A MODEL STUDY OF THE END BEARING CAPACITY OF PILES IN LAYERED CALCAREOUS SOILS

by

Keith Martin Evans

A Thesis submitted for the Degree
of Doctor of Philosophy at the
University of Oxford

Keble College

Trinity Term, 1987

A MODEL STUDY OF THE END BEARING CAPACITY OF PILES IN LAYERED CALCAREOUS SOILS

K.M.Evans

Keble College, University of Oxford

A Thesis submitted for the Degree of Doctor of Philosophy

Trinity Term, 1987

ABSTRACT

The results of a series of over 120 model tests to study the end bearing capacity of piles in layered calcareous soils are described. The tests were carried out on samples enclosed in a cylindrical testing chamber, 450 mm diameter and 450 mm high, which allowed independent control of horizontal and vertical stress in the range 25 kPa to 500 kPa.

The samples consisted of a loose, uncemented calcareous sand consisting predominantly of foraminifera and mollusc micro-organisms (D_{50}= 0.2 mm, calcium carbonate content 92%). Into this was built a layer of the same material artificially cemented by a gypsum plaster. The layer had similar properties to naturally cemented deposits, and layers with unconfined crushing strengths in the range 500 kPa to 4000 kPa have been prepared. All samples were tested dry.

Closed end model piles of 16mm diameter were jacked at 0.1 mm/s into the sample, and continuous profiles of end bearing capacity obtained during penetration. A parametric study has been carried out to examine the effects on the bearing capacity of stress level, K_0, cemented layer thickness (0.5 pile diameters to 5.0 pile diameters) and layer strength. In addition, tests have been conducted with different pile geometry, multiple cemented layers, and using dynamic installation techniques.

The study has identified ranges of parameters for which brittle failure of the cemented layer occurs (low stress levels and high layer strengths) and ranges where the failure is ductile (high stresses and low layer strengths). Characteristic patterns have been observed of the variation of end bearing with position as a layer is penetrated. Examination of the samples after testing has revealed details of failure mechanisms.

Simple procedures are proposed for modelling the bearing capacity of such layered systems, and some implications of the results for design methods are discussed.

Acknowledgements

I wish to thank Mr. Mike Sweeney of B.P. International Ltd. for organising the finance from within the B.P. company to support the work reported in this thesis, and for initially stimulating and directing the research to an interesting and exciting area.

I am grateful to Dr. Guy Houlsby, who as my supervisor has provided encouragement and guidance when required, and whose enthusiasm and standards have been a constant motivation. I also wish to thank Professor Peter Wroth for his many useful comments, which were always an education.

The development and commissioning of the experimental equipment was achieved with the help of the Soil Mechanics laboratory technicians, Mr. Chris Donnelly and Mr. Bob Earl.

My time as part of the Soil Mechanics Research Group has been made very enjoyable by the friendship of other members of the group, and to those people I have known I extend my thanks.

Personally, I would like to thank my parents for their support in many ways over many years, and my wife for her constant encouragement, understanding and tolerance of my preoccupation.

Keith Evans

CONTENTS

CHAPTER 5 BEARING CAPACITY OF A MODEL PILE IN CARBONATE SAND

CHAPTER 6 TESTS ON SINGLE CEMENTED LAYERS

CHAPTER 7 VARIATION OF PILE GEOMETRY

CHAPTER 8 TESTS WITH SPECIAL APPLICATIONS

CHAPTER 9 APPLICATION TO DESIGN

CHAPTER 10 DISCUSSION AND CONCLUSIONS

CHAPTER 1 INTRODUCTION

1.1 Piled foundations in calcareous soils

The present day need for hydrocarbons has led to an increase in offshore exploration and production platforms on the continental shelves of the world. Within the last two decades the major areas of activity have coincided with areas where the sea bottom sediments are predominantly of a carbonate nature and generally termed calcareous soils. They comprise variably layered cemented and uncemented carbonate sands, and examples are found in the Arabian Gulf, the north west and south east coasts of Australia, the west coast of India and the south east coast of Brazil.

The presence of calcareous soils has presented the geotechnical engineer with foundation difficulties, as so little is known about their geomechanical behaviour. It is readily recognised that the origin and composition of such sediments differ significantly from the more well known terrigenous silica sands. The problem is compounded by the special nature of the sediments which:-

(i) exhibit extreme variations in void ratio due to variations in the size and shape of their particles.

(ii) do not compact to as low a void ratio as non carbonate sediments.

(iii) have very low grain strengths.

(iv) are very susceptible to post-depositional alteration in the form of dissolution, cementation and bioerosion, and such alteration may be extremely variable.

Early offshore construction experiences clearly showed the dangers of applying criteria established from tests conducted on silica sand to calcareous material. Of particular concern are the low values of driving resistance and load capacity of foundation piles driven into such sediments. Therefore, much research is being directed at the conception and evaluation of methods of analysis for structures on calcareous soils, and in particular for the behaviour of piled foundations.

A recent project on the continental shelf off North West Australia, the North Rankin platform, has foundation strata consisting of calcareous soils and illustrates a number of typical geotechnical problems. Here the cemented layers are quite thick and occur periodically throughout the soil profile, a schematic example is illustrated in Figure 1.1.

The development of pile resistance by skin friction in calcareous soils has been shown to be limited (Angemeer et al. (1973), McClelland(1974), Fugro (1981)) and therefore maximum use must be made of the end bearing characteristics of cemented layers (where they exist). However, due to the special nature of calcareous material and the geometry of the cemented layers, the appropriate form of the limit state failure mechanism for such layered configurations is at present in doubt. Therefore, even though it is accepted that the fundamental behaviour of calcareous soils is not understood fully, since the limit state analysis forms such an important part of the design methodology for piled foundations, the understanding and evaluation of such mechanisms has been identified as the primary objective of this research programme.

Physical modelling was proposed as a method of investigating this type of problem and the research concept is illustrated in Figure 1.2. A cemented layer (or layers) was created within a sand stratum, and a pile installed into this system, inducing failure in the cemented layer. A parametric model study was carried out to study the effects of cemented layer strength, cemented layer thickness, pile diameter, pile type, and stress level (using a stress controlled testing chamber). The resulting failure mechanisms could be physically examined and classified, and when related to the measured test results allowed comparison with appropriate existing semi-empirical or numerical solutions.

Based on the acceptance of physical modelling techniques (the philosophy of modelling regarding similarity between model and prototype is discussed in Section 4.1), a number of tasks was clearly defined:-

* establish satisfactory calcareous testing materials (cemented and uncemented).
* conceive and develop testing equipment.
* conduct parametric model tests.
* compare the test results with available semi-empirical/numerical predictions.

The extent of these tasks was curtailed by applying the following limitations:-

(i) the tests were conducted in a dry state.

(ii) only monotonic loading was considered.

(iii) no comparative testing was carried out using silica sand.

The tasks identified have been completed within this research programme and are presented in subsequent chapters.

Before discussing the engineering behaviour of calcareous soils, it is felt to be beneficial to review the geology of calcareous soils, since such sediments represent relatively new materials to foundation engineers.

1.2 The geology of calcareous soils

1.2.1 Formation, diagenesis and lithification

A review of the associated literature soon indicates that the terminology used to describe calcareous soils can be confusing, some authors preferring to use the word 'carbonate' in preference to 'calcareous'. Tentative guidelines do exist on the division of sediments into calcareous or carbonate, a sediment being classified as calcareous if it contains more than 30% and less than 50% calcium carbonate, and carbonate if it contains more than 50% calcium carbonate. The word 'calcareous' seems to have been adopted by the engineering profession as the generic description for all material (soil and rock) containing calcium carbonate, and has been used in that context in this thesis. However, when discussing sedimentological and classification aspects of this material the stricter terminology should be applied, and it is therefore, primarily carbonate sediments that are of major interest.

In order to understand the geomechanical behaviour of any soil type, a thorough knowledge of the geology of that soil is required. This section therefore attempts to present an overview of the sedimentology, diagenesis and lithification of carbonate sediments and is drawn primarily from published works by carbonate sedimentologists and limestone geologists. A more detailed account is provided by Evans (1985).

Carbonate sediments are presently forming on many parts of the ocean floor, the areas of which are defined by fairly complex controls. Excluding cases where direct inorganic precipitation occurs, the common means by which the principal constituent of a carbonate sediment i.e. calcium carbonate, is transferred to the sea floor is biological. Organisms living in the sea water (pelagic) and on the sea floor (benthonic) utilise dissolved calcium carbonate to construct portions of their bodies (tests), usually in the mineral form of calcite or aragonite. Their remains settle on the sea floor, and if the rate of sedimentation is greater than the rate of dissolution, a bed of carbonate sediment forms. The same has been true throughout geological time, and because organisms have deposited the carbonate, the controls have changed as the organisms have evolved.

The rate of organic productivity in the marine environment is controlled by many variables but in general there is a progressive increase from the higher to lower latitudes. Temperature combines with other factors like salinity, carbon dioxide balance, water depth, nature of local current regimes, light penetration, effective day length, nature of substrates and turbidity in controlling carbonate deposition (Reading, 1978). Carbonate deposits are not, however, restricted to latitudes between 30°N and 30°S as reported by many recent authors. For example many thousands of square kilometres of virtually pure shelf carbonates are currently accumulating off southern Australia, between latitudes 30° and 40°S (Angemeer, 1973) and in smaller, discrete patches elsewhere in the world, including areas as far north as Ireland and Scotland, with deep sea deposits extending beyond the Arctic Circle (Rodgers, 1957).

Three broad classes of modern marine carbonate sediments may be recognised, though there are of course gradations: the calcareous oozes found over great parts of the worlds deep sea floor: the deposits forming organic

reefs in both the ocean and shallow water; and the carbonate sands and muds of certain continental shelves.

Organic reef complexes have presented geotechnical engineering problems on near shore structures (Hagenaar (1982), Hagenaar and Vandenberg (1981)) but recent offshore hydrocarbon explorations on the continental shelves of many regions of the world have encountered carbonate sand and mud deposits, and it is only this class of deposit that will be considered.

The dominance of carbonate deposits upon certain sectors of the world's continental shelves is directly related to two major factors, the relative lack of clastic deposition, and high organic productivity. All modern carbonates occur in areas that are not generally receiving large amounts of silicate detritus, and the bulk of carbonate material on modern shelves is ultimately of organic origin, either directly as skeletal material or indirectly as a precipitated by product of organic activity.

It has now been established that marine carbonate sands occupy significant areas of the continental shelf between the equator and latitudes 60°S and 60°N. Lees and Buller (1972) reviewed the global distribution of grain types in the sand and coarser fractions in carbonate sediments deposited in less than 100m of water on open continental shelves between these latitudes, and found that they could be grouped into a few grain associations. On tabulating the skeletal grains in terms of major taxonomic groups they discovered a systematic difference between those carbonates forming well outside the tropics and those of warm water type.

The main groups of organisms represented in the temperate water associations are; (i) Animals - molluscs, foraminifera (benthonic), echinoderms, bryozoans, barnacles, ostracods, sponges, worms and ahermatypic

corals, (ii) Plants - calcareous red algae (eg. Lithothamnium). The warm-water association may include most of the above mentioned components but differs in that:- (i) it always contains significant contributions from corals and/or calcareous green algae (eg. Halimeda); (ii) barnacles never contribute measurably to the sediments, and (iii) bryozoans are rarely more than minor constituents.

These associations of skeletal grains have therefore been termed, CHLOROZOAN (Chlorophyla + Zoanthoria) for the warm-water group, and FORAMOL (Foraminifera + Molluscs) for the other association. The predicted distributions of these two associations are shown in Figure 1.3. The non-skeletal grains were classified as pellets, ooliths, and aggregates (ex. grapestone). The majority of pellet records occupied the chlorozoan association in areas bordering the chlorozoan/foramol boundary. The other non-skeletal grains are largely restricted to areas with chlorozoan sediments. The predicted distribution of the non-skeletal grain associations is shown in Figure 1.4. It should be noted that Figures 1.3 and 1.4 have been prepared from direct sampling in limited areas, together with salinity and temperature data (thought to be the major contributing factors, Lees (1975)). They should therefore only be viewed as tentative predictions to a depth of about 100m, due to the unknown effects of other environmental conditions which may prevail.

Until recently, little was known about carbonate sediments from shallow temperate waters. However, it is now evident that they do occur along many western coastal regions in the Northern Hemisphere, generally in isolated patches scattered amongst the predominantly terrigenous sediments, (sometimes referred to as 'neritic' deposits). Documentation exists for deposits in Norway, Isle of Skye, Scotland, Brittany, S. Cornwall, and the west coast of Ireland, (Wilson (1979), Lees et al. (1969), Lees, (1975), Boillot et al.

(1971), Buller, (1969)). These deposits are discussed in more detail in section 2.1.

Diagenesis and lithification include processes which convert sediment into rock. They are of special importance when studying carbonate sediments because of the ease with which they modify the texture, structure and composition of the original sediment. The onset of diagenesis is often difficult to define in a carbonate sediment and an understanding of the mineralogy of the sediments must be gained in order to grasp the inherent processes. In Recent and Subrecent sediments, two calcium carbonate minerals predominate: aragonite (orthorhombic) and calcite (trigonal). The mineralogy of a modern carbonate sediment depends largely on the skeletal and non skeletal grains present. Carbonate skeletons of organisms have a specific mineralogy or mixture of mineralogies and during diagenesis, these mineralogies may be altered or replaced, in particular aragonite, being metastable, is invariably replaced by calcite.

Diagenesis of a carbonate sediment to a limestone rock is often referred to as isochemical when there is no major change in the chemistry of the sediment, and allochemical when chemical changes are involved. The principal diagenetic isochemical processes taking place are cementation and neomorphism, and allochemical changes of dolomitisation and silicification. The process of cementation is of particular interest to the geotechnical engineer.

Until the 1950's it was tacitly assumed that carbonate sediments could only ultimately be converted into limestones through burial. It was then realised that Recent and Pleistocene carbonate sediments were being cemented through contact with fresh, meteoric waters (water which penetrates the rocks from above - rain, dew, snow, rivers and streams) and so cementation through uplift became the accepted process. Discoveries in the 1960's of cemented

sediments on the sea floor in shallow and deep waters (areas which are now receiving some geotechnical exposure eg. Arabian Gulf, Australia, Brazil, Florida, India), showed that neither burial nor uplift was necessary, and that simultaneous sedimentation/cementation was occurring. More recently cores through pelagic carbonates from the ocean floors have demonstrated cementation with increasing depth of burial. The process of cementation is therefore very much environment controlled and no single hypothesis can explain the process. There are thought to be five main types of cementation process:-

(i) meteoric cementation,

(ii) intertidal zone cementation producing cemented beach sands known as beach rock,

(iii) shallow subtidal cementation to produce surface crusts, (sometimes termed 'hardrock' or 'caprock'). This process is well documented for the Arabian Gulf and has featured in a number of geotechnical papers (Shin (1969), Broadhead (1970), Dennis (1976)),

(iv) deep water cementation,

(v) burial diagenesis through pressure solution,

Having discussed the formation, diagenesis and lithification of calcareous soils, where are the divisions drawn between sediment type, and what descriptive nomenclature has been developed for each?

1.2.2 Classification systems

Geologists and geotechnical engineers, whilst dealing with the same material, often require different classification systems. In general the geotechnical engineer will need to categorize to a greater extent on the basis of engineering properties. It is therefore often the case that an original geologically derived classification will be subdivided by an engineer to

produce a system suitable to his/her requirements. This is the case with carbonate sediments.

Generally sedimentologists need to classify the visible limestones of today in order to construct facies models for present carbonate sediments and to understand ancient limestone formations. While the late 1950's witnessed many advances in the facies approach there was still no satisfactory classification. Grabau (1913) introduced the twofold grain-size terms calcirudite, calcarenite, calcisiltite and calcilutite, and these terms are still in common useage. Pettijohn (1957) simply divided limestones into allochthonous, autochthonous, biohermal, and biostromal, but the subtleties of differentiating between limestone types was not possible before Folk's (1959) paper on petrographic classification was published. The Folk classification, was later restated by Ham (1962) which gives the major classification in common contemporary usage, that of Dunham (1962) whose prime concern was the nature of the grain-support. The present classification system for limestones is shown in Figure 1.5.

This terminology is of limited use to the geotechnical engineer as it gives very little indication of engineering behaviour. Fookes and Higginbottom (1975) were perhaps the first to attempt classification of carbonate soils from an engineering viewpoint, largely derived from Pettijohn (1957). They chose grain size and post-depositional induration (cementation) as the main parameters of engineering significance, but also recognised the possible importance of other factors such as mineral composition, origin and strength.

Clark and Walker (1977) rationalized and expanded the previous scheme to include the range of mixed carbonate and non-carbonate materials which they encountered in the Middle Eastern sedimentary rocks. Their scheme is shown in Figure 1.6. The three main classification parameters are grain size, carbonate

content, and degree of induration. They also emphasized the use of Grabau's original grain size terms, calcirudite, calcarenite, calcisiltite, and calcilutite, and the importance of the carbonate content (%) which was beginning to become apparent.

King et al. (1980) developed a site specific system for the classification of carbonate sediments for the North Rankin, North West Australian Shelf project based on Clark and Walker's system. The system incorporates modifications in both the grain size, description, and evaluation of induration/cementation, CPT data being used as an indicator for the latter. The basis of the classification is shown in Figure 1.7 and is only applicable to sediments with 90-100% carbonate content. The main components of the modified system are derived from visual description by microscope, grain size analysis and cone resistance data. Full classification of a carbonate sediment involves the items shown in Table 1.1.

This system certainly goes someway to providing a description and classification of carbonate sediments which will satisfactorily reflect the engineering behaviour of a sediment. However, Datta et al. (1982) illustrate that the type of carbonate material can significantly influence both the magnitude of crushing under stress and the degree of cementation, and both factors vary over a wide range and can have a markedly different influence on engineering behaviour. They illustrated that there is as yet no method of readily identifying and quantitatively expressing the degree or the uniformity of cementation. Table 1.2 illustrates their proposed systems of description.

In terms of practical application it is felt that use of the King et al. classification system should be continued, but that every opportunity should be taken to obtain information on the exact nature of the carbonate material being sampled or tested in line with Datta et al.'s recommendations.

Table 1.1

1.	Grainsize of Main fraction	fine/medium/coarse
2.	Name	see classification diagram
3a.	Degree of induration (fine grained deposits)	very soft/soft/firm/stiff/very stiff/hard/ weak/mod.weak/mod.strong/strong/extr.strong
3b.	Degree of cementation (medium-coarse grained deposits)	uncemented/very weakly cemented/weakly cemented/firmly cemented/well cemented/hard cemented
4.	Bedding and lamination	thinly laminated/laminated/thinly bedded/ medium bedded/thickly bedded
5.	Origin of carbonate (medium-coarse grained deposits)	bioclastic/clastic/oolitic/reefoidal
6.	Colour	Munsell soil colour charts
7.	Minor fractions	clean/with some/muddy/silty/sandy/gravelly

Table 1.2

Description of	Remarks
1. Cementation	
(*a*) No cementation	
(*b*) Weak cementation	
(*c*) Strong cementation	
(i) uniform	the soil has a soft rock-like appearance. Unconfined compressive strength should be indicated
(ii) partial	the soil contains cemented aggregates—this should be noted
2. Grain Size Distribution (GSD) and Plasticity	
(*a*) Grain size distribution	for strongly cemented soils, GSD is not very relevant; for uniform cementation, size of constituent particles should be indicated; for partial cementation, GSD of soil after removing aggregates should be indicated and size and proportion of aggregates noted separately
(*b*) Plasticity	for fine-grained soils in which intraparticle voids cause error in GSD and Atterberg limits, field classification procedures may be used for providing the relevant information in a qualitative sense
3. Nature of Carbonate Component	
(*a*) Carbonate content	soils having more than 30% carbonate content should be termed as carbonate soils
(*b*) Particle size of carbonate material	the carbonate content in the sand and in the silt-clay fractions should be determined separately and indicated. Microscopic studies mentioned below will also give information about particle size
(*c*) Particle characteristics and origin	microscopic studies—optical microscope for sands and scanning electron microscope for fine-grained soils—should be conducted. Presence of thin-walled material and intraparticle voids should be highlighted
(*d*) Mineralogy	X-ray diffraction analysis should be performed
(*e*) Geologic name	if possible to identify, the geologic name may be indicated
4. Nature of Noncarbonate Component	information on noncarbonate material is determined by dissolving the carbonate material in HCl, separating the remaining soil, and conducting the following tests on it
(*a*) Particle size	grain size distribution analysis
(*b*) Particle characteristics	microscopic studies
(*c*) Mineralogy	X-ray diffraction analysis

1.3 Review of engineering behaviour

It is not intended to discuss in detail the mechanical behaviour of calcareous soils, as such details are not yet clearly established, nor was the primary aim of this research to establish such behaviour. However, certain behavioural characteristics have been identified, and these will be highlighted. It is convenient to discuss these characteristics separately for uncemented and cemented deposits.

1.3.1 Uncemented deposits

Laboratory investigations on the behaviour of uncemented deposits (primarily carbonate sands) have been directed towards the evaluation of shear strength and deformation properties.

Datta et al. (1979, 1979a, 1981, 1982) conducted extensive studies on four carbonate sands of skeletal origin from the west coast of India, all having a calcium carbonate content greater than 85%, and gradings ranging from coarse to fine sand. In order to investigate the stress-strain-volume change behaviour, together with the extent of sand crushing, a series of consolidated drained triaxial tests were performed at low and elevated (6280 kPa) cell pressures.

The results, when defined in terms of the peak effective stress ratio show the angle of shearing resistance decreasing with increasing confining pressure. Datta et al. (1979) attribute this decrease to the effects of particle crushing and found the following empirical relationship between the degree of particle crushing and the decrease in angle of shearing resistance.

$$\frac{K}{K_1} = (\overline{C}_c)^{-0.6} \qquad \ldots\ldots (1.1)$$

where K = maximum principal effective stress ratio

K_1 = K corresponding to no crushing, i.e. $\bar{C}_c = 1$

$\bar{C}_c$ = crushing coefficient, defined as

$$\frac{\%\text{ particles finer than } D_{10} \text{ of original soil after stress application}}{\%\text{ particles finer than } D_{10} \text{ of original soil i.e. } 10}$$

Values of $\bar{C}_c$ up to 7.0 were measured for soils subjected to high confining pressure and then failed in drained triaxial compression. The tests also showed that increased crushing altered the behaviour from that of a dilatant brittle material to a more plastic material, exhibiting volume reduction during shear, as illustrated in Figure 1.8.

Datta et al.'s investigation revealed the importance of particle crushing and concluded that crushing increases with: increasing confining pressure, application of shear stress, increasing abundance of intraparticle voids and plate-like shell fragments, increasing angularity of particles, increasing size of particles, and decrease in mineral hardness.

Poulos et al. (1982) recognised the need for further data on strength and deformation properties of carbonate soils in order to understand more fully their behaviour under both static and cyclic loading. Motivated by the offshore exploration off the southern coast of Australia, they presented the results of a series of static laboratory tests carried out on two types of carbonate sand of biogenic origin from Bass Strait, Australia (sand A & B). The tests included drained triaxial compression tests, direct shear tests, hydrostatic consolidation tests, K_o consolidation tests and oedometer tests. The tests were carried out on reconstituted samples so that the effects of any cementation which may have been present in the in-situ soil were not accounted for.

When tested under drained conditions in the triaxial apparatus, failure was defined in terms of the maximum principal stress difference, and the corresponding angle of shearing resistance ϕ was found to decrease with increasing confining pressure, as noted by Datta et al.. Also in line with Datta et al.'s findings, Figure 1.9 shows that as the confining pressure increases the soil behaviour changes from that of a dilatant brittle material to that of a more plastic material, exhibiting volume reduction during shear.

Following the triaxial tests, changes in grading due to particle crushing were investigated, and the coefficient $\bar{C}_c$ as defined by Datta et al. was evaluated. For soil B a value of 1.6 was found but soil A did not show measurable crushing, this being attributed to the fact that the soil was re-used several times for a number of tests.

In evaluating deformation properties values of drained Young's modulus E' and drained Poisson's ratio ν' (corresponding to a deviator stress of 50% ultimate) were obtained from the triaxial tests. Both E' and ν' were found to vary linearly with consolidation pressure.

Six conventional oedometer tests were performed, and for the stress range 69 - 552 kPa the values of the compression index C_c fall within the range 0.09 to 0.14, which is considerably more compressible than normal silica sands. Eight tests on sand A were carried out in the K_o test apparatus at Sydney University, resulting in a range of K_o values of 0.16 - 0.41.

Conclusions are drawn by Poulos et al. that the tested carbonate soils are: susceptible to crushing at relatively low stress levels, have values of Young's modulus and Poisson's ratio which vary linearly with confining pressure in the triaxial apparatus, and are significantly more compressible than normal silica sands.

Due to the extremely variable nature of the calcareous soils at the North Rankin gas exploration site the sediments have been tested extensively to evaluate appropriate geomechanical properties. Unfortunately, the vast majority of the data remains unreported in the open literature, but the author has been given access to the files of B.P. International, and some of the data presented are drawn from such files. However, the results presented do not attempt to constitute a full review of the extensive testing programmes undertaken.

The early design philosophy applied to the North Rankin platform directed the investigations to the upper stratum carbonate sands and silts. Dames and Moore (1974) measured unit weights of 10.5 to 15.4 kN/m^3 with void ratios in the range 1.4 to 0.75. Specific gravity was quoted at an average value of 2.67 with calcium carbonate content varying from 88% to 99%. Triaxial shear and direct shear results indicated angles of friction of approximately 45°. This angle was found to reduce with increasing confining pressure, but no quantitative data were given.

Fugro carried out investigations in 1978 and 1981, and Rupp (1984) reviews the extensive laboratory tests undertaken. These tests included classification tests, oedometer tests, and various triaxial tests. Oedometer tests indicated slightly overconsolidated to normally consolidated soils with the compression index C_c ranging from 0.21 to 0.73. Consolidated drained and undrained triaxial tests gave effective angles of shearing resistance in the range 33° to 44°.

The following points become apparent from a review of the laboratory work previously performed on uncemented deposits:

(i) hardness of grains - even though the angle of shearing resistance of carbonate sand is in the same range as that of silica sands, the difference in values for the hardness of the principal minerals (7 for silica, 3 for calcite) could explain the weaker behaviour of carbonate sands. This is characterized by the changing of its grain size distribution under stress, and has been quantified by Datta et al. (1979) by a crushing coefficient $\overline{C}_c$, which in itself is related to a number of parameters.

(ii) compressibility - the compressibility of a carbonate sand is the result of four mechanisms (Nauroy and Le Tirant, 1983):-

- elastic deformation of the materials,
- re-arrangement of the grains,
- crushing of the grains,
- breakdown of cementation bonds (when they exist).

The first two mechanisms are common to all granular materials, the last two are important for carbonate sands. Their compressibility and long term creep rate have been shown to be significantly greater than those of silica sands.

(iii) Void ratio / porosity - not only is the void ratio of carbonate sands larger than for silica sands, but also the presence of intraparticle voids, in addition to interparticle voids, plays an important role. Voids internal to the particles mean that their breakdown will always be accompanied by a net decrease in volume, and this has been illustrated by Datta et al. (1979) and Poulos et al. (1982).

1.3.2 Cemented deposits

Well known and documented calcareous rocks are chalk and limestone. Unfortunately, the diagenetic processes which control lithification are complex and lead to the weak cementation and variable stratification presently encountered in cemented calcareous soils, this consequently avoids a comparison with the fully lithified chalk and limestone rocks.

Many authors have reported the occurrence of cemented horizons within an otherwise uncemented sand or silt. The engineering behaviour of such sediments has not, however, been so well reported, primarily due to the difficulty in obtaining representative samples from the weakly cemented strata due to sample disturbance.

Again the North Rankin site provides the most comprehensive data available on the strength and deformation properties of cemented carbonate sands. Figure 1.10 presents the results of five oedometer tests performed on specimens from generally well cemented layers. These tests show similar compression indices (C_c = 0.25 - 0.58) to the carbonate sand even though the void ratios quoted are substantially less. Interestingly, the apparent pre-consolidation pressure is of the order 2 to 5 MPa, and well above the in-situ effective stress, 0.5 MPa. Such behaviour has been previously reported by Miller and Richards (1969) who found the apparent pre-consolidation pressure of a calcareous ooze core from the Bahamas to be sixty times greater than the in-situ effective stress (σ'_v), 0.5 MPa. This difference was attributed to cementation occurring in place, and Miller and Richards suggest that consolidation test results should be interpreted with caution for such materials.

Strength tests in the form of uniaxial unconfined compression and consolidated drained triaxial tests were performed on the North Rankin cores by Fugro (1981). For the uniaxial compression tests most of the stress-strain curves have sharp peaks and show the post peak strain softening associated with brittle fracture. However, some curves have unusual shapes and the sketches of the test specimens after testing show an unusual range of fracture planes.

For the series of consolidated drained triaxial compression tests specimens were consolidated under isotropic pressures of 0.5 and 1.0 times the estimated mean in-situ effective stress. The specimens exhibited a variety of failure modes including the formation of a single shear plane, ductile bulging, tilting and/or crushing at the ends, and the formation of sub-horizontal fracture surfaces or zones. Fugro (1981) plot the results in terms of Mohr's circles and conclude that the cemented sand should be treated as a layered material with the less well cemented layers behaving as $c - \phi$ soils.

Brown (1984) has studied the laboratory data from the North Rankin field and makes the following conclusions on the strength and deformation behaviour of the cemented sand, classified as calcarenite :-

(a) the calcarenite is a weak, high porosity rock composed of a self supporting framework of uniform grain sized clastic and bioclastic material.

(b) the degree of cementing varies with depth, but is not related to depth of burial.

(c) if the calcarenite is treated as a single layer with uniform properties, drained strength and modulus values of $c' = 400$ kPa, $\phi' = 35^{\circ}$, unconfined strength $\sigma_{fc} = 1.5$ MPa, and $E' = 150$ MPa could be used.

(d) if the calcarenite is treated as a layered material, suitable drained strength and modulus parameters would be; $c' = 1.0$ MPa, $\phi' = 35^{\circ}$, $\sigma_{fc} = 3.8$ MPa, $E' = 350$ MPa for the stronger layers, and $c' = 100$ kPa, $\phi' = 35^{\circ}$, $\sigma_{fc} = 0.38$ MPa and $E' = 100$ MPa for the weaker layers.

(e) in the oedometer test, specimens of well cemented calcarenite exhibited an apparent pre-consolidation pressure, generally of 2 - 3 MPa, above which compressibility increased considerably. This phenomenon is probably associated with failure of the cementing between the grains, and progressive collapse of the open pore structure, causing volume decrease during shear.

In the early 1980's the pile design concept for the North Rankin platform changed from friction piles to end bearing piles, with maximum end bearing mobilised from the cemented layers. This change resulted in numerous triaxial, shear, model pile and grouted section tests by several organisations throughout Australia.

The triaxial and shear tests conducted are extensive and provide valuable comparative and calibration data for the detailed numerical modelling undertaken. It is not proposed to review such data, as it is felt that the characteristic behaviour of the material has already been conveyed, and any analysis of such results will in itself be subjective. The model tests carried out will be discussed in section 1.4.

Studies of the microstructural fabric of the undisturbed calcarenites and the changes to those fabrics induced by the laboratory tests detailed above will be presented, as they are of direct application to the investigation area of this dissertation, and will be referred to in subsequent sections.

By studying thin sections of both the undisturbed calcarenites and tested samples, Price (1985) describes the fabrics of the undisturbed calcarenites, in particular the components which are significant to mechanical performance, and the pronounced changes which occurred to those fabrics during the laboratory tests.

The deformation fabrics were categorised into two types :-

(i) fabrics characterised by consolidation and repacking of the original grains into denser arrangements, with the consequent closure of open pores. A moderate degree of grain fracturing was involved and this produced a wide range of fragment sizes. The broken grains and fragments were tightly pressed together with only a little fine ground matrix, so that continued deformation would involve considerable grain interaction. This type of fabric was described as a high particle density breccia.

(ii) fabrics characterised by relative shear displacement between grains, the disintegration of carbonate pellets and most of the shells and shell fragments, and the formation of an abundant matrix of very small carbonate granules. This matrix surrounded and separated the few remaining large grain fragments such that further deformation would not involve grain interaction but would be lubricated by the matrix. This fabric was described as a low particle density breccia.

Price (1985) proposes that during the tests conducted, one or both of these fabric types were developed in different regions of the tested specimens, and concludes that these two types of fabric have characteristicly different stress-strain responses and govern the performance of the bulk calcarenite specimens during the test. The consolidation type fabric results in a strain hardening response after yield, and the shear type fabric results in a strain softening response after yield.

1.4 Previous model testing and applied research

Over the last few years there has been a dramatic increase in research activity in the area of calcareous soils; this of course has been driven by the many problems encountered in offshore pile installation in such soils. Much of this research has been directed at the pile soil interface characteristics in order to understand the very low skin friction values which have been observed. The end bearing problem has so far received limited exposure primarily due to the difficulty in obtaining consistent, representative and repeatable test samples, and the difficulty in producing artificial material. It is however beneficial briefly to review the research on side friction to appreciate the techniques employed, but specific details will not be discussed.

Research has primarily been carried out using three techniques:

(i) laboratory scale models (approx. 1:100 scale) tested in either a modified triaxial cell or a purpose built testing chamber. Dames and Moore (1974) and Fugro (1981) used such techniques for the North Rankin materials. Nauroy and Le Tirant (1983) carried out tests to link the compressibility of calcareous sand with bearing capacity parameters. Poulos (1984) investigated the cyclic degradation of pile performance for Bass Strait, Australian carbonate sands. Ertec Western Inc. (1983) studied the effects

of grain crushing on the engineering behaviour of calcareous sediments, and Lu (1986) used similar apparatus for an investigation with an instrumented pile.

(ii) laboratory shear tests to understand the pile/soil/(grout) interface characteristics. Such tests have been discussed by Agarwal et al. (1977), Datta et al. (1981), Dutt et al. (1986), but perhaps the most revealing are tests by Noorany (1985) who found that no change was evident in the friction angles and average soil-steel friction angles when testing highly crushed or uncrushed calcareous sand. This illustrates an important aspect which is consistently revealed in the previous literature i.e. the low skin friction of steel piles driven in calcareous sands is caused by low effective soil-pile interface stresses rather than small soil-pile friction angles.

(iii)Field performance observations have been conducted using different scale models to assess skin friction or grout adhesion values. Details of such tests for calcareous soils have been presented by Angemeer et al. (1973), Fugro (1981), Dutt and Cheng (1984), Nauroy and Le Tirant (1985) and Withers et al.(1986).

More applicable to the end bearing behaviour in layered calcareous soils are tests performed by Poulos et al.(1984) and Jewell (1985a,b).

Poulos et al. describe a series of model footing tests (25 mm diameter) on calcareous and silica sands carried out in a stress controlled testing chamber. Despite the high angle of internal friction of the calcareous sand, they found the bearing capacity to be significantly less than that of silica sand. They attribute this difference to the compressive plastic volume strain of the calcareous sand even at low confining stresses, which contrasts with

the dilatant plastic volume strain in the silica sand. Conventional bearing capacity theories were found seriously to overestimate the bearing capacity on calcareous sands, but reasonable predictions were provided by spherical cavity expansion theories which take into account the variation of friction angle and plastic volume strain with mean normal stress. The application of such theories will be discussed in Chapter 5.

As part of the North Rankin investigations a series of model pile and rod index tests were carried out at the University of Western Australia and reported by Jewell (1985a,b).Some of these results provide comparative data for the model tests which will be presented in this thesis.

A series of model pile tests were carried out, with one of these series becoming standardised as the Rod Index Test (RIT). The samples used in each series were obtained from coring operations at the North Rankin platform, and consisted of cemented carbonate sand (calcarenite). Two types of model pile were used, a closed and open end, and this review will be restricted to the 16 mm diameter closed end model pile.

The first series of tests consisted of drilling a 19 mm diameter by 35 mm deep hole through the centre of an 83 mm diameter by 160 mm long core sample, and positioning this sample in a triaxial cell. The model pile was lowered into the preformed hole and the cell pressure raised to 500 kPa. The pile was then jacked into the sample at a constant rate of displacement, with load and penetration being constantly monitored. Different samples were penetrated to different depths, with the samples retained for micro-fabric analysis. The resulting load-displacement plots are presented in Jewell (1985a) who concludes that the response is irregular, and observed oscillations are due to build up of end resistance followed by sudden decrease, probably due to particle crushing or breakdown of cementation.

Whilst the primary aim of the model tests was of a qualitative nature, it was felt that useful quantitative information could be obtained. The need for such data was due to the inconsistency of the uniaxial compressive strength in providing a satisfactory strength measurement for the North Rankin calcarenites. The RIT was established to provide a more satisfactory strength measurement.

Test samples were prepared by cutting sections of the 83 mm diameter core to a length of 120 mm and grouting these sections into a 130 mm long PVC tube. After the grout had set a 19 mm diameter hole was drilled into the centre of the core and a guide tube inserted into this hole. The base of the hole was cleaned and the sample placed between the top and bottom platens of a loading frame as illustrated in Figure 1.11.

Testing was conducted at a constant rate of displacement of 0.5 mm per minute, and taken to a displacement of 16 mm (if possible) i.e. a displacement/diameter ratio of 1.0. After testing the sample was oven dried and cut down the centre to reveal the shape and extent of the sample deformation. The primary results from these series therefore include the load-deformation curves and the visual assessment of the split sample after testing.

Jewell considered that most of the curves could be characterised by three linear phases, each of decreasing stiffness, and representing elastic, crushing and particle rearrangement responses. These were defined as the three stages of "crush up" and are illustrated in Figure 1.12. In order to classify the calcarenite, loads at a rod penetration of 8 mm (designated as "P_8") have been adopted as the strength criterion.

From an inspection of the samples split after testing, Jewell (1985b) suggested that the compression zones could be classified into five types. However, further detailed study of the fabric changes by Price (1985a) revealed only two characteristic shapes; one a spherical shaped bulb, and the other a vertically elongated bulb, both illustrated in Figure 1.13. Such fabric studies have been previously discussed, and these two characteristic shapes correspond to the consolidation and shear mechanisms previously identified.

The Rod Index Test results and "P_8" values will be referred to in subsequent chapters.

1.5 Existing design practice

The design of piled foundations for calcareous soils is at present empirical and does not conform easily to the guidelines established for silica based marine soils.

It is not proposed to state the design methods presently applied to calcareous soil as these are comprehensively presented by Datta et al. (1980) and Poulos (1985), and simply use reduced values of limiting unit skin friction and end bearing in relation to values used for the design of piles in non calcareous soils. Further discussions on the applicability of static design methods will be presented in subsequent chapters.

Attempts have been made to relate in-situ test results to pile behaviour. The simplest of in-situ tools, the SPT hammer, has been used by Hagenaar (1982) and Puyuelo et al. (1983), who conclude that the results can be misleading, and substantiation of interpretation is required in the form of full scale pile load tests. Stevenson and Thomas (1978) have used instrumented

piles to facilitate prediction by wave equation methods, and report limited success, but Dutt and Teferra (1986) claim good results from such techniques.

Extensive investigations have been conducted off the Australian coast, originally in the south east at Bass Strait, and reported by Angemeer et al. (1973) and Withers et al. (1986), and at the North Rankin platform, Dames and Moore (1978) and Fugro (1978, 1981). The devices used have been: the cone penetrometer, instrumented piles, pressuremeter, and specialised in-situ tests such as pull out tests on small scale piles and down hole plate bearing tests. These tests have been assessed by; Poulos (1981, 1982, 1983), Poskitt (1983), Houlsby and Wroth (1983), Parry (1983) and Brown (1984). The conclusions are varied and must reflect the difficulty of interpretation in such deposits.

The design of piles in cemented strata appears to be based more on local experience and judgement rather than on geotechnical theory. However, literature reports are available for drilled and grouted piles, Fuller (1979), Settgast (1980) and Abbs and Needham (1985). Also the design of socketed piles in weak rock is theoretically well advanced, Williams et al. (1980) provide a good summary, and here the trend is towards "rock mechanics" type solutions.

Bearing in mind the limited knowledge of pile behaviour in uncemented and cemented strata, the added effect of strata thickness introduces additional complexities and doubt to the solutions. It is the aim of this research to identify appropriate solutions for such layered problems.

Possible failure mechanisms for a layered system include punch through, flexural or indentation failure mechanisms. It is not proposed to start with a discussion of such mechanisms but to present the test results and then apply appropriate theories to the actual mechanisms identified.

1.6 Summary

In this chapter the background to the research has been discussed. It was necessary to discuss the sedimentology of calcareous soils as they present a relatively new material to the geotechnical engineer. The review has highlighted some of the fundamental characteristics applicable to calcareous soils, and how such characteristics are transformed into design concepts by the use of model tests and applied research. A brief review of relevant engineering practice was presented, reflecting the present indefinite state of design methods for calcareous soils.

CHAPTER 2 CALCAREOUS SOILS USED FOR MODEL TESTS

2.1 Carbonate sand

The previous chapter has illustrated the unique nature of calcareous soils in terms of their physical and mechanical characteristics. These special characteristics preclude the use of fabricated calcareous soils such as crushed chalk or limestone. It was therefore considered essential to obtain 'real' calcareous materials. It is unfortunately not economically possible to obtain a sufficiently large amount of calcareous material from an offshore site where in-situ investigations have been carried out, therefore a real surrogate material was required. The material had to exhibit the essential characteristics of the in-situ materials observed, and be able to be obtained economically and in bulk quantity.

In view of the vast amount of geotechnical data obtained for the North Rankin site in Western Australia, it was considered prudent to try and produce materials comparable with those of the North Rankin site. However, no samples were available for examination, therefore, the site information was based on the Dames and Moore (1974) and Fugro (1978) foundation investigations, together with the analysis of sea bottom sediments performed by Woodside Petroleum Development Pty. Ltd (1979). This included petrological examination of thin sections using scanning electron microscope techniques (SEM), washed sample descriptions, and paleoecology.

Details of these studies are discussed by Evans (1985), and in terms of the terminology introduced in Chapter 1 the deposits can simply be classified as 'FORAMOL' type, with limited algae, and an abundance of benthonic deposits, particularly foraminifera, and exhibiting varying degrees of cementation.

Calcium carbonate content was generally in excess of 90%, and grain size distribution tended from silty sand for the uncemented deposits to fine/medium sand for the cemented deposits. It was decided to search for an uncemented carbonate sand, and then investigate controlled laboratory cementation to produce indurated samples of known and repeatable strength properties, rather than try to identify field cemented samples.

The fact that the North Rankin deposits tend to the 'FORAMOL' type grain association fortunately allows consideration of the northern hemisphere carbonates. In order to assess the compatibility of any sand type the following criteria were applied:-

(i) Calcium carbonate content - must be of the order of 90% (evaluation of this property is discussed in Chapter 3).

(ii) Particle size distribution - the sand must be of fine gradation, $D_{50} < 0.5$ mm.

(iii) The micro-organism compilation must be of a similar nature to that of North Rankin.

Within an economically viable circumference, the following [illegible] were considered, and samples obtained for evaluation where possible.

(a) Brittany, France - Nauroy and Le Tirant (1983) carried out [illegible] in calcareous soils. They were contacted and it was confirmed that the sand types used were readily accessible beach and quarry deposits from the Northern Brittany region.

(b) Falmouth Bay, Cornwall - certain types of carbonate deposits [illegible] fertilizers, and via the Ministry of Agriculture Fisheries [illegible] was established that a Cornish firm, 'Cornish Calcified Seaweed [illegible]', dredged such carbonate deposits from Falmouth Bay, and samples obtained

(c) Dogs Bay, Connemara, W. Ireland - extensive research on the sedimentology of carbonate deposits of the Connemara region had been carried out at Reading University, [Buller (1969), Scott (1970), Gunatilaka (1972), Bosence (1976)]. Dr. Bosence, now at Goldsmith College, University of London, is continuing this study and was able to relate accurately the various sand types of the region, and provide a sample of Dogs Bay sand.

(d) Red Crag complex, Suffolk - details were established of this complex, Boatman (1976), the site visited and samples taken.

The sands were tested, and the compatibility criteria established, the results of which are summarized in Table 2.1.

Table 2.1

Sand Type	Test			
	$CaCO_3$	Grade	D_{50}(mm)	Micro Organisms
Brittany	90	Coarse	0.8	Shelly (Bryozoan)
Falmouth Bay	95	Medium	0.5	Algal
Dogs Bay	90	Fine	0.2	Mollusc, Forams
Red Crag	50	Medium	0.4	Shelly sand

The Dogs Bay material was chosen as the surrogate carbonate sand.

2.1.1 Dogs Bay, Connemara, W. Ireland

Extensive deposits of present day shallow-water biogenic carbonate sediments occur along the Connemara coast on the Atlantic seaboard of Western Ireland (Figure 2.1). Patch sands, shells and gravels occur in exposed areas, extensive spreads of sand occur in less exposed areas and muds are found in the shelter of islands, headlands and narrow inlets (Figure 2.2).

In order for the carbonate deposits to exist there must be as little admixed terrigenous clastic sediment as possible and the rate of carbonate sedimentation must be greater than the accumulation of terrigenous material (i.e. dilution by clastics should be small). For the Connemara coastline the rocks are mainly metamorphic and igneous, relief is low and there are no major rivers. Thus, the hard coastal rocks provide little or no clastic detritus, and riverine contributions are slight. Some Pleistocene glacial boulder clays outcrop along the coast, and although many are being actively eroded by the sea, their clastic contribution attains only local, rather than regional dominance, and certainly have no major input into Dogs Bay (Plates 2.1 to 2.3).

The degree of shelter provided by the coastline is reflected in the grain size and biogenic composition of the sediments. The sediments in the exposed area contain much coarse barnacle and mollusc detritus, where as in more protected areas such as that of Dogs Bay the fine sands contain smaller and lighter biogenic components (ex. Foraminifera, echinoderm, and bryozoan fragments). The beach at Dogs Bay is some 400m long and backed by dunes 5-10m high. A slight platform is created at the high tide mark, with some evidence of cementation. The beach drops gently away from the dunes into a calm protected bay (Plate 2.2).

Permission to remove sand was obtained from the Irish Agricultural Department, and 2.5 tonnes were transported to the Oxford Soil Mechanics laboratory in January 1985. The sand gradation varied across the beach, with the finer material being extracted from the location shown in Plate 2.2

2.2 Cemented carbonate sand

Some aspects of the diagenetic and lithification process have been presented in Chapter 1. The main interest is that of cementation, which is seen as a process by which calcium carbonate precipitates in the form of an interparticle cement, bonding the sand into a cemented mass. The true nature and control of this precipitation is not yet understood fully by sedimentologists, and is the subject of research.

Present areas of research are looking at the physico-chemical processes which control diagenesis and involve variable parameters of pressure, temperature and time. In a geotechnical context Poulos et al. (1987) made some attempts to promote cementation of a carbonate sand by leaving samples in the oedometer under stress in the presence of;

(i) a supersaturated solution of calcium carbonate for a period of ten weeks,

(ii) a lime rich solution for four weeks,

(iii) the sample was mixed with 6% cement and left under stress for four weeks.

Only the cement treated sample showed signs of cementation.

Also Ertec Western Inc.(1983) used 0.5 to 2 % ordinary portland cement mixed with carbonate sand and water, and cured for 3 to 7 days to produce weakly cemented samples.

Therefore, in order to produce controlled, consistent and repeatable cemented carbonate sand strengths, in a timescale suitable for this geotechnical study the material was formulated on the basis of mixing the carbonate sand with a cementing agent to promote artificial cementation. A number of criteria was established for this cementing agent:

(i) the amount of cement introduced into the soil matrix would be comparable to in-situ values (5-50%) i.e. to give similar porosity,

(ii) the strength and deformation properties of the cemented material formed must be similar to that of the in-situ material,

(iii) rapid curing to enable testing in the shortest possible time,

(iv) good workability to facilitate placement and production of high quality models.

Stimpson (1970), Barton (1970) and Sabins and White (1967) have discussed a number of materials used in rock mechanics studies, leading to a number of possible cementing agents being investigated i.e. portland cement, engineering plasters and casting plasters.

The process of sample preparation simply involved the dry mixing of controlled quantities of carbonate sand and cementing agent, and when thoroughly mixed introducing a specific amount of water and remixing. The fluid mix can then be introduced into a sample former and cured for a defined period to produce a cemented material of specified strength.

Portland cements were found to take between seven and fourteen days to develop the correct strength characteristics, whereas suitable strengths could be achieved in twenty four hours using gypsum based plasters. A number of laboratory tests resulted in the choice of a fine casting plaster as the cementing agent. Specific details of the laboratory preparation and strength and calibration tests are discussed in Chapter 3.

CHAPTER 3 STANDARD TESTING OF CALCAREOUS SOILS

3.1 Introduction

Standard laboratory tests and special tests have been conducted on the carbonate sand and cemented carbonate sand. Although it is accepted that the fundamental behaviour of such materials is not understood fully, it was not intended to carry out a full investigation of the strength and deformation properties of the materials, but merely to characterize the materials used, and evaluate the parameters required for subsequent analysis of the main test results. The laboratory tests have therefore been carried out within the limits of the available equipment, and only with materials and test parameters relevant to the main test series.

3.2 Carbonate Sand

3.2.1 Grain size distribution

The grain size distribution has been determined using the standard 'dry method', and is illustrated in Figure 3.1. The material is classified as a fine sand with a D_{50} value of 0.2 mm, and a coefficient of uniformity of 1.9.

3.2.2 Carbonate content

The methods of determining calcium carbonate content have been reviewed by Chaney et al. (1982). Based on this review the acid-soluble weight loss

method was carried out giving a calcium carbonate content varying from 88% to 94%.

3.2.3 Specific gravity

The specific gravity was determined using the pycnometer method. An average value of 2.60 was obtained and has been used in subsequent analyses.

3.2.4 Particle characteristics

An optical microscope and a scanning electron microscope were used to study grain shape and characteristics, and a selection of photomicrographs are presented as Plates 3.1 to 3.3. These illustrate the variable nature of the fossil fragments which constitute the grains, ranging in shape from angular to well rounded. The grains are clearly skeletal remains (tests) of biogenic populations, with the main contributors being the mollusc and foraminifera groups, with some coral and algae present. The mollusc fragments are mostly platey and include large curved shell pieces (bivalves) and some gastropod cones and rods. The foraminifera grains are well rounded fragments and complete spherical shells, and where fractured illustrate the thin walled nature of the shells and the occurrence of intraparticle voids.

3.2.5 Principal mineralogy

To determine the principal mineralogy, X-ray diffraction analysis was performed on the carbonate sand. This has shown the principal minerals to be

high magnesium calcite (foraminifera grains) and aragonite (mollusc grains), with the non carbonate grains being quartz, feldspar, and zircon.

3.2.6 Specific volume

An important aspect of the project was the use of realistic material properties in the laboratory, and modelling of the density (and hence the void ratio) of the carbonate sand was of prime importance. The aim was to produce a sand sample in a test chamber of consistent and known density. Sand pouring techniques were therefore investigated. Cole (1967) reviews the techniques that had been implemented in tests involving silica sand, in which raining techniques were found to produce the most uniform samples, with aperture size and fall height being primary controls.

Comparative tests incorporating aperture (% free area) and fall height variables, and using the carbonate sand and a similarly sized silica sand illustrated that carbonate sand does not conform to the criteria established for silica sand. It was possible to obtain only two consistent and repeatable states for the carbonate sand, 'loose' and 'dense'. The 'loose' state was achieved by carefully hand placing the sand into the test chamber in a consistent manner to achieve a unit weight of 9.3 kN/m^3 ($e = 1.70$). The 'dense' state was achieved by pouring the sand into the test chamber via a discharge hopper and then densifying the sand by the controlled use of vibration, both in the sand and on the chamber walls (vibration was chosen in preference to direct compaction to avoid the possible crushing effect of direct compaction on the soft carbonate grains). This process produced a consistent sample unit weight of 10.9 kN/m^3 ($e = 1.34$).

The 'loose' state was chosen as the set up state for the test samples, as the sample compression experienced upon application of the confining stress (10%) would result in a test sample of acceptable properties. Also preliminary tests carried out by jacking a model pile into a stressed sample produced bearing stresses comparable with field cone resistance values for samples in a 'loose' state. All subsequent tests were carried out with the carbonate sand in this state.

3.2.7 Direct shear tests

A series of direct shear tests was performed on dry carbonate sand (set up in a 'loose' state) in a standard 60 x 60 x 35 mm shear box. The results are presented in standard shear stress/shear displacement format in Figure 3.2. The test at a normal stress of 114 kPa showed peculiar characteristics and was therefore repeated, giving similar results. Some interesting characteristics are evident, namely the plateau which appears to be developed at a shear displacement of 0.8 mm, and seems to be dependent on the magnitude of normal stress.

Such results are consistent with ring shear tests performed by Fugro (1981) on the North Rankin sediments, and presented in a similar format in Figure 3.3.

If the shear stress is normalised by dividing by the normal stress and plotted against the shear displacement, as shown in Figure 3.4, a unique stress ratio is established for tests with normal stress above 114 kPa. This ratio is equal to tan ϕ as shown in Figure 3.4 ($\phi = 34^{o}$). A normal stress of 114 kPa therefore seems to represent the division between two characteristic modes of behaviour, additional evidence being provided by Figure 3.5, which

shows the sand tending towards dilatant behaviour for normal stresses less than 114 kPa.

Figure 3.6 shows the maximum shear stress for various normal stresses compared to the range of results for the North Rankin material. Consistent properties are evident.

3.2.8 Oedometer tests

Dry oedometer tests were performed on 'loose' and 'dense' samples, and the resulting void ratio-vertical pressure plots are shown in Figure 3.7. Load increments were applied when sample compression had stopped, and this was generally of the order of five minutes.

Compression indices (C_c) of 0.78 and 0.70 were obtained for the 'loose' and 'dense' samples respectfully, and these are comparable with those quoted by Fugro (1981) for the North Rankin sediments. The apparent pre-consolidation pressures (which must in some way relate to the crushing of the sand) are 1.05 MPa (loose) and 1.55 MPa (dense). The unloading part of the curve illustrates that the sample has undergone permanent deformation, and represent volumetric strains of the order of 30%.

The samples were sieved after testing to assess the extent of particle crushing. When defined in terms of Datta et al.'s (1979) crushing coefficient values of 4.2 and 3.5 were obtained for the 'loose' and 'dense' samples. These values are consistent with those quoted by Datta when extrapolated to the appropriate vertical stress.

3.2.9 Triaxial tests

A series of unconsolidated drained triaxial tests were performed on dry samples, set up in a 'loose' state. Samples were tested at three confining pressures and the results are presented in Figure 3.8 as a plot of deviator stress against axial strain. Figure 3.9 represents a diagram of deviator stress (q) against mean principal stress (p) and illustrates the difficulty in interpreting strength parameters from the results. The curvature of the illustrated envelope representing the effects of confining pressure and crushing.

However, since an attempt must be made at property characterization to allow subsequent analysis, and in the absence of a clearly defined failure point, parameters have been evaluated at 10% axial strain. If the angle of shearing resistance defined at this point on the q-p plot is evaluated a relationship of the form,

$$\phi = 131 \left(\frac{p'}{p_a} \right)^{-0.61} \qquad \ldots\ldots (3.1)$$

is established, where, ϕ = angle of shearing resistance (degree s), p′ = mean principal stress and p_a = atmospheric pressure. The drained Youngs modulus E' may also be evaluated in terms of the mean principal stress, and when defined in terms of a secant modulus at 10% axial strain,

$$\left(\frac{E'_{1o}}{p_a} \right) = 4.90 \left(\frac{p'}{p_a} \right)^{0.44} \qquad \ldots\ldots (3.2)$$

and in terms of the initial tangent modulus,

$$\left(\frac{E_i'}{p_a}\right) = 182.87 \left(\frac{p'}{p_a}\right)^{0.73} \quad \ldots\ldots (3.3)$$

These values are of a similar range to those obtained by Poulos et al. (1982). The samples showed increasing particle degradation with increasing confining stress, and when defined in terms of Datta et al.'s (1979) crushing coefficient, values ranged from 1.8 to 2.5.

3.3 Cemented Carbonate Sand

3.3.1 Characteristics and calibration

It was stated in Chapter 2 that a fine casting plaster was chosen as the artificial cementing agent, and the cemented material formed required characterisation and calibration against the real North Rankin soils. At the time of the calibration process results from a series of uniaxial compressive strength tests were available and there were a number of important features to be modelled: peak strengths (σ_{fc}) in the range 0 - 5 MPa, initial tangent moduli E_i in the range $E_i = 60\sigma_{fc}$, and the brittle strain softening nature of the stress-strain curve. The tests were performed at comparable moisture contents (approx. 25%). Following a number of trial mixes and testing series three materials were selected and have been termed weak, medium, and strong, with mix proportions and strengths as shown below.

Composition: Material →	Weak	Medium	Strong
plaster/carbonate sand ratio (by wt.)	0.3	0.4	0.6
water/plaster ratio (by wt.)	1.8	1.5	1.1
Uniaxial compressive strength σ_{fc} (MPa)	0.65	1.5	4.0

The mixing technique was:-

(i) Weigh out required quantity of carbonate sand, plaster and water.

(ii) Dry mix plaster and sand to consistent appearance (approx. 2 minutes).

(iii) Introduce water and quickly mix to uniform texture (approx. 2 minutes).

(iv) Introduce fluid mixture into former of required shape.

(v) Cure samples in a controlled manner (i.e. constant temperature for specified time period).

In this way samples of a variety of shapes could be made, for example triaxial sized samples 38 mm diameter by 76 mm long, oedometer samples 70 mm diameter by 20 mm thick, or larger samples for the main test series 200 mm diameter by 80 mm thick. It was important that whatever the sample size it should possess a known and consistent strength. Considering the results of Johnston and Chiu (1984) based on strength tests of a weak mudstone at different moisture contents, the moisture content would appear to be an important control on strength. Therefore, whatever the size of sample, wherever possible a consistent moisture content was maintained. This resulted in different types of tests being performed after specified periods of curing. Details will be discussed in section 3.3.6.

The cemented material will be referred to as 'weak', 'medium' or 'strong'. Photomicrographs of the fabric of the cemented material are shown in Plates 3.4 and 3.5, and illustrate the nature of the interparticle cementing.

3.3.2 Uniaxial unconfined compressive strength

Uniaxial unconfined compressive strengths were evaluated for the three material types, 'weak', 'medium' and 'strong' from 38 mm diameter by 76 mm long samples (L/D = 2). The samples were tested in a conventional displacement controlled testing machine at a rate of 0.5% axial strain per

minute. The values quoted in section 3.3.1 are mean values based on a number of tests carried out for the calibration exercise and during the course of the main test series. Typical stress-strain plots for the three materials are illustrated in Figure 3.10, and show the brittle strain softening nature of the failure, with increasing initial tangent modulus with strength and decreasing failure strain with strength. Inclined shear planes formed the failure mode for all tests, with negligible end effects.

The variation of the initial tangent modulus (E_i) with strength is shown in Figure 3.11. Also plotted is the North Rankin relationship $E_i = 60\ \sigma_{fc}$ and the relationship for similar material from the Zakuum and Umm Shaif fields, Abu Dhabi $E_i = 290\ \sigma_{fc}$, reported by Dames & Moore (1982). It is noted that the moduli values are above the North Rankin values, but below the Zakuum and Umm Shaif values and therefore considered acceptable. The relationship can be represented by:-

$$\left(\frac{E_i}{p_a}\right) = 66.2 \left(\frac{\sigma_{fc}}{p_a}\right)^{1.29} \qquad \ldots\ldots (3.4)$$

where E_i is the initial tangent modulus, σ_{fc} the uniaxial compressive strength and p_a atmospheric pressure.

3.3.3 Rod Index Tests (RIT)

The details of the rod index test have been previously presented in section 1.4. The test was established as the strength criterion for the North Rankin calcarenites due to the inconsistency of results from the uniaxial compressive strength tests. It is accepted that the RIT is not a universally used classification test, but due to the unique nature of calcareous soils new techniques for their classification will evolve and therefore it was

considered beneficial to calibrate the artificial material using such new techniques.

The method of testing was similar to that described in section 1.4 with the following exceptions. A sample was directly cast into an 88 mm diameter by 130 mm long UPVC pipe, the pipe was cut down the side to facilitate removal of the sample after testing. During the test three jubilee clips were fixed around the diameter of the pipe to provide constraint and simulate an uncut pipe.

Typical results for the 'weak', 'medium' and 'strong' materials are shown in Figure 3.12, together with comparative North Rankin results from Jewell (1985a). The artificial material shows similar features to naturally cemented sediments. The compression zones revealed by splitting the samples after the test identified two distinct mechanisms, a spherical bulb for the 'weak' material and a restricted elongated bulb with shear cracks for the 'strong' samples, as shown in Plates 3.6 and 3.7, and comparable with those identified by micro fabric studies of Jewell's tests (Figure 1.13).

The relationship between uniaxial compressive strength and RIT is shown in Figure 3.13. The non linearity of this relationship can be explained by the change of mechanism which occurs from the 'weak' to the 'strong' material. The RIT has been used for the majority of the test series to check strength consistency.

The uniaxial compressive strength (σ_{fc}) - RIT (P_8) relationship can be expressed by:-

$$\left(\frac{P_8}{p_a}\right) = 28.8 \left(\frac{\sigma_{fc}}{p_a}\right)^{0.39} \quad \ldots\ldots (3.5)$$

where p_a = atmospheric pressure.

3.3.4 Tensile Tests

In order to evaluate the tensile strength a number of 'Brazilian' type tensile tests were carried out by loading a sample diametrically to induce tensile failure.

The results are plotted in Figure 3.14 against uniaxial compressive strength (σ_{fc}), and can be defined by the relationship:-

$$\sigma_{ft} = 0.16\ \sigma_{fc} \quad \ldots\ldots (3.6)$$

where σ_{ft} = tensile strength.

3.3.5 Point Load Index Tests

A simplification of uniaxial strength testing which can give a rapid strength index is the point load index test, and is now widely used as a field index test. Good relationships have been established between point load index (I_s) and uniaxial compressive strength (σ_{fc}) for strong rocks; however, its applicability to weak rocks is not so certain, where localised crushing may occur beneath the load points, and this was visible in the tests carried out. Nevertheless, the test has been performed using the conventional point load index test apparatus and the results are presented in Figure 3.15. The relationship can be defined by:-

$$\sigma_{fc} = 11.5\ I_s \qquad \ldots\ldots (3.7)$$

Also plotted on Figure 3.15 are the standard relationship for all rock types suggested by Bieniawski (1974), $\sigma_{fc} = 24I_s$, and the relationship for the Zakuum and Umm Shaif fields carbonate deposits, $\sigma_{fc} = 3.7\ I_s$.

3.3.6 Specific volume

A diverse range of sample sizes has been tested. For the standard laboratory tests sample sizes included 38 mm diameter triaxial samples, 70 mm diameter oedometer samples, 88 mm diameter RIT samples and slabs of approximately 200 mm diameter by 8 to 80 mm thick for the main test series. Obviously these would have significantly different drying characteristics under constant curing conditions. As stated in section 3.3.1 the initial calibration tests were performed at moisture contents comparable to the North Rankin soils (25%). This was therefore considered to be the target moisture content for the majority of the tests, the alternative being to conduct all the tests in a dry state, which would then preclude direct comparison with the available data-base of information on calcareous soils.

A series of 'drying tests' was therefore carried out which monitored the variation of moisture content with time for different sized samples in their particular sample formers. The variation of moisture content throughout samples was also monitored. This exercise resulted in the curing periods shown in Table 3.1 being adopted.

Table 3.1

Sample Size	Curing Period
38 mm diam. x 76 mm (TXL)	48 hours
70 mm diam. x 20 mm (oedometer)	24 hours
88 mm diam. x 130 mm (RIT, Point load index)	48 hours
>200 mm diam. x 8-80 mm (Test layers)	24 hours

This procedure resulted in all tests being performed at comparable moisture contents (25%) and therefore comparable strengths. The resultant material properties are presented in Table 3.2.

Table 3.2

Material Type (classification)	Unit Weight (at test) (kN/m^3)	Void Ratio (-)	Porosity (%)
Weak	15.00	0.7	41
Medium	15.25	0.67	40
Strong	15.50	0.65	39

3.3.7 Oedometer tests

Oedometer tests were performed on the three material types in a dry oedometer cell with the samples loaded up to 6 MPa vertical pressure. Load increments were applied when initial sample compression had appeared to stop, and this was of the order of ten minutes. The resulting void ratio - vertical pressure plot is shown in Figure 3.16, and these should be compared with the North Rankin data presented in Figure 1.10.

The apparent pre-consolidation pressures (as discussed in section 1.3.2) are clearly evident in Figure 3.16, which increase with sample strength and must therefore be related to the degree of cementation of the sample. The three tests illustrate that as the sample strength increases so the initial stiffness will be greater. However, when the cementation strength has been overcome (vertical pressure greater than apparent pre-consolidation pressure) then the 'weak', 'medium' and 'strong' samples have comparable compression indices, C_c = 0.42, representing the behaviour of a crushed sample.

The compression indices and apparent pre-consolidation pressures are comparable with those of the North Rankin sediments as presented in section 1.3.2.

3.3.8 Triaxial tests

In order to investigate the effect of confining pressure on the stress-strain behaviour of the cemented material, a number of unconsolidated drained triaxial tests was performed on the 'weak', 'medium' and 'strong' materials at their test moisture contents (25%) and for confining pressures in the range 0 - 575 kPa. The results are presented in Figures 3.17 to 3.19, and illustrate a number of important features.

There is a clear trend from brittle strain-softening behaviour to ductile and strain hardening behaviour as the confining pressure is increased, with this tendency diminishing with increasing strength. The modes of failure also change from cataclastic shear fractures for the brittle failures to multiple shear planes with plastic deformation (lateral bulging) for the ductile and strain hardening failures. Also the magnitude of the confining pressure has

little influence on the pre-yield behaviour of the materials which show consistent initial moduli for each material type.

A study of rock mechanics literature soon established that this behaviour is typical for rocks tested at elevated confining pressure (Jaeger and Cook, 1969, Hoek and Brown, 1980, Farmer, 1983). However, the majority of rocks require significant confining pressures to induce ductile behaviour in the rock mass. This is not the case for calcareous rocks which are very weak and consequently the confining pressures required to induce ductility are comparable to the in-situ effective stresses for offshore foundation environments. The most comparable data for this brittle to ductile transition is provided by Elliott (1983) who tested a soft high porosity oolitic limestone (Bath stone, uniaxial compressive strength = 23 MPa, void ratio 0.23 - 0.37) at confining pressures in the range 0.4 to 30 MPa. A typical set of results is illustrated in Figure 3.20 and clearly shows similar characteristics to Figures 3.17 to 3.19. A number of workers have quantified a brittle to ductile transition line based on a wide variety of rock types and strengths, Mogi (1966) found the transition for most rocks could be defined by,

$$\sigma_1' = 3.4\sigma_3' \qquad \ldots\ldots (3.8)$$

where σ_1' = axial stress and σ_3' = radial stress. Barton (1976) suggests,

$$\sigma_1' = 3\sigma_3' \qquad \ldots\ldots (3.9)$$

and Elliott and Brown's (1985) results indicate

$$\sigma_1' = 7\sigma_3' \qquad \ldots\ldots (3.10)$$

In order to investigate these relationships the triaxial test results have been plotted as shown in Figure 3.21, where the failures have been classified as brittle (b) or ductile (d). Equation 3.10 provides a reasonable prediction of the division between brittle and ductile behaviour.

These results indicated that any strength criterion developed for application to calcareous material would have to describe both brittle and ductile behaviour. Presently, criteria used in rock mechanics are only applicable to the brittle range and usually take the form of the Mohr-Coulomb criterion or Griffith type criteria ('modified' or 'extended') with the most recent empirically based developments given by Hoek and Brown (1980) and Johnston (1985). Attempts are being made to identify a strength criterion which will encompass ductile behaviour, mainly by the application of the concepts of critical state soil mechanics, but these are not yet well established, Chiu and Johnston (1984), Elliott (1983), Price and Farmer (1981).

It is felt that there is insufficient high quality laboratory test data available to discuss the application of such criteria to the test results, but it is important to observe that brittle and ductile mechanisms can be induced within the cemented materials at moderate stress levels. Such mechanism changes have been observed in the main test series, and are discussed in subsequent chapters. Appropriate strength parameters for the cemented material are derived from these laboratory tests in Chapter 9.

CHAPTER 4 EXPERIMENTAL EQUIPMENT

4.1 The modelling of end bearing capacity

The advantages of model testing have been comprehensively discussed by Bassett (1979), and the use of such techniques is accepted. However, having decided that modelling techniques are to be applied, a number of questions still remains to be addressed. What type of modelling should be performed, should it be in a centrifuge or on a laboratory floor, and how should boundary stresses be controlled? Also, what size of equipment is required, and what should the relative dimension between the model and testing chamber be? These particular questions will be considered for this investigation.

The aim of any model analysis is to achieve complete similarity between model and prototype, and if similarity is not fully achieved then departure must be justified (Ovesen, 1979). If the techniques of dimensional analysis are used to establish a set of similarity requirements, then the results of the analysis will indicate the most appropriate testing technique. Ovesen (1979) sets out a case for the use of a centrifuge to determine the bearing capacity of a circular footing on a dry sand surface; a similar analysis will be presented for the case of a pile in dry sand with particular application to end bearing capacity and calcareous sand.

Figure 4.1 illustrates the independent variables which might influence the end bearing stress - displacement response, with skin friction considered negligible and variation of geostatic stress at the base of the pile neglected order for a deep pile analysis.

The variables can be defined as :

r = radius of pile shaft	ν = Poisson's ratio for sand
q = end bearing stress	$E(G)$ = Young's(Shear) modulus
δ = pile displacement	d_g = average sand grain size
e = void ratio for sand	σ_g = sand grain crushing strength
ϕ = angle of shearing resistance	σ'_H = effective horizontal stress
σ'_V = effective vertical stress	K_o = effective stress ratio

If σ'_V and σ'_H are expressed in terms of the effective mean stress p' and K_o, then the displacement of the pile may be written as a function of the other variables :

$$\delta = f_1(\phi,\ e,\ \nu,\ K_o,\ E,\ q,\ \sigma_g,\ r,\ d_g,\ p') \qquad \ldots\ldots (4.1)$$

The quantities entering the problem have two independent dimensions, length and stress. Following the techniques of dimensional analysis the quantities r and p' are chosen to represent the independent dimensions, leading to nine dimensionless groups,

$$\frac{\delta}{r} = f_2(\phi,\ e,\ \nu,\ K_o,\ \frac{E}{p'},\ \frac{q}{p'},\ \frac{\sigma_g}{p'},\ \frac{d_g}{r}) \qquad \ldots\ldots (4.2)$$

where the displacement ratio (δ/r) is a function of the other eight dimensionless groups. In order to obtain complete similarity the model test must be designed in such a way that the independent dimensionless groups attain the same values for the model and prototype. If a model of scale 1:n is used, with a similar sand to the prototype condition, then similarity requirements can be written as shown in Table 4.1.

Table 4.1

Prototype Scale 1:1	Model 1:n	Similarity Condition
ϕ	ϕ	Similar
e	e	Similar
ν	ν	Similar
K_o	K_o	Similar
E/p'	E/p'	?
q/p'	q/p'	?
σ_g/p'	σ_g/p'	?
d_g/r	$d_g/(r/n)$	Not similar

The unique nature of calcareous soil particles eliminates the possibility of scaling particle size, and for this type of material departure from similitude is considered justified. Therefore, accepting this dissimilarity Table 4.1 shows the importance of attaining similar stress levels (p') in the model and prototype. If this is satisfied then all the remaining groups become similar. One method of achieving such a condition is to use a testing chamber in which boundary stresses can be imposed on the soil sample.

Dimensional analysis has therefore shown that 1g model tests can be performed provided they are carried out in a test chamber capable of applying boundary stresses of similar levels to perceived in-situ stresses.

The scaling factor (n) is another important parameter to determine. Here, the availability of existing laboratory equipment has been influential. A previous research project investigated the ground heave around driven piles in clay (Gue, 1984) using 16 mm diameter model piles and 450 mm sample diameter test chambers. To maximise the use of existing equipment it was considered

The dimension of

beneficial to use similar dimensions. A 16 mm essentially represents a 1:100 scale model of realistic pile diameters, and gives a diameter to mean particle size ratio of 80, well above the scale effect threshold established by Kerisel (1972). However, the majority of offshore piles are open pipe piles, and logically it would seem correct to model these piles as open ended sections with comparable diameter to wall thickness ratios (approximately 30). Applying this criterion to the 16 mm diameter piles results in a wall thickness of approximately 0.5 mm. With a mean particle size of 0.2 mm, this presents a major scaling problem. It was therefore decided that the majority of the tests would be carried out using a solid 16 mm diameter section, but an open ended section would form part of a subsidiary pile type series.

A sample diameter of 450 mm represents a sample to pile diameter ratio of 28. Considering the localised crushing behaviour of the carbonate sand, and likely reduction in lateral stresses during model pile installation (Nauroy and Le Tirant, 1983), this diameter ratio was considered acceptable. Also, stress controlled boundaries would be adopted, with any pressure fluctuations being monitored.

In the previous project (Gue, 1984) the model piles had been installed by using a model 'driving rig'. This was not considered to be the most suitable method for this investigation where it was required continuously to monitor load build up of a pile during installation. A displacement jacking mechanism was therefore chosen to represent pile installation.

The philosophy behind the choice of the main pieces of experimental equipment has been presented, and the mechanical details of these will now be discussed.

4.2 Testing chamber

The two main functions of the test chamber were to provide a means of forming a uniform test sample of defined dimensions, and facilitating the application of predetermined boundary stresses to that sample. A number of chambers exists which perform these functions, mainly in the field of in-situ device calibration, and are commonly referred to as calibration chambers. The Norwegian Geotechnical Institute (NGI) commissioned the construction of a chamber which is now located at Southampton University, and the Italian companies ENEL and ISMES each possess a chamber. Details of these chambers are outlined in the report produced following the 'Calibration Chamber Testing Seminar' held at Southampton University, Last (1984). Also, Dr. Martin Fahey produced such a chamber during his research work at Cambridge on the calibration of the pressuremeter in sand, and details are given in Fahey (1980).

All these chambers show a number of consistent features;

(i) each use flexible rubber membranes to separate the sample from the pressurising fluid,

(ii) vertical stress is applied by pressurising the base of the sample,

(iii) rigid top plates are used.

These details have been successfully proven by producing consistent test results, and were consequently incorporated into the testing chamber design. However, differences in calibration chamber design were evident in the methods of fixing and sealing flexible membranes, and in the type and operation of sample formers. Modifications were therefore made to these details.

The testing chamber designed is conceptually shown in Figure 4.2 and a schematic section is shown in Figure 4.3.

Flexible circumferential and vertical stress boundaries are formed by the use of rubber membranes, and the sample is initially laterally restrained by an internal sample former. The sample former consists of three 5 mm thick 120° perforated segments (Figure 4.4) supported by two push rods per segment which pass through the outer shell of the chamber, and fixed by sealing and adjustment units (Figure 4.5). These units allow the segments to be pushed against the circumferential membrane to form a rigid boundary against which the sample may be formed. By introducing the pressurising fluid into the cavity between the membrane and the outer shell of the chamber, and balancing the hydrostatic and geostatic stresses the segments can be withdrawn from the membrane to create a flexible (stress controlled) boundary with minimum disturbance to the sample.

The flexible membranes were cut from sheets of 1.5 mm thick 'shotblasters rubber'. The circumferential membrane was made by lapping the rubber and sealing with 'Belzona fortified fluid rubber' at the lap joint. The membranes were fixed in position by means of diametric clamping rings as illustrated in Figures 4.6 and 4.7. The sequence of membrane fixing is shown in Plates 4.1 to 4.4.

Figure 4.8 illustrates the top plate showing the 'o' ring seatings to compensate for surface imperfections, and the slot adaptor to maintain a constant aperture to diameter ratio during pile diameter changes.

One input pressure port is provided to the circumferential stress boundary and one to the base stress boundary. Details of the input ports and associated bleed valves are shown in Figures 4.9 and 4.10.

The testing chamber was structurally designed as a pressure vessel with an internal design pressure of 1000 kPa, approximately one and a half times

the proposed maximum working pressure. A non-ferrous alloy, duralumin, was chosen as the manufacturing material because of the ease with which fabricated elements could be handled, and also its good corrosion resistance properties. Due to its size, the chamber was manufactured outside the Department of Engineering Science by Freeland Engineering Ltd., Oxford, with minor modifications being carried out by the soil mechanics laboratory technicians.

4.2.1 Testing chamber pressurisation system

It was decided at an early stage that K_o would constitute an important variable in the parametric study. To facilitate K_o change, two independent pressurisation systems were required, one for the lateral pressure and one for the vertical pressure. In addition to providing these pressures, the system was also required to measure and control such pressures.

The system components are shown schematically in Figure 4.11 and comprise: an oil reservoir (oil being the pressurising fluid), pneumatic pump, pressurised gas supply (oxygen free nitrogen), gas pressure regulator, two gas/oil interfaces (bladder type accumulators), two pressure gauges, various hydraulic control valves and associated hydraulic fittings and hosing

A complete cycle of sample formation and stressing was as follows:-

(i) testing tank empty - close valves (9a), (9b) and (9f to 9i), and connect hydraulic coupling to (10a).

(ii) pump required amount of oil into base pressure bag to form oil base.

(iii) form test sample.

(iv) connect hydraulic coupling to (10b) and pump oil into circumferential bag until full.

(v) close valves (9c) to (9e) and open/close valves (9a)/(9b), pump required amount of oil into accumulators (one at a time, and not required for every test).

(vi) close valves (9a) and (9b), open valves (9c) and (9d).

(vii) charge accumulators with required gas pressure (i.e. just above the test pressures) by means of regulator (2), divertor valve (3) and pressure release valve (4).

(viii) slowly open valves (9f) and (9g) to transfer pressure onto sample

(ix) top up gas pressure to give required lateral and vertical test pressures on pressure gauges (8).

(x) perform test with constant pressures, i.e. stress controlled boundaries.

(xi) after completion of test, release pressure through pressure release valves (4).

(xii) close valves (9f) and (9g) and open valves (9h) and (9i) allowing pressurising fluid to drain back into oil reservoir.

This represents a lengthy description for what in practice was a simple operation.

4.3 Jacking mechanism

Having established that the piles would be installed by a jacking mechanism, criteria were needed on which to base the design. These were defined as follows:-

(a) A slow installation speed was envisaged for the majority of the tests, but it was also considered prudent to have the standard 'in-situ speed' of 20 mm/s available for comparative tests.

(b) The load capacity was difficult to assess initially as no bearing capacity theories could be applied to the problem with confidence, that being a

primary research objective. However, a review of CPT profiles, and some speculative calculations resulted in an upper limit bearing stress of 30 MPa for the proposed cemented layer strengths. This was applied to the solid 16 mm diameter piles giving a design axial thrust of 6 kN.

(c) Positional accuracy was considered important if piles were to be terminated in cemented layers at predetermined penetrations. Therefore, a positional accuracy of 0.5 mm was applied.

(d) If accurate data acquisition techniques were employed then the system must not be suspect to flexural displacements during loading. The system must therefore be rigid enough to restrict such displacements to 0.2 mm at full working load.

Based on the above criteria a number of options were assessed and compared in terms of cost and availability, viz. linear actuators, hydraulic pump/piston, motor (d.c. and stepping) and lead screw. The preferred and adopted system is illustrated in Figure 4.12.

A control box provides the power supply, logic circuits and controls for the 1.8° stepping motor, which is fitted with a 15:1 ratio gearbox to increase torque capacity. The motor drives the shaft of a ball screw which moves at the preset penetration rate (the ball screw and shaft were replaced by a power nut and shaft towards the end of the project due to excessive wear in the ball screw). A load transmission plate was fixed to the ball screw to which the pile could be attached, and was restrained from lateral motion by linear bearings aligned on a shaft parallel to the main screw shaft. Axial thrust generated by the pile is transmitted via the load transmission plate to the main shaft and subsequently into the jacking frame by the thrust and radial bearings located in the shaft housings. Reaction forces are provided by bolting the frame to the top plate of the testing chamber.

The frame was manufactured and the mechanism assembled by the soil mechanics laboratory technicians, duralumin being used wherever possible. A general view of the jacking mechanism and testing chamber is shown in Plate 4.5.

4.4 Model piles

The philosophy of using 16 mm diameter model piles has previously been discussed, and most of the tests have been performed using this diameter. Subsidiary test series have been carried out incorporating open ended and 60° cone tipped sections, together with a series investigating size effect using 8 mm and 32 mm diameter solid section piles.

Figure 4.13 shows details of the model piles used. All were manufactured from duralumin, except the open ended sections which were made from stainless steel tubing. The model piles are illustrated in Plate 4.6.

4.5 Preparation equipment

The preparation of a uniform sand sample and consistent cemented sand samples will be discussed in subsequent chapters, therefore, this section will only discuss the equipment used to form cemented samples of specified shape and thickness.

The cemented samples were pre-cast in the mould shown in Figure 4.14. The thickness of the sample was controlled by the adjustable base plate, and the shape achieved by polystyrene formers. These polystyrene formers consisted of the required number of 6 mm thick ceiling tiles, cut to shape and placed together. During casting a pneumatically driven vibrating unit was attached to the mould frame to help eliminate air voids. Curing was

controlled by maintaining a polythene membrane 50 mm above the surface of the sample for the whole of the curing period (detailed in Chapter 3).

The preparation process consisted of:-

(i) Prepare constituent materials (sand, plaster, water).

(ii) Manually mix materials until consistent texture is achieved (5 minutes).

(iii) Place fluid material into vibrating mould.

(iv) Switch off vibrating unit and level surface with flat edge.

(v) Place polythene curing membrane above sample.

(vi) Cure in temperature controlled laboratory for specified period.

This process proved satisfactory in producing consistent samples. When cured the samples required no special equipment for transportation and placement as the samples possessed sufficient rigidity if carefully handled. The preparation mould is shown in Plate 4.7.

4.6 Instrumentation and data acquisition

4.6.1 Instrumentation

Instrumentation was required to monitor jacking force and pile penetration.

Sangamo 'D95 Series Load Transducers' were used to measure the total jacking force at the pile head, with fixing details as illustrated in Figure 4.15(a). The transducer consists of a one piece Z-beam type body machined from a billet of stainless steel alloy, and employs foil strain gauges bonded into the Z-beam body. In order to maximise accuracy, two capacity ranges were used to cover the varying test conditions, 0 to 2.5 kN and 0 to 10 kN, the fixing detail facilitating easy interchange. For each transducer a 10V d.c.

electrical excitation voltage was applied with full scale output of 30 mV/V being achieved.

Pile penetration was measured by attaching a linear variable differential transformer (LVDT) to the pile head, the LVDT body being supported by a frame fixed to the top of the testing tank, as illustrated in Figure 4.15(b). Depending on the planned penetration, a long stroke (± 200 mm) or short stroke (± 50 mm) LVDT was used. RDP Electronics Ltd. a.c. series transducers were used, Ref. No's D5/8000C, D5/2000, and required a 5V a.c. power supply to give outputs of the order of 0.8 mV/V/0.1 mm.

RDP Electronics Ltd. transducer conditioning units (E307, E307-2) supplied the excitation power supply to the LVDT and load transducer, and allowed signal conditioning to maximise instrumentation accuracy when linked to the data acquisition system.

4.6.2 Data acquisition, storage and processing

Measurement transducers produce d.c. analogue signals as an output. These analogue outputs can either be recorded on x-y or strip chart recorders, or preferably be converted to digital signals and directly recorded to a data file in a microcomputer, allowing instant data storage and easy data transfer and processing. The equipment items required were therefore identified as an analogue to digital converter and a microcomputer, together forming a data acquisition system. A cost budget was defined and certain criteria established for the individual items of the system.

The microcomputer had to have sufficient memory capacity to process data files without extensive shuttling to and from the disk, possess good on-screen graphics capability, be capable of serving as a work station for further

engineering computations, and be able to communicate with other computers in the laboratory and department.

The analogue to digital converter had to be fast enough to sample a signal at least ten times a second, and have at least eight channels. Also, the software accessing and controlling the system had to be a high level language such as Basic or Fortran, requiring no special knowledge of the system architecture or machine language.

An IBM-XT was chosen as the microcomputer, with specifications of: 256 kilobytes of accessible memory with a 10 megabyte Winchester hard disk and one floppy disk drive for data storage, a monochrome monitor with enhanced graphics via a 'Hercules' graphics card, and serial and parallel communication ports.

There is a number of analogue to digital (A/D) converters on the market, with the majority able to satisty the established criteria (which are modest by comparison with other application areas). Metrabyte's DASH-8, 8 channel 12 bit successive approximation A/D converter was chosen. The DASH-8 requires a full scale input of $\pm$ 5 volts to give a resolution of 2.44 millivolts, and required conditioning the transducer outputs to this range. This gave scanning accuracies of 0.1 mm and 0.02 mm for the large and small LVDT and 4.9N (500g) and 1.2N (122g) for the large and small scale load cells. A/D conversion time is quoted at 25 microseconds giving throughputs of up to 30,000 channels per second, resulting in the transducer accuracies being used to control the scanning speed (discussed later). The DASH-8 was fitted on a 'half' slot of the IBM's internal PC Bus, and all transducer signal connections were made through a standard 37 pin 'D' male connector at the rear of the computer.

A schematic diagram of the data acquisition system is shown in Figure 4.16. Utility software was provided which allowed initial set-up, installation and calibration, together with a machine language Input/Output I/O driver for selecting multiplexer channels, setting scan limits, and performing A/D conversions, all accessed via BASIC, using 'CALL' sub-routines.

For all the tests carried out a 'displacement control' program was used in which data capture was initiated by movements of the LVDT, the displacement scanning interval having been pre-programmed. This allowed flexibility in the frequency of data capture, for example where the pile was penetrating a sand layer prior to reaching a cemented layer, data capture may take place at pile penetration intervals of 1.0 mm, but on reaching a penetration of say 200 mm (somewhere near the cemented layer) data capture may take place at pile penetration intervals of 0.2 mm, allowing the load build up to be monitored closely. By simply programming the input of limit displacement at the start of the test a very flexible data acquisition system was created; a flow chart of the program is shown in Figure 4.17.

On completion of a test, the data file created was stored in an appropriate test directory within the hard disk memory of the microcomputer. Further processing either took place locally at the microcomputer, or by the Department's VAX II/780 mainframe computer following data transfer via established communication lines. This system allowed maximum benefit to be taken of proprietary software such as 'Lotus 123' or the 'Ginc' graphics routines which aided considerably the processing of results into meaningful engineering format.

CHAPTER 5 BEARING CAPACITY OF A MODEL PILE IN CARBONATE SAND

5.1 Introduction

Whilst the primary aim of the research programme was to study the failure mechanisms for piles in layered calcareous soils, it was important to establish the bearing response of the model pile in a uniform sample of carbonate sand. This would quantify one of the variables when interpreting the layered test results.

A series of fourteen tests was carried out in the test chamber, with varying confining stress and K_o, and using a 16mm diameter solid section model pile jacked into the test chamber at 0.1mm/s. Details of the tests are given in Table 5.1.

Table 5.1

Test No.	Vertical Stress (kPa)	Ko
D3	50	0.5
S2	100	0.5
S3	200	0.5
S4	300	0.5
S5	400	0.5
D10	500	0.5
S6	25	2.0
S8	50	2.0
S9	100	2.0
S10	150	2.0
S11	200	2.0
S12	250	2.0
S13	100	0.25
S14	400	0.25

5.2 Laboratory tests results and observations

Figure 5.1 shows the set of results for K_o = 0.5, and illustrates the typical features obtained. The results have been presented as bearing stress,

which represents the total force measured at the pile head divided by the end area of the pile (discussed later), plotted against pile penetration in terms of pile diameters. Each of the curves shown represents some 500 data points and is therefore presented as a continuous line plot in preference to a data point plot. The spikes represent points at which the jacking mechanism was stopped and restarted.

The results show that the bearing stress increases up to a penetration of approximately four pile diameters where a steady state is reached, with this steady state bearing stress being dependent on the confining stress. The consistency of the steady state is a good indication of the uniform nature of the sand sample.

On examination of the sample after testing two significant features appeared. Firstly the pile wall was surrounded by an annulus of crushed material, shown in Plate 5.1 and Figure 5.2, and secondly a sphere or bulb of crushed material had formed at the base of the pile (Figure 5.3), which was sufficiently firm to be held in the hand, and crumbled under slight finger pressure. The crushed material was sieved and the particle size found to be < 125 μm.

In order to evaluate the skin friction contribution a number of pull out tests was performed following the jacked-in tests. Figure 5.4 shows the resulting back calculated skin friction-penetration plot from a test carried out at confining stresses 500 kPa vertical and 250 kPa horizontal. A unit shaft friction of the order of 13 kPa is shown, and this is considered negligible by comparison with the end bearing stress (5MPa), hence the bearing stress referred to previously is based on the end bearing area only, as are all subsequent bearing stress calculations. Also, during the pull out tests it was noted that on examination of the sand sample after the test, the hole

formed by withdrawal of the model pile had remained open, i.e. the open hole was able to sustain a lateral stress of up to 250 kPa at the chamber boundary (highest tested value) without collapse. The importance of this behaviour for the skin friction mechanism is discussed in the next section.

For the end bearing response, it would appear from the results that a penetration of four diameters was required to form the crushed bulb at the base of the model pile and hence reach a steady state. However, this penetration distance also includes any effect of the top plate aperture, which is 20 mm compared to the model pile diameter of 16 mm. To isolate these effects a test was carried out with the pile embedded 100 mm into the sample i.e. built into the sample. The result is shown in Figure 5.5, and it can be seen that approximately four diameters of penetration are still required to reach the steady state bearing stress. It is therefore inferred that the aperture effect is small, and four diameters is a true measure of the penetration required to form the crushed bulb.

The test results show the influence of stress level on bearing capacity and also allow isolation of the effects of horizontal and vertical confining stress. The steady state bearing stress is plotted against horizontal confining stress (σ_h), vertical confining stress (σ_v), and mean confining stress ($p = \frac{1}{3}(\sigma_v + 2\sigma_h)$) in Figures 5.6, 5.7 and 5.8 respectively. The horizontal confining stress gives a better correlation with bearing stress than the vertical confining stress, and this has been shown to be the case in test chamber work in other areas, (Houlsby and Hitchman (1987), Jamiolkowski (1986)), but the best correlation is that of mean stress, which virtually eliminates any variation due to K_o. The relationship between steady state bearing stress (q) and mean confining stress may be expressed by:-

$$\left(\frac{q}{p_a}\right) = 37.9 \left(\frac{p}{p_a}\right)^{0.6} \qquad \ldots\ldots (5.1)$$

where p_a = atmospheric pressure

This solution is compared with other available bearing capacity solutions in the next section.

5.3 Interpretation and comparison with design methods

5.3.1 Skin friction

The formation of an annulus of crushed material around the model pile during driving, and the unit skin friction achieved on pull out have already been discussed. It is intended to compare this behaviour with other available data and with current design methodology.

Unit skin friction (τ_s) is conventionally expressed in terms of the normal effective stress (σ'_n) acting on the pile shaft and an interface friction angle (δ) to give:-

$$\tau_s = \sigma'_n \tan\delta \qquad \ldots\ldots (5.2)$$

The normal effective stress is expressed as a multiple K times the effective overburden pressure (σ'_v) and the final expression for skin friction becomes:

$$\tau_s = K\,\sigma'_v \tan\delta = \beta\sigma'_v \qquad \ldots\ldots (5.3)$$

where $\beta = K \tan\delta$

The inclusion of σ'_v in equation 5.3 implies that the skin friction will increase with depth as the effective overburden pressure increases with depth. However, experimental evidence in non-calcareous soil (Vesic, 1967) indicates

that unit values do not increase linearly with depth, but rather the rate of increase reduces with depth. This behaviour has often been represented in design approaches by introducing limit valves. Appropriate values for these limits, and whether true limits are reached in practice, are matters of considerable debate (Randolph, 1985, Kulhawy, 1984). A conventional design in non calcareous soil would incorporate a linear increase in skin friction up to a 'critical depth' or a limit value, and remain constant thereafter. For calcareous soils, where skin friction has been shown to be significantly less than that predicted using data from non-calcareous soil, the current practice is simply to reduce the value of K, δ and τ_{limit} to give results comparable to field values. Such reduced values are reported in McClelland (1974), Angemeer et al. (1973) and Datta et al. (1980). Such an empirical approach is accepted where no data are available to justify a more systematic approach. However, the limited skin friction tests carried out within this study, combined with other experimental observations now available, can provide an alternative approach.

It is important to establish the reason for the low skin friction values; is it a reduction in K resulting in a low effective normal stress, or a reduction in the interface friction angle δ due to extensive particle degradation? Noorany (1985) has investigated the soil-steel frictional behaviour of two calcareous sands, with particular emphasis on the effects of grain crushing on these properties. The results indicate that grain crushing does not appear to reduce the high friction angles (45^{o}) and average soil-steel friction angles (20^{o}) originally measured. This implies that the grain crushing observed for the present tests, and by Ertec (1983) in similar tests, cause a reduction in the effective normal stress σ'_{n} acting on the pile wall. This has also been suggested by Nauroy and Le Tirant (1983) and Dutt and Cheng (1984). Such ideas can be supported by the open-hole observations discussed in section 5.2, and it must be inferred that the annulus of crushed

material formed during the installation process possesses sufficient strength and stiffness to restrict the transfer of lateral stress onto the pile wall, resulting in the low skin friction values observed.

In line with Nauroy and Le Tirant's (1983) observations the unit skin friction was found to increase rapidly before reaching a reasonably constant limit value (approximately 13 kPa), and found to be relatively independent of confining pressure. This limit value is consistent with field observations.

The skin friction pull-out tests were carried out simply to show the limited contribution of skin friction to bearing capacity, but they have also provided some observations pertinent to the understanding of the skin friction mechanism.

5.3.2 End bearing

It is generally accepted (Randolph, 1985, Poulos and Chua, 1985, Kulhawy, 1984) that three principal failure modes may occur beneath a pile; general shear, local shear, and punching shear. At shallow depths an unconfined failure mechanism can occur and the bearing capacity can be computed from Terzaghi's theory for general shear failure (Terzaghi, 1943). At intermediate depths a limited flow mechanism exists close to the pile, confined by external stresses, and solutions may be based on local shear failure mechanisms. At greater depths, the flow mechanism may not occur, leaving a punching form of failure, with the end bearing pressure closely linked to the limit pressure for spherical cavity expansion (Vesic, 1972).

Randolph (1985) states that the transition depth between these various mechanisms will depend on the dilation characteristics of the soil, and thus on relative density and effective stress level, and adds that in loose sands,

where compactive volumetric strains occur during shearing, the 'deep' punching mechanism may occur at relatively shallow depths. Based on the test observations of a crushed bulb of material beneath the pile tip, together with the loose and contractile nature of carbonate sand, the application of Vesic's spherical cavity expansion method will be considered further, together with a local shear failure analysis, and the results compared with those presented in Figure 5.8.

Vesic (1972) calculates the end bearing resistance of driven piles in terms of the ambient stress level, the internal angle of friction for the soil, and the rigidity index, I_r, defined as

$$I_r = G / (p'_o \tan\phi) \qquad \ldots\ldots (5.4)$$

where G is the soil shear modulus and p'_o the ambient (mean) effective stress level. The solutions allow for volumetric compression during plastic shearing of the soil, and are therefore particularly attractive for calcareous soils. As the mean effective stress level increases, the rigidity index of the soil decreases, and there will also be a greater tendency for volumetric compression to occur during plastic shearing. Vesic's work has been extended by Baligh (1976) and Carter et al. (1985), but the solutions presented herein have been based on Vesic's original work, using the relationships presented in Chapter 3 for the variation of friction angle and elastic modulus with confining pressure, and supplemented with volumetric strain data from Poulos and Chua (1985). The results are presented in Figure 5.9.

A local shear failure mechanism has also been evaluated, and uses Vesic's rigidity index concept to provide a rigidity factor for the general shear failure solution, usually represented as

$$q_b = N_q \sigma'_v \quad \ldots\ldots (5.5)$$

where q_b is the end bearing pressure, N_q a bearing capacity factor, and σ'_v the effective overburden pressure.

Kulhawy (1984) discusses this local shear failure mechanism and based on Vesic's (1977) work introduces the term ξq_r as a rigidity factor to give:-

$$q_b = N_q \sigma'_v \xi q_r \quad \ldots\ldots (5.6)$$

The local shear bearing stress has been evaluated as set out in Kulhawy (1984) and the results are presented in Figure 5.9, which indicate that the spherical cavity expansion forms a lower bound solution to the laboratory results. A similar trend was observed by Poulos and Chua (1985) for model footing tests on calcareous sand.

As stated in Section 5.3.1 the conventional design approach is to introduce limited values, and this is the case for end bearing as well as skin friction. The most widely used guidelines are those of the American Petroleum Institute, API RP2A (1984), who make no specific recommendations for calcareous soils, but Dennis and Olson (1983), on who's database of pile load tests the API regulations are based, have proposed some values for calcareous soils, N_q = 8 to 12. Also Datta et al. suggest an N_q of 20 and a limit bearing pressure of 3 MPa, while McClelland (1974) recommends a limit bearing pressure of 4.8 MPa. These results are plotted on Figure 5.9 for comparison (assuming K_o = 0.5).

In the light of the experimental results it would seem best to model the end bearing as a power function of the ambient mean stress.

CHAPTER 6 TESTS ON SINGLE CEMENTED LAYERS

6.1 Introduction

The results of a basic test series which encompassed the extremes of the proposed investigation in terms of layer strengths, layer thicknesses and confining stresses are presented in this chapter. The other sections detailed are developments based on the initial test series, and will be introduced individually.

It is considered beneficial to discuss briefly the general method of sample preparation and the format of the results presented.

Single layer tests consisted of a single cemented layer within a sample of uniform sand. The cemented layer was placed at the mid height of the test chamber by forming first a bottom layer of uniform sand, onto which was placed by hand the preformed cemented layer, having previously levelled the sand surface. Minor adjustments were then made to the cemented layer top surface to maintain level. The distance from the top of the test chamber to the top of the cemented layer was measured and recorded. Sand was uniformly placed on top of the cemented layer to the top of the test chamber. The top plate was fixed, the sample stressed by application of the vertical and lateral confining stresses (following the procedure given in Section 4.2.1). The jacking mechanism and instrumentation were attached and the model pile was brought in contact with the top of the sand surface. The model pile was then jacked into the sample at a rate of 0.1 mm/s, and readings from the load cell at the top of the pile and the displacement transducer were digitally recorded at specified displacements, usually 0.5 mm while penetrating the sand, and 0.2

mm when the pile was within three diameters of the cemented layer (as discussed in section 4.6.2).

Before adopting this procedure a number of preliminary tests was performed to identify and eliminate any potential sources of error. By using thin steel rods attached to the top of the cemented layer the movement of the layer during application of the confining stresses was monitored. A maximum vertical upward movement of 2 mm occurred under maximum confining stress conditions, depths to cemented layers were consequently adjusted to compensate for this effect. The movement of the cemented layer was monitored during pile penetration, and was found to be negligible.

Initially the cemented layers were cast 400 mm in diameter, but after performing some initial tests to identify the extent of the failure zone their diameter was reduced to 250 mm. Comparative tests showed that this diameter reduction had no effect on the load-penetration response.

This study is directed at the drained behaviour, therefore tests were performed at jacking rates slower than 0.1 mm/s to ensure that drained conditions occur. No significant difference in response was noted and 0.1 mm/s has been used for the majority of the tests.

The standard format of the test results is illustrated in Figure 6.1. Pile penetration is represented in terms of pile diameters relative to the top of the cemented layer, which is taken as the datum. The bearing stress represents the jacking force measured at the head of the pile divided by the area of the end of the pile (skin friction having been shown to make a negligible contribution). A continuous profile of bearing stress variation with penetration is shown, and typically consists of 500 data points. Where no cemented layer is present then the response represents the steady state

behaviour for carbonate sand, as previously discussed. Where a cemented layer has been tested then its thickness is represented by an arrow ▲, and the test was usually terminated just after penetration of the base of the sample to allow physical examination of the failure mechanism.

6.2 Results and observations of basic test series

The aim of the basic test series was to identify and categorize the likely failure mechanisms and their controlling parameters. To limit the number of variables the following investigation parameters were adopted. The confining stresses were limited to 'low' (vertical stress 50 kPa) and 'high' (vertical stress 500 kPa), with a K_o value of 0.5 used for all tests. The tests were carried out using the 'weak', 'medium' and 'strong' cemented materials previously defined. Layer thicknesses were 'thin' layer (0.5 pile diameters) an 'intermediate' layer (1.5 diameters) and a 'thick' layer (5.0 pile diameters) in which failure purely in the cemented layer was assumed to prevail (discussed later). Subsequently two tests were performed on layers 3.0 pile diameters thick, and these have been included in this test series. All the tests were performed using a 16 mm diameter solid section model pile (i.e. closed end analogy) and a summary of the tests performed is given in Table 6.1, including the tests on sand alone.

Table 6.1

Test No.	Vertical Stress (kPa)	Ko	Cemented Layer Strength (Classif.)	Cemented Layer Thickness * D (D=pile diam.)
D3	50	0.5	-	-
D10	500	0.5	-	-
D4	50	0.5	Weak	0.5
D6	50	0.5	Weak	1.5
D7	50	0.5	Weak	5.0
D17	500	0.5	Weak	0.5
D16	500	0.5	Weak	1.5
D20	500	0.5	Weak	5.0
F3	50	0.5	Medium	0.5
F5	50	0.5	Medium	1.5
E9	50	0.5	Medium	5.0
F8	500	0.5	Medium	0.5
F11	500	0.5	Medium	1.5
E11	500	0.5	Medium	5.0
D8	50	0.5	Strong	0.5
D9	50	0.5	Strong	1.5
E21	50	0.5	Strong	3.0
D21	50	0.5	Strong	5.0
D18	500	0.5	Strong	0.5
D19	500	0.5	Strong	1.5
F2	500	0.5	Strong	3.0
D26	500	0.5	Strong	5.0

The results are presented in Figures 6.2 to 6.7, where tests with similar strength and confining stress conditions are grouped together, so that each Figure shows several cemented layer thicknesses. Consistent behavioural patterns are evident and also, important mechanism changes are apparent. Figures 6.2 and 6.3 show the results for the 'weak' material at 'low' and 'high' confining stresses, Figures 6.4 and 6.5 the 'medium' material at 'low' and 'high' confining stresses, and Figures 6.6 and 6.7 the 'strong' material at 'low' and 'high' confining stresses.

With the exception of Figure 6.3, which will be discussed later, the results present consistent 'failure' patterns controlled by the thickness of the cemented layer. As the pile penetrates the carbonate sand a steady state bearing stress is achieved, as defined in Chapter 5, and dependent on the confining stress level. However, when the pile is approximately two and a

half diameters from the top of the cemented layer the bearing stress begins to increase i.e. the pile is sensing the cemented layer. The bearing stress continues to increase with penetration, at a rate dictated by the strength of the cemented layer (discussed in section 6.4), until failure occurs. The point at which failure occurs is governed by the thickness of the layer and significantly, occurs above the cemented layer for layers of less than three diameter thickness, i.e. before the pile has penetrated into the layer. This result is consistent with the observations of a bulb of crushed material in the carbonate sand tests, and discussed in Chapter 5.

This behaviour is consistent up to the failure point, the behaviour after failure, or post-peak, is very much controlled by the strength of the cemented sample and the magnitude of the confining stresses. Reference should be made to the triaxial tests carried out on the cemented samples and discussed in Section 3.3.8 of Chapter 3, where it was shown that the magnitude of the confining stress relative to the sample strength dictated the subsequent compression failure mode. This failure mode changing from brittle strain softening behaviour, to ductile strain hardening behaviour. Similar characteristics can be observed in Figures 6.2 to 6.7. Consider Figure 6.6, here the results clearly show a sharp peak and a decreasing post peak response. Figures 6.2, 6.4, 6.5 and 6.7 show various stages of the brittle to ductile transition, and Figure 6.3 clearly shows a ductile strain hardening response which has even masked out the effect of thickness variation. In addition to the characteristics of Figures 6.2 to 6.7 different failure mechanisms are evident on exposure of the underside of the cemented layers after the tests. Plates 6.1 to 6.6 show the failure mechanism for the test results represented in Figures 6.6 and 6.3. The brittle type bearing stress response represented in Figure 6.6 is shown by Plates 6.1 to 6.3, where the three layer thicknesses tested (0.5, 1.5, 5.0 pile diameters) all show consistent patterns of failure i.e. the formation of radial and

circumferential cracks. The results represented in Figure 6.3 are shown in Plates 6.4 to 6.6, and illustrate the plastic flow of the ductile mechanism with no fracture cracks evident (the cracks shown in Plate 6.4 are due to sample extraction). Again the features are consistent for the three layer thicknesses tested (0.5, 1.5, 5.0, pile diameters).

The contrasting mechanisms are schematically illustrated in Figures 6.8 and 6.9 , and show the cone of material formed at the tip of the pile, this cone tending to be more spherical in the case of the ductile mechanism. It was not clear whether this material was from within the cemented layer or perhaps the bulb of crushed sand simply pushed through the cemented layer. In order to clarify this uncertainty a small amount of blue dye was introduced into the water used to manufacture the cemented layer, resulting in a blue coloured cemented layer. A number of tests was carried out using such layers and showed that the cone formed at the tip of the pile was formed from the originally cemented material (i.e. the cone was coloured blue).

After failure the response tends towards the steady state behaviour of the model pile in carbonate sand. The actual mechanisms of failure will be discussed in greater detail in section 6.5.

There is a number of important features highlighted by the basic test series, and further tests discussed in the next sections have been performed to investigate these features.

6.3 Tests on piles embedded at the top of the cemented layer

It was noted in the previous section that where an effect due to thickness was apparent then failure occurred prior to the pile reaching the cemented layer. This has an important effect when considering driven piles, but what of drilled piles, where no crushed materials can form beneath the

pile tip during installation, and the pile is loaded from the top of the foundation stratum? Will the same failure patterns emerge for this case?

In order to investigate the behaviour of drilled piles a series of tests were carried out as detailed in Table 6.2.

Table 6.2

Test No.	Vertical Stress (kPa)	Ko	Cemented Layer Strength (Classif.)	Cemented Layer Thickness * D (D=pile diam.)
E25	50	0.5	Strong	0.5
E24	50	0.5	Strong	1.5
TV18	50	0.5	Strong	3.0
E23	50	0.5	Strong	5.0
E26	500	0.5	Strong	0.5
E17	500	0.5	Strong	1.5
TV11	500	0.5	Strong	3.0
E16	500	0.5	Strong	5.0

The 'strong' material was tested at 'low' and 'high' confining stresses, with tests conducted using cemented layer thicknesses of 0.5, 1.5, 3.0 and 5.0 pile diameters. The analogy with a drilled pile was achieved by embedding the model pile during sample preparation, i.e. the bottom sand stratum was formed, the cemented layer placed in position with the model pile resting directly on top of the layer and restrained from moving while the upper sand stratum was formed. The testing chamber top plate was placed over the protruding model pile and the jacking mechanism attached.

The 'low' confining stress tests are presented in Figure 6.10 and the 'high' confining stress tests in Figure 6.11. Failure patterns are evident, but the importance of the steady state condition of the underlying material (shown as the broken line) is clear.

For the 'low' stress condition (Figure 6.10), the 0.5D (D = pile diameter) layer hardly makes a contribution to bearing stress response, the

1.5D, 3.0D and 5.0D however, all show the brittle peaks at failure before tending towards the steady state stress in the underlying sand. If this steady state is increased (by increasing the confining stresses) then the effect can be seen in Figure 6.11. Now the limit bearing stress is not influenced by the 0.5D or the 1.5D cemented layer, but the limit value for the 3.0D layer has been increased. Quantitatively, the results of Figures 6.10 and 6.11 should be compared with Figures 6.6 and 6.7, and it can be seen that there is a significant difference in peak values of bearing stress and in response characteristics. This comparison of driven and drilled piles raises significant questions with respect to design applications, as does the fact that for the drilled tests, depending on the steady state stress of the underlying weaker material, 'strong' layers of significant thickness do not control limit state calculations. Such considerations will be discussed in greater detail in Chapter 9 - 'Application to Design'.

The one consistent feature between the drilled and driven tests was the observed failure mechanism, with similar characteristics being evident on the underside of the samples after testing. This is expected, as it is the layer strength and confining stress which dictate the failure mode, and these were the same for both sets of tests.

6.4 Behaviour of a pile in an infinitely thick cemented layer

It was originally assumed that a cemented layer five pile diameters thick would be similar in behaviour to an infinitely thick layer, and failure within this layer would not be subject to any effects of thickness. In order to verify this assumption a cemented layer was made eight and a half diameters thick and tested ('weak' strength at 'low' confining stress). The result is shown in Figure 6.12 together with a comparative 5.0D test, previously shown in Figure 6.2. Clearly the results are similar and the peak bearing stress

achieved therefore represents in this case a limit state value for an infinite cemented layer thickness. An important observation is also the point at which departure from this limit state occurs, and this is shown to be when the pile is approximately three and a half diameters from the base of the sample. Therefore, this must represent the extent of the stressed zone within the sample during penetration, the departure occurring as this stressed zone senses the underlying weaker material. If the results for the 5.0D layers in Figures 6.2, and 6.4 to 6.7 are studied it will be seen that this is a consistent feature.

If the limit state value for the 'weak', 'medium' and 'strong' material is quantitatively assessed then an important feature can be observed. By comparing the 5.0D layer results in Figures 6.2 and 6.3, 6.4 and 6.5, 6.6 and 6.7, and 6.10 and 6.11, it can be seen that the peak values are comparable for similar strength material i.e. the confining stress has little or no effect on the limit state value (it should also be noted that the confining stress does significantly affect the results where layer thickness effects occur). In order to investigate this behaviour further a series of tests was carried out as detailed in Table 6.3.

Table 6.3

Test No.	Vertical Stress (kPa)	Ko	Cemented Layer Strength (Classif.)	Cemented Layer Thickness * D (D=pile diam.)
E9	50	0.5	Medium	5.0
E10	250	0.5	Medium	5.0
E11	500	0.5	Medium	5.0
E2	50	0.5	Strong	5.0
E3	250	0.5	Strong	5.0
E4	500	0.5	Strong	5.0
K1	250	0.25	Medium	5.0
K2	250	0.5	Medium	5.0
K3	250	1.0	Medium	5.0
K4	250	2.0	Medium	5.0

Again a 16 mm diameter solid section model pile was used, and 'medium' and 'strong' 5.0D thick cemented layers were tested at three different confining stresses. The effect of varying K_o was studied by testing a 'medium' strength 5.0D layer at K_o values ranging from 0.25 to 2.0, using a maximum confining stress of 250 kPa. The results are presented in Figures 6.13 to 6.15, and show that even though the confining stress controlled the type of failure mechanism i.e. brittle or ductile, it had little effect on the limit state bearing stress. Consequently, variation of K_o also showed little effect.

The limit state bearing stress for the 'strong', 'medium' and 'weak' samples created for this study can be correlated with the Rod Index Test, P_8 stress (section 3.3.3) by the equation:-

$$\left[\frac{q_{cl}}{p_a}\right] = 1.94 \left[\frac{P_8}{p_a}\right] - 34.20 \qquad \ldots\ldots (6.1)$$

where p_a = atmospheric pressure, and for $(P_8 / p_a) > 18$

q_{cl} = cemented layer limit state bearing stress

6.5 Failure mechanisms

From the results presented so far, there is a number of observations which can be made regarding the failure mechanisms for a pile jacked into a single cemented layer within a sand stratum:-

(i) the cemented layer begins to contribute to the bearing stress response when the pile is approximately two and a half diameters above the top of the cemented layer.

(ii) the rate at which the bearing stress increases as the pile approaches the cemented layer is dependent on the strength of the cemented layer and the confining stress level.

(iii) for an infinitely thick cemented layer a limit state bearing stress is reached within the cemented layer, this limit state is reached at a penetration of about half a pile diameter for a pile jacked through a stratum above the cemented layer, and at one and a half diameters for a pile jacked from the top of the cemented layer.

(iv) for a cemented layer of thickness comparable to those previously presented (i.e. 0.5, 1.5, 3.0 pile diameter) then failure may occur prior to this limit state, and before the pile tip has penetrated the cemented layer.

(v) the possible limit state value for a cemented layer is independent of the confining stress state, and is controlled by the strength of the cemented layer.

(vi) the limit state is maintained within a cemented layer until the pile tip is three and a half diameters from the base of the layer, where it responds to a change in underlying material, and for the case of sand, the bearing stress tends towards the steady state stress for the carbonate sand.

(vii) the nature of the failure mechanism has been described as brittle or ductile, and is controlled by the level of the confining stress relative to the cemented layer strength.

In order to supplement this information a number of additional tests was performed, specifically aimed at investigating the failure mechanisms at various stages of their formation. These tests were carried out using a 16 mm diameter solid section pile and are detailed in Table 6.4.

Table 6.4

Test No.	Vertical Stress (kPa)	Ko	Cemented Layer Strength (Classif.)	Cemented Layer Thickness * D (D=pile diam.)
K9	50	0.5	Medium	5.0
K10	50	0.5	Medium	5.0
K5	250	0.5	Medium	5.0
K6	250	0.5	Medium	5.0
K7	250	0.5	Medium	5.0
K8	250	0.5	Medium	5.0

By replacing the cemented layer with a 10 mm thick steel plate an infinitely strong cemented layer was modelled. Tests were carried out at three different confining stress states and provided additional information on the bearing stress increase as the pile tip approaches a layer. The results are presented in Figure 6.16.

Figure 6.17 shows the results of the six tests carried out on medium strength cemented layers, five pile diameters thick and tested at 'low' and 'medium' confining stress levels. For the two tests at 'low' confining stress level, where a brittle type failure occurred, the pile was stopped at penetrations of one and a half and two and a half diameters into the cemented layer. For the tests at 'medium' confining stress level the pile was terminated one and a quarter diameters above the top of the cemented layer, at the layer surface, and one and a half and two and a half diameters into the cemented layer. The mechanisms observed are schematically represented in Figures 6.18 to 6.20.

Figure 6.18 shows the development of the mechanism for a brittle type failure. Figure 6.18(a) shows a section through the cemented layer at failure and it can be seen that the fracture cracks have radiated to the base of the sample and precipitated failure. The punched-out section is shown in Plate

6.7, and is very similar to those observed by Braestrup (1979) who studied punching shear in concrete slabs (further analogies with this work will be discussed in Chapter 9). As penetration continues Figure 6.18(b) shows that the pile indents into the punched out section causing more extensive crack propagation within the section. The final condition on full penetration is shown in Figure 6.18(c) and Plate 6.8, and represents the full indentation of the pile into the punched out section.

For the ductile tests Figure 6.19 shows the mechanism of loading prior to penetration, and before the limit value in the cemented layer has been reached. Zones where the fabric of the cemented material has been modified were identified by close inspection with a hand magnifying glass. Such changes could be readily identified and obviated the need to employ thin section and petrographic techniques. The identification of such zones was particularly important for the ductile mechanisms due to the lack of fracture (shear) cracks. Figure 6.20 shows the continued penetration of the pile into the cemented layer at penetrations of one and a half and two and a half diameters, and full penetration.

The difference between the two deformation mechanisms i.e. brittle and ductile, is clearly apparent, and characterized by the presence of a fracture crack at the boundary between the modified (crushed) and normal soil fabric for the brittle mechanism, and the appearance of significant plastic flow for the ductile mechanism. This behaviour is similar to that described for the Rod Index Tests (section 3.3.3) and detailed in Plates 3.6 and 3.7.

The mechanism formation has been described for a cemented layer thickness sufficient to allow failure to occur within the layer. If the thickness of the layer is reduced, causing failure prior to reaching a limit value for the layer strength, then the mechanism formation is seen as similar to that

described above, with premature failure resulting from the pile tip sensing the bottom of the sample. This behaviour will be quantified in Chapter 9, as will all other quantifiable facets of the behaviour presented in this chapter.

CHAPTER 7 VARIATION OF PILE GEOMETRY

7.1 Introduction

Whilst a case has been presented for using a 16 mm diameter solid section model pile (section 4.1), it was necessary to examine some variations on this geometry by testing different diameter model piles, and varying the nature of the pile type i.e. considering an open ended section or a cone tipped section.

Significant changes in the order of magnitude of controlling parameters should be examined if scale effects are to be studied. However, changes in such parameters can only be achieved within the limits of the available testing equipment. Consequently, a series of tests has been carried out using 8 mm and 32 mm diameter sections.

7.2 Variation of pile diameter

Table 7.1 summarizes the tests carried out using the 8 mm and 32 mm diameter solid section model piles. The tests have been conducted in carbonate sand at various stress levels, and on single cemented layers of a variety of strengths and thicknesses.

Table 7.1

Test No.	Pile Diam	Vertical Stress (kPa)	Ko	Cemented Layer Strength (Classif.)	Cemented Layer Thickness * D (D=pile diam.)
SC1	8	50	0.5	-	-
SC7	8	200	0.5	-	-
SC15	8	500	0.5	-	-
SC6	8	50	0.5	Weak	1.0
SC8	8	50	0.5	Weak	3.0
SC9	8	50	0.5	Weak	5.0
SC5	8	50	0.5	Strong	1.0
SC3	8	50	0.5	Strong	3.0
SC2	8	50	0.5	Strong	10.0
SC4	32	50	0.5	-	-
SC10	32	50	0.5	Weak	0.5
SC11	32	50	0.5	Weak	1.5
SC12	32	50	0.5	Strong	0.5
SC17	32	50	0.5	Strong	1.0

The results of the carbonate sand tests are compared with the results achieved for the 16 mm solid section model pile in Figure 7.1. in which 'steady-state' bearing stress is plotted against mean confining stress. In addition to the good agreement of 'steady-state' values, the relative dimensions of the visible bulb of crushed material formed beneath the advancing pile were also comparable, i.e. one diameter wide and one and a half diameters deep.

The results of the cemented layer tests are shown in Figures 7.2 to 7.5. Figure 7.2 shows the results for the 8 mm diameter pile jacked into 'weak' cemented layers, one, three and five diameters thick at low confining stress level (σ'_v = 50kPa, K_o = 0.5). These results should be compared with Figure 6.2 which represent 16 mm diameter tests carried out within the same limits. Peak bearing stresses and failure patterns were similar for both diameters. Also, the type of failure mechanism was similar i.e. ductile.

Figure 7.3 shows the results for the 8 mm diameter pile jacked into 'strong' cemented layers, one, three and ten diameters thick and again at low confining stress level. These results should now be compared with Figure 6.6 where again similar peak bearing stresses, failure patterns and type of failure mechanism (brittle) were observed. The ten diameter thick cemented layer test provides additional support for the limit state concept of an infinitely thick cemented layer discussed in section 6.4. Previously an eight and a half diameter thick 'weak' layer was tested, within which the bearing stress was shown to reach a limit state, failure being characterized by a ductile type mechanism. The ten diameter thick cemented layer test shown in Figure 7.3 has induced a brittle type failure mechanism, but a limit state bearing stress is still maintained, although the response is more 'peaky'.

Figures 7.4 and 7.5 show the limited number of tests performed using the 32 mm diameter solid section model pile. By making similar comparisons to the results of the basic test series as previously discussed, then consistent features are evident, and the results for the different diameters are comparable.

The results have shown that 8mm, 16mm and 32mm diameter solid section model piles produce similar patterns of behaviour for the stress range and material types tested.

7.3 Variation of pile type

Variation of the pile type was based on a 16mm diameter section, and the pile types considered were an open ended section, and a 60^{o} cone tipped section. The details of these piles have been previously defined in section 4.4, and doubts about the use of an open ended section have been discussed in section 4.1. The tests carried out using these two types of model pile are shown in Table 7.2.

Table 7.2

Test No.	Pile Type	Vertical Stress (kPa)	Ko	Cemented Layer Strength (Classif.)	Cemented Layer Thickness * D (D=pile diam.)
TV6	Open	50	0.5	-	-
TV8	Open	50	0.5	Weak	0.5
TV4	Open	50	0.5	Weak	1.5
TV3	Open	50	0.5	Weak	5.0
TV9	Open	50	0.5	Strong	0.5
TV5	Open	50	0.5	Strong	1.5
TV7	Open	50	0.5	Strong	5.0
TV16	Cone	50	0.5	-	-
TV23	Cone	50	0.5	Weak	0.5
TV20	Cone	50	0.5	Weak	1.5
TV25	Cone	50	0.5	Weak	5.0
TV22	Cone	50	0.5	Strong	0.5
TV21	Cone	50	0.5	Strong	1.5
TV29	Cone	50	0.5	Strong	5.0

7.3.1 Open ended section

The results of the open ended model pile tests are shown in Figures 7.6 and 7.7, where the abscissa has been changed from bearing stress (as shown in previous Figures) to jacking force. This is because of the difficulty in assessing the appropriate bearing area of the open-ended section. The ratio of the end bearing area of the open ended section to the solid section model pile is 12.1%, and in order to determine if this ratio was consistent for the tests carried out a comparison was made with the 16 mm diameter solid section results given in Chapter 6 by Figures 6.2 and 6.6. Direct comparisons which can be made are the steady state value in the carbonate sand and the limit state value in the five diameter thick cemented layer, for which force ratios have been determined and are shown below:-

Force ratio for steady state value in carbonate sand	= 22.9%
Force ratio for limit state value in 'weak' material	= 38.7%
Force ratio for limit state value in 'strong' material	= 25.3%

(Note: contribution of skin friction assumed negligible).

Clearly, the results are inconsistent with the bearing area ratio. Also, the open ended section was observed to remain unplugged during installation in the carbonate sand and partially plugged during installation through the cemented layer. It must be inferred that, as feared, the geometry of the open ended section has resulted in a scale effect problem. However, qualitatively the results do exhibit some consistent features; such as load pick up prior to reaching a cemented layer (for this case two and a half diameters above the top of the cemented layer), thickness effects causing failure prior to penetration of the cemented layer, and the load decrease at two diameters from the base of a 'thick' cemented layer.

No firm conclusions can be made regarding the behaviour of an open ended section model pile.

7.3.2 Cone tipped section

In order to investigate if a change in the shape of the pile tip was significant a number of tests were carried out using a 60° cone tip. This was chosen to consider the implications of using a cone penetrometer in-situ. The results of the tests carried out are shown in Figures 7.8 and 7.9. The solid lines represent the results based on the penetration of the tip of the cone and the broken lines represent the results based on the penetration of the shoulder of the cone. If the 'shoulder' results are compared with the corresponding tests using the 16 mm diameter solid section pile shown in Figures 6.2 and 6.6 it can be seen that there is good qualitative and quantitative agreement. Additionally, it was observed that the bulb of material formed at the base of the model pile had enveloped the cone tip (Figure 7.10). Therefore, apart from the initial penetration of the carbonate sand (where a slight reduction in penetration required to reach steady state was observed - not shown in the Figures) the cone tip has made no change to the bearing stress response, and it is the effective diameter of the cone tip (i.e. 16mm) which has dictated the bearing stress. This behaviour was consistent for the material types and cemented layer thicknesses tested.

CHAPTER 8 TESTS WITH SPECIAL APPLICATIONS

8.1 Introduction

A number of special application tests was carried out either as extensions of the tests discussed previously, such as multiple layer tests and embedded pile tests, or as comparative tests, such as the tests where the pile was installed by driving rather than jacking. A series of tests for comparison with numerical analyses was included. The details and results of such tests are discussed in the following sections.

8.2 Tests on multiple cemented layers

The tests discussed so far have all been performed using single cemented layers placed in a uniform sand stratum i.e. sand above and below. However, in practice this is not usually the case; a more realistic profile contains cemented material of a variety of strengths and thicknesses. Having built up a data base of tests using single cemented layers, and gained an understanding of the dominant behavioural mechanisms, the multiple layer problem was approached, the main aim being to establish if superposition procedures could be applied to multi-layer systems based on single layer tests. The geometries of the multi-layer systems were based on the stratigraphic details of the North Rankin 'A' platform foundations, and it was hoped that the results would provide information relevant to the design of the platform. Details of the tests performed are given in Table 8.1.

Table 8.1

Test No.	Vertical Stress (kPa)	Ko	Cemented Layer Strength (Classif.)	Cemented Layer Thickness ÷ D (D=pile diam.)
E8 (full penetration)	500	0.5	Strong/Weak	1.5/3.5
E18 (full penetration)	50	0.5	Weak/Strong	3.5/1.5
TV17 (penetration from top of cemented layer)	500	0.5	Strong/Weak	0.7/5.0
TV10 (penetration from top of cemented layer)	500	0.5	Strong/Weak	1.5/3.5

Two layers were combined to form a double layer system, this being achieved by casting the cemented layers independently then roughening the contact surfaces and joining the two layers by applying a thin coat of gypsum plaster to the contact surface. This technique proved successful in producing a double layer unit.

Figure 8.1 shows the result for a 'strong' layer one and a half diameters thick overlying a 'weak' layer three and a half diameters thick with the system tested at a high confining stress. The results should be compared with Figures 6.3 and 6.7 in which similar features for the strong layer are clearly evident i.e. 'failure' above the cemented layer, and fall off to the steady state stress of the underlying material, which in this case is that of the carbonate sand. The weak material has therefore had minimal contribution to the bearing stress response. It is perhaps useful to explain this in terms of a step by step account of the load build up.

As the pile approaches the cemented layer an increase in resistance begins to occur at approximately two and a half pile diameters above the cemented layer. This increase is continued until failure of the 'strong' layer occurs, i.e. approximately half a diameter above the cemented layer

(point A on Figure 8.1). Up to this point the behaviour has been similar to that of Figure 6.7. The weak material is now controlling the load response, which tends towards the limit state value of the weak material at high confining stress level (given by Figure 6.3). This is shown by section A-B of Figure 8.1. At point B the pile is three and a half diameters above the base of the weak sample, and from the previous results presented, we should expect a drop off to the steady state of the underlying material, which is represented by section B-C in Figure 8.1.

The sample configuration was then inverted i.e. 'weak' over 'strong' and the confining stress dropped to a low condition to give the result shown in Figure 8.2. As with the previous result the initial behaviour is dictated by the upper cemented layer (in this case of 'weak' strength). The limit state value reached should be compared with that of Figure 6.2, and can be seen to be consistent. When the pile penetration reaches half a diameter the pile tip is within the important three and a half diameters from the base of the weak layer and would be expected to sense the strong layer. However, although some fluctuation of response is noted, the 'strong' layer does not seem to influence significantly the bearing stress until the pile is two and a half diameters from its top surface. The response continues to increase, controlled by the strong layer until the pile tip is just over three diameters from the base of the sample, and this induces failure and a drop off to the steady state stress of the underlying carbonate sand.

Two other tests were performed where the pile was embedded at the top of the cemented layer, and penetration was commenced from this point, as discussed in section 6.3. The results are shown in Figure 8.3 and should be compared with Figure 6.11. It can be seen that the results are comparable, with the 'weak' underlying material not influencing the bearing stress response of the 'strong' layer, but simply providing an underlying limit state

(which is almost indistinguishable from the carbonate sand steady state value).

This section has shown that multiple layers behave in a consistent manner, and that the behaviour of single cemented layers can be used to predict the behaviour of multi-layered systems.

8.3 Test on a pile embedded into a cemented layer

A test was devised to provide an analogy with a full scale 'rock insert' type pile. This was achieved by casting a short section of 16 mm solid section model pile into the cemented layer. When cured this section of model pile was removed, leaving an opening into which a full length model pile could be inserted. A five diameter thick 'strong' cemented layer was manufactured with a 1.5 diameter insert. The cemented layer and embedded model pile were built into a sample in the test chamber and tested at a low confining stress level (σ'_v = 50 kPa, K_o = 0.5). The result of the test is shown in Figure 8.4.

By comparing the results with Figure 6.10 it can be seen that the embedded insert pile behaved in a similar manner to the piles embedded at the top of the cemented layer, indicating that there appears to be no advantage in embedding a pile into a cemented layer (although in practice this may be done to overcome surface weathering or for other reasons).

8.4 Tests on piles installed by a driving rig

A jacking mechanism was used to install the model piles to allow continuous recording of jacking force during penetration. However, as the majority of piles are installed in the field using dynamic techniques it was considered sensible to carry out a number of tests using a dynamic

installation technique. A model pile driving rig has been constructed for a previous project. Details of the driving rig are given by Gue (1984), and essentially the rig provided a mechanism for applying a constant rate of blows to a model pile by dropping a specified weight (hammer) through a controlled drop height. This mechanism was considered adequate to simulate dynamic installation techniques.

The main aim of this comparative series was to investigate if the characteristic features observed for jacking installation would be reproduced during driving installation. These characteristic features were identified as the bulb of crushed material formed beneath the pile tip during installation in carbonate sand, and the mode of failure of a cemented layer during pile penetration.

To investigate the behaviour in carbonate sand two tests were performed. A carbonate sand sample was prepared in the test chamber and stressed to a vertical confining stress of 200 kPa (K_o = 0.5). A 16 mm diameter solid section model pile was dynamically installed into the sample over its full length at approximately 15 blows/diameter (i.e. a steady state was reached), after installation the sample was examined for evidence of a crushed bulb of material beneath the pie tip. A bulb of crushed material was found, but of approximately half the dimensions of that observed for jacked installation. In order to investigate this behaviour further a second test was performed using the same test conditions and the same model pile, but this time the pile was dynamically installed to a penetration of approximately 100 mm, and then jacked from this penetration. The result is shown in Figure 8.6 where it can be seen that a penetration of approximately two diameters is required to reach the steady state bearing stress for the carbonate sand. This should be compared with the four diameters previously identified in section 5.2 for full

formation of the crushed bulb, and indicates that the bulb of crushed material is partially formed during dynamic installation, as previously observed.

To study the behaviour of a cemented layer under dynamic penetration of a model pile, a sample with a one and a half diameter thick 'strong' cemented layer was tested at a vertical confining stress level of 200 kPa ($K_o = 0.5$). The result is shown in Figure 8.7 on which the comparable result for a driven pile in sand only is also shown. It can be seen that a significant increase in blow count is required to penetrate the layer, this value being about four and a half times the result in sand, and this is comparable with the jacked installation results. The failure mode observed was similar to those previously identified, for this strength and confining stress condition a brittle type failure with radial and circumferential cracking of the cemented layer.

From these tests it is inferred that within the limits of the testing equipment similar results would be achieved by using a driving rig to install the piles as have been achieved by using a jacking mechanism for installation.

8.5 Tests for comparison with numerical analyses

As part of the foundation studies for the North Rankin Project emphasis was placed on producing a numerical model of the foundation material. This work was primarily carried out by Fugro B.V. Ltd and is detailed in Fugro (1986). Tests were carried out for comparison with the analysis. To carry out this exercise the laboratory material must be fitted into the strength classification of the North Rankin materials, and this is done in Table 8.2, based on the Rod Index Test (RIT) bearing stress at 8 mm displacement (P_8).

Table 8.2

North Rankin Category	RIT, P_8 (MPa)	Oxford Material (P_8, MPa)
5	>24	
4	16 - 24	
3	12 - 16	'strong' (12.3)
2	8 - 12	'medium' (8.5)
1	<8	'weak' (6.0)

It can be seen that the Oxford material is comparable to the lower strength North Rankin material. However, having identified the strength to confining stress ratio as a major controlling parameter, and for an in-situ vertical effective stress of 910 kPa (130 m below mud line) compared to a maximum vertical confining stress of 500 kPa in the test chamber the strength (RIT) to stress (vertical) ratios are shown in Table 8.3.

Table 8.3

Category	NORTH RANKIN RIT, P_8 (MPa)	P_8/σ_v'	P_8/σ_v'	OXFORD RIT, P_8 (MPa)	Category
5					
	24	26.4	24.6	12.3	'strong'
4					
	16	17.6	17.0	8.5	'medium'
3					
	12	13.2			
2			12.0	6.0	'weak'
	8	8.8			
1					

The physical modelling was therefore based on the following comparison:-

North Rankin Category	5,4	3	2,1
Oxford Category	strong	medium	weak

with a quantitative sealing factor of 0.6 between the strengths and stresses used in the Oxford tests compared to the North Rankin prototype.

The numerical model required the specification of boundary conditions. The problem was considered as axisymmetric with a free vertical boundary placed at a radial distance of three diameters from the centre line of the pile and the material beneath the pile tip terminated at a distance of two diameters by a fixed rough boundary. In order to model such boundary conditions, a container was manufactured to simulate the boundary restraints. The container is shown in Figure 8.8 and Plate 8.1, and provides physical boundaries of the specified dimensions based on a 16 mm model pile, with the free boundary vertical movement modelled by lubricating the inside face of the container, and the rough base created by gluing sand to the bottom face. This container was placed inside the test chamber to carry out the tests, thus imposing a stress boundary on the open top face of the sample through the carbonate sand.

Two numerically modelled cases were tested, representing a 4.5 m diameter belled pile, and a 10.3 m diameter pile group. The North Rankin strength categories used for the numerical model and the comparative Oxford strength categories are shown in Figures 8.9 and 8.10.

For each of the above cases two tests were carried out, one with a sample cast inside the container (the layers prepared directly on top of each other at ten minute intervals) and then tested in the test chamber, and the other with a 200 mm diameter sample of similar layer configurations tested in the test chamber but without the physical restraints of the container. For each, a uniform sand sample was prepared up to mid depth in the chamber, the sample placed in the chamber, the pile placed on the surface of the sample and carbonate sand uniformly placed on top of the sample up to the top of the test

chamber i.e. the pile was embedded at the top of the sample, the sample was stressed and the test carried out to a pile penetration of one diameter. The results of the tests together with the drained finite element analyses (FEA), scaled and unscaled, are shown in Figures 8.11 and 8.12.

Firstly, the numerical analyses and physical test results give broadly comparable loads. There is very little detail to discuss for the finite element analyses, the results simply showing a stiffer response for the stronger stratification of Figures 8.9 and 8.11. For the physical tests the results can be explained in terms of the observations made previously for layer thickness effects.

Remembering that only two diameters of foundation material are considered, based on the results of section 6.3 (Figure 6.11) the upper material would control the initial stiffness with the underlying material controlling the limit state. This can be seen to be the case for the large test samples. By introducing the container, the effect of the lateral stress is reduced, allowing the change from the material strengths to be picked up, with the introduction of the rigid bottom plate causing a continual increase in bearing stress with penetration. These are consistent features for both tests and show that sample thicknesses greater than two diameters should be considered when performing numerical analyses, whilst being imperative for limit analyses; the thickness effect can be seen to affect the results within the 10% working displacement range.

The results from this comparative study have shown that although the bearing stress values are of comparable magnitudes for the numerical and physical experiments, the physical tests have shown greater detail in terms of response characteristics.

CHAPTER 9 APPLICATION TO DESIGN

9.1 Introduction

It is felt that the unique characteristics and behaviour of calcareous soils has been clearly illustrated. However, when faced with such sediments as foundation strata, analyses must be performed. It is therefore the aim of this chapter to compare existing methods of analysis (primarily semi-empirical, and derived for non calcareous soils) with the test results obtained, in order to provide some direction to the design process. It should be clearly stated that the test results can only be applied to a limit state drained bearing capacity analysis, where displacements to limit state may be large and possibly unacceptable for design purposes.

For a pile foundation analysis in layered uncemented and cemented calcareous soils the design process for a single driven pile can be greatly simplified into (i) assessing self weight penetration (ii) assessing driving resistance (iii) calculating bearing capacity for a chosen bearing stratum (assumed to be cemented). Driving resistance is considered to be highly dependent on the equipment used and therefore will not be considered. Other factors are subsequently discussed.

9.2 Bearing Capacity in Layered Strata

9.2.1 Bearing capacity in carbonate sand

Details of the determination of bearing capacity in carbonate sand have been discussed in Chapter 5 where it was shown that skin friction made a negligible contribution to bearing capacity, and end bearing could be

quantified by equation 5.1. This solution may be used not only to determine the end bearing capacity of a pile in carbonate sand, but also to determine self weight penetration during installation.

If a typical offshore pipe pile is considered of 1800 mm diameter and 50 mm wall thickness, 100 m long, for an unplugged analysis the self weight bearing stress is 8.1 MPa. By substitution into equation 5.1 a mean effective stress of 355 kPa is obtained, and for a soil with a K_o value of 0.5 and an effective unit weight of 7kN/m^3, this represents a penetration value of 76 m. This value is not unreasonable for completely uncemented sediments (Offshore Engineer, 1985).

9.2.2 End bearing capacity in cemented layer

Intuitively there is a number of possible mechanisms to consider, and these are sketched in Figure 9.1 (a) to (d). For a relatively thin layer a form of punching shear (a) may occur; however, if this layer is very strong and the underlying material weak then the layer may fail in flexure, with circumferential and radial yield lines prominent (b). For a thick layer then a classical bearing capacity failure may occur beneath the pile tip (c), but for a reasonably strong material with a high porosity, compression and indentation may result beneath the pile tip (d). A primary aim of this research programme has been to verify if such mechanisms occur, and identify controlling parameters in the formation of such failure modes. Only the flexural mechanism (b) can be eliminated immediately as no flexural failures were observed for the range of tests carried out. The other mechanisms will be discussed further.

The problem can be dissected into two areas. Firstly the determination of the bearing capacity for an infinitely thick cemented layer where failure

occurs within the rock mass and is unaffected by the thickness of the layer, and secondly where the layer thickness plays an important role in directing the resultant bearing capacity. This is seen as less than that for an infinitely thick layer and may result from punch through or some other form of mechanism. The bearing capacity for an infinitely thick layer will be discussed first.

The question which comes to mind for the analysis of this problem is should rock mechanics or soil mechanics bearing capacity theory be used? This question has been addressed by Pells and Turner (1980) and Brown (1984) who suggest that there are two major reasons why the standard bearing capacity analyses developed for soils may not be applicable to rock:-

(i) many rocks behave as brittle or strain-softening materials under the stress regimes to which they are submitted under foundations, whereas soils tend to behave plastically.

(ii) the presence of discontinuities (joints, bedding planes etc.) influences the behaviour of the rock mass by providing planes of weakness on which slip may occur preferentially.

The presence of discontinuities has not been observed for cemented calcareous soils and they may therefore be treated as a homogeneous rock mass, and therefore (ii) is not applicable. Based on the results presented in Chapter 3 and Chapter 6 it has been shown that the cemented carbonate sand (being classified as a very soft rock) can behave in both a brittle and ductile manner under the envisaged foundation stress regimes. Soil and rock mechanics bearing capacity theory must therefore be considered. As indicated in Chapter 3, defining strength parameters for the cemented material is extremely difficult, but is essential since such parameters need to be used in bearing capacity analyses.

The material might be expected to show c'-ϕ' characteristics, with the cohesion representing the interparticle cementing and shearing resistance being provided by the crushed particles. Figures 9.2 to 9.4 clearly show that this is not the case, where the 'medium' and 'strong' material should be treated as a $\phi' = 0$ material. Assuming the Mohr-Coulomb failure criterion appropriate parameters have been derived from Figures 9.2 to 9.4, and together with parameters derived in Chapter 3, the cemented materials may be classified as follows:-

'weak' - $\phi' = 23^{\circ}$, $c' = 203$ kPa, $\sigma_{fc} = 0.65$ MPa, $E' = 74$ MPa, $\sigma_{ft} = 0.1$ MPa, $\upsilon = 0.30$

'medium' - $\phi' = 0$, $c' = 0.78$ MPa, $\sigma_{fc} = 1.5$ MPa, $E' = 217$ MPa, $\sigma_{ft} = 0.24$ MPa, $\upsilon = 0.30$

'strong' - $\phi' = 0$, $c' = 2.05$ MPa, $\sigma_{fc} = 4.0$ MPa, $E' = 770$ MPa, $\sigma_{ft} = 0.64$ MPa, $\upsilon = 0.30$

where σ_{fc} = uniaxial crushing strength, and σ_{ft} = uniaxial tensile strength.

As previously stated, both brittle and ductile failure mechanisms have been observed and therefore the three categories of theoretical approach suggested by Pells and Turner (1980) will be considered, i.e.

(i) methods based on plasticity.

(ii) simplified methods allowing for brittleness effects.

(iii) methods based on limiting the bearing stress to a value less than required to initiate fracture.

9.2.2.1 Methods based on plasticity

Bearing capacity analysis for soils make use of the Limit Theorems of Plasticity Theory for finding upper and lower bounds to the true failure load. Based on this approach Pells and Turner (1980) suggest that for rock material, the cohesion term in Terzaghi's bearing capacity formula dominates, reducing the formula to

$$q_u = \sigma_{fc} \frac{N_c}{2\sqrt{N_\phi}} \qquad \ldots\ldots (9.1)$$

where

q_u = ultimate bearing pressure

σ_{fc} = uniaxial compressive strength

N_c = bearing capacity factor (a function of ϕ)

$$N_\phi = \tan^2 (45 + \frac{\phi}{2})$$

Equation (9.1) must be modified by a shape factor, s_c for a circular footing, and a depth factor d_c (Brinch Hansen, 1970). Equation (9.1) becomes

$$q_u = \sigma_{fc} \frac{N_c}{2\sqrt{N_\phi}} s_c d_c \qquad \ldots\ldots (9.2)$$

The results of applying this solution to the 'weak', 'medium' and 'strong' materials are given in Table 9.1 (page 9-11).

Nielsen (1984) defines concrete as a rigid, perfectly plastic material with the modified Coulomb failure criterion as yield condition and deformations governed by the associated flow rule (normality condition), and discusses limit analysis based on concrete plasticity. The theoretical

results achieved have to be modified by an empirical factor, but the application of such concepts has been successful. Of particular interest is the determination of an upper bound solution for the ultimate punching force in concrete slabs (punching shear) originally discussed by Braestrup (1979). Here the shape of the failure surface (shown in Figure 9.5) and the features of the punched out section (Plate 9.1) show remarkable similarity to those achieved during the present tests which were discussed in detail in section 6.5 and classified as brittle type failures, therefore the analysis is considered applicable. Jiang and Shen (1986) have modified the Braestrup-Nielsen solutions for practical use in which the ultimate punching load (P in Figure 9.5) is given by

$$P = (K + 1)\ \sigma'_{ft} s\ h \qquad \ldots\ldots (9.3)$$

where

P = ultimate punching load

s = $(d + h)$

d = diameter of loaded area

h = thickness of slab (taken as 3.5d, this being the thickness at which punch through failure occurred, see section 5.6)

$K = \frac{1}{4}\ [\ m + 2\ (1 - \sqrt{m + 1})]$

m = ratio of compressive to tensile strength

σ'_{ft} = effective tensile strength = $\upsilon_t \sigma_{ft}$

σ_{ft} = uniaxial tensile strength

υ_t = effectiveness factor = $\frac{0.6}{\sqrt{\sigma_{fc}}}$

σ_{fc} = uniaxial compressive strength (MPa)

The results of applying equation (9.3) to the 'weak', 'medium', and 'strong' materials are given in Table 9.1 (it should be noted that the effectiveness

factor has been derived in a similar format to that given by Nielsen (1984) but with the numerator derived for the range of calcareous soil strengths).

9.2.2.2 Simplified methods allowing for brittleness effects

Davis and Booker (1974) have used a simple 'box model' (Figure 9.6) to show that for a frictionless material the bearing capacity is significantly reduced when brittleness is introduced into the material. Based on a series of model footing tests using the 'box model' Pells and Turner (1980) found that at an early stage failure occurred beneath the footing and the material in this zone was crushed (reduced to residual strength), with all cohesion destroyed but with the same angle of friction as the intact material. They proposed a modification to the Simple Bell analysis, Bell (1915), in which the material beneath the footing is at residual strength with no cohesion and friction angle ϕ_r equal to that for the crushed material, giving

$$q_u = \sigma_{fc} N_\phi \qquad \ldots\ldots (9.4)$$

where $N_\phi = \tan^2(45 + \frac{\phi_r}{2})$

with ϕ_r taken as 45° (an explanation for this choice is given later) for the 'weak', 'medium' and 'strong' materials the results of applying equation (9.4) are given in Table 9.1.

As stated, Pells and Turner (1980) found the failure of rock under a footing to be characterized by the formation of a completely crushed zone beneath the footing, either taking the shape of a truncated cylinder or roughly hemispherical. Similar observations had been previously made by Ladanyi (1966, 1967, 1972, 1976) and Ladanyi and Roy (1972), and sketches of the failure modes observed in tests at different depths of embedment are shown

in Figure 9.7. On the basis of such observations Ladanyi proposed that the bearing capacity failure of a deep circular punch in brittle material consists of the following sequence:-

(i) Incipient failure - the stress distribution is elastic and first cracks appear where the failure criterion is satisfied.

(ii) Intermediate phase - a roughly hemispherical zone of crushed rock forms beneath the bearing area. With increasing load, the crushed zone expands radially into the surrounding elastic material causing radial cracks to develop.

(iii) Ultimate failure - horizontal pressure from the crushed zone leads to spalling outside the loaded area.

Ladanyi analyses the intermediate phase using his theory for the expansion of a spherical cavity in an infinite elastic brittle - plastic medium (Ladanyi, 1967). This concept appears particularly attractive in view of the observations made during the test series. Ladanyi's solutions were developed for shallow foundations on very strong rocks, and for the case of zero initial stress in the rock mass. Brown (1984) has used the methods set out by Ladanyi (1967) to develop 'high' ambient stress solutions, and Brown's and Ladanyi's ultimate bearing capacity solutions are presented.

Ladanyi gives an approximate upper bound solution for the ultimate bearing capacity of a foundation on brittle c' - ϕ' rock as,

$$q_u = p_u (1 + \tan \phi_c) + c_c \qquad \ldots\ldots (9.5)$$

where

$$p_u = (\sigma_{fc} + s_c) \left[3\alpha \frac{\sigma_{fc}}{E} + e_{av}\right]^{-a} - S_c \qquad \ldots\ldots (9.6)$$

σ_{fc} = uniaxial compressive strength of the intact rock

$s_c = c \cot \phi_c$ = Coulomb shear strength parameters for the crushed rock

E, υ = Young's modulus and Poisson's ratio of the intact rock

$\alpha = 1 - \frac{1 - \upsilon}{\sqrt{2n}}$

$n = \sigma_{fc}/\sigma_{ft}$

σ_{ft} = tensile strength of intact rock

e_{av} = average volumetric strain (positive for a volume decrease) undergone by the rock in reaching the crushed state

$a = 4 \sin \phi_c / 3(1 + \sin \phi_c)$

Equation (9.6) will apply to equation (9.5) if

$$\frac{p_o}{\sigma_{ft}} < \frac{n}{3} - \frac{3 - \sin \phi'}{3(1 - \sin \phi')} \qquad \text{(9.7)}$$

where p_o = initial lateral stress in the rock

ϕ' = angle of shearing resistance of intact rock

if this is not the case then equation (9.8) will apply to equation (9.5)

$$p_u = (p_o + S_c + \sigma_{fc}F) \left[\frac{3(1 + \upsilon)}{2E} \sigma_{fc}F + e_{av} \right]^{-a} - S_c \qquad \text{(9.8)}$$

where $F = \frac{4}{n + 4} + \frac{2(n - 2)}{n + 4} \cdot \frac{p_o}{\sigma_{fc}}$

There are a number of parameters which must be estimated i.e. c_c, ϕ_c and e_{av}. As discussed in Chapter 5, Noorany (1985) carried out tests on crushed carbonate sand and found no deterioration in the friction angle, so that, the friction angle has been taken as that of carbonate sand and determined from equation (3.1), Chapter 3. The crushed material formed beneath the pile tip for the model tests detailed in Chapter 6 was found to possess a certain amount of inherent strength but could be displaced by moderate finger

pressure, a nominal cohesive strength (c_c) of 100 kPa has therefore been assigned to this material. The volumetric strain to crushing e_{av} is a difficult parameter to quantify; here it is considered that the best estimate can be made from the oedometer tests on the cemented material, where the strain required to cause the change in slope of the e - log p' curve (section 3.3.7) has been taken as e_{av} (range 6.5% to 11.5%).

The results of applying Ladanyi's cavity expansion theory to the 'weak', 'medium' and 'strong' materials are given in Table 9.1 (where p_o has been taken as 0.25 MPa to correspond to the laboratory test conditions).

9.2.2.3 Incipient Fracture Solutions

The incipient fracture theory aims at quantifying the bearing pressure for the start of failure at some point in the material beneath a footing based on the Griffith crack model. It is felt that such a model, which assumes a number of small inherent cracks in the material does not provide a realistic model of the high porosity, soft rock. Also the available solutions do not allow for the influence of depth of embedment or overburden pressure, and are not considered further.

Table 9.1 provides a comparison of the methods of analysis and the model test results, and Figure 9.8 gives a graphical representation of the calculated ultimate bearing capacity as a function of the uniaxial strength.

Table 9.1

Solution/Material q_u	'weak' (MPa)	'medium' (MPa)	'strong' (MPa)
Model Test Results	8.2	13.0	20.8
Plasticity Solutions			
Pells and Turner	5.9	9.7	25.9
Jiang and Shen	8.0	12.7	20.8
Simplified Solutions Allowing for Brittleness Effects			
Modified Bell	3.8	8.7	23.7
Ladanyi's cavity expansion	6.6	12.5	25.5

The results show reasonably good agreement; it can be seen that all theories underestimate the test results for the 'weak' and 'medium' material, and three out of four overestimate for the 'strong' material. It is not considered of advantage to recommend the use of any particular solution for a given case as each of the above solutions can be subjected to theoretical criticism, and all are empirical. It must be emphasized that the most difficult parameters to assign are the strength parameters and it should be noted that the 'medium' and 'strong' cemented materials have not been assigned any frictional resistance in the intact state for the confining stress range used.

Having considered an infinitely thick cemented layer, the question must be addressed, when does layer thickness become important? Before defining critical dimensions based on the model tests carried out, it is perhaps worth reviewing the available literature.

Meyerhof (1976), in association with a number of co-workers (Valsangkar, Sastry, Hanna) has studied the behaviour of foundations in layered soils. Of particular interest are the tests on loose and dense sand. Generally on jacking model piles into layered strata the limits (or controls) defined in Figure 9.9 were established. The bearing stress was found to increase when the pile was three diameters above the dense sand and required ten diameters of penetration to reach the limit bearing capacity in the dense layer. Also, the bearing stress dropped from this limit bearing stress when the pile was ten diameters from the bottom of the dense sample. This would imply that a layer must be greater than 20 diameters not to exhibit a layer effect.

In contrast Hanna (1981) found that surface footings loaded on dense sand overlying loose sand did not sense the underlying loose material when the dense layer was thicker than two footing diameters, though this value is of course dependent on the relative strengths of the two layers.

Meyerhof (1960) studied the bearing capacity of floating ice sheets by field observations and small-scale loading tests. He concluded that if the contact radius (a) is greater than about one-fifth of the thickness of the bearing material (ice sheet), the surface penetration resistance decreases with smaller ratios of h/a until the lower limit of punching resistance is obtained at about a = h.

If a foundation stratum is thought to be suspect to punch through there are two methods of analysis in general use; the punching coefficient method, and the projected area method.

The punching coefficient method is based on the punching theory developed by Meyerhof (1974) for cohesionless soils. The assumptions involved in predicting the ultimate bearing capacity state that at the ultimate load a

soil mass in the upper sand layer, roughly a truncated pyramid in shape, is pushed into the lower sand layer (Figure 9.10). Empirical punching coefficients and shape factors are derived from model tests.

The projected area method, popular in the analysis of jack up rig stability problems, has been derived mainly for the case of sand overlying clay. It also considers that at the ultimate load a soil mass of roughly truncated conical shape is pushed into the underlying deposit, Figure 9.11. However, it is assumed that the applied load is transmitted through a failure zone in the upper layer to a fictitious foundation at the top of the underlying strata. The area of this fictitious foundation is related to the assumed slope of the failure surface in the upper soil layer. Different values of the slope of the failure surface have been proposed.

- Young and Focht (1981) have proposed side slopes of three vertically to one horizontally.
- Jacobsen et al. (1977) propose an empirical equation related to the relative bearing capacities of the upper and lower layers.
- Baglioni et al. (1982) propose that the sides of the failure zone make an angle equal to the angle of shearing resistance of the upper sand layer with the vertical.

The ultimate bearing capacity is then simply computed for the lower stratum using the projected load area and standard bearing capacity theory.

A similar concept has been proposed (McClelland, 1985) for a cemented layer, incorporating a circumferential shear surface, and mobilising the shear resistance on this surface together with the bearing capacity of the underlying material.

Whilst these methods of analysis and controls are considered applicable to surface loading problems, they are not considered applicable to deep foundation problems as they are based on, or incorporate, empirical factors primarily derived from model tests in which the similarity requirements of dimensional analysis are not satisfied. The model tests carried out within this research programme have clearly shown the primary importance of incorporating the confining stress into any form of analysis for layers subject to a thickness effect (controls subsequently defined), so that an empirical prediction model will be derived based on the model tests carried out.

Before dealing directly with the formulation of the empirical prediction model, it should be mentioned that additional techniques are available for determining pile bearing capacity in layered strata. These are based on in-situ testing of the soil profile, and are known as the 'CPT calibration method' determined from a cone penetrometer profile, Fugro (1981) and the 'semi-empirical PLT method' derived from plate load test load-displacement curves, Parry (1978). It is not proposed to discuss the application of these tests.

9.3 The formulation of an empirical prediction model

As previously stated, it is considered more useful to develop empirical solutions based directly on the model test results than to try to apply existing empirical solutions, which have themselves been derived from model tests in which the testing procedure is not entirely satisfactory.

There are two major cases to consider, the pile driven (jacked) through overlying strata into the bearing stratum, and the pile directly loading the bearing stratum (i.e. drilled in place). These cases will be discussed seperately as driven piles and embedded piles, and only refer to closed end sections.

9.3.1 Driven piles

Based on the model tests a number of characteristic features has been observed and these have been discussed in section 6.5, in which a number of controlling parameters was defined. Based on these parameters the following procedure may be used to predict the bearing stress response of a pile jacked into a single cemented layer within a sand stratum.

1. Calculate the mean effective stress at foundation level (σ_m).
2. Calculate the steady state bearing stress in sand stratum (q_s) from equation 5.1.
3. From determined value of uniaxial compressive strength or rod index test 'P_8' stress calculate limit bearing stress for cemented layer (q_{cl}) from equation 6.1.

4. Set up failure envelope, with envelope line running from 2.5 pile diameters above the surface of the cemented layer on the steady state sand bearing stress line to 0.5 pile diameters below the surface of the cemented layer on the limit state bearing stress line of the cemented layer. This constructs the failure envelope for the system, as shown in Figure 9.12.

5. The thickness effects may now be applied. If the cemented layer is less than three pile diameters (D) thick, departure from the failure envelope will occur when the pile has moved a distance below the 2.5D change point (point A on Figure 9.12) equal to the thickness of the cemented layer. If the layer is equal to or thicker than three pile diameters then departure from the failure envelope will occur when the pile tip is 3.5D above the base of the cemented layer.

6. The failure envelope may be completed by a line running from the envelope departure point to the steady state bearing stress for the underlying material at the elevation of the bottom of the cemented layer. The actual closure line will be dependent on the cemented layer strength to confining stress ratio, and may be of a brittle or ductile form.

   Examples are shown in Figures 9.13 and 9.14 for cemented layers of two and eight pile diameters thick.

The controls defined above imply a change of failure mechanism at a cemented layer thickness around three pile diameters. No physical characteristics were observed to support this theory, and further work would be required around these thicknesses to provide additional information. However, it would appear that a minimum thickness of four pile diameters is required to avoid thickness effects and reach a limit state.

This methodology may be applied to multi-layered systems by calculating the appropriate limit state values for the cemented layers above and below the proposed bearing stratum. An example is illustrated in Figure 9.15 for a 'strong' cemented layer, one diameter thick, sandwiched between a 'weak' strength layer above and a 'medium' strength layer below.

The prediction procedure outlined can be programmed into a microcomputer to generate results similar to those previously defined.

9.3.2 Embedded piles

The formulation of a similar procedure for embedded piles is not as clear as for driven piles as the data base is smaller, and tests have only been evaluated at one strength. Therefore, only limited recommendations can be made as no existing solutions are directly applicable to the results (no punch through failures were observed). The following procedure should be carried out.

1. Calculate the mean effective stress at foundation level (σ_m).
2. Calculate the steady state stress, or limit state stress of the underlying material.
3. Construct the failure envelope, with the envelope line running from zero bearing stress to the limit state bearing stress for the cemented layer at a penetration of one and a half diameters. A linear line should not be drawn between these two points, but the line should show increasing curvature, in accordance with values established from rod index tests if they have been carried out (see Figures 6.10 and 6.11).
4. Any layering analysis should be carried out within the established criteria.

5. The failure envelope should be closed as detailed for the driven pile case.

Reference should be made to Figures 6.10 and 6.11 for typical features.

CHAPTER 10 DISCUSSION AND CONCLUSIONS

10.1 Summary discussion of test results and observations

10.1.1 Materials

A satisfactory testing material was found which exhibited the essential characteristics, both in physical properties and engineering behaviour, of calcareous soils. An artificially cemented material was created by using gypsum plaster as a cementing agent, resulting in the production of a material of controlled and repeatable strength and deformation properties.

A limited number of standard laboratory tests has been conducted, primarily to quantify significant engineering parameters and allow comparison with similar parameters observed for other materials.

10.1.2 Experimental equipment

Equipment was developed especially to carry out this investigation. The major item was a stress controlled testing chamber which allowed independent application of a horizontal and vertical confining stress to a test sample; this was necessary to satisfy dimensional analysis modelling criteria, and has played a critical role in understanding the effect of confining stress on the failure mechanisms for layered strata. Model piles of 16 mm diameter were installed into the dry test sample by the use of a displacement controlled jacking mechanism at a displacement rate of 0.1 mm/s. Other items of equipment have been developed to support the experiments.

10.1.3 Bearing capacity in carbonate sand

A number of tests was carried out in which the model pile was jacked into carbonate sand only for a variety of confining stress levels. Consistent observations were observed of an annulus of crushed material around the pile wall and a bulb of crushed material beneath the pile tip. The annulus of crushed material was found to limit the transfer of lateral stress onto the pile wall resulting in low values of skin friction (negligible by comparison with the end bearing stress). A steady state bearing stress was achieved for each confining stress level, and this has been quantified as a power law function of the mean confining stress. The relationship is non-linear and found to increase at a decreasing rate with increase in mean confining stress. Such behaviour has been compared with existing design concepts for skin friction and end bearing in calcareous soils.

10.1.4 Tests on single cemented layers

A series of tests was performed incorporating a variety of cemented layer strengths, thicknesses and confining stress levels. The results indicated consistent failure patterns and modes of behaviour. The importance of cemented layer thickness was identified, and samples with a layer thickness less than four pile diameters were found to be liable to layering effects, where the bearing capacity will not reach the limit state value identified for an infinitely thick cemented layer, and the peak bearing capacity may be achieved prior to the pile penetrating the cemented layer. The limit state value was found to be independent of confining stress level and remained constant throughout a layer until the pile tip was three and a half pile diameters from the base of the layer, at which point the bearing capacity reduced to the value appropriate for the underlying material. The post peak behaviour for all cemented layer thicknesses was found to be dependent on the

strength of the cemented layer relative to the magnitude of the confining stress, and this dictated whether a brittle or ductile type failure mechanism occurred. The brittle mechanism resulted in radial and circumferential cracking at the base of the sample with the ductile mechanism showing a complete absence of cracks and exhibiting significant plastic flow in the penetration area.

The behaviour of a pile loaded directly above the cemented layer surface i.e. an embedded or drilled pile, showed significantly different behaviour from the pile jacked through upper strata, but the final failure mechanisms observed were comparable.

10.1.5 Brittle and ductile behaviour

A general trend from brittle to ductile behaviour for the cemented material under increasing confining stress has been observed, both in the triaxial tests and the bearing capacity tests in the testing chamber. From the limited range of tests carried out it would appear that the transition from brittle to ductile behaviour (ductile being applied in the absence of radial and circumferential cracking) very approximately occurs when the ratio of the uniaxial compressive strength to the mean effective stress falls below 20. The smaller this ratio the more ductile the behaviour, the greater the ratio the more brittle the behaviour. This can be an important guideline in understanding the deformation mechanism of any problem, although it should be emphasized that the limit bearing stress (applicable only to cemented layers greater than four pile diameters) remains unaffected by the confining stress level.

10.1.6 The effect of pile geometry

Tests were carried out to study the effect of changing the pile diameter and the pile type. A limited number of tests was performed using model piles of 8mm and 32mm diameter. The results were found to be quantitatively consistent with the 16mm diameter tests. Two pile types were examined, an open ended pile, and a 60° cone tipped pile. The open ended section remained essentially unplugged during installation through carbonate sand and partially plugged in cemented carbonate sand. It was concluded that the open ended section was subject to a scaling problem due to the thickness of the wall relative to the soil particle size. The cone tipped pile was found to behave in a similar manner to the solid section pile of equivalent diameter, with the bulb of crushed material formed beneath the pile tip, enveloping and masking out the effect of the cone.

10.1.7 Tests with special applications

A number of tests was performed to investigate a variety of application problems. Multiple cemented layers were considered, and it was shown that the principles established for the single layer tests could be successfully applied to multi-layer systems by using superposition techniques. A rock socket simulation was considered and it was found that the thickness beneath the insert controls the bearing capacity response, and therefore there is no embedment effect. Installation by dynamic techniques was considered by the use of a driving rig with which it was shown that similar results could be achieved to those observed for jacked installation. Extensive independent numerical analyses on pile end bearing in layered strata has been performed, similar physical tests were carried out to allow comparison of the two techniques. The results were found to be quantitatively comparable, with the physical tests providing much greater qualitative data.

10.1.8 Application to design

Design considerations have been discussed and existing semi empirical solutions have been compared with the test results. Plasticity solutions and solutions allowing for brittleness effects have been shown to produce consistent results, though the design process is highly dependent on the choice of strength parameters, and this is itself of great difficulty for such materials. No existing solutions were found to simulate the layering effects observed in the model tests, so that, entirely empirical procedures have been developed which allow prediction of pile behaviour in layered strata.

10.2 Recommendations for future work

There remain many unanswered questions concerning pile behaviour in calcareous soils. This project has attempted to identify mechanisms and their controlling parameters and tried to provide direction to the design process. By touching on a number of areas the work has illuminated many possible extensions, where investigations could be more specific. Some of these areas are identified below.

10.2.1 Standard laboratory tests

Only very crude laboratory tests have been performed as part of this project, but these have clearly illustrated the unconventional behaviour of calcareous soils. Perhaps the direct shear results and the triaxial tests on the cemented material are the most striking, and present ample justification for additional work.

10.2.2 Parametric model studies

Apart from moving up a scale with the model study to model piles of the order of 50mm, there are two main areas where progress can be made using the existing equipment. Firstly, the framework of tests performed could be 'filled in' with more tests at intermediate thicknesses, stress levels and strengths, also greater attention could be paid to the mechanism formation and propagation. Secondly, the undrained problem could be tackled. This would involve using a different cementing agent as the gypsum based plaster is susceptible to breakdown on contact with water; however, plasters are available which do not suffer from this problem. A careful study of the dimensional analysis of the problem should be undertaken before attempting to study undrained behaviour under dynamic loading.

10.2.3 Theoretical developments

Before any advance can be made in meaningful theoretical analysis a yield criterion must be developed for cemented calcareous soils which can cope with the full range of behaviour which this material can exhibit i.e. brittle, transitional and ductile with contractile volumetric strains and particle crushing.

10.2.4 Field work

Wherever possible, advantage should be taken of field conditions to verify (or disprove) the observations and inferences made from this series of model tests.

10.3 Main conclusions

The main conclusions from this study can be identified as :-

* Pile skin friction was shown to be minimal in carbonate sand due to the formation of an annulus of crushed material around the pile, and it was inferred that this annulus limits the transfer of lateral stress onto the pile wall resulting in low skin friction values.

* A bulb of crushed material was found to form beneath a closed end model pile jacked into carbonate sand. This resulted in a steady state end bearing stress for a given confining stress. The bearing stress was found to increase at a decreasing rate with increase in confining stress level.

* A self consistent set of results has been achieved for the study of end bearing capacity in layered strata, covering a variety of material strengths, thicknesses and confining stress levels. A critical layer thickness of four pile diameters has been identified, below which layer thickness effects dominated the bearing stress response.

* For layer thicknesses greater than four pile diameters a limit state value was reached which was dependent only on the strength of the cemented layer. Fall off to a weaker sub layer occurred when the pile tip was three and a half diameters from the base of the strong layer.

* For layer thicknesses less than four diameters the peak bearing stress was confining stress dependent, for layer thicknesses more than four diameters the limit state bearing stress was independent of confining stress.

* Driven (jacked) and drilled (embedded) piles showed significantly different peak bearing stresses for consistent material and confining stress properties when layer thickness effects dominated.

* Two consistent failure mechanisms have been observed for all cemented layer thicknesses, classified as brittle and ductile types. Brittle type failures exhibited extensive radial and circumferential cracking on the underside of the layer, and ductile mechanisms showed plastic flow with no evidence of cracking. The transition from brittle to ductile behaviour occurred when the ratio of uniaxial compressive strength (σ_{fc}) to mean confining stress (σ_m) fell below 20.

* Model pile diameters of 8, 16 and 32 mm showed consistent behaviour.

* A 60° cone tipped model pile showed behaviour consistent with a flat ended section of similar diameter.

* Multiple cemented layers behaved as a series of single cemented layers, encouraging the use of superposition techniques for prediction purposes.

* The depth of embedment of a pile in a cemented layer (i.e. socket or insert piles) had little effect on the bearing stress response which was controlled by the thickness of material beneath the embedment.

* Dynamic installation of a pile by a driving rig showed consistent behaviour patterns to jacked installation, and the results achieved by jacked installation are considered applicable when dynamic techniques are used.

* The results obtained by physical modelling, and independent numerical modelling, were consistent for similar strata configurations, with physical modelling providing greater qualitative data.

* Existing semi-empirical solutions have been compared with the test results and were found to be capable of predicting a limit state value for a cemented layer , but unable to predict layering effects. Empirical prediction procedures have been developed which allow both effects to be evaluated.

It is considered that this study has been successful in its intention to provide an understanding of the end bearing capacity of piles in layered calcareous soils, and a number of problems has been addressed However, whilst every effort has been made to satisfy scaling laws, the application of these results to full scale problems should be considered carefully. The use of qualitative concepts is encouraged, but the use of quantitative data should be approached with caution until field verification can be obtained.

FIGURES

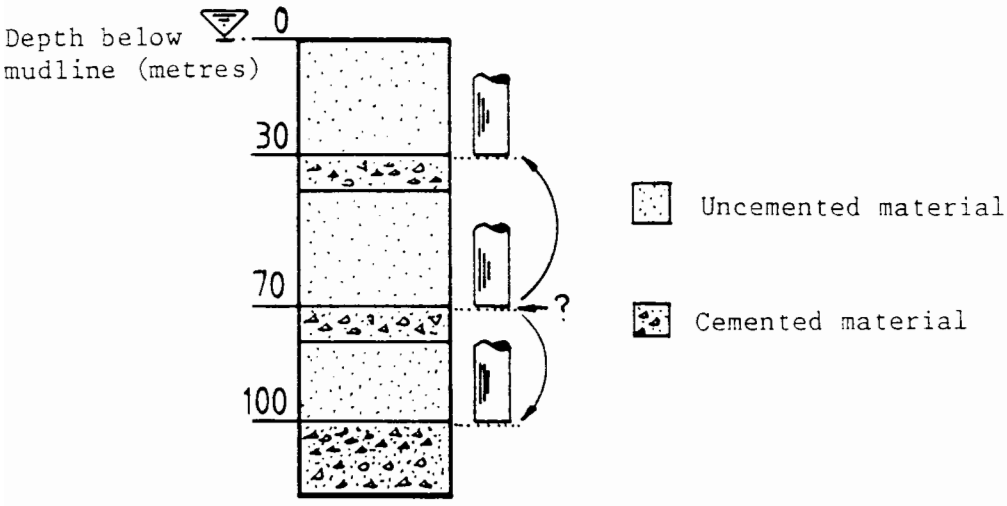

Figure 1.1 - Schematic soil profile

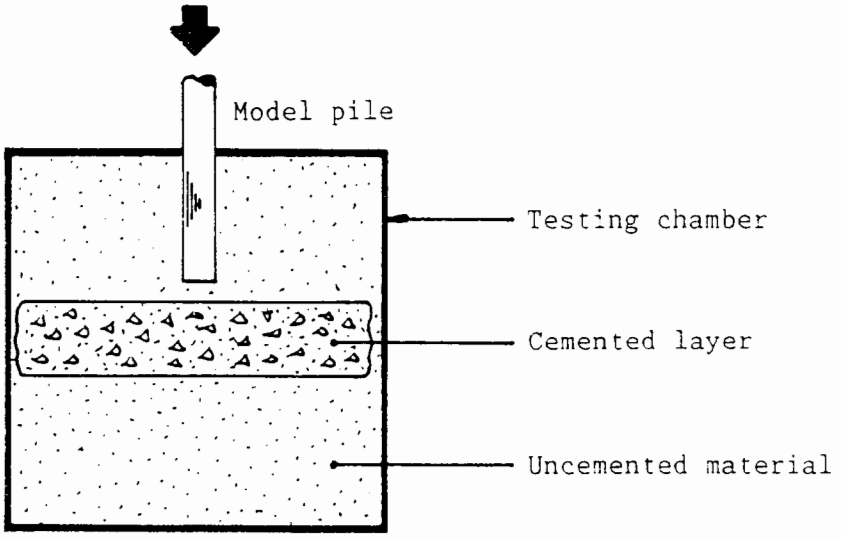

Figure 1.2 - Research concept

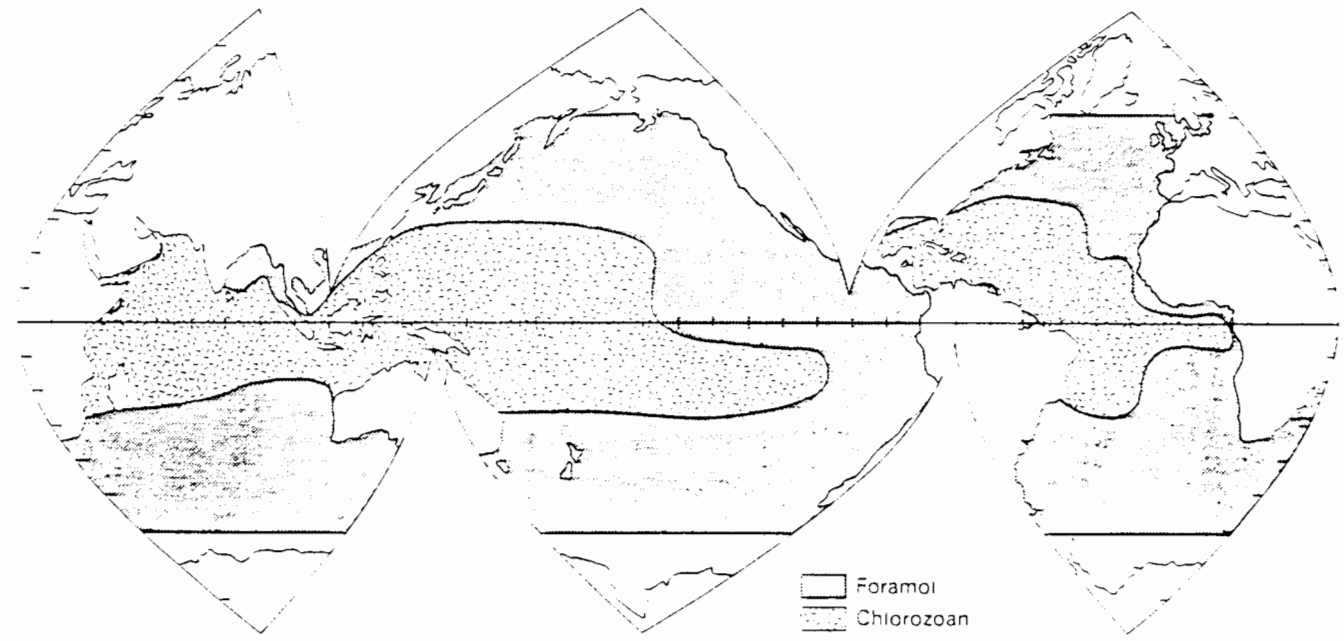

Figure 1.3 - Predicted distribution of skeletal grain associations (after Lees, 1975)

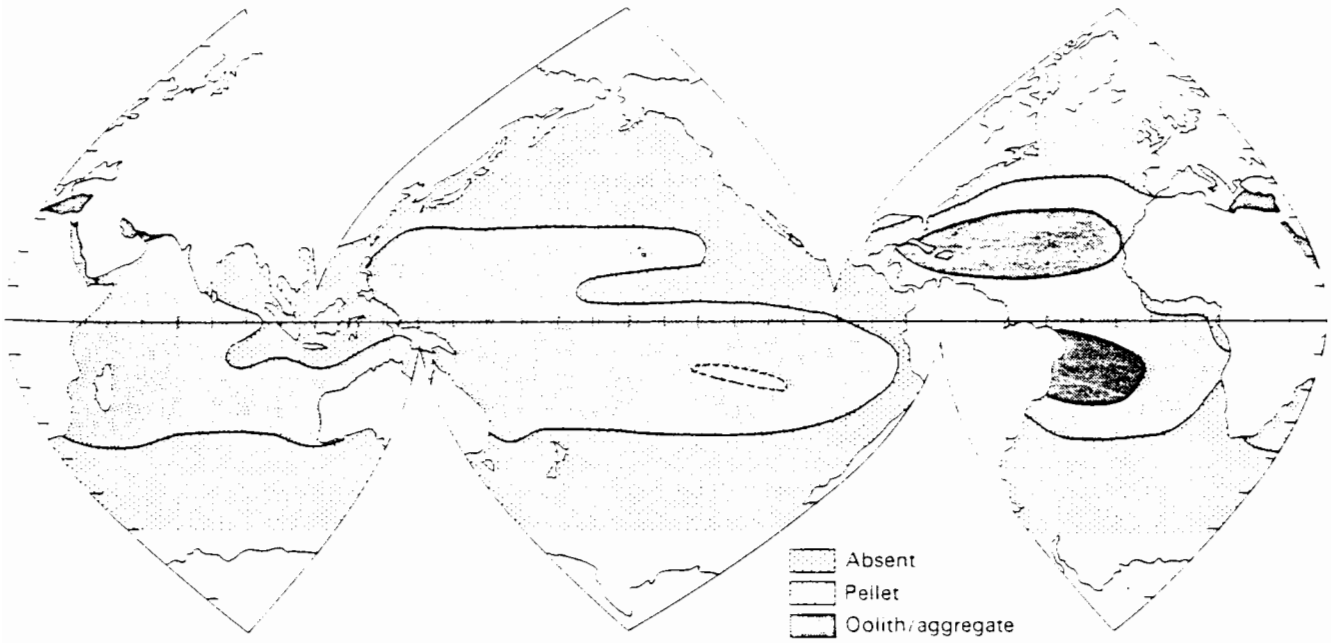

Figure 1.4 - Predicted distribution of non-skeletal grain associations (after Lees, 1975)

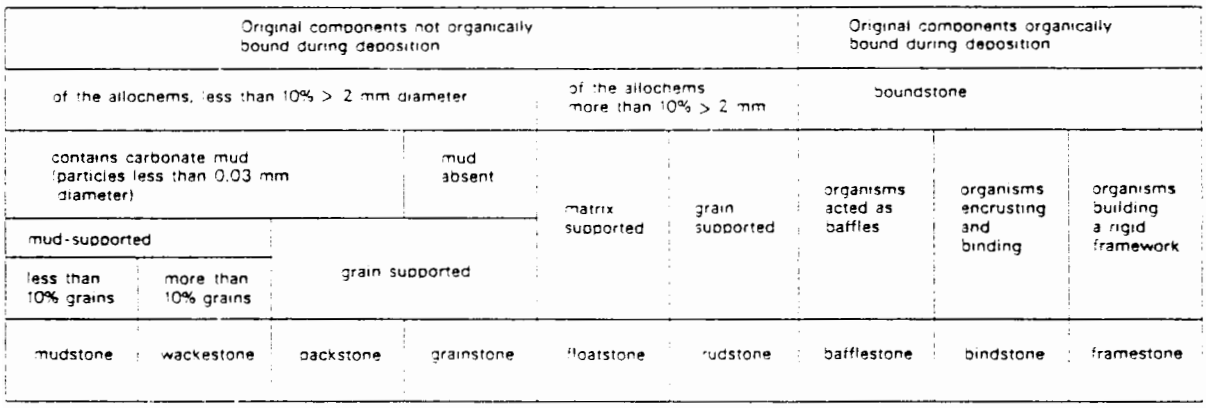

Figure 1.5 - Limestone classification (after Dunham, 1962)

Figure 1.6 - Proposed classification system of Clark and Walker (1977)

Figure 1.7 - Classification of carbonate sediments, 90 - 100% calcium carbonate (after King et al., 1980)

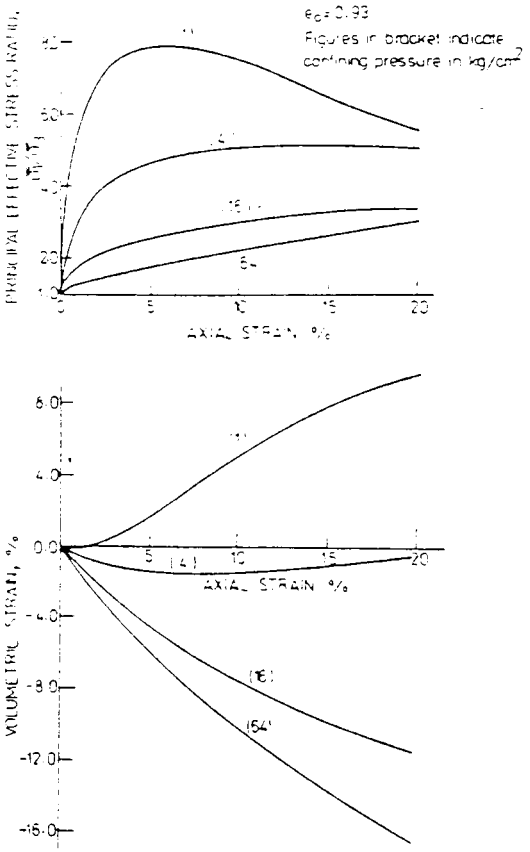

Figure 1.8 - Stress-strain-volume change behaviour, carbonate sand, India (after Datta et al., 1979)

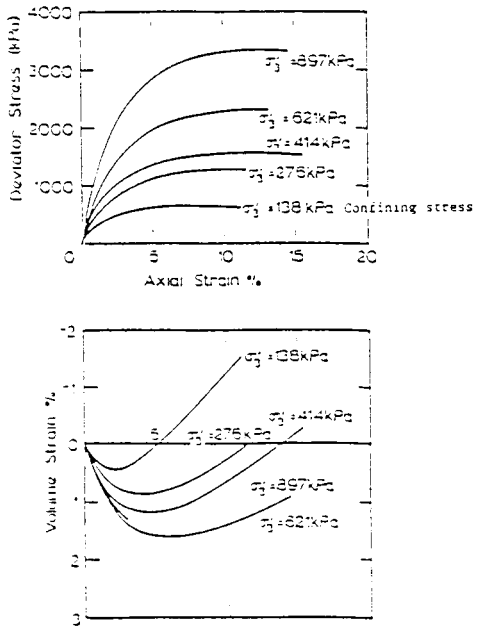

Figure 1.9 - Stress-strain-volume change behaviour, carbonate sand, Bass Strait, Australia (after Poulos, 1982)

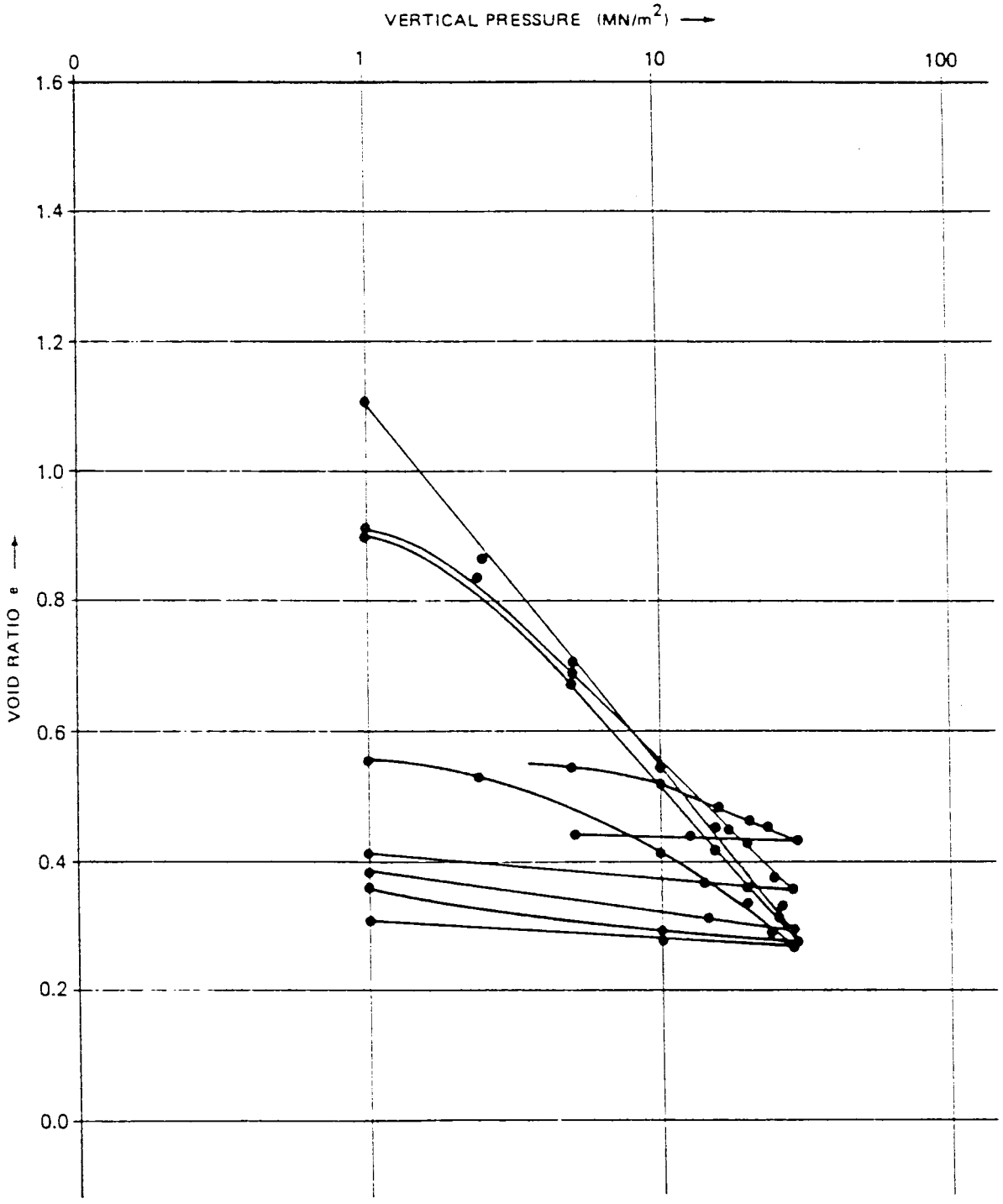

Figure 1.10 - Oedometer test results, North Rankin, Australia

(after Fugro, 1981)

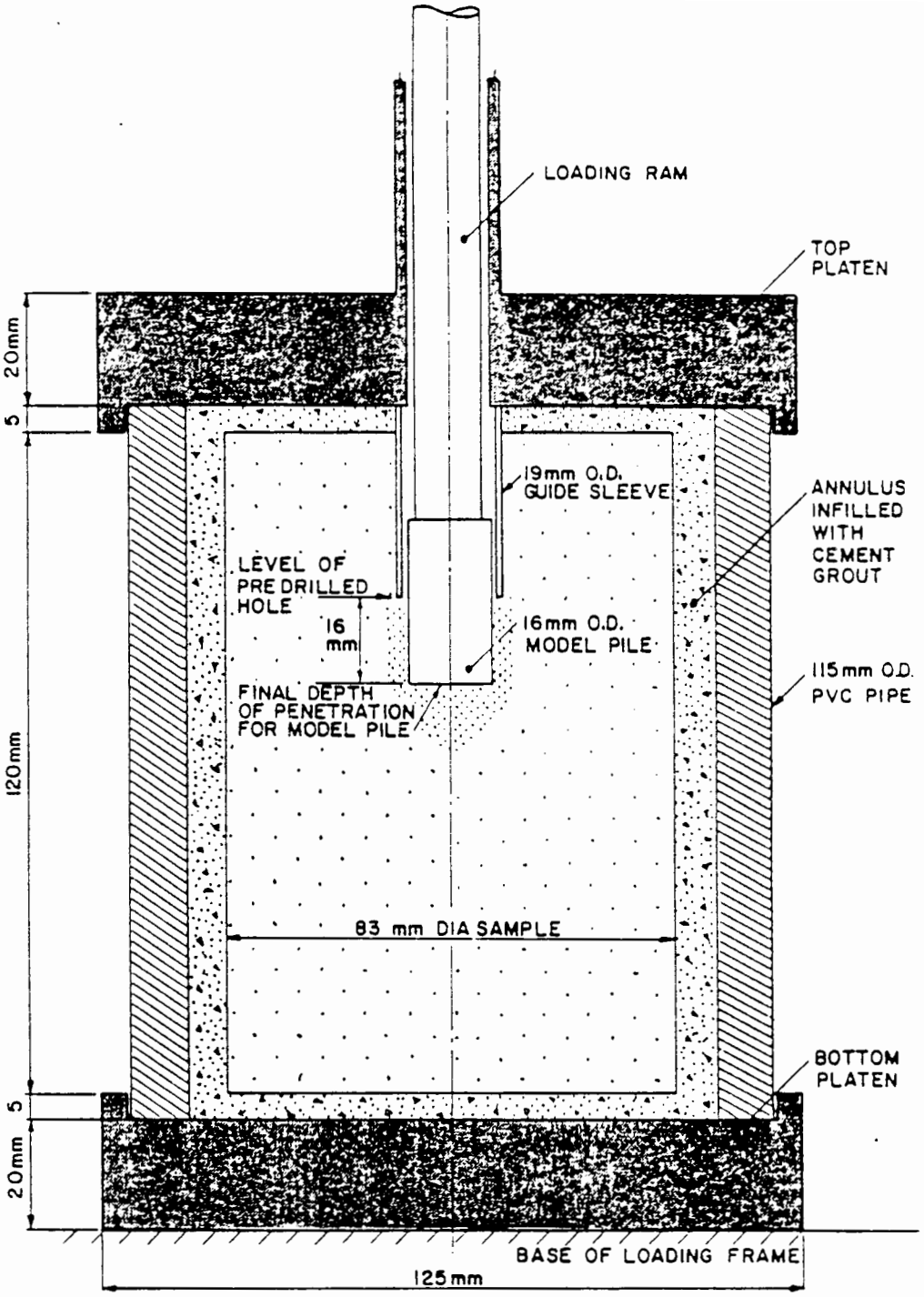

Figure 1.11 - Test arrangement, rod index test (after Jewell, 1985a,b)

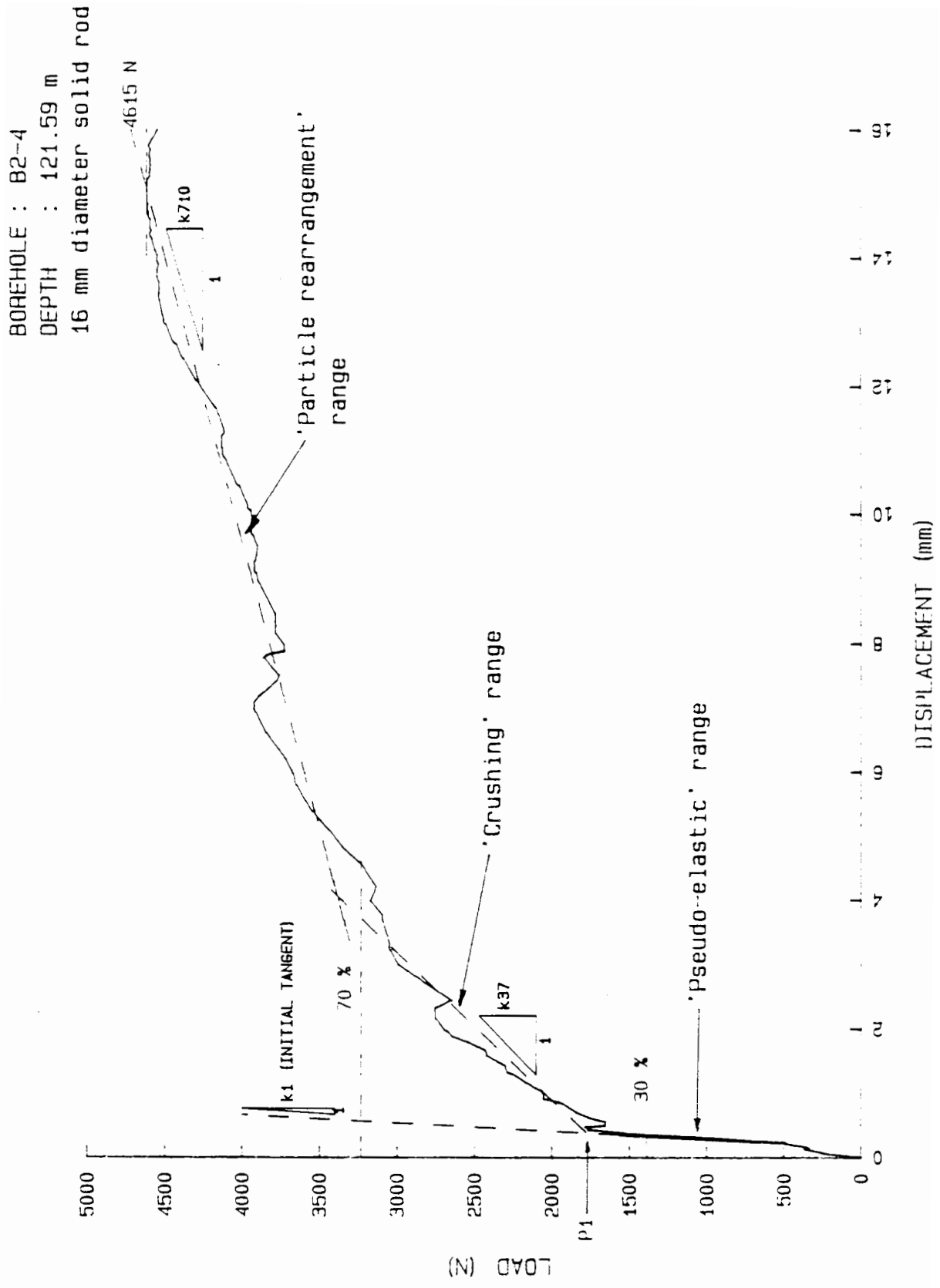

Figure 1.12 - Typical load - displacement result from rod index test (after Jewell, 1985a,b)

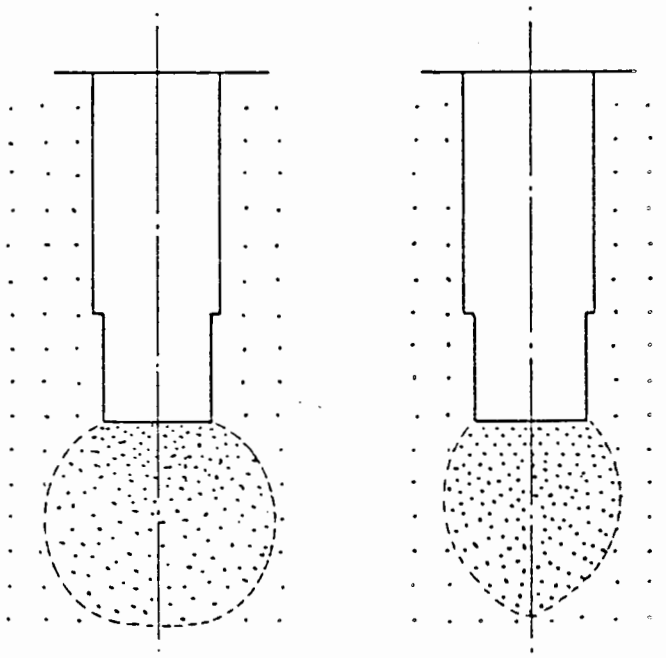

Figure 1.13 - Typical shapes of compression zones from model [illegible] (after Jewell, 1985a,b)

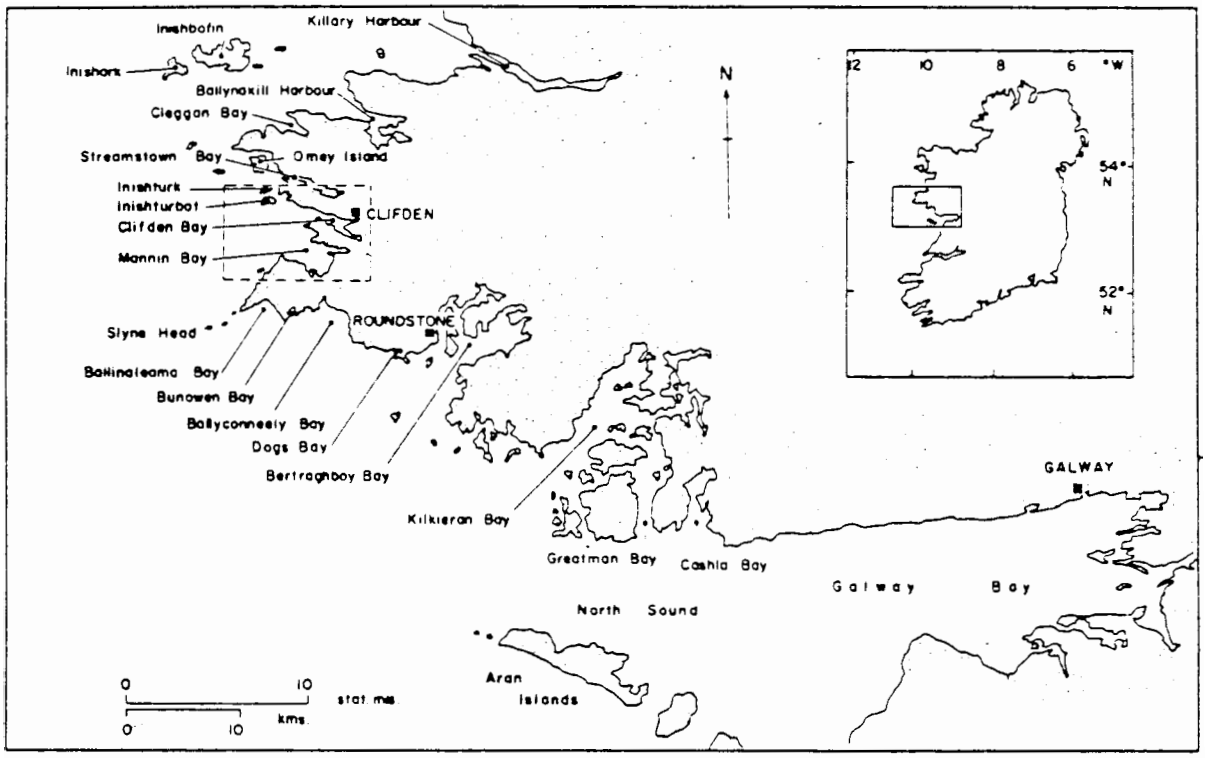

Figure 2.1 - Locality map, coastal region of Connemara

(after Lees et al. 1969)

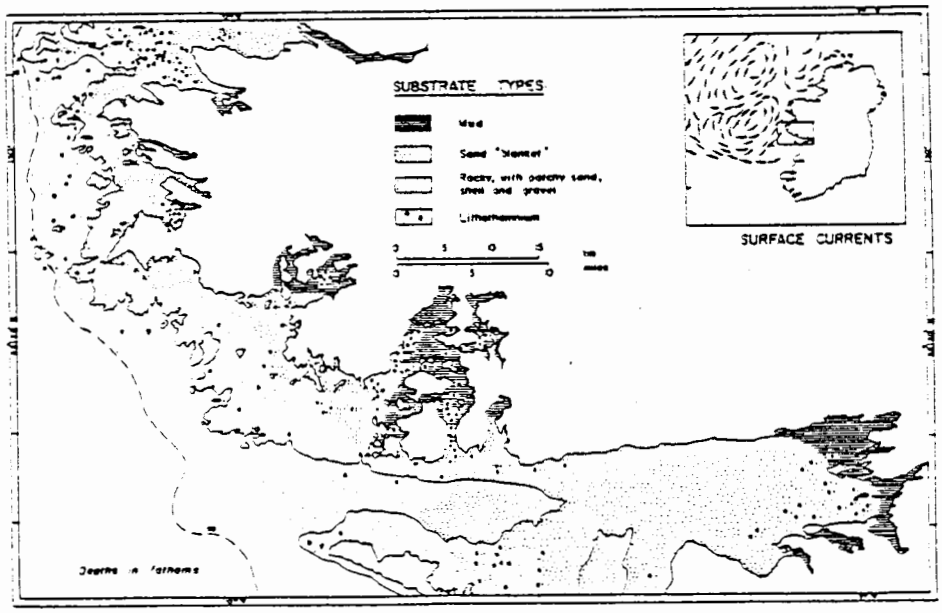

Figure 2.2 - Distribution of main substrate types - Connemara region

(after Lees et al., 1969)

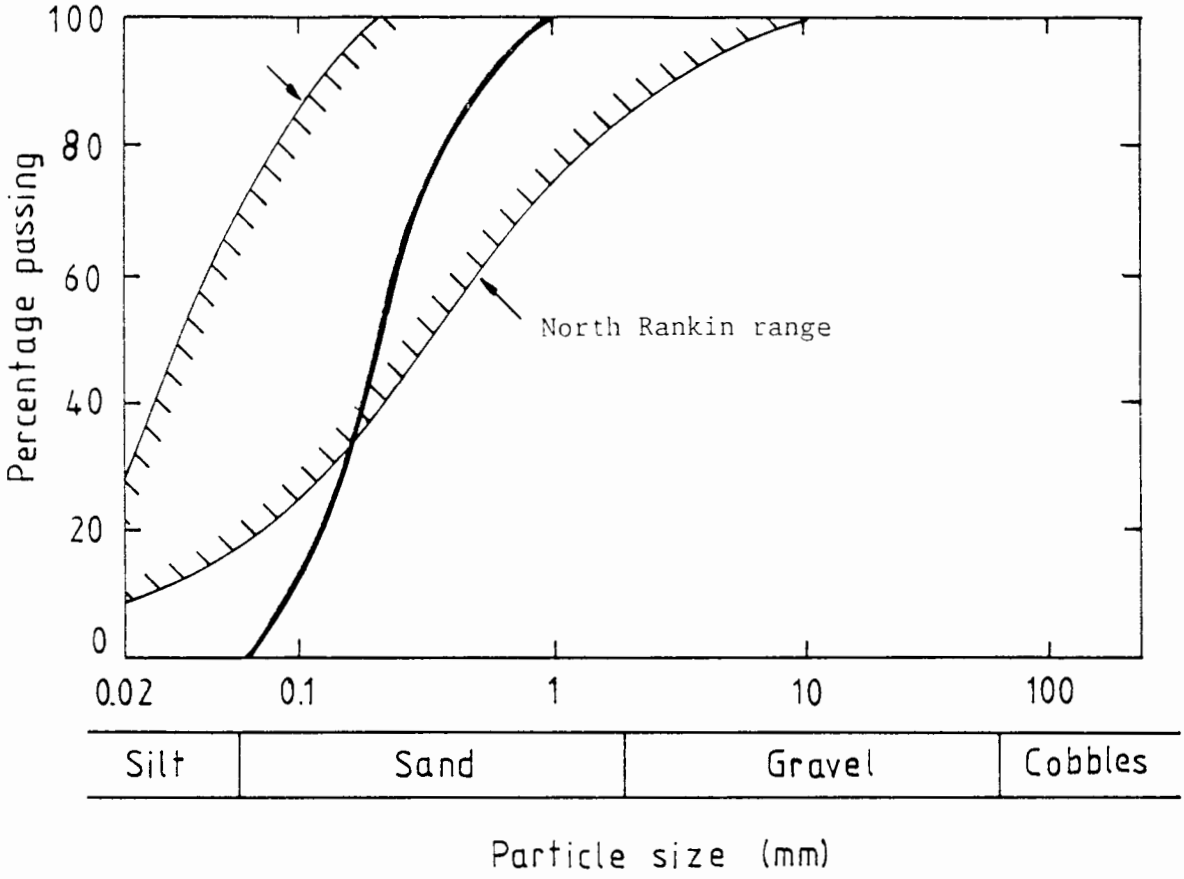

Figure 3.1 - Grain size distribution. Dogs Bay carbonate sand

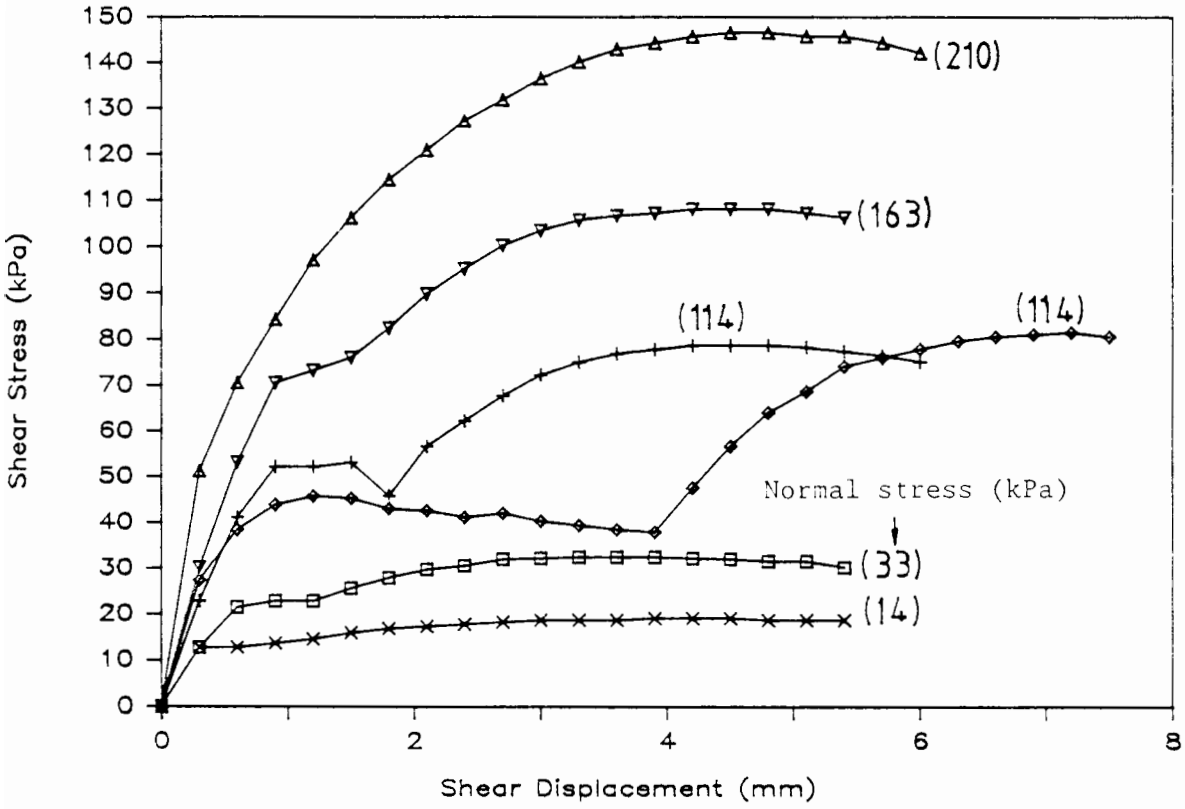

Figure 3.2 - Direct shear test results (1/5)

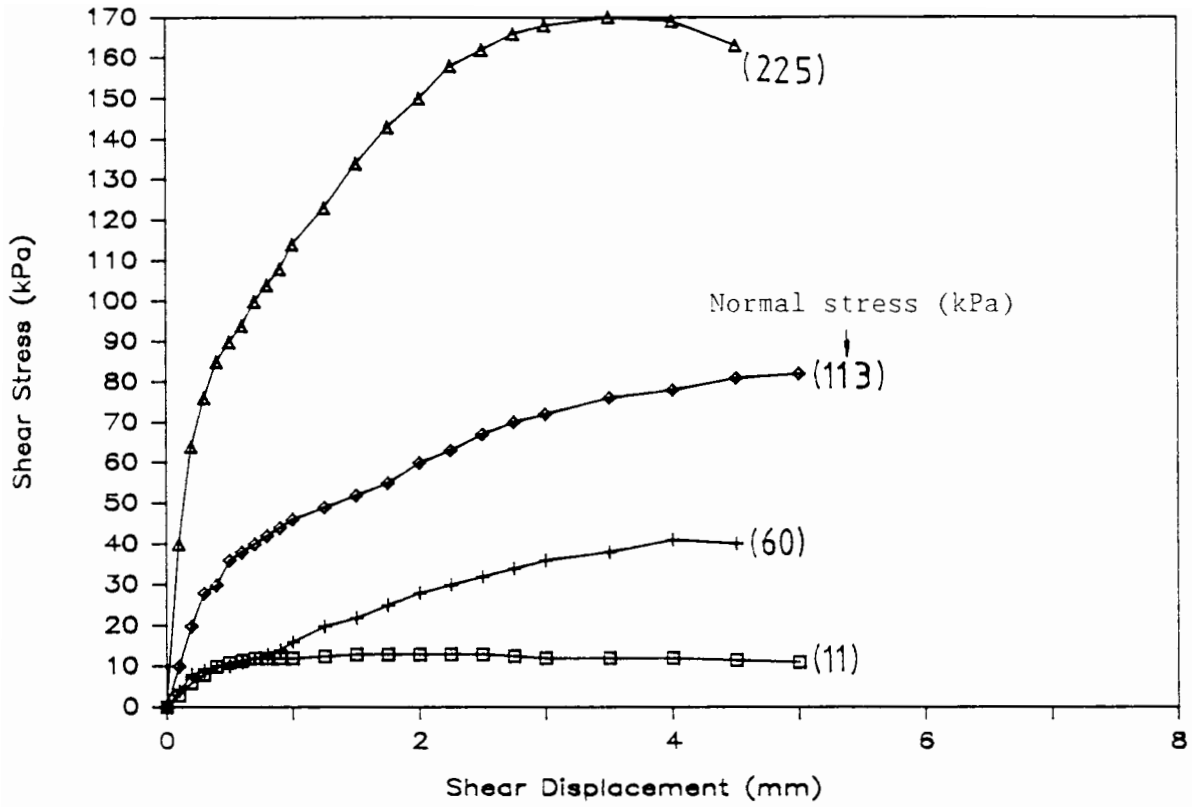

Figure 3.3 - Direct shear test results (2/5), North Rankin material (after Fugro, 1979)

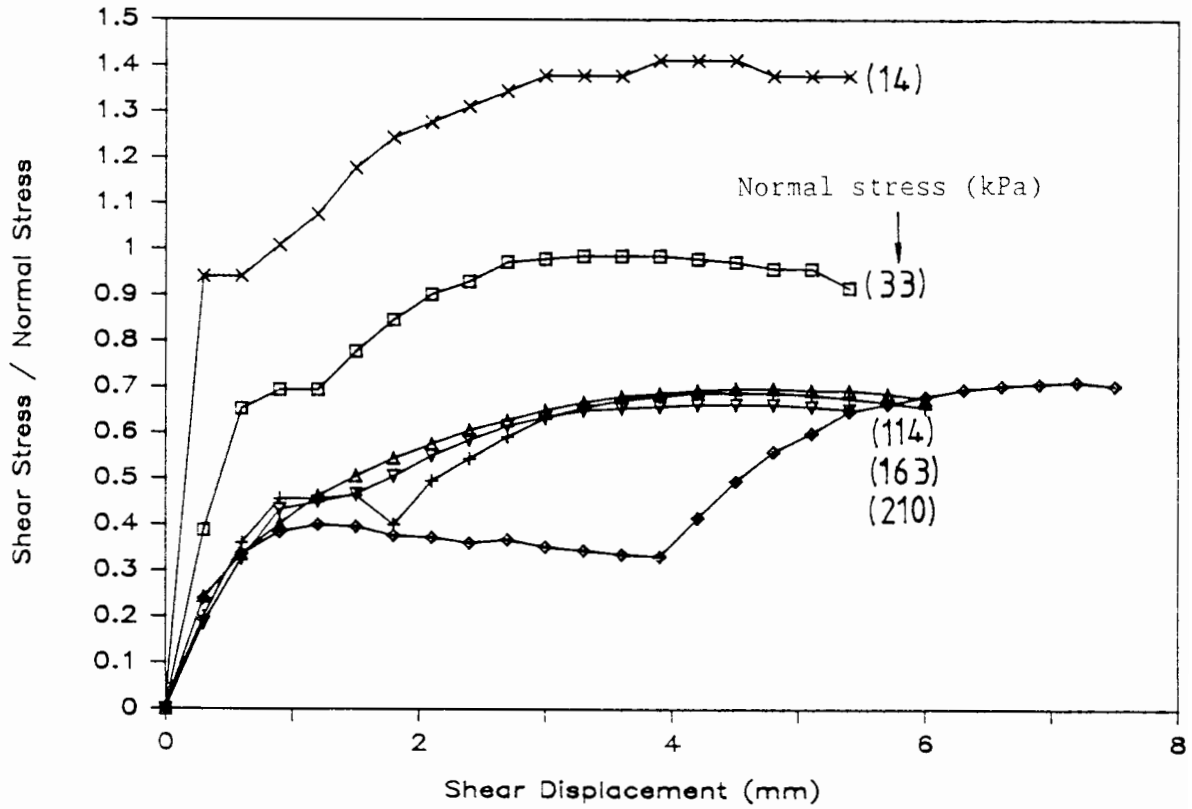

Figure 3.4 - Direct shear test results (3/5)

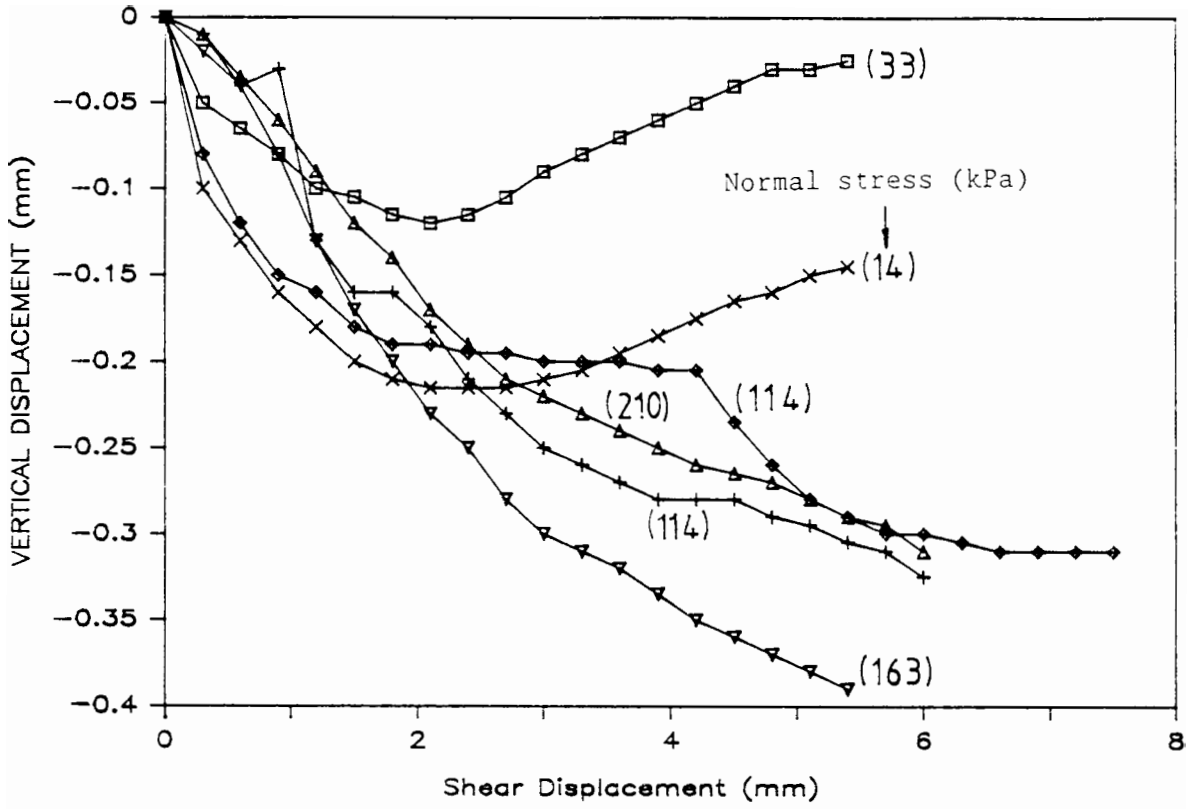

Figure 3.5 - Direct shear test results (4/5)

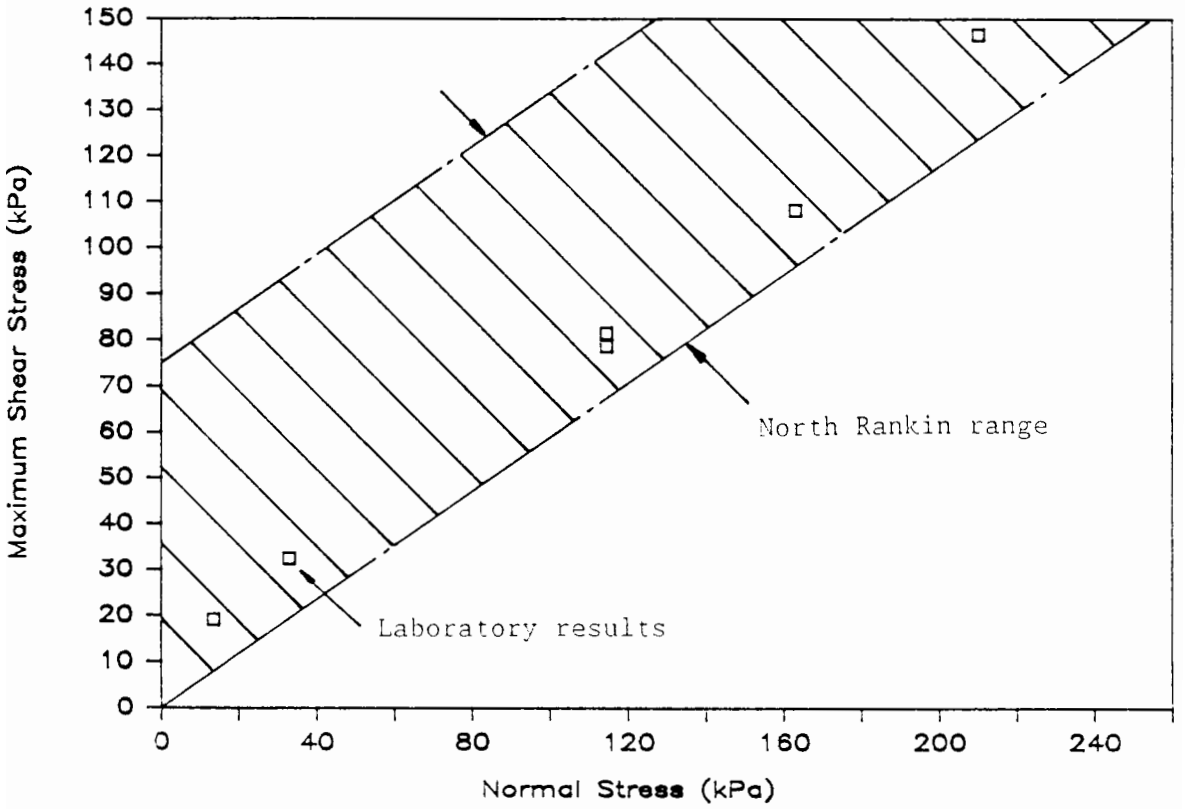

Figure 3.6 - Direct shear test results (5/5)

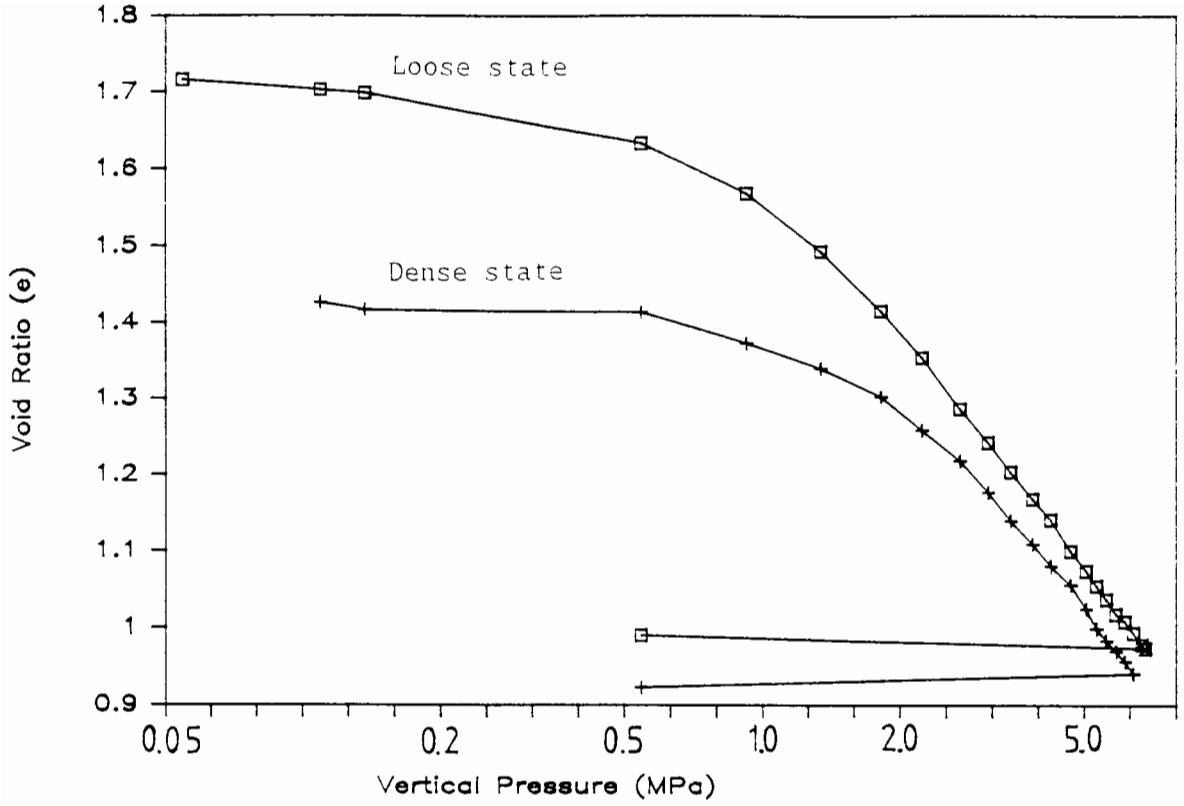

Figure 3.7 - Oedometer test results

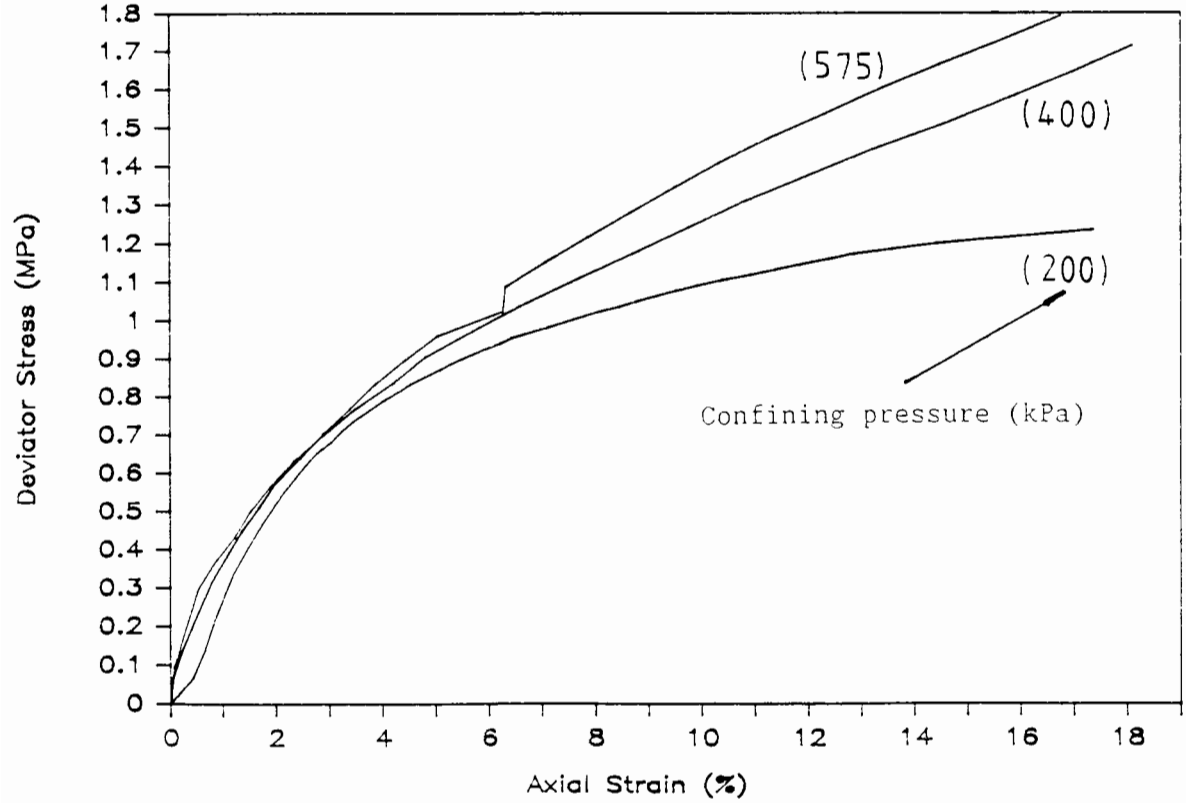

Figure 3.8 - Triaxial test results

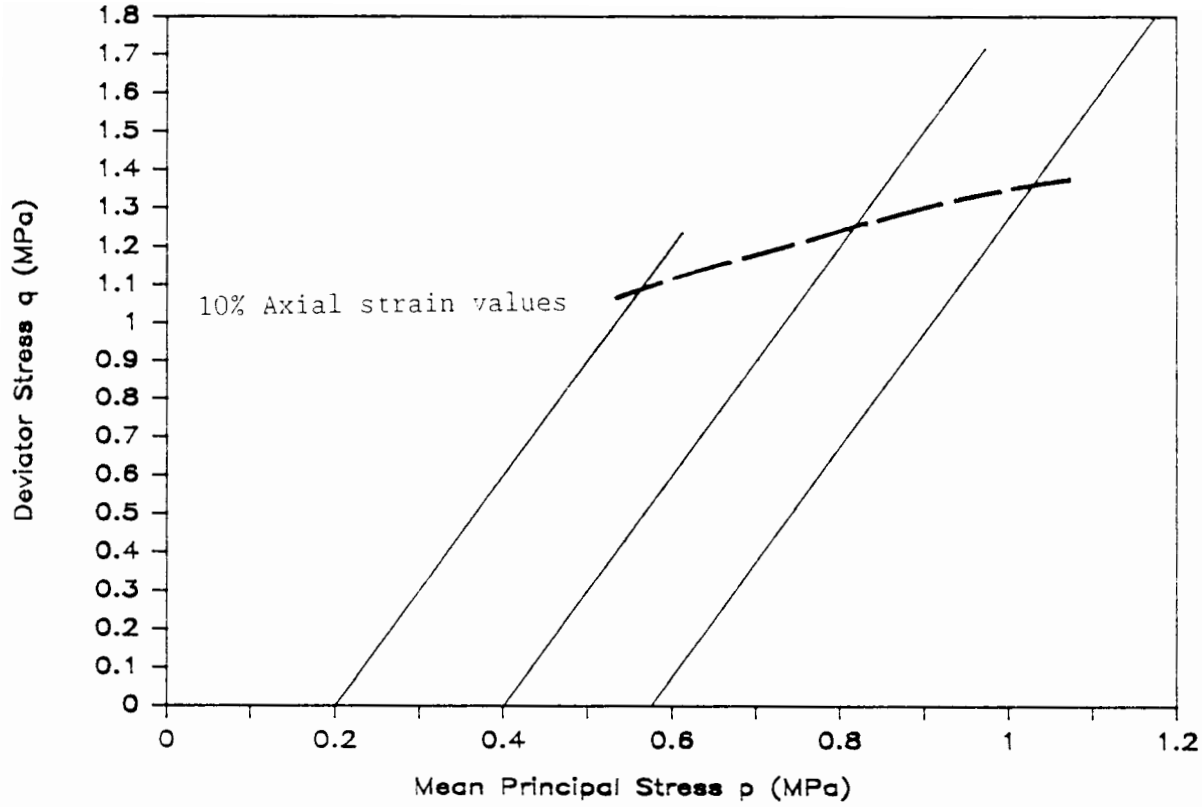

Figure 3.9 - q - p diagram of triaxial test results

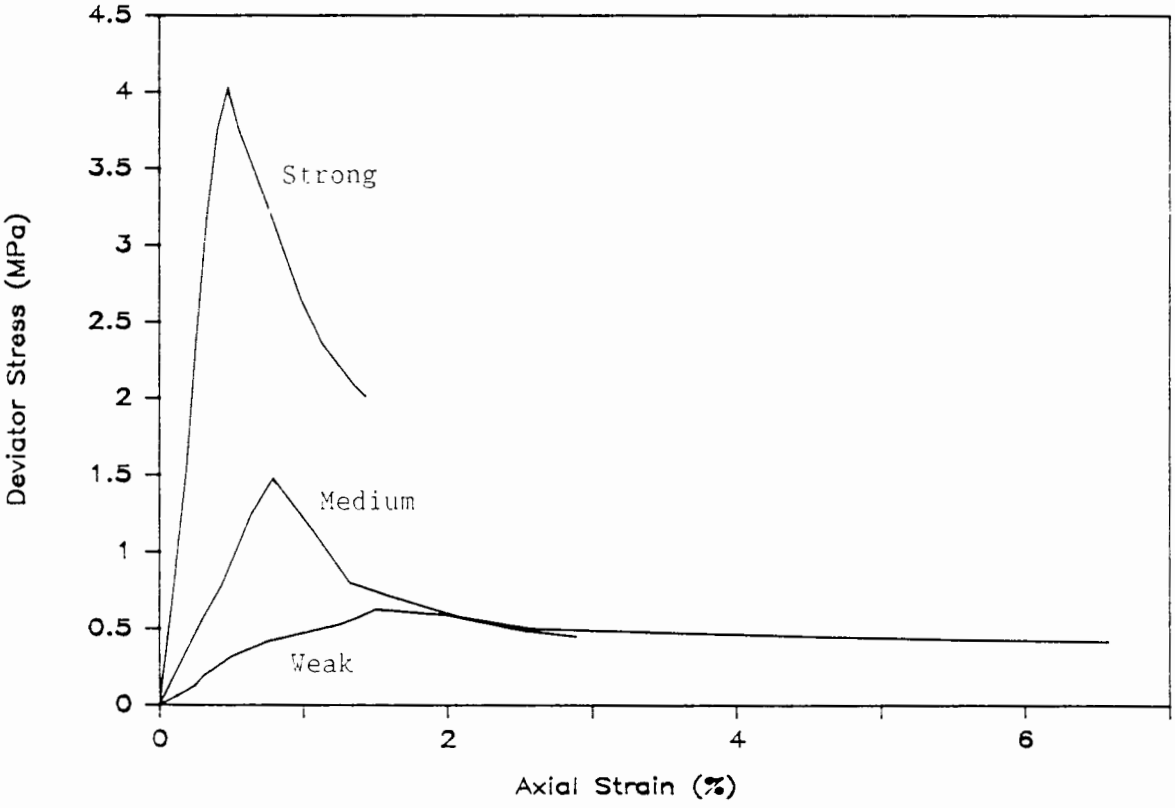

Figure 3.10 - Uniaxial unconfined compressive strength tests on cemented materials ($\sigma'_3 = 0$)

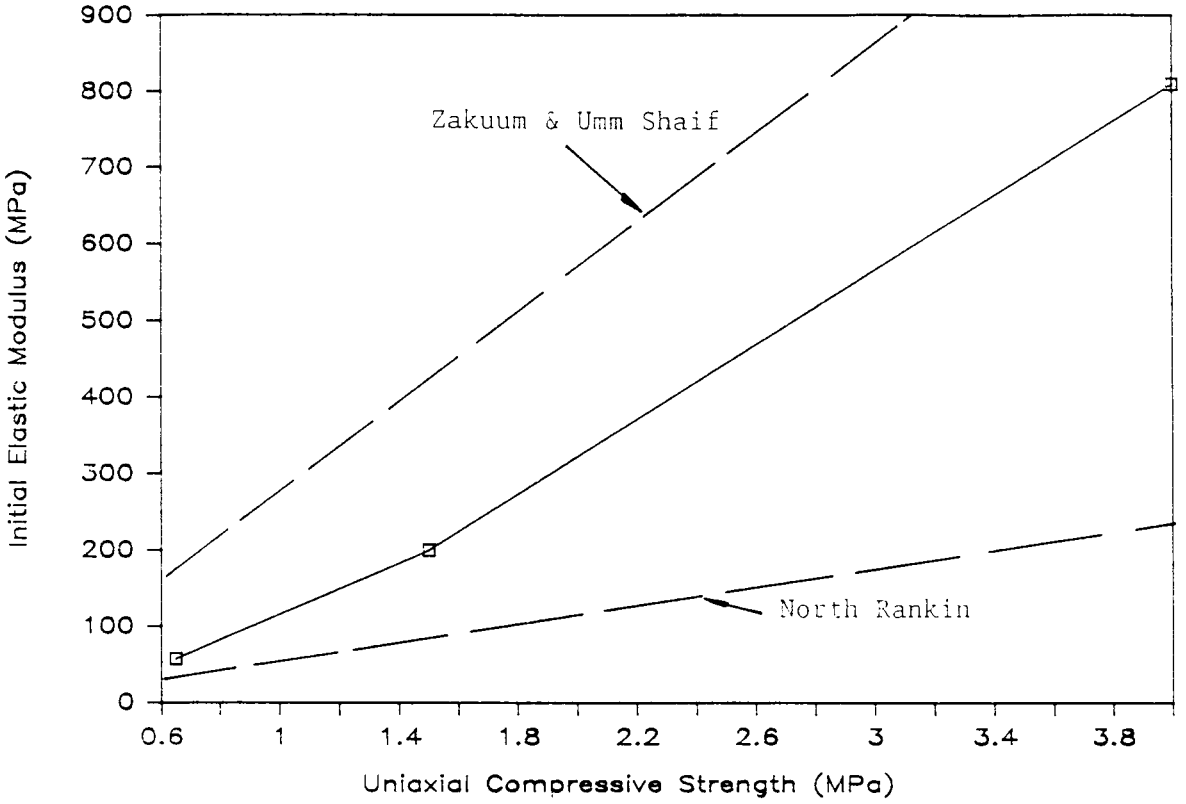

Figure 3.11 - Variation of initial elastic modulus with uniaxial compressive strength

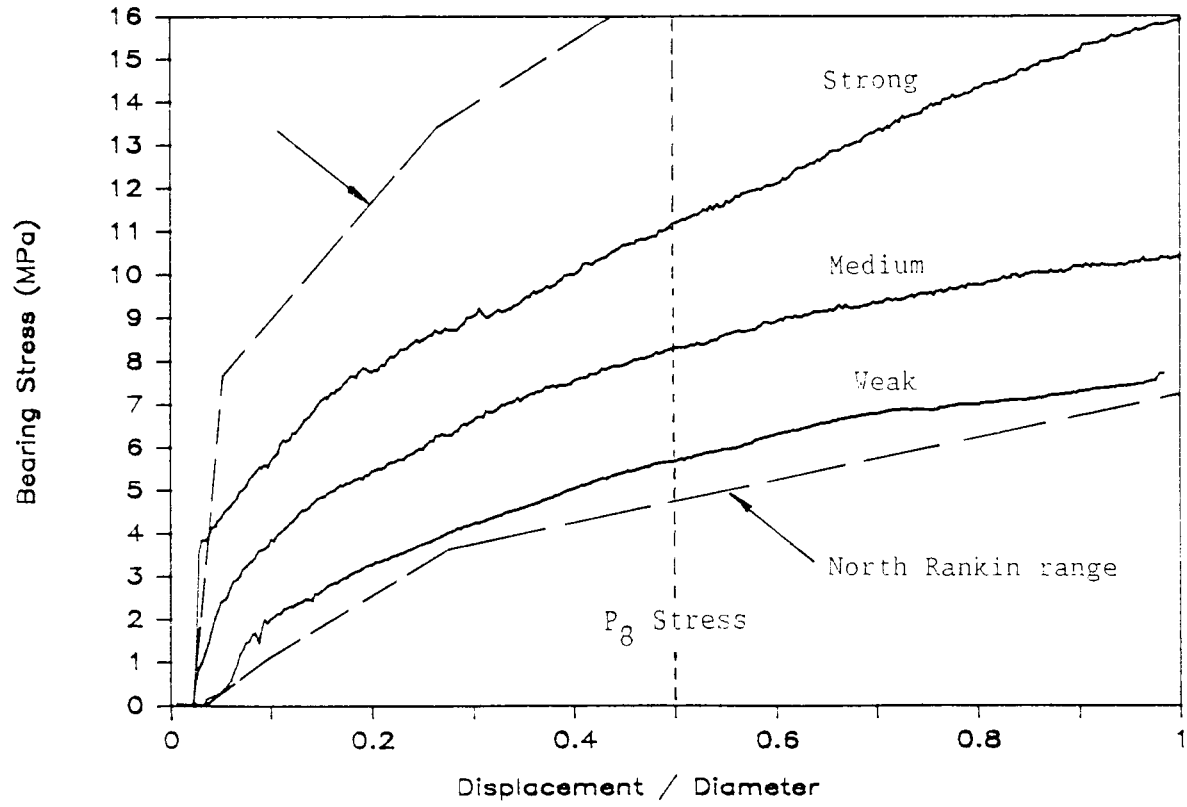

Figure 3.12 - Rod index test results

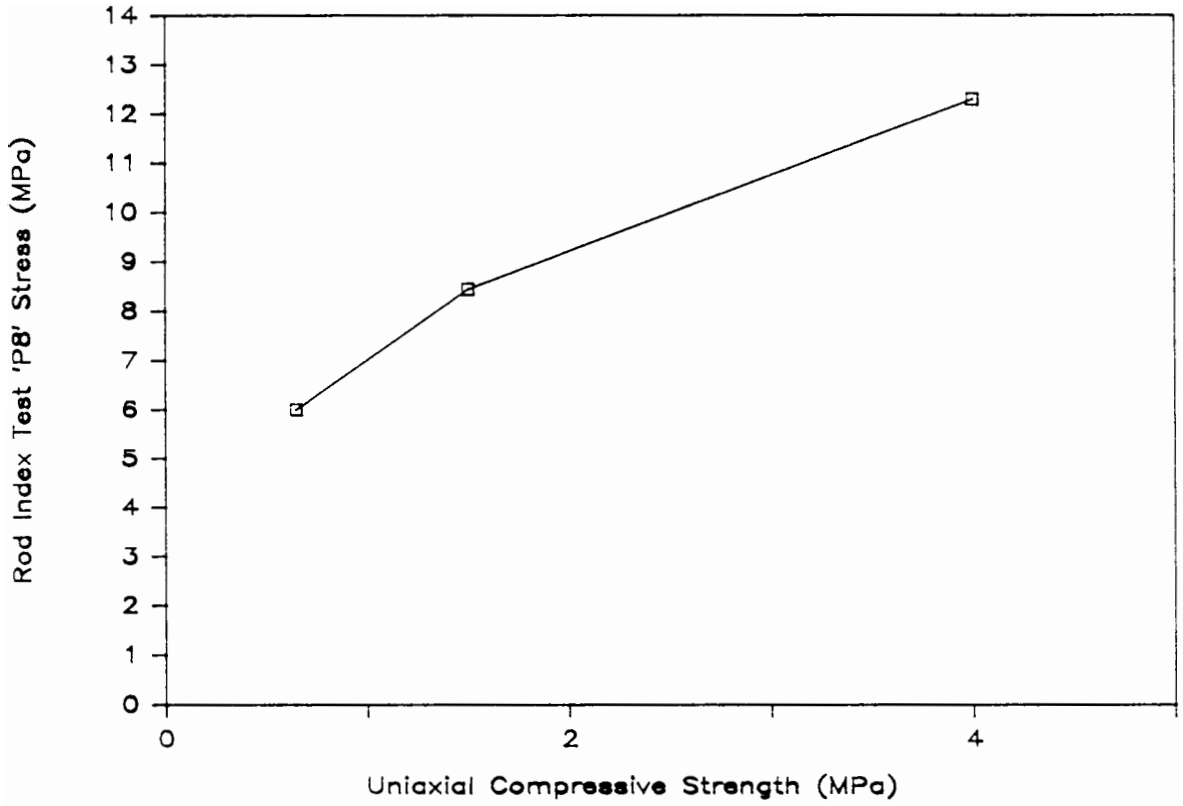

Figure 3.13 - Variation of RIT 'P_8' stress with uniaxial compressive strength

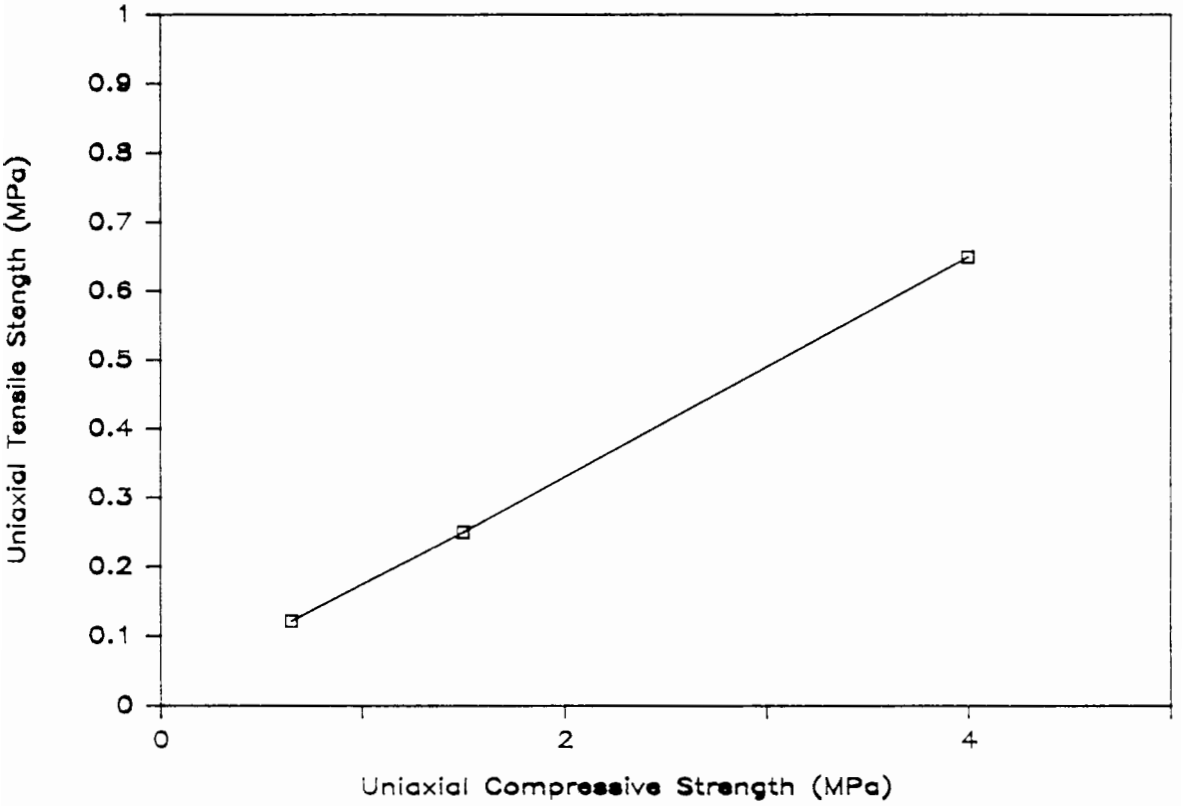

Figure 3.14 - Variation of tensile strength with uniaxial compressive strength

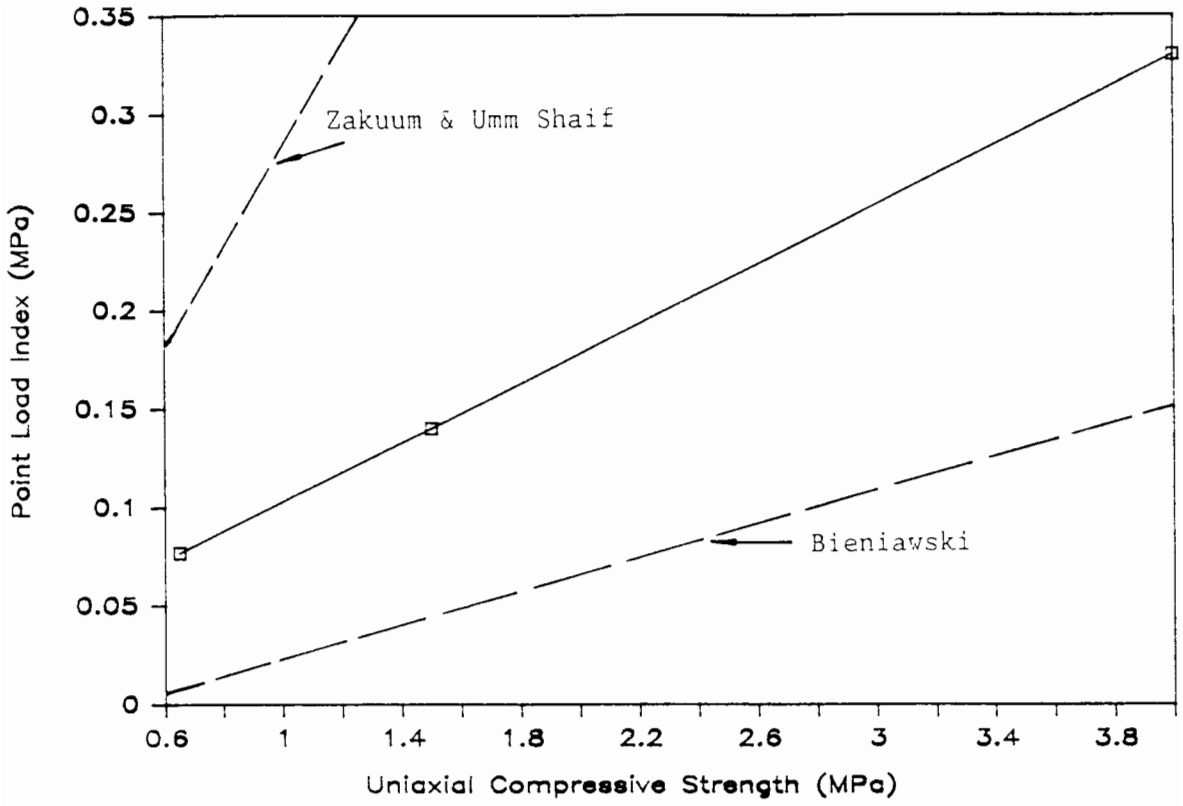

Figure 3.15 - Variation of Point load index with uniaxial compressive strength

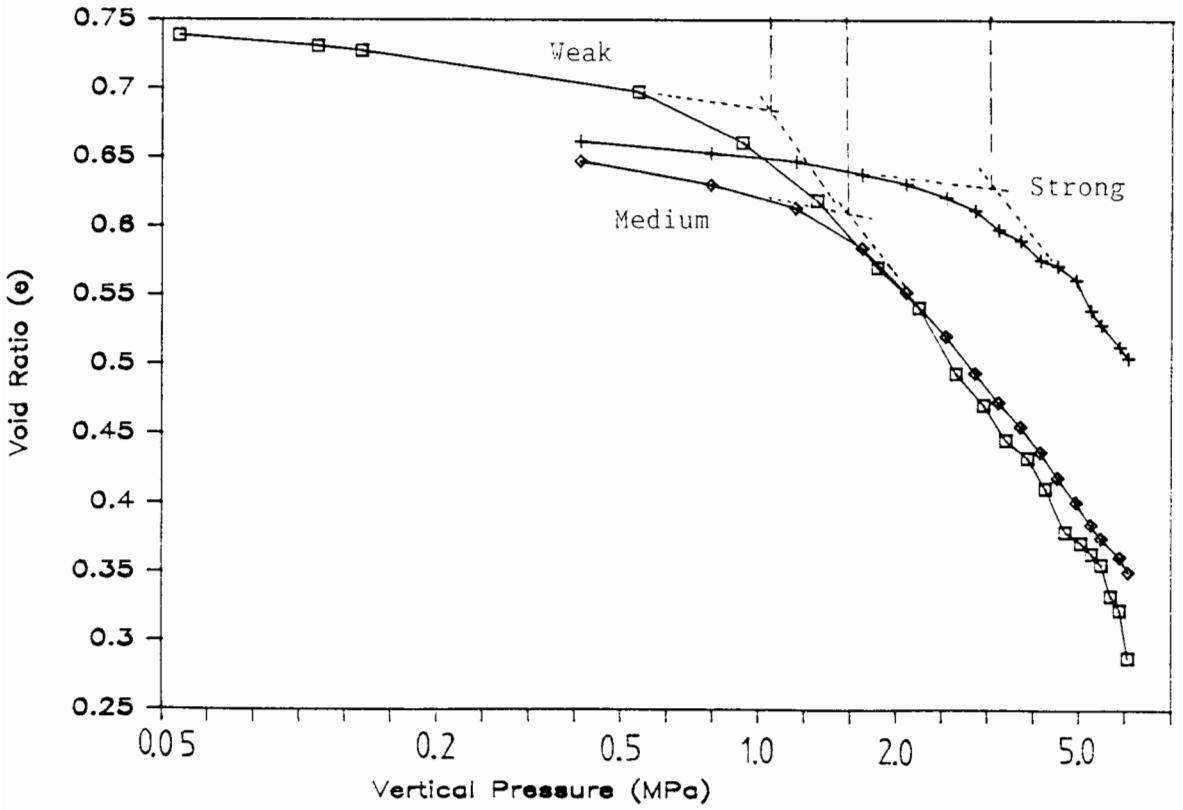

Figure 3.16 - Oedometer test results. cemented material

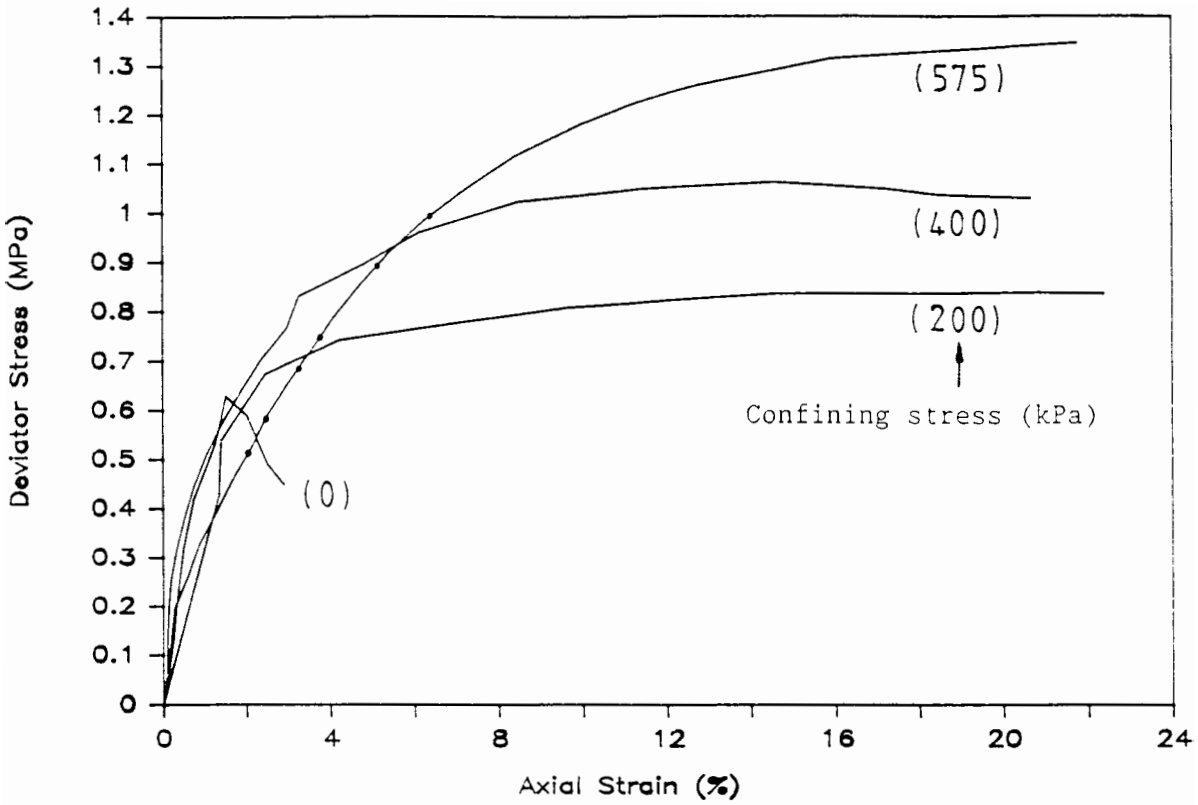

Figure 3.17 - Triaxial test results, 'weak' strength material

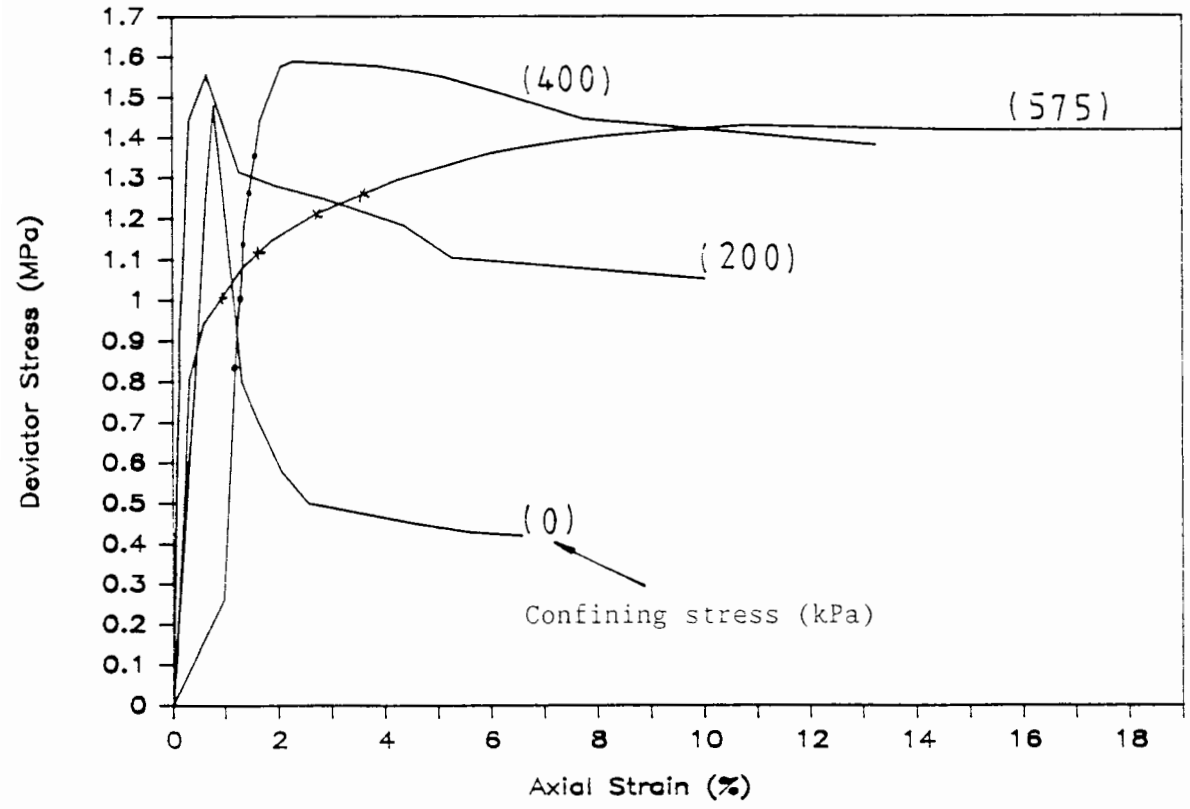

Figure 3.18 - Triaxial test results, 'medium' strength material

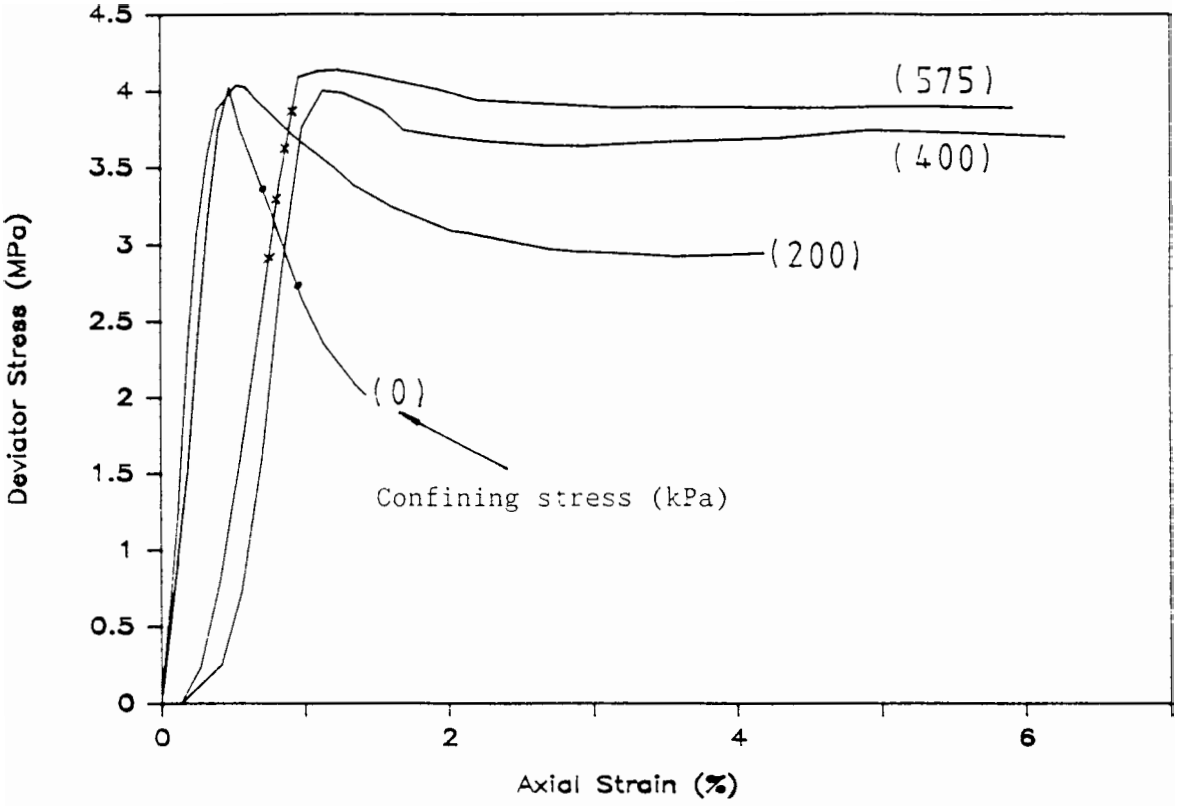

Figure 3.19 - Triaxial test results, 'strong' strength material

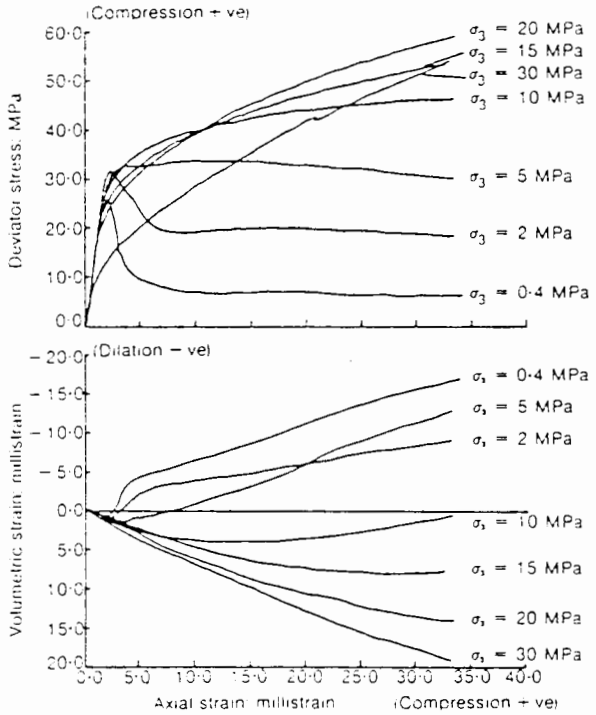

Figure 3.20 - Triaxial test results, Bath Stone (after Elliott, 1983)

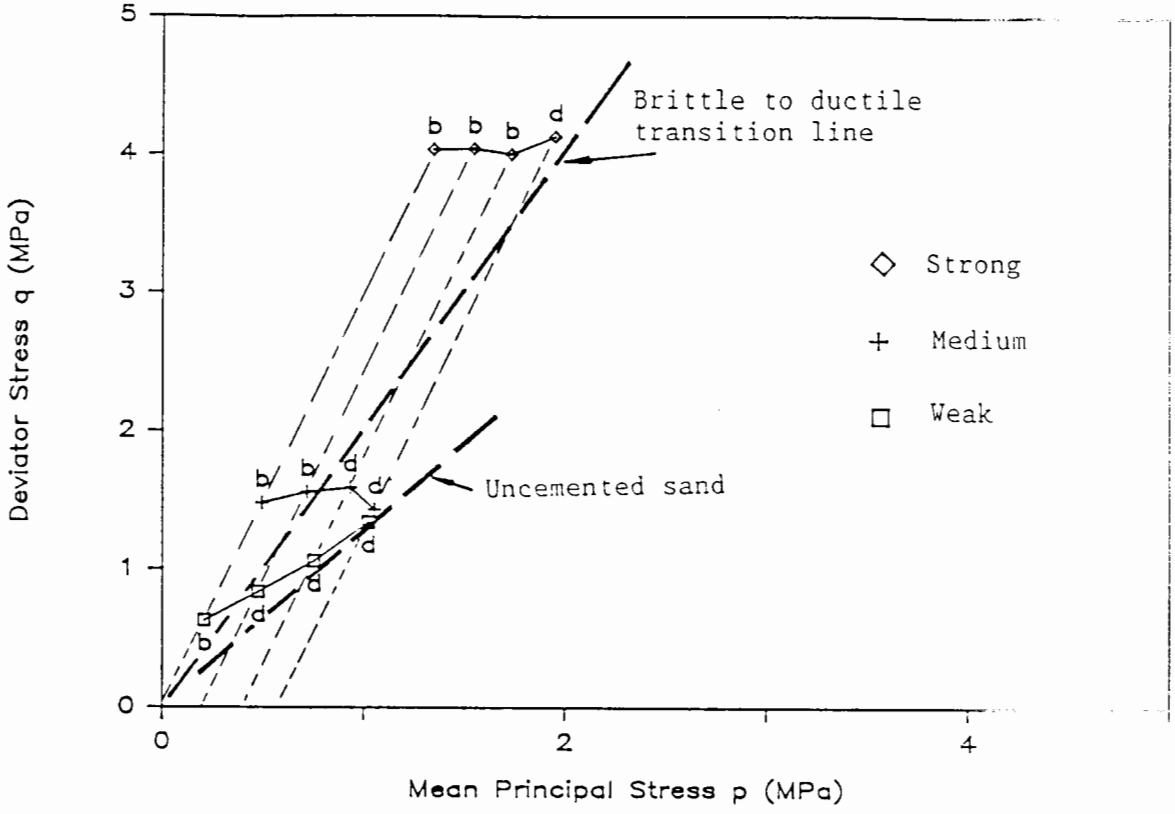

Figure 3.21 - q - p diagram of triaxial test results

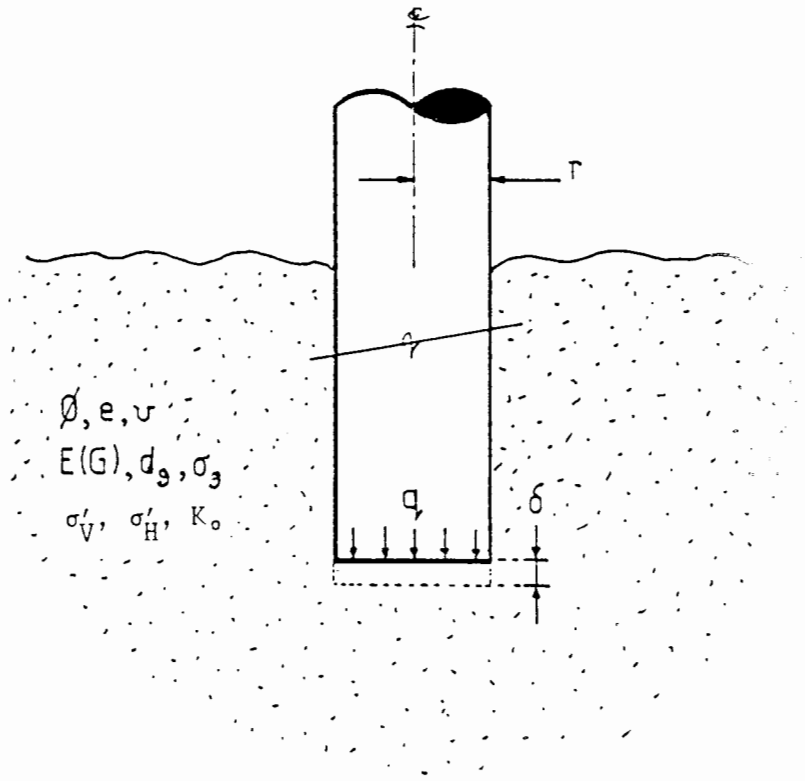

Figure 4.1 - Independent quantities for a dimensional analysis of a deep foundation in dry sand

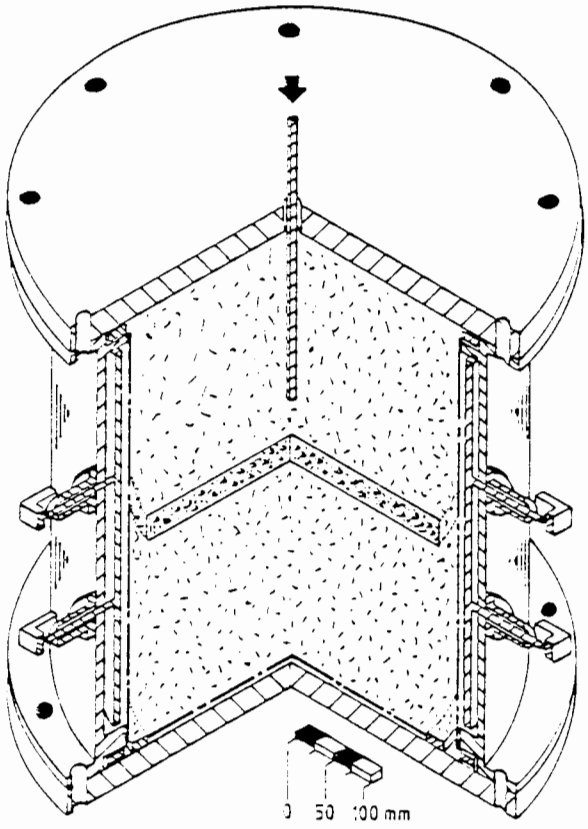

Figure 4.2 - Conceptual diagram of testing chamber

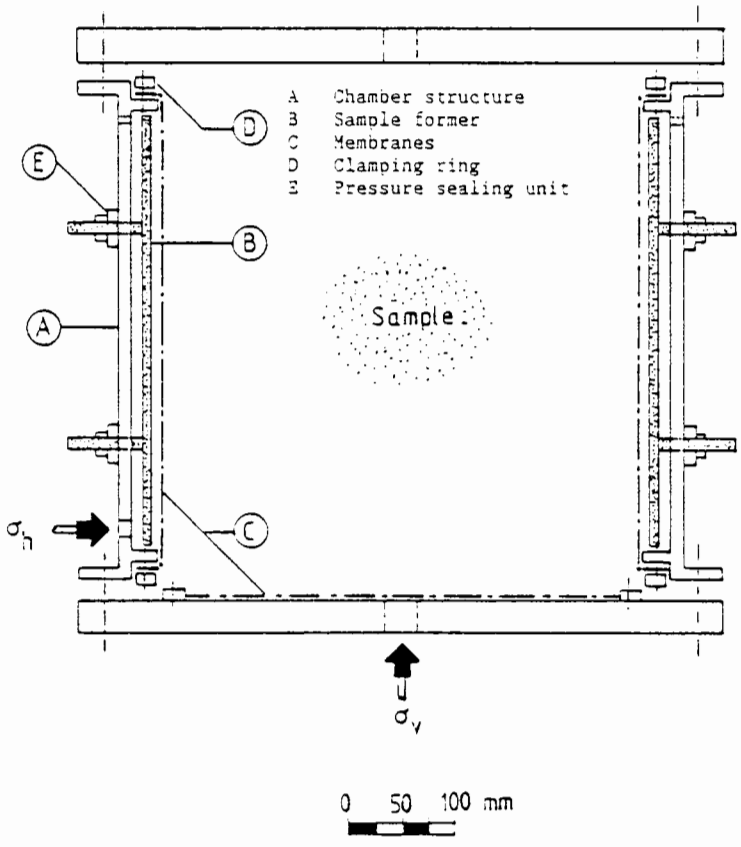

Figure 4.3 - Schematic diagram of testing chamber

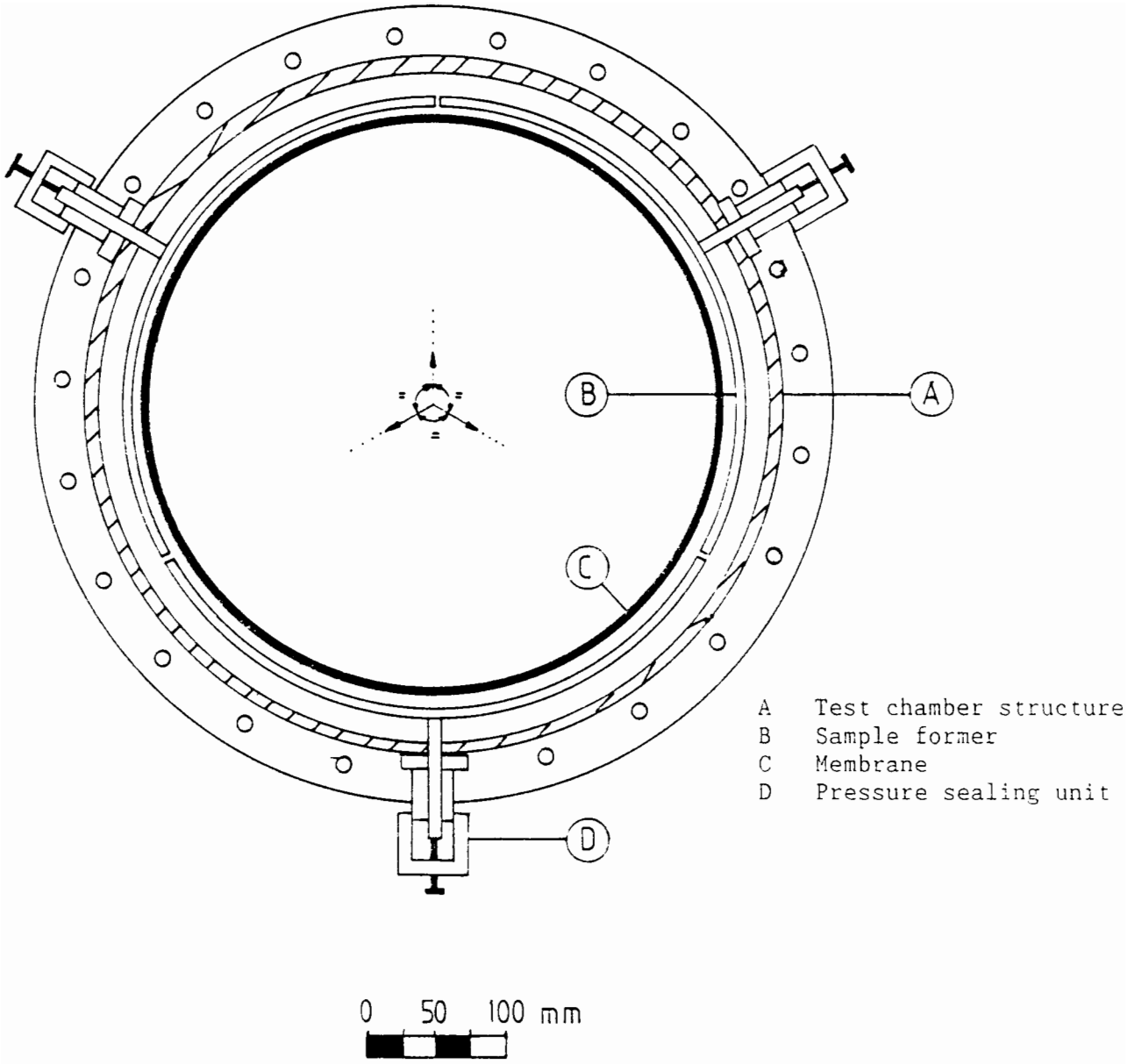

Figure 4.4 - Section through testing chamber illustrating sample former details

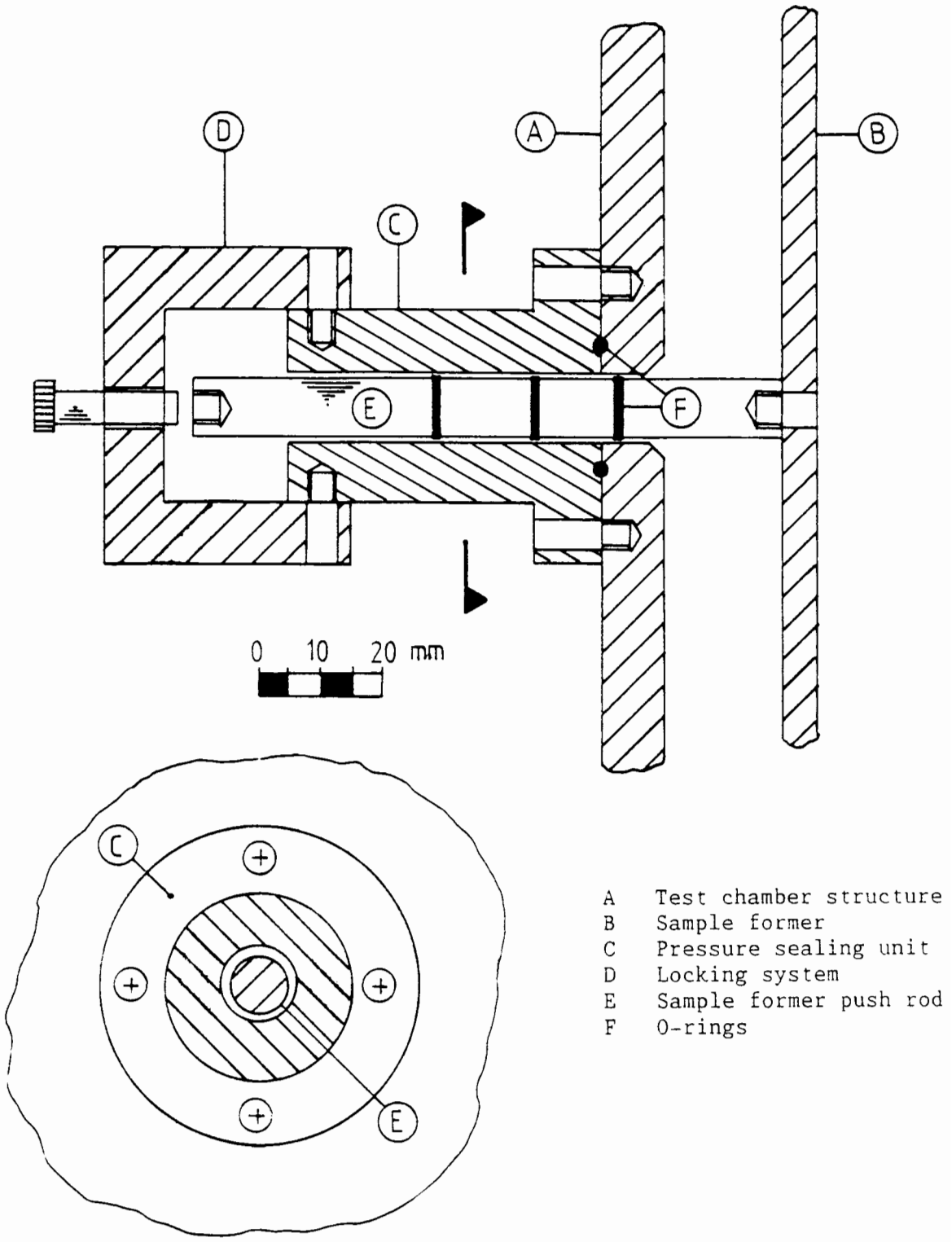

Figure 4.5 - Testing chamber sealing and adjustment units

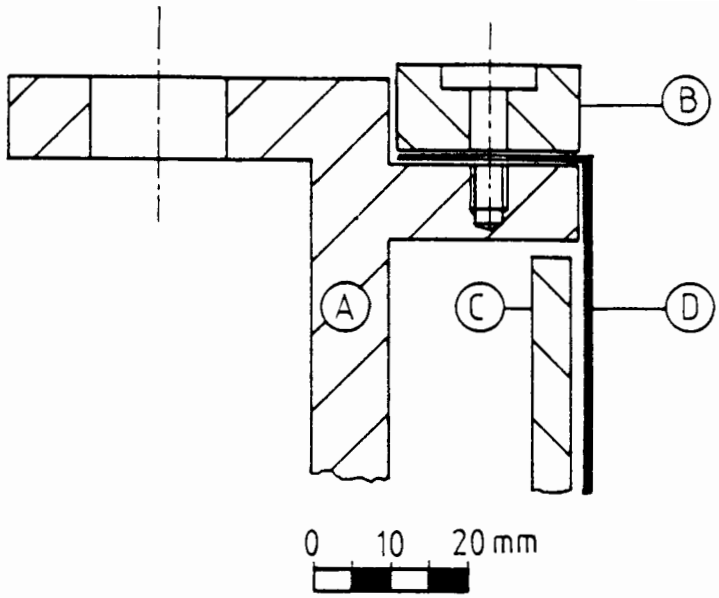

A Test chamber structure
B Lateral membrane clamping ring
C Sample former
D Lateral membrane

Figure 4.6 - Diametric clamping ring for circumferential membrane

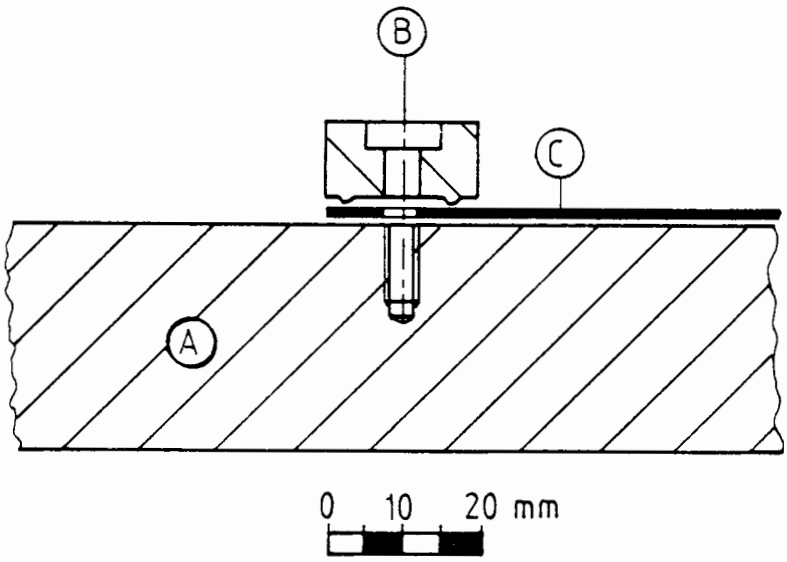

A Bottom plate
B Bottom membrane clamping ring
C Bottom membrane

Figure 4.7 - Diametric clamping ring for base membrane

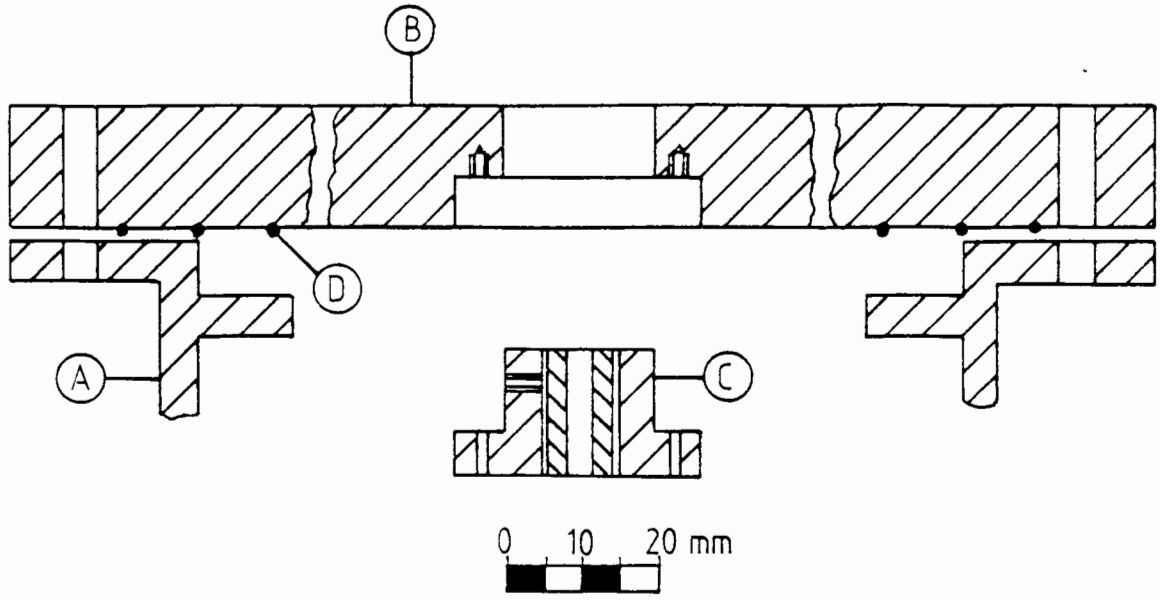

A Test chamber structure
B Top plate
C Pile size adaptor
D O-rings
E Lateral pressure input port
F Air bleed valve
G Bottom plate
H Vertical pressure input port

Figure 4.8 - Top plate details

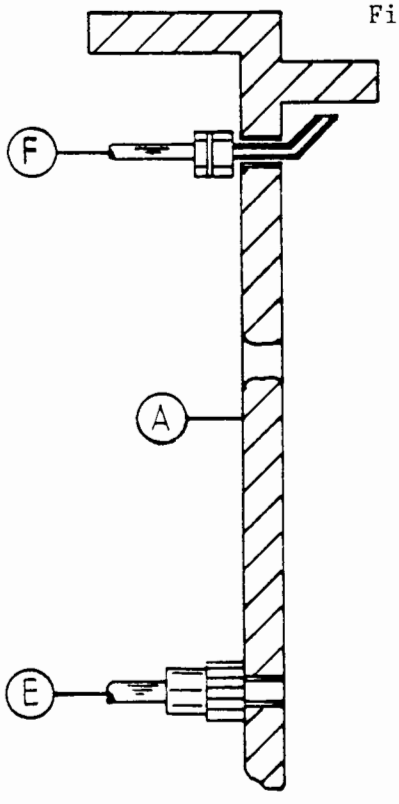

Figure 4.9 - Circumferential pressure ports

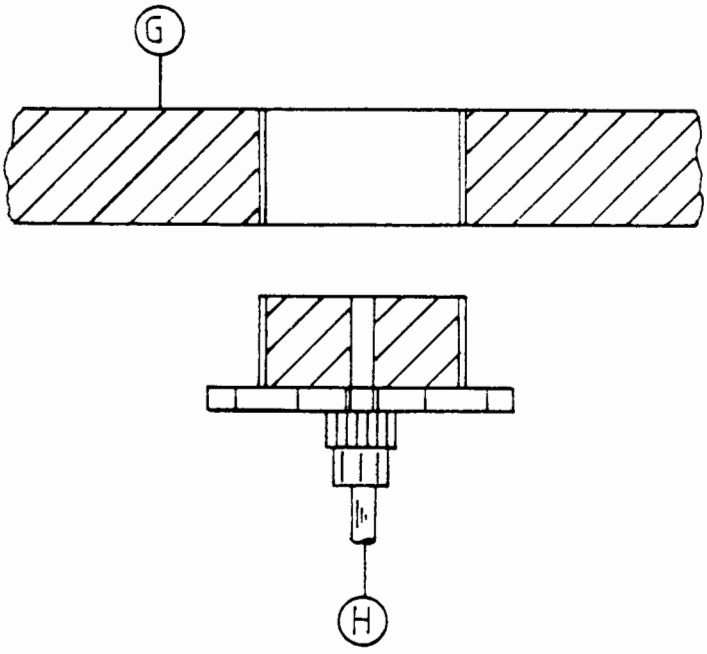

Figure 4.10 - Base pressure ports

Figures 4.8, 4.9 and 4.10

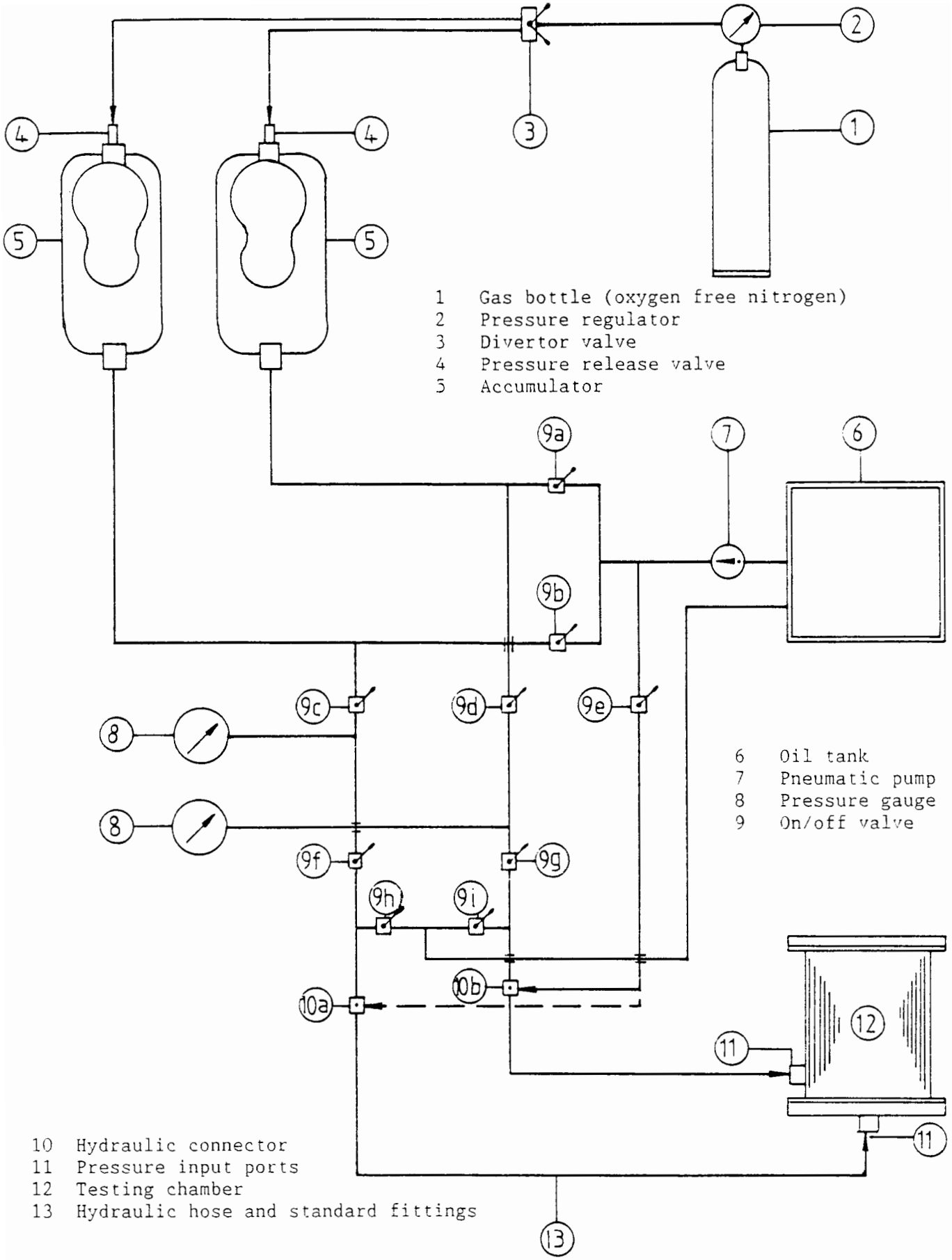

Figure 4.11 - Testing chamber pressurisation system

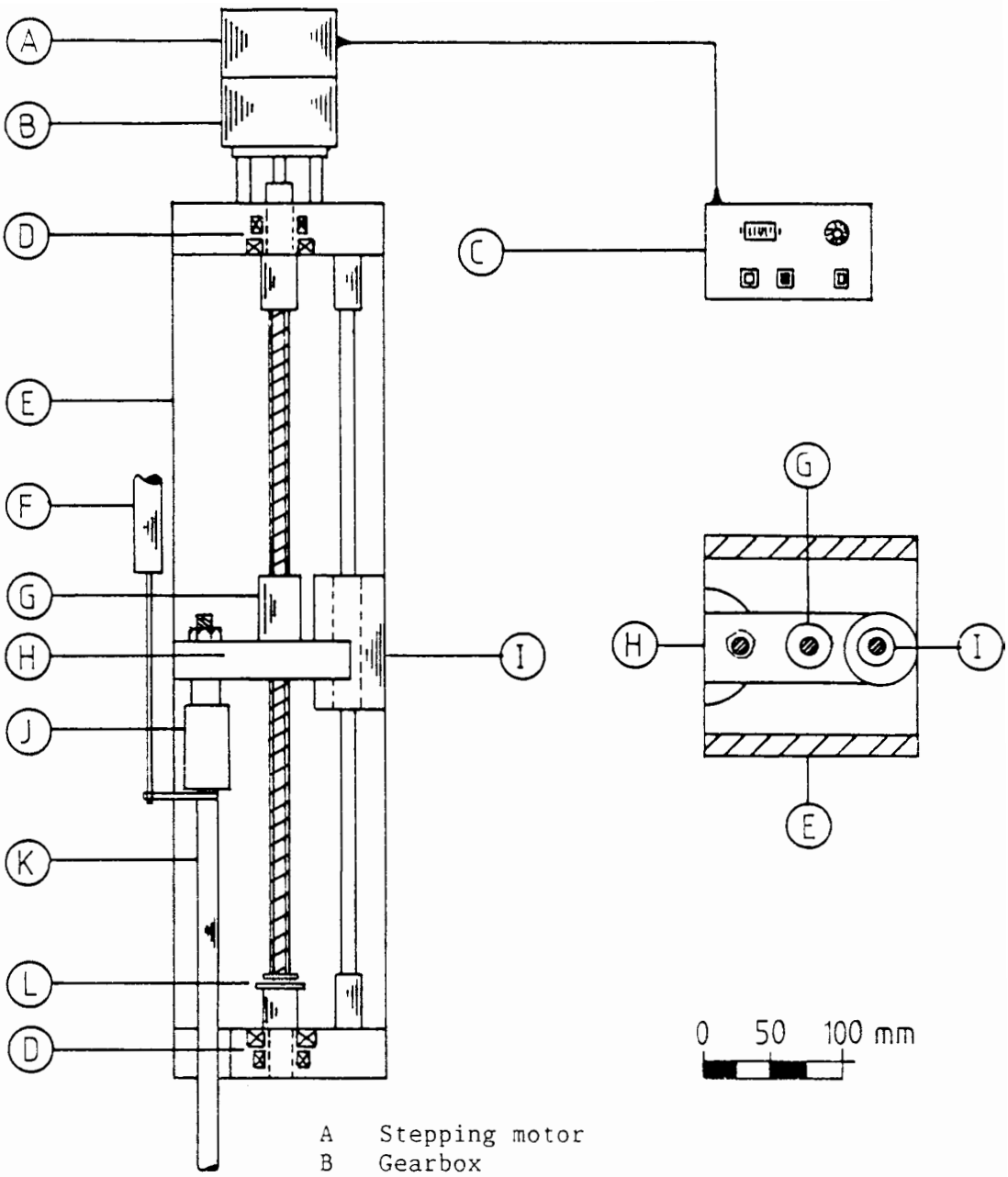

A Stepping motor
B Gearbox
C Stepping motor control box
D Radial and thrust bearings
E Support frame
F LVDT
G Ball screw and thread
H Load transmission plate
I Restraint fixing
J Load transducer
K Model pile
L Thread adjustment nut

Figure 4.12 - Jacking mechanism

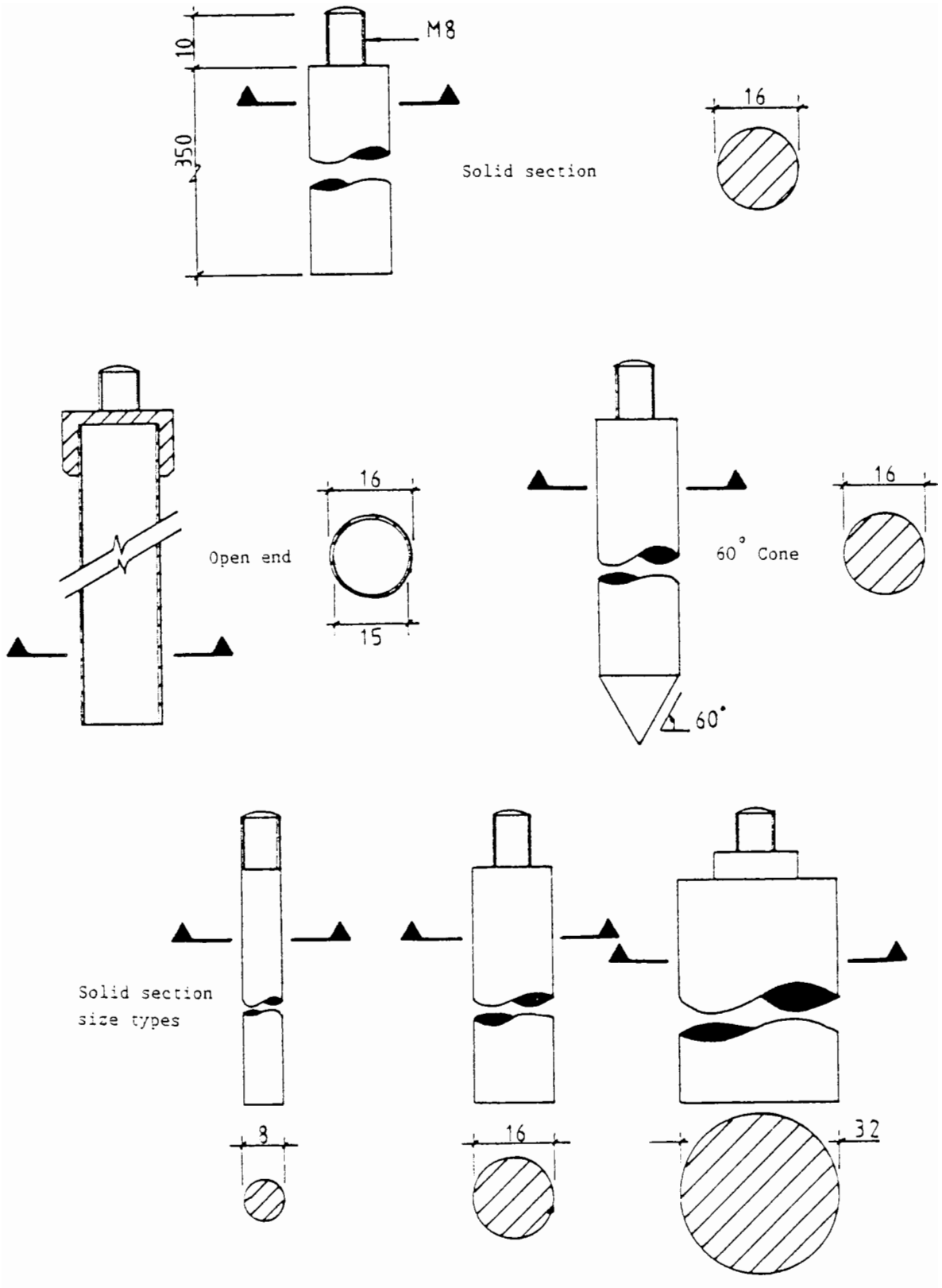

Figure 4.13 - Model piles (all dimensions in millimetres)

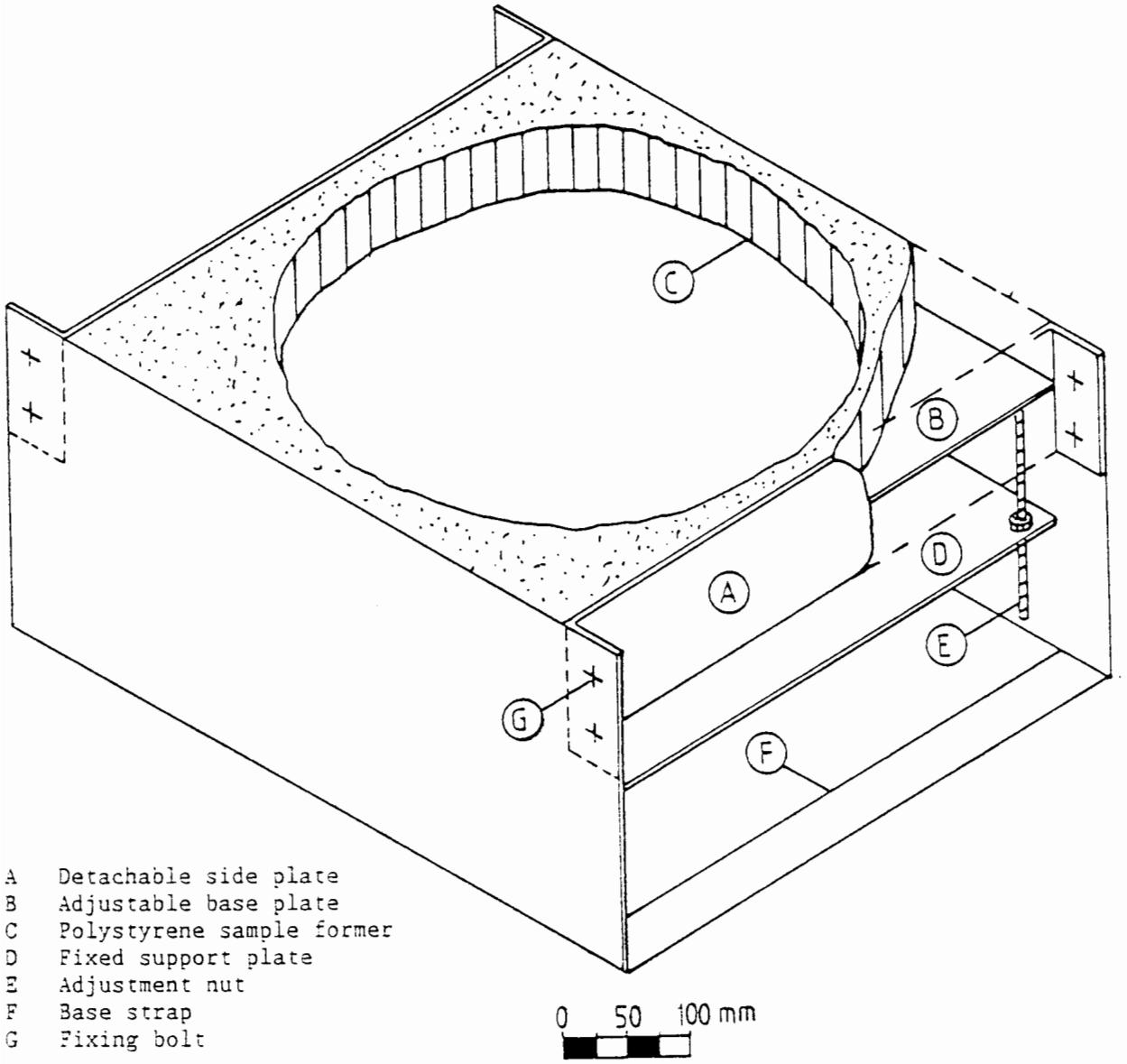

Figure 4.14 - Cemented sample preparation mould

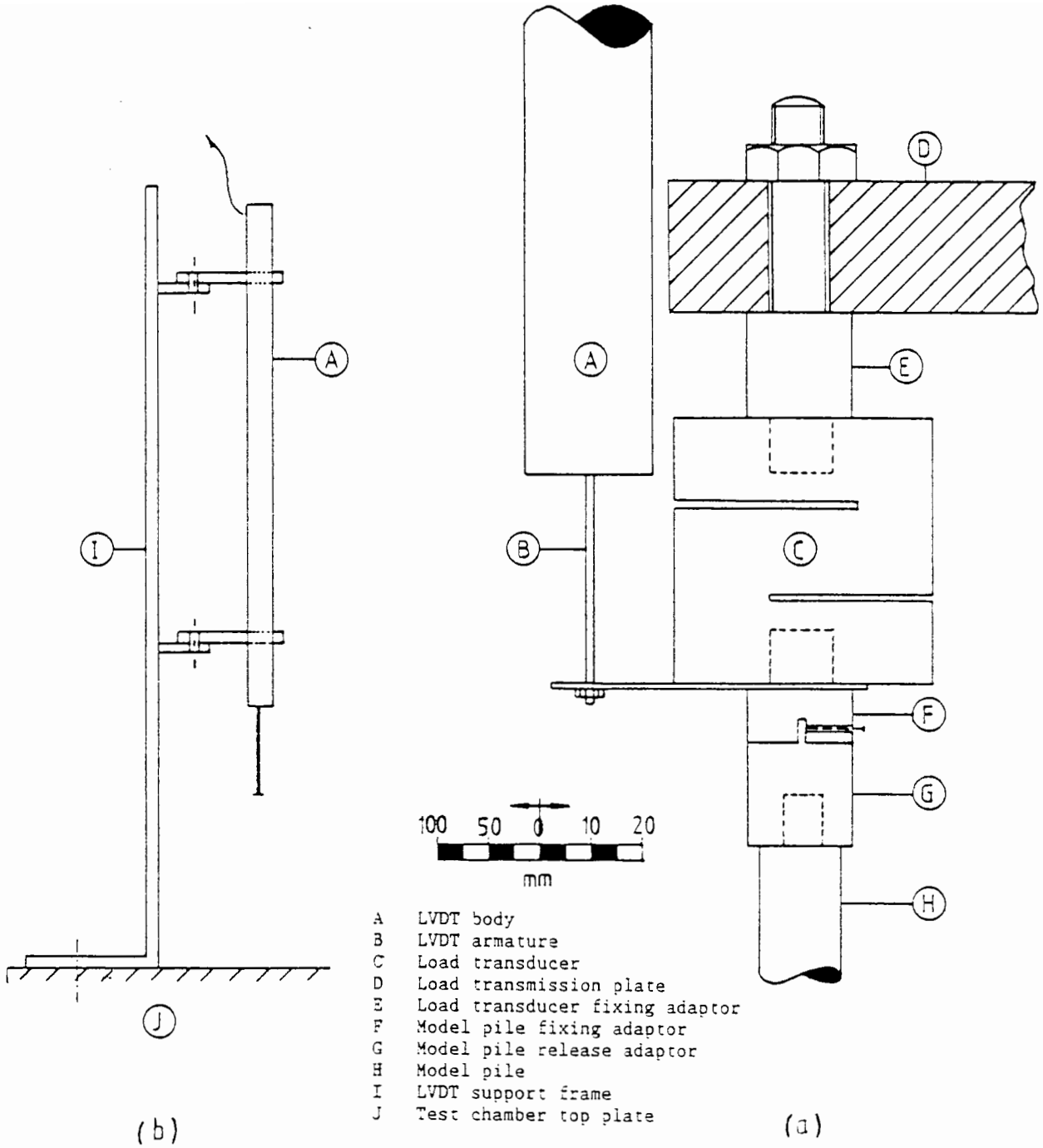

Figure 4.15 a,b - Instrumentation details

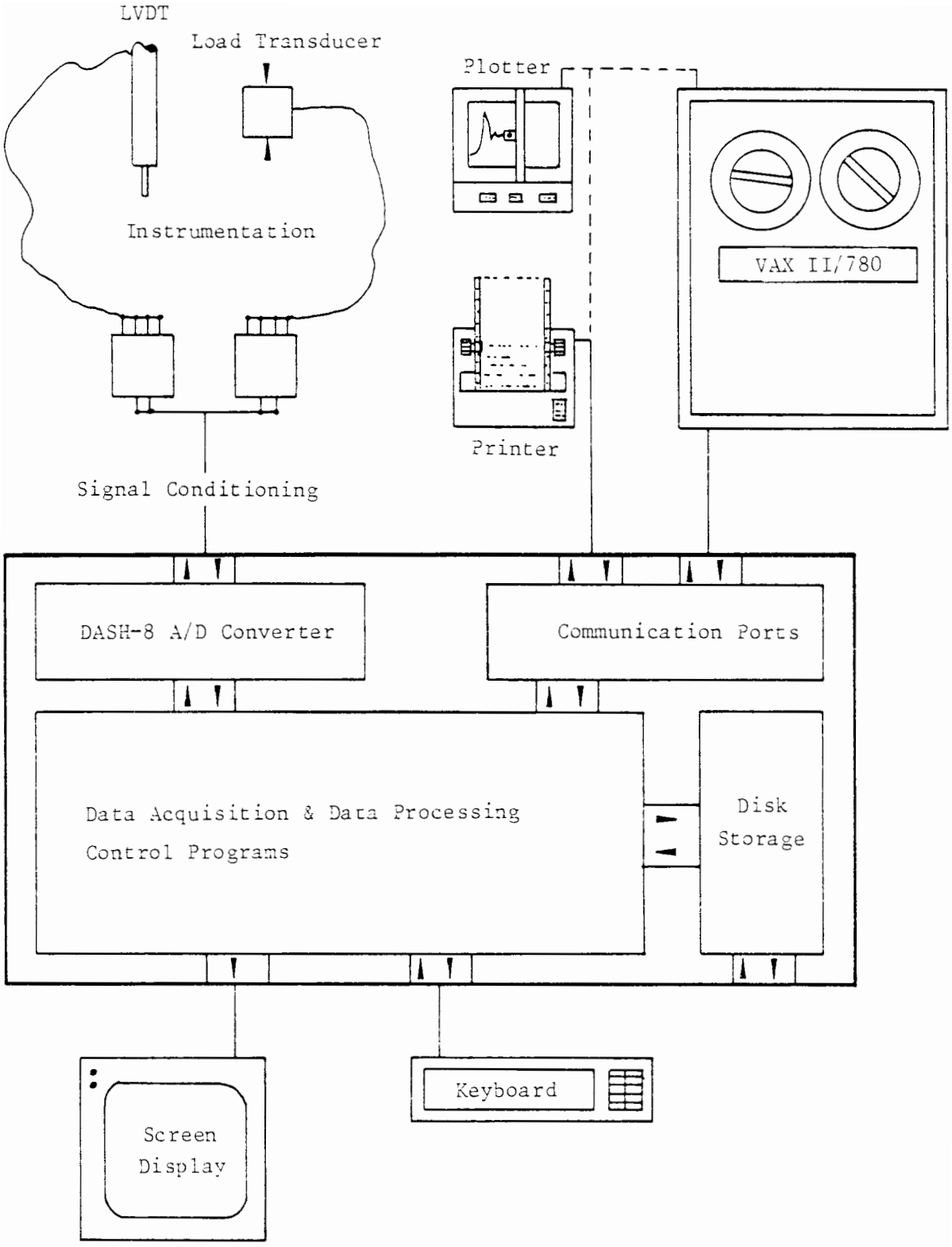

Figure 4.16 - Schematic diagram of data acquisition system

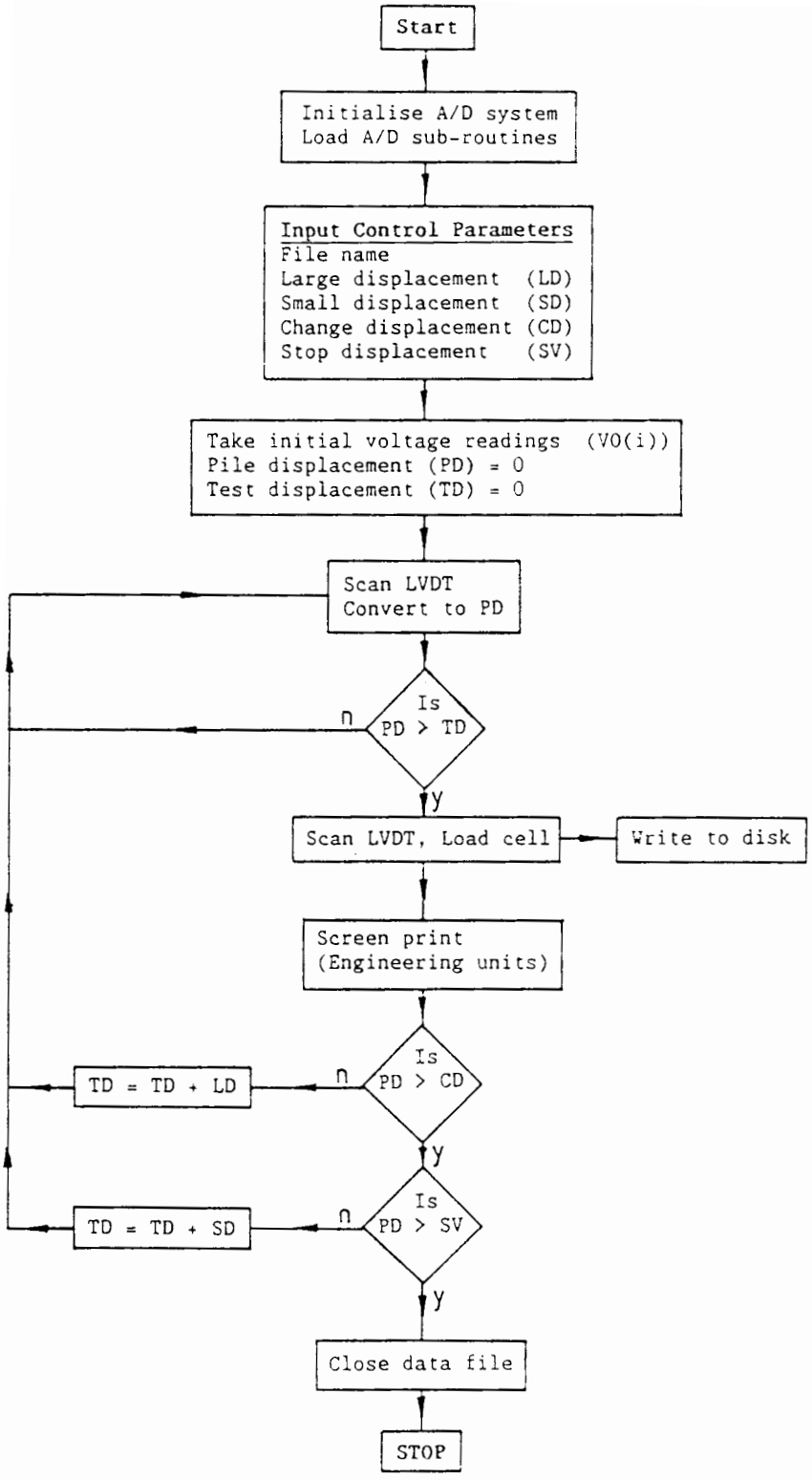

Figure 4.17 - Data acquisition program flow chart

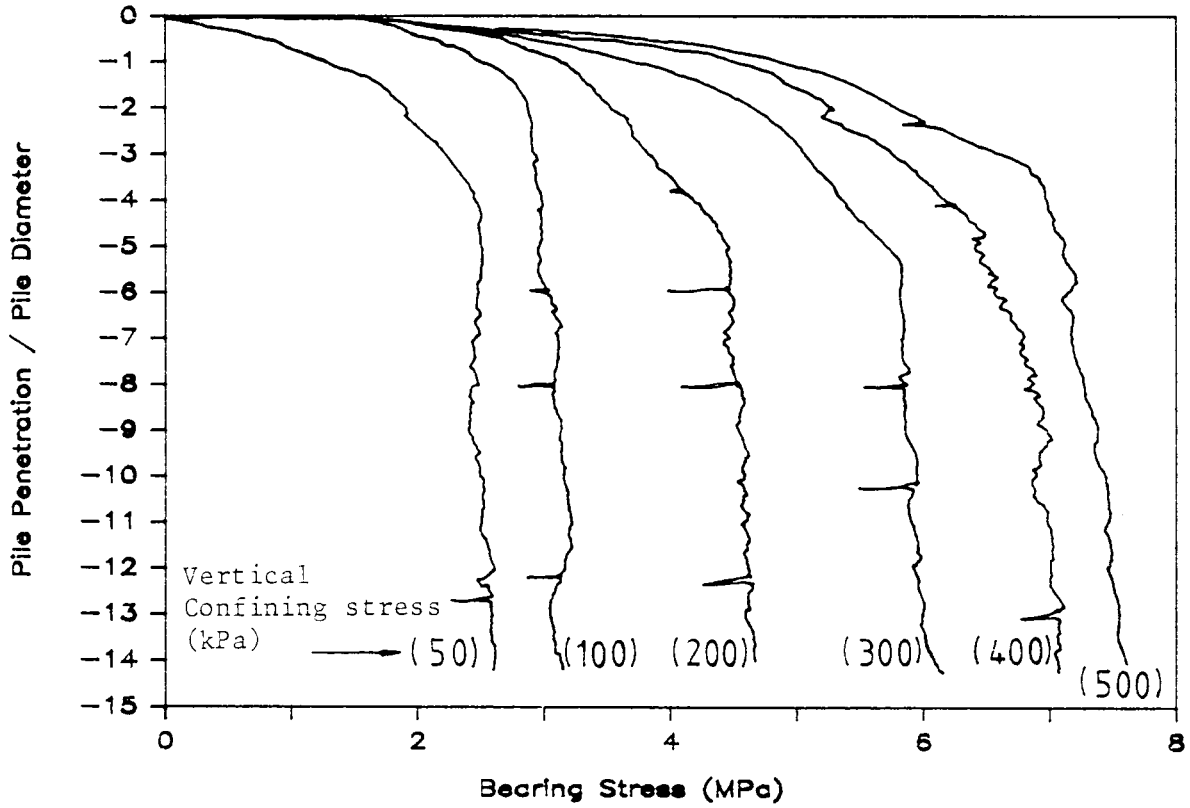

Figure 5.1 - Effect of confining stress on bearing stress response

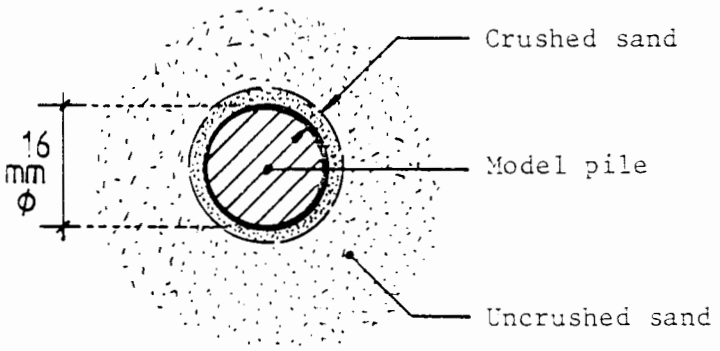

Figure 5.2 - Annulus of crushed material formed during pile installation

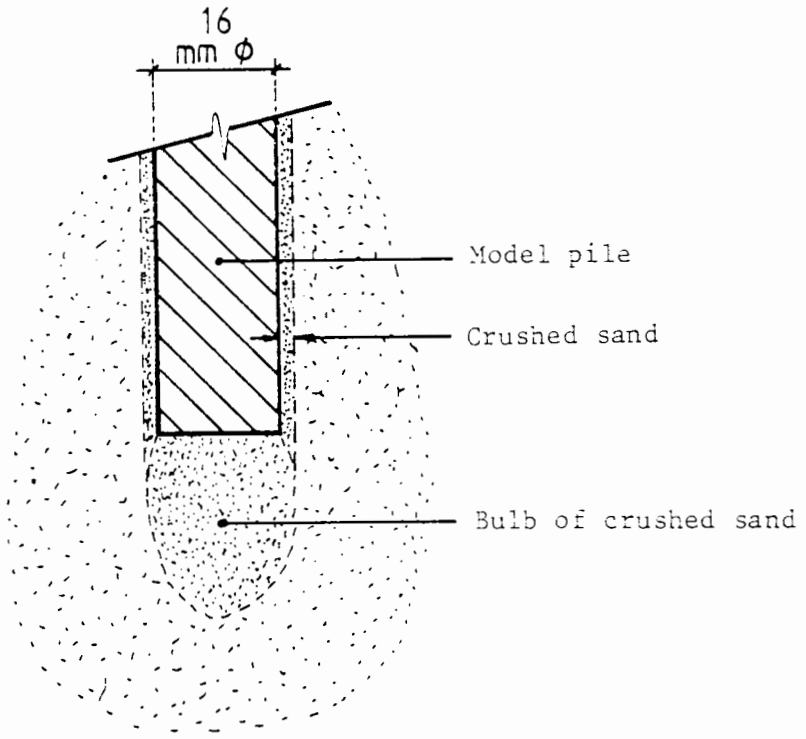

Figure 5.3 - Bulb of crushed material formed during pile installation

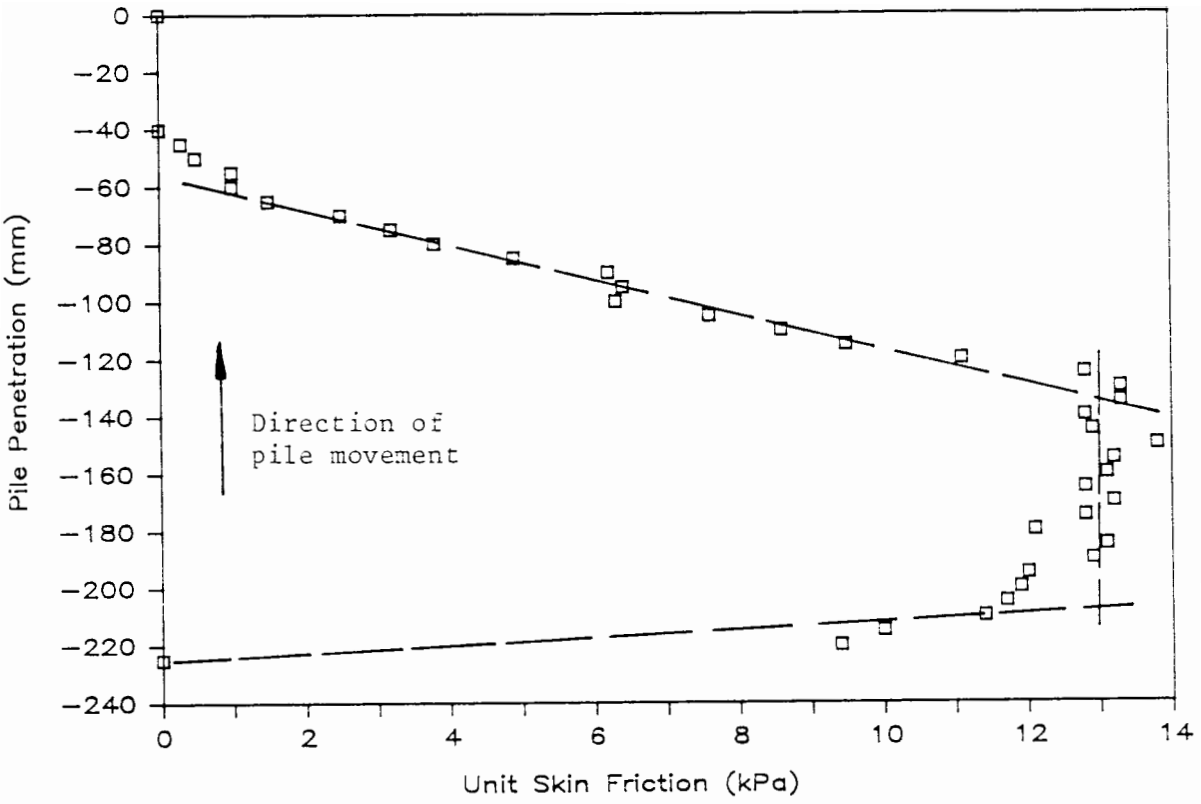

Figure 5.4 - Skin friction values determined from pull-out test

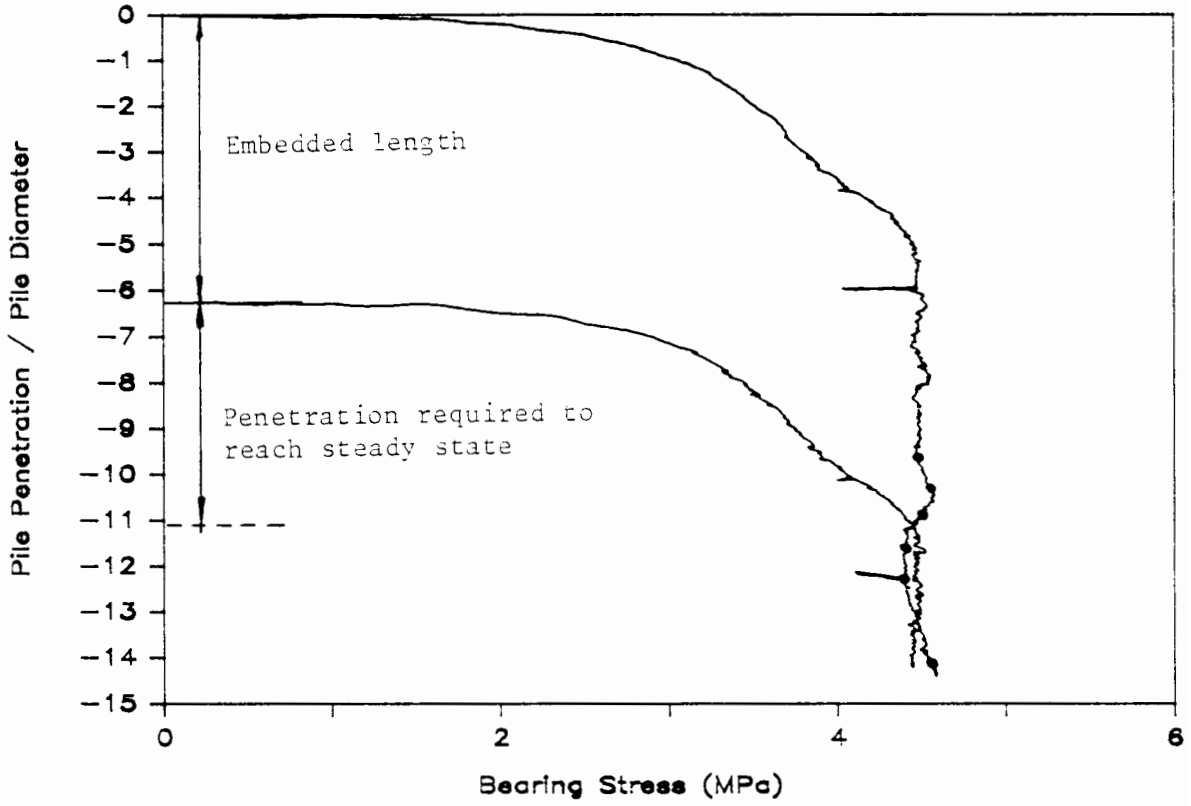

Figure 5.5 - Aperture effect

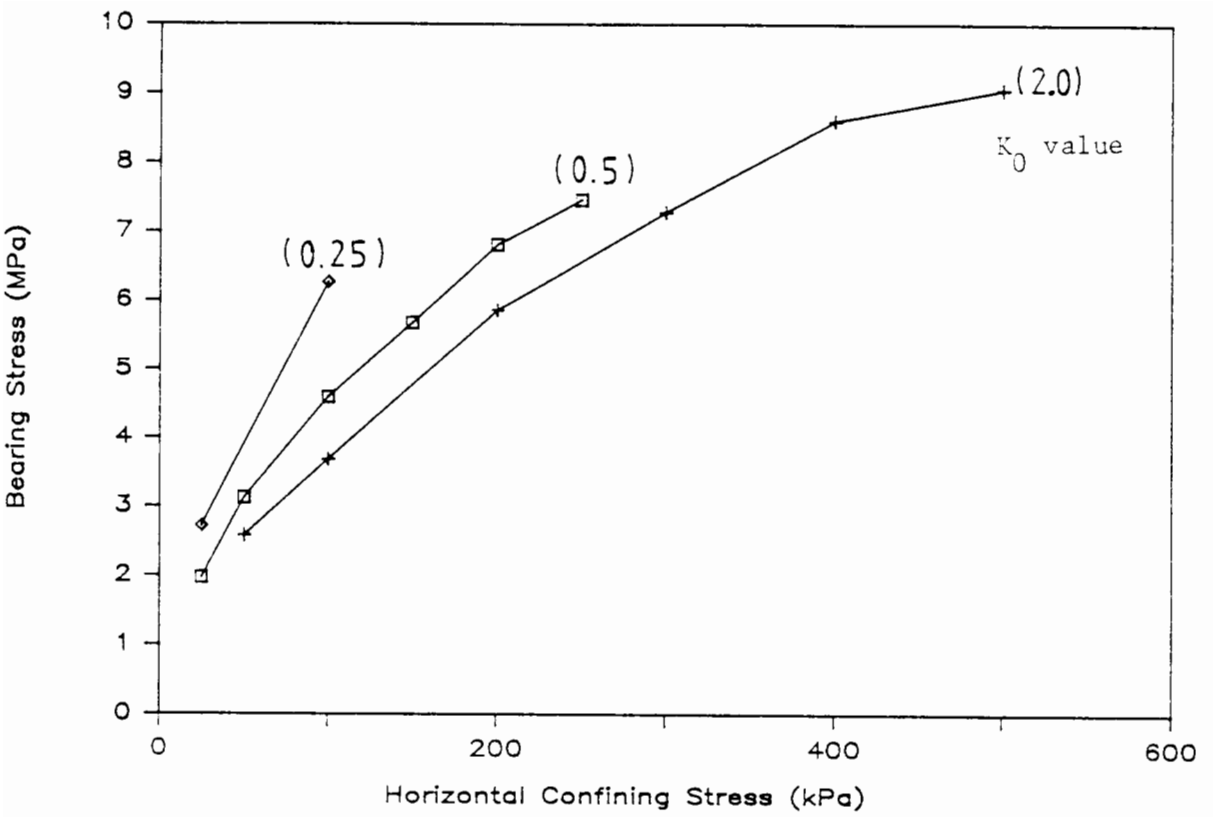

Figure 5.6 - Variation of bearing stress with horizontal confining stress

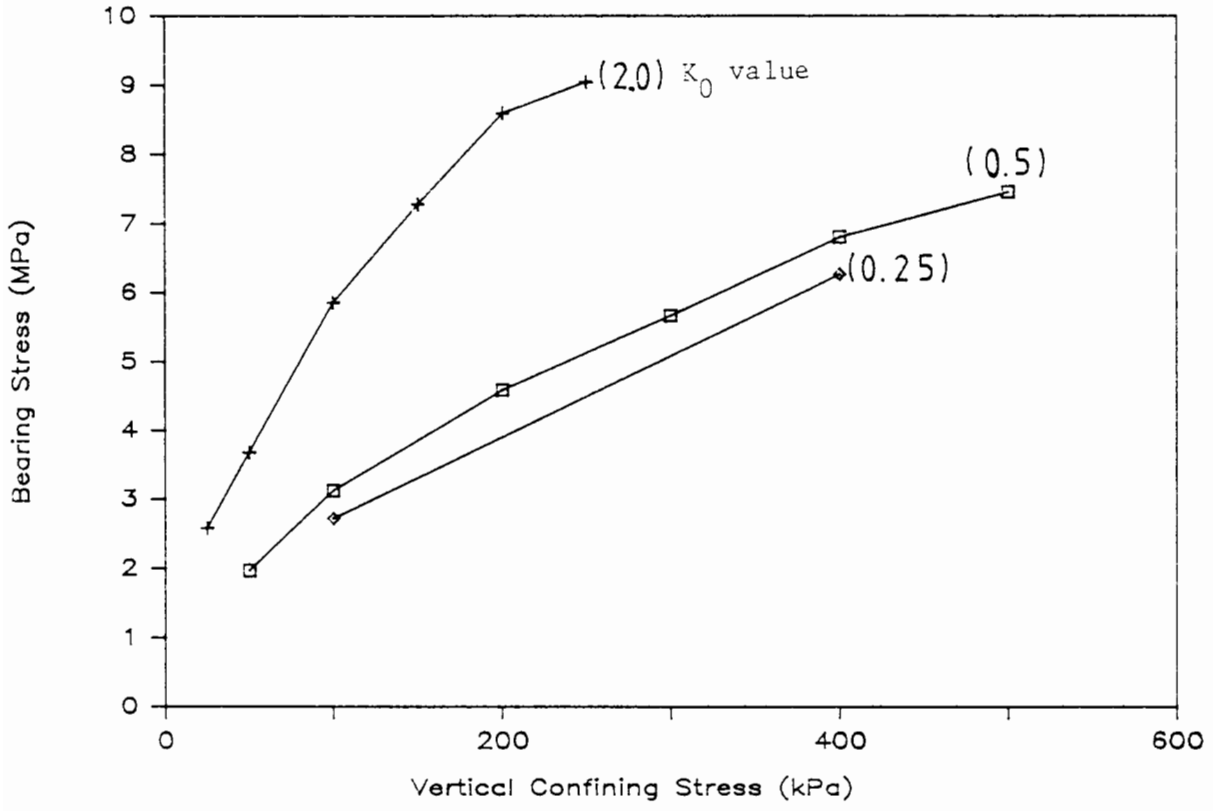

Figure 5.7 - Variation of bearing stress with vertical confining stress

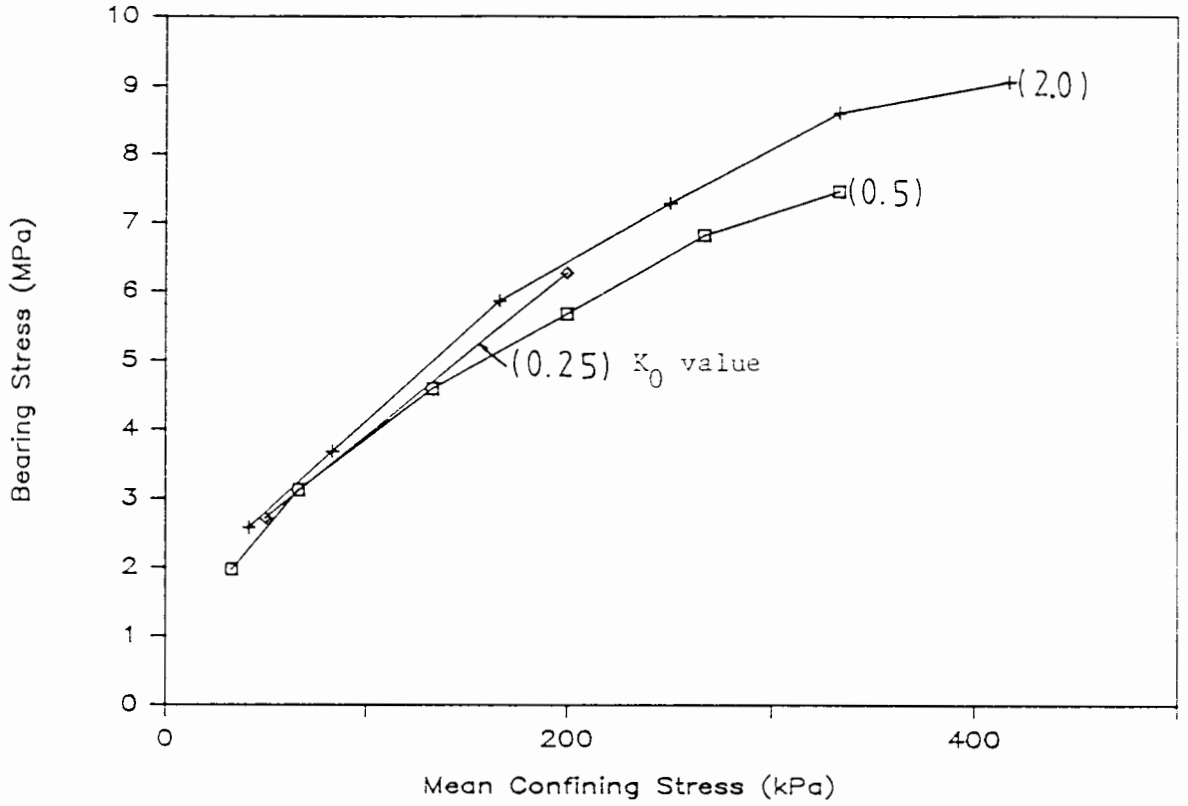

Figure 5.8 - Variation of bearing stress with mean confining stress

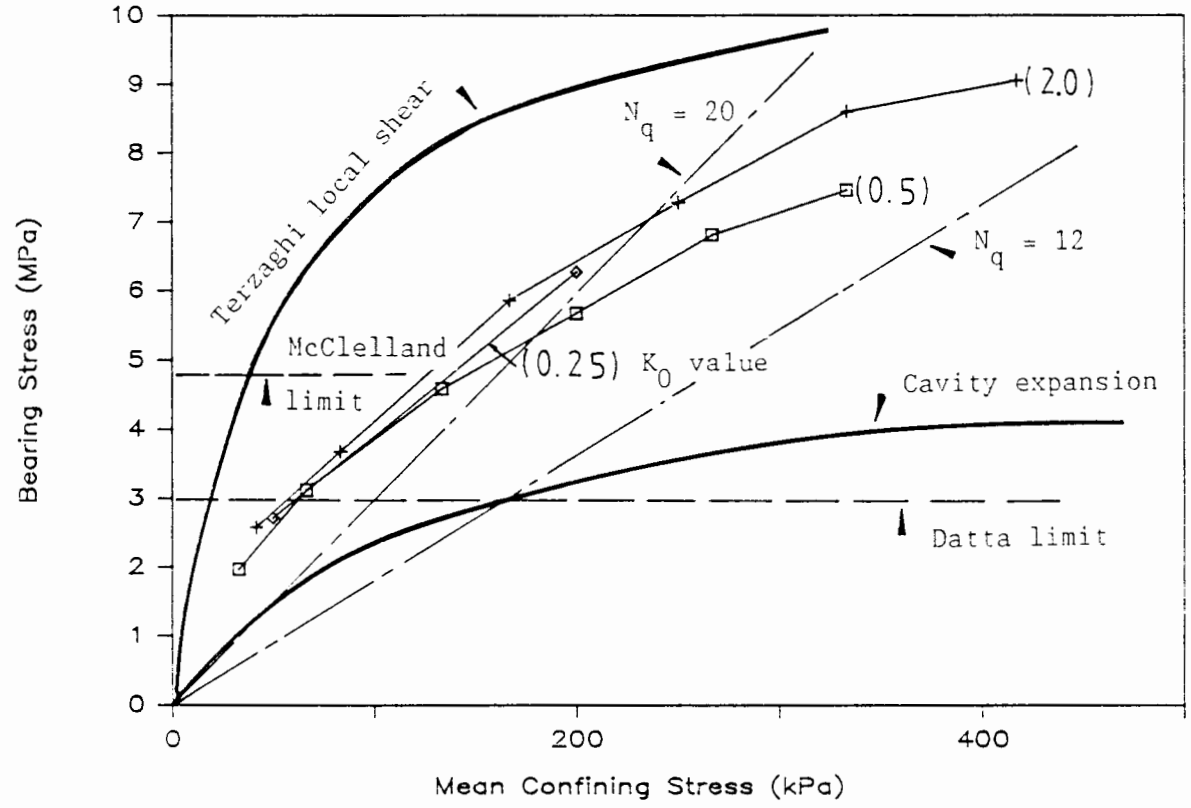

Figure 5.9 - Comparison of end bearing capacity solutions

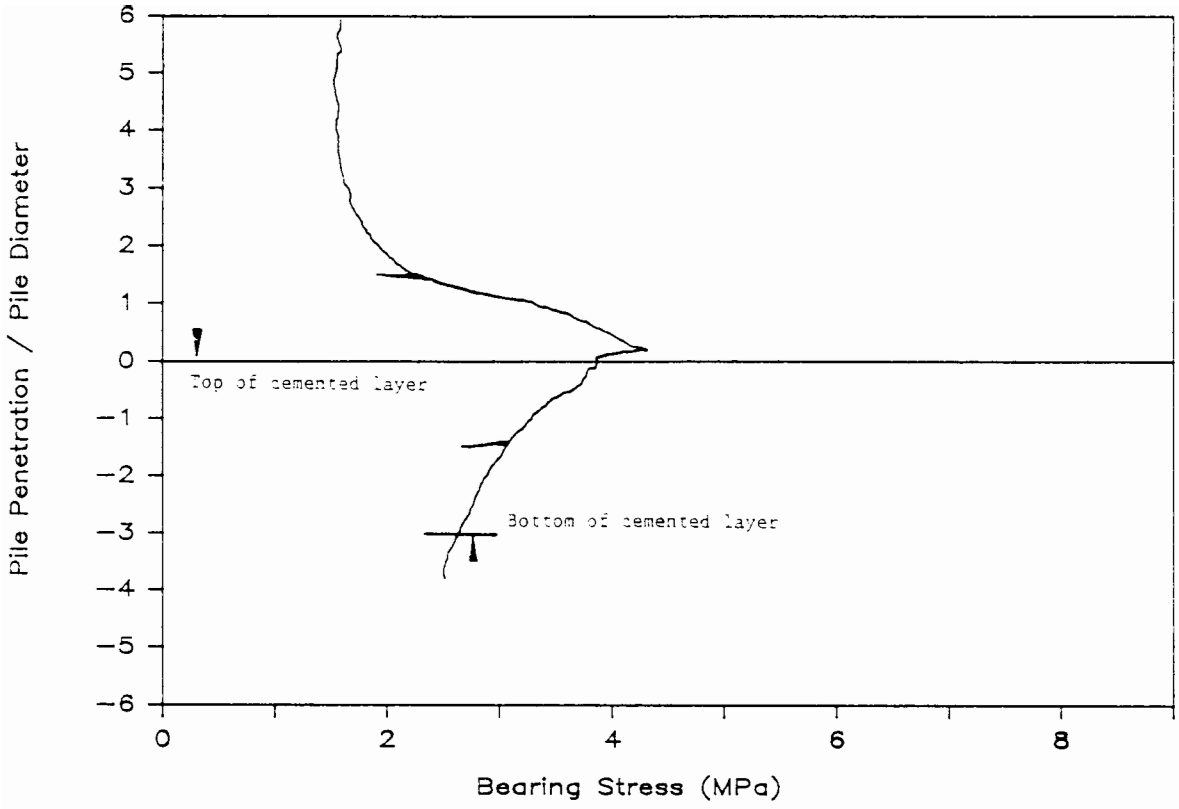

Figure 6.1 - Standard format of test results

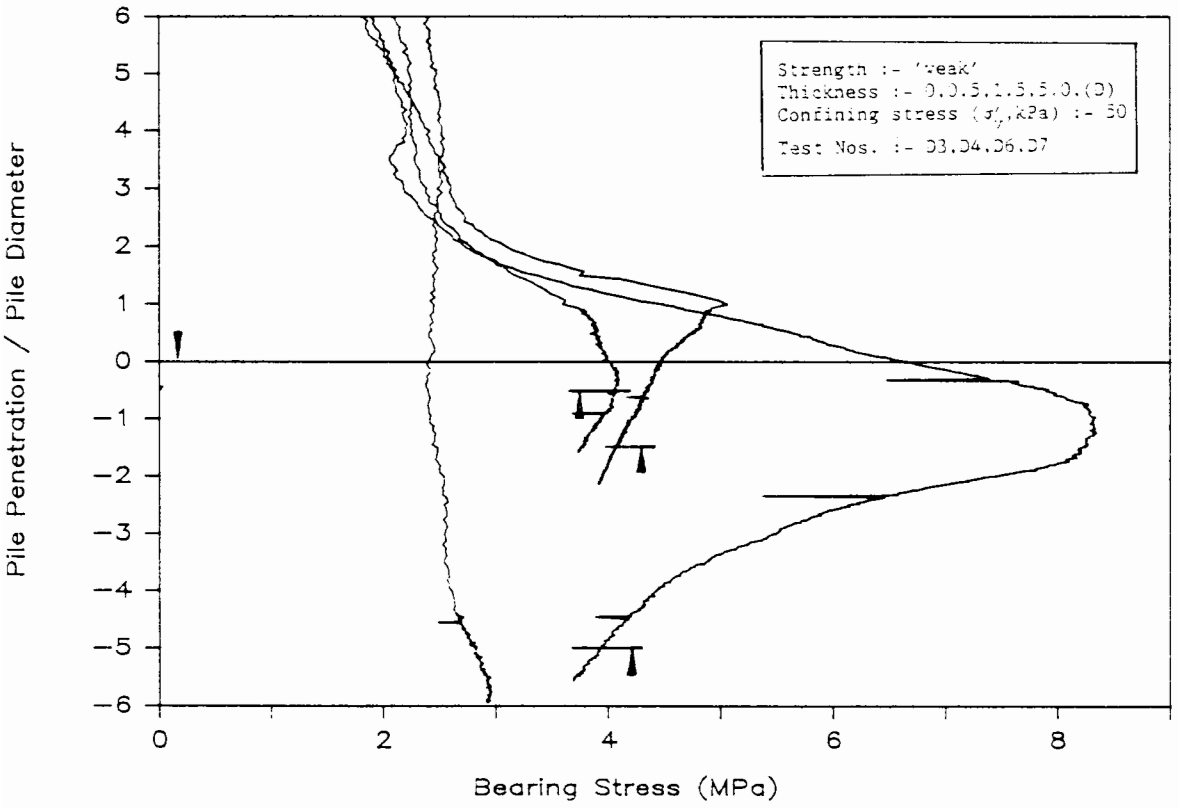

Figure 6.2 - Basic test series (1/6)

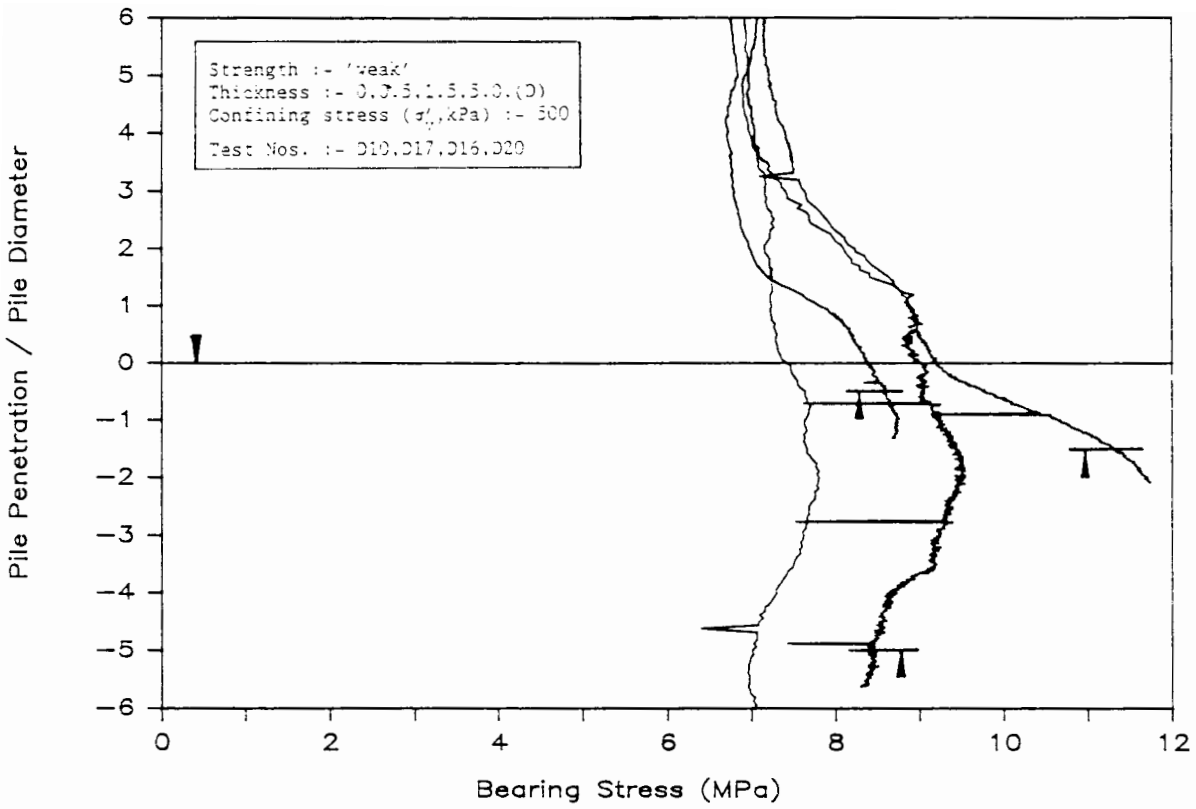

Figure 6.3 - Basic test series (2/6)

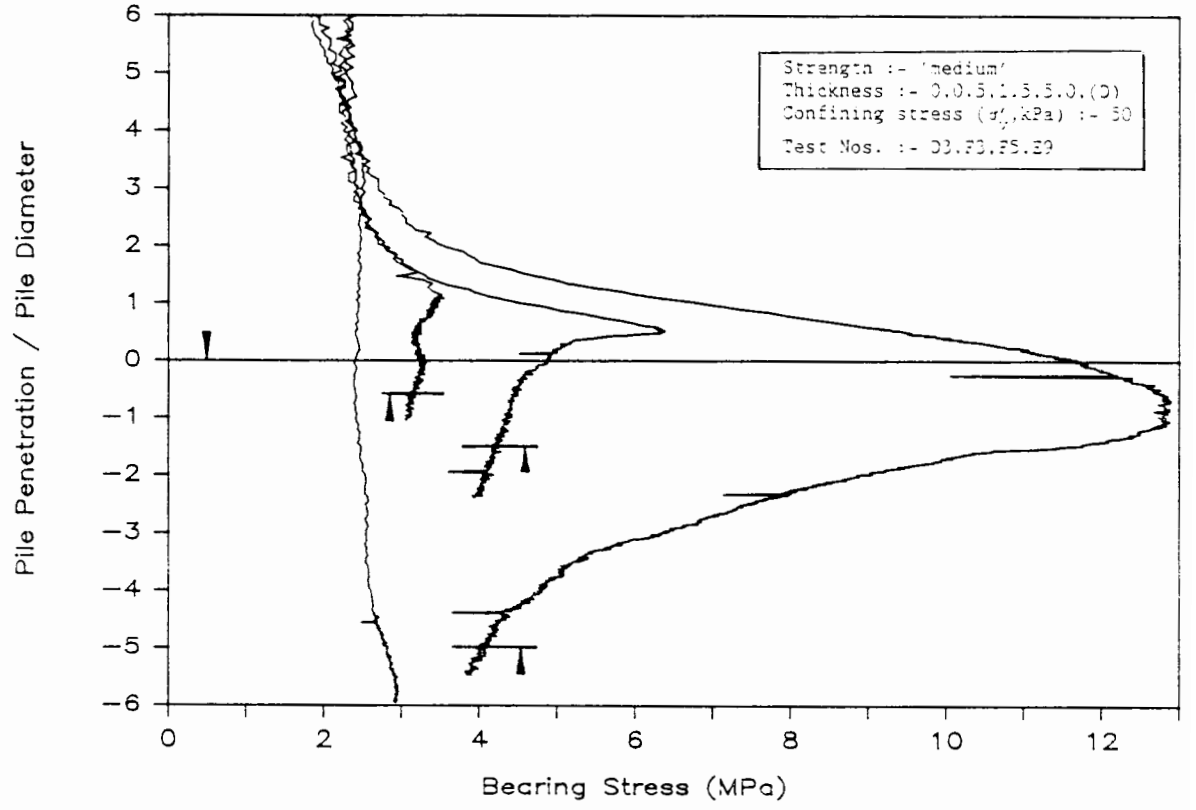

Figure 6.4 - Basic test series (3/6)

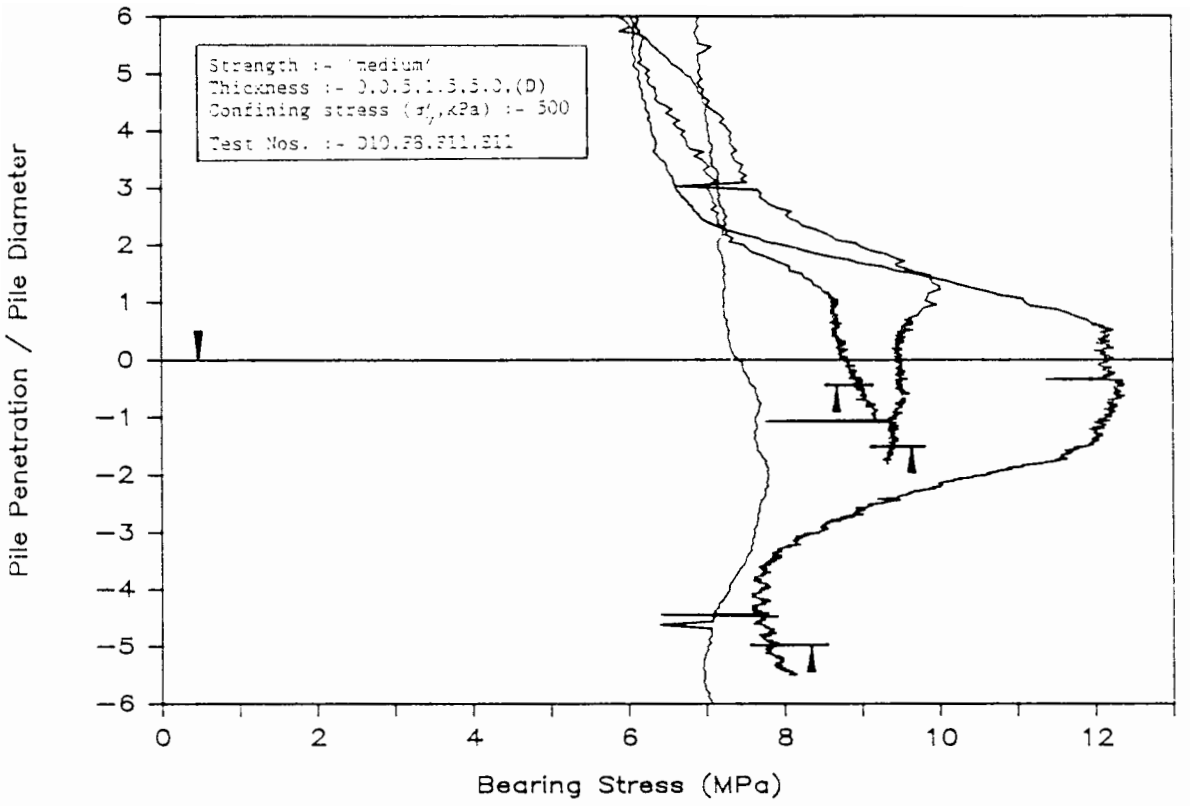

Figure 6.5 - Basic test series (4/6)

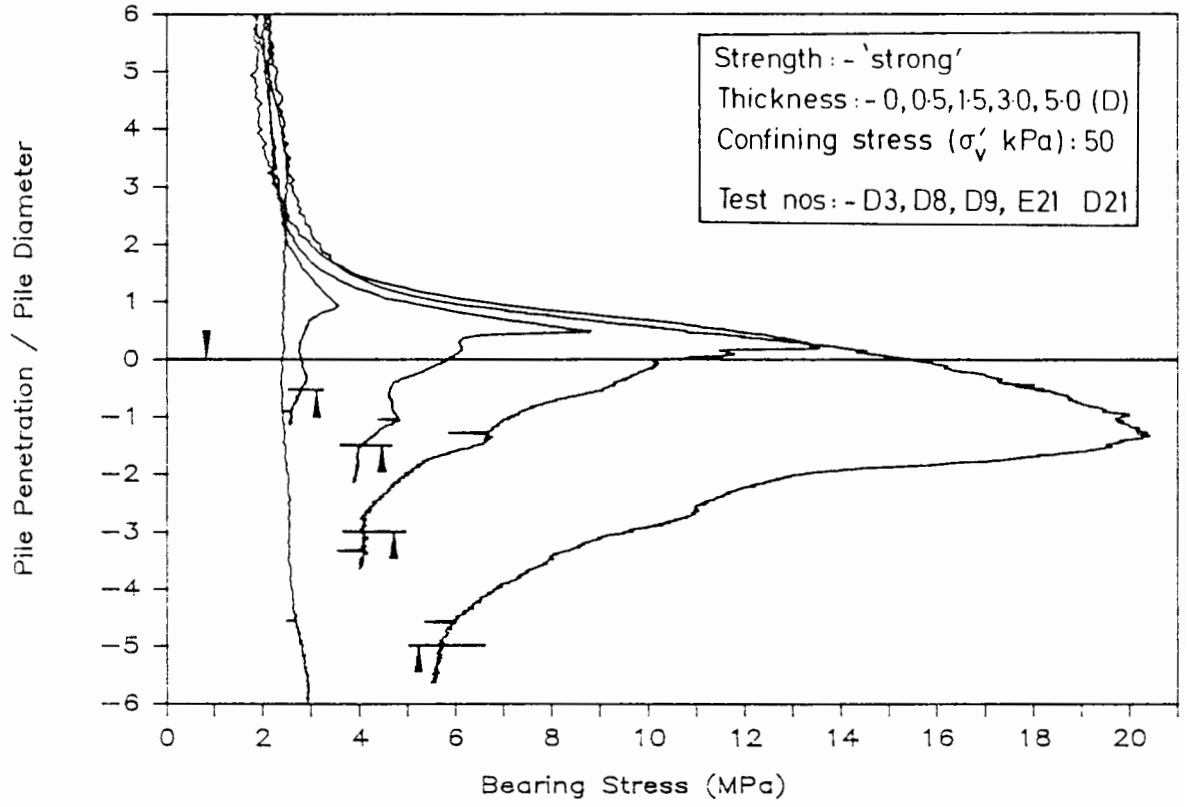

Figure 6.6 - Basic test series (5/6)

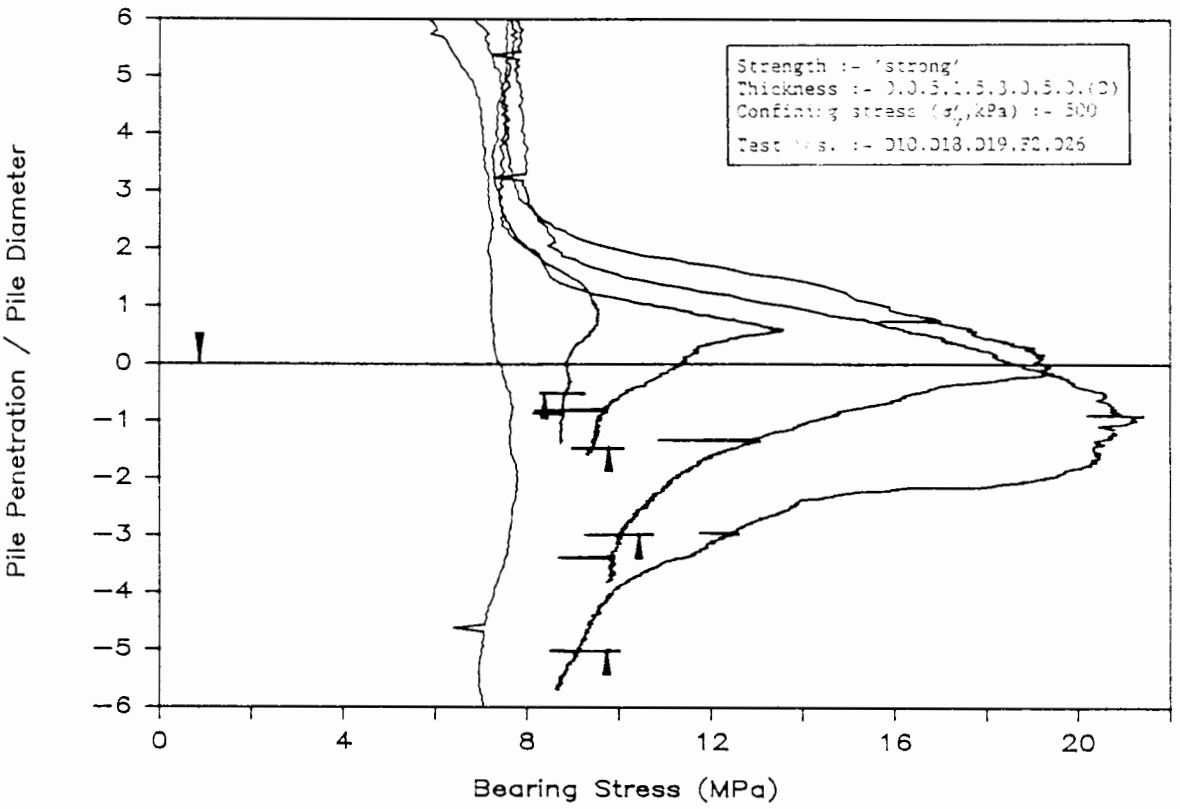

Figure 6.7 - Basic test series (6/6)

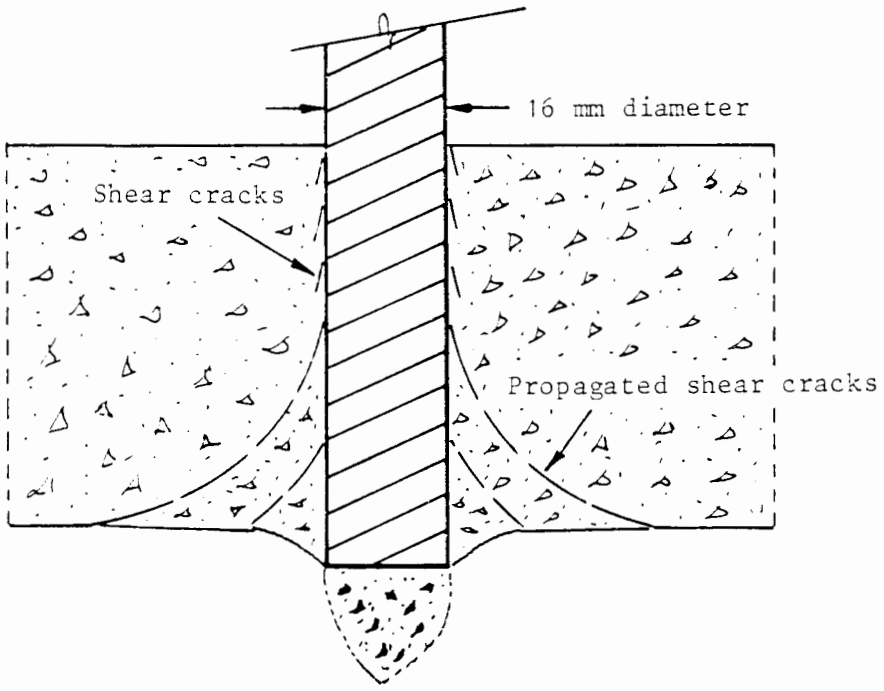

Figure 6.8 - Brittle failure mechanism

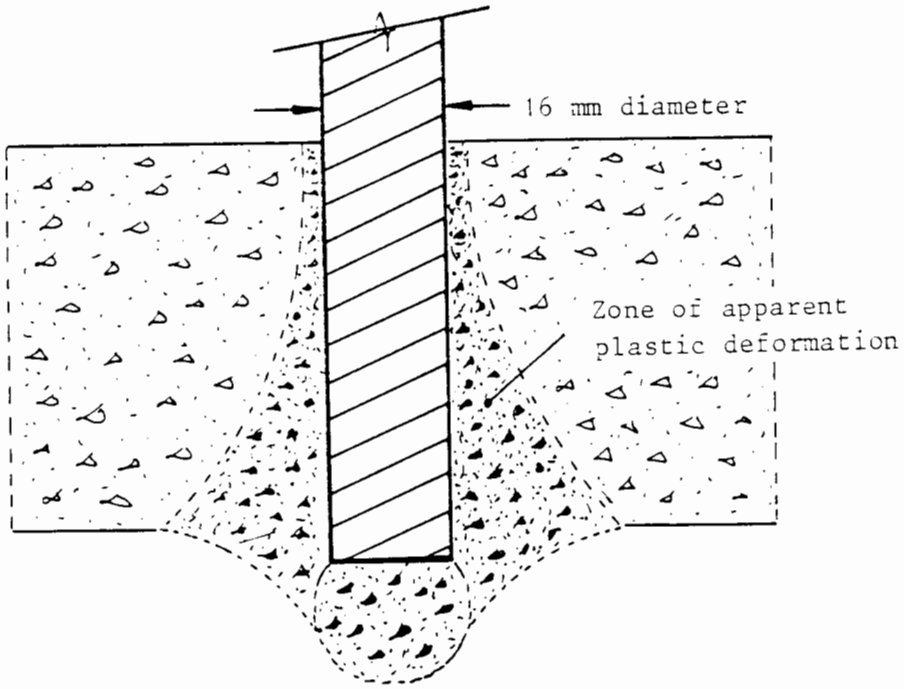

Figure 6.9 - Ductile failure mechanism

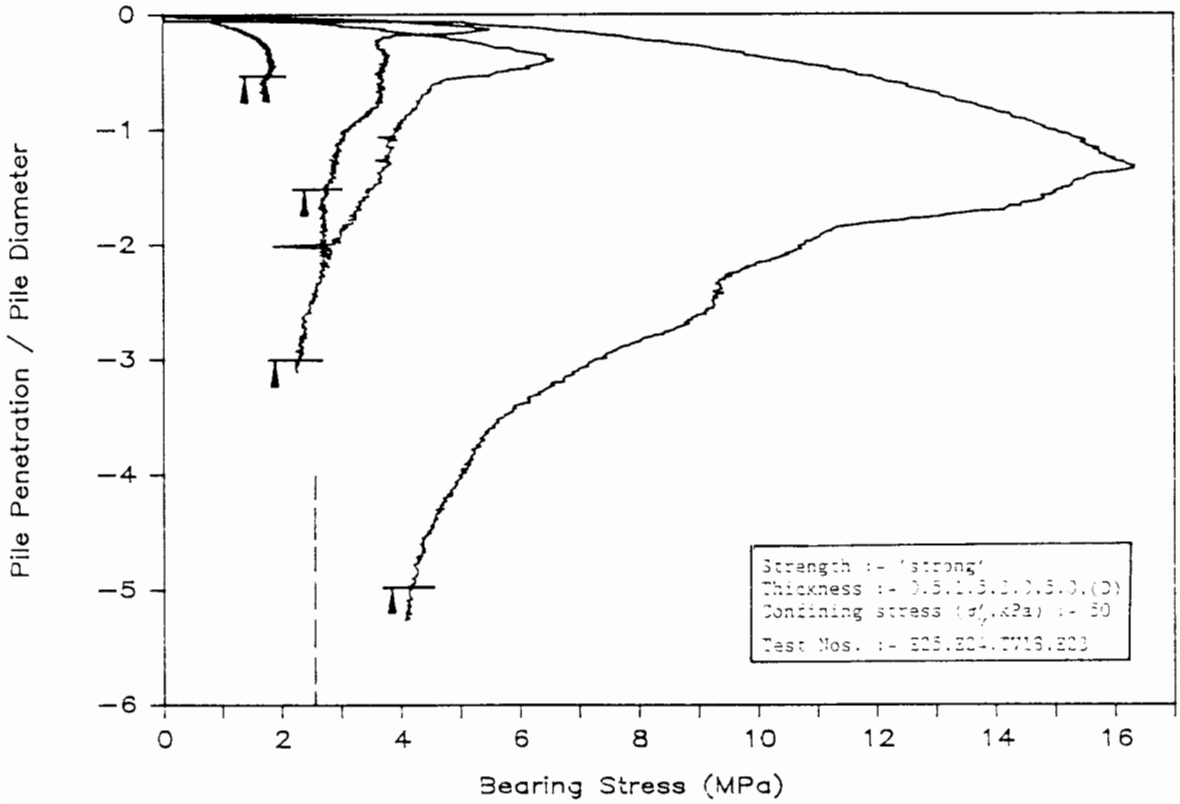

Figure 6.10 - Embedded pile test (1/2)

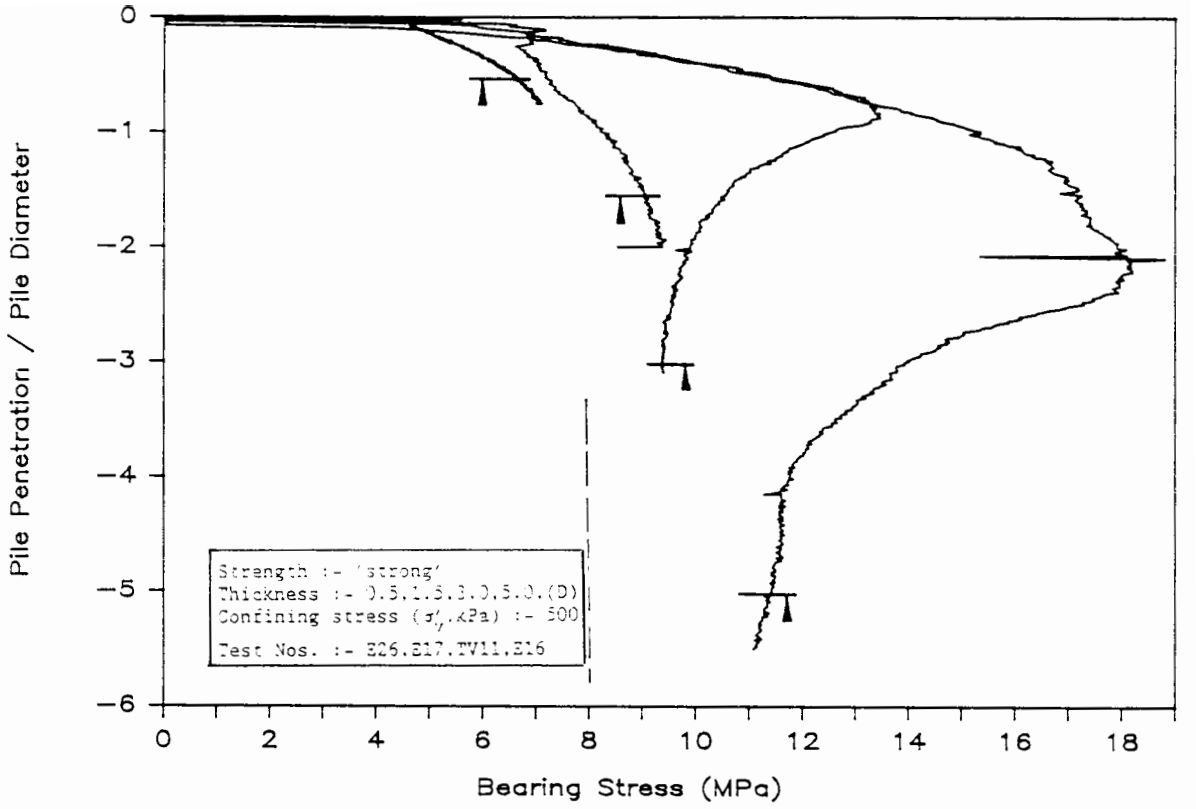

Figure 6.11 - Embedded pile test (2/2)

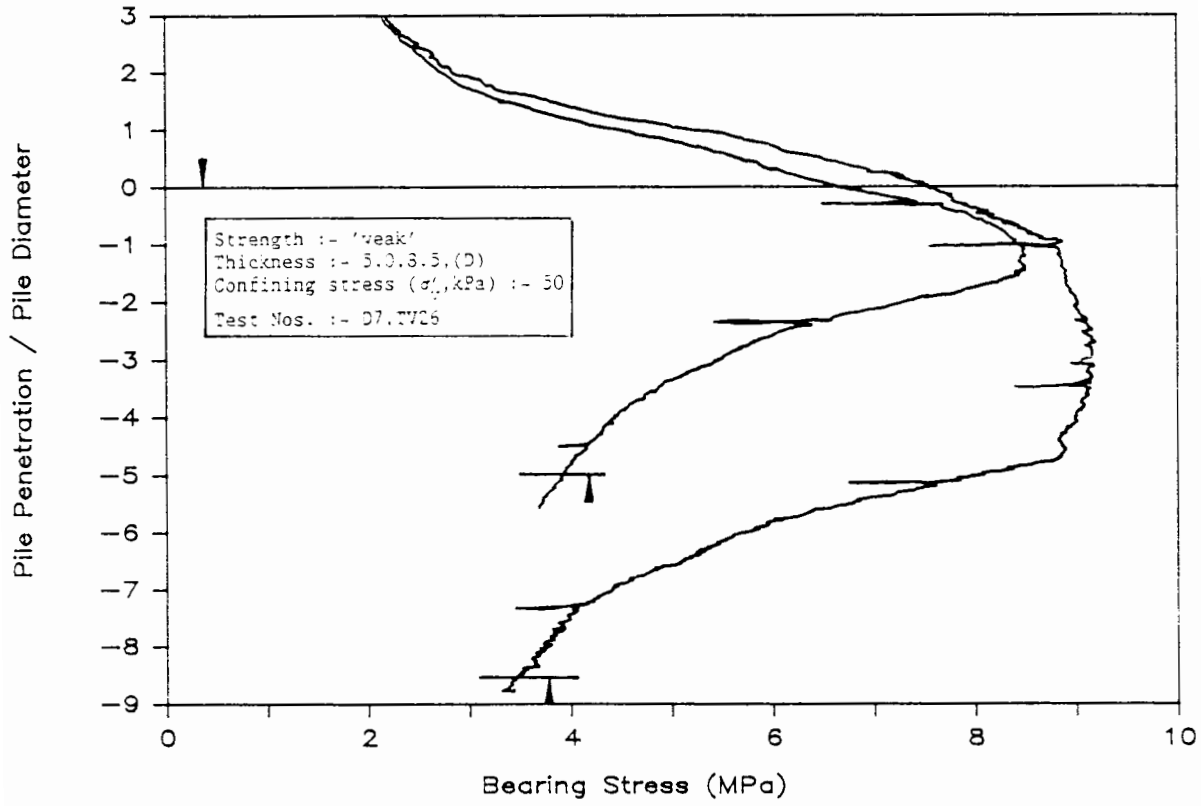

Figure 6.12 - Infinitely thick layer test (1/4)

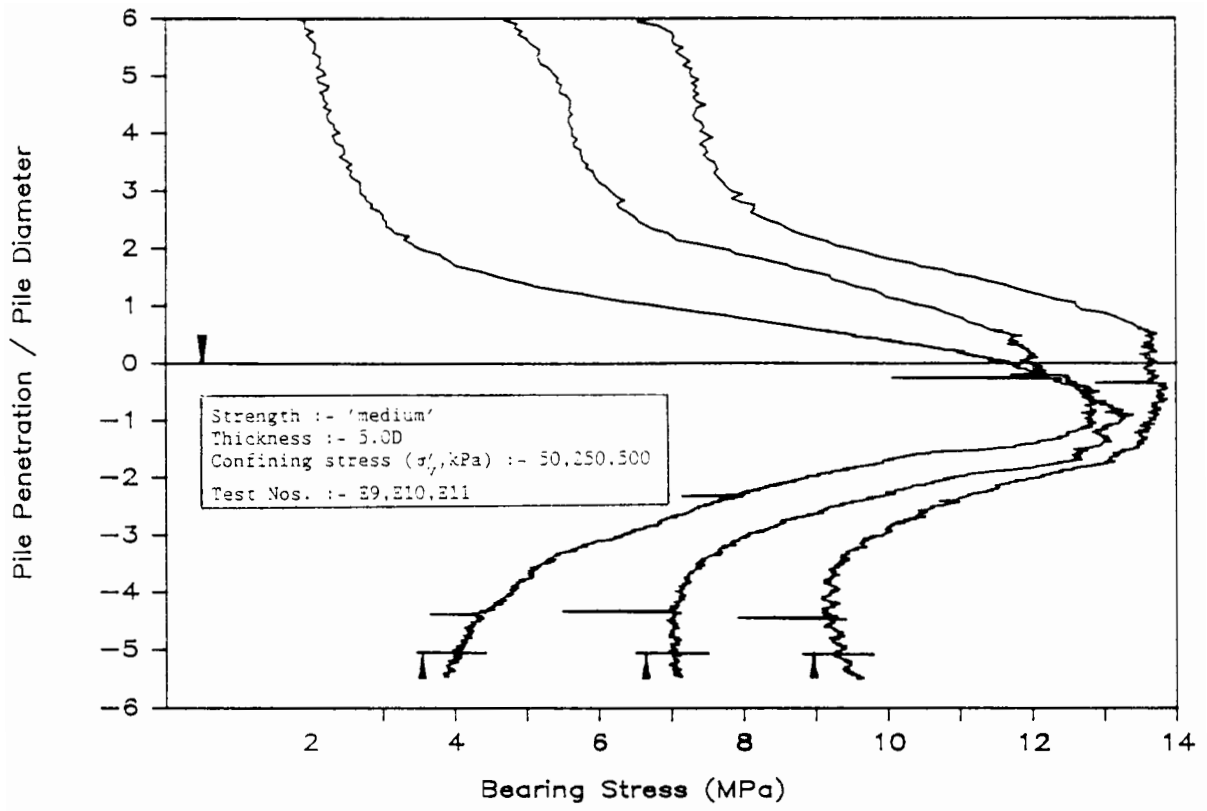

Figure 6.13 - Infinitely thick layer test (2/4)

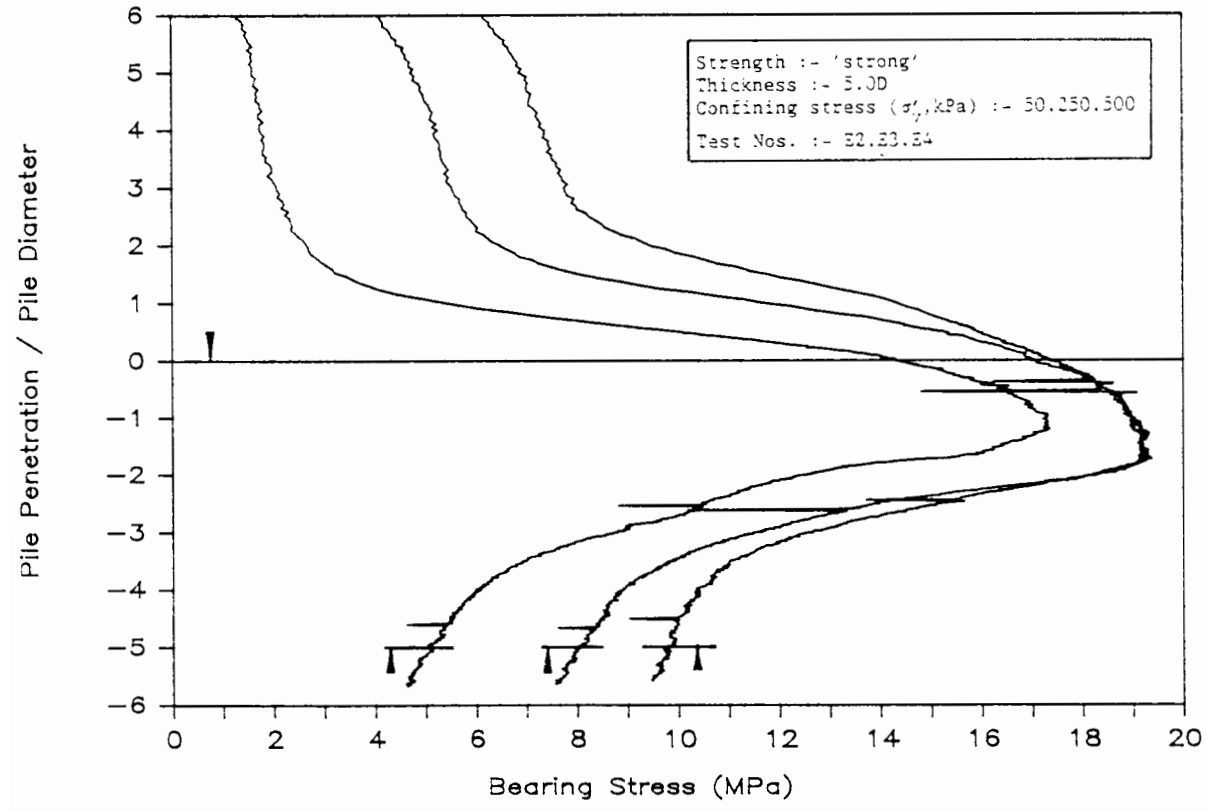

Figure 6.14 - Infinitely thick layer test (3/4)

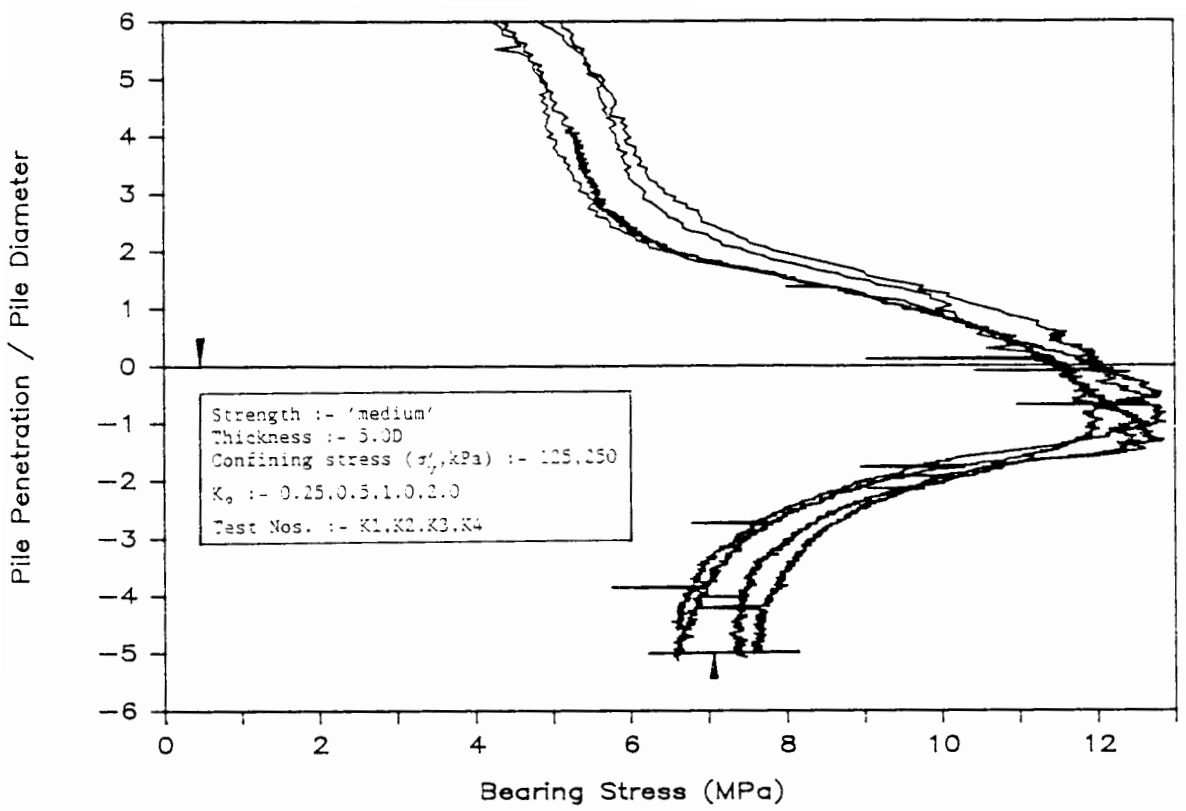

Figure 6.15 - Infinitely thick layer test (4/4)

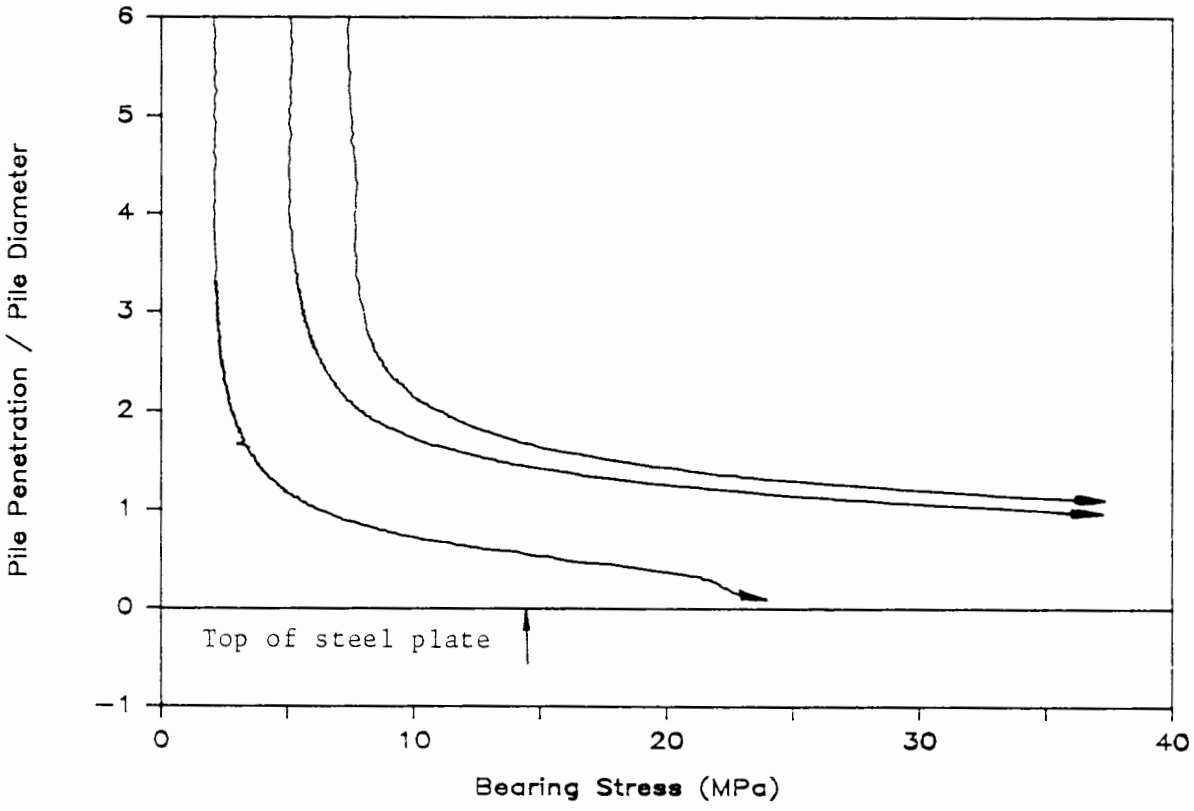

Figure 6.16 - Steel plate test results

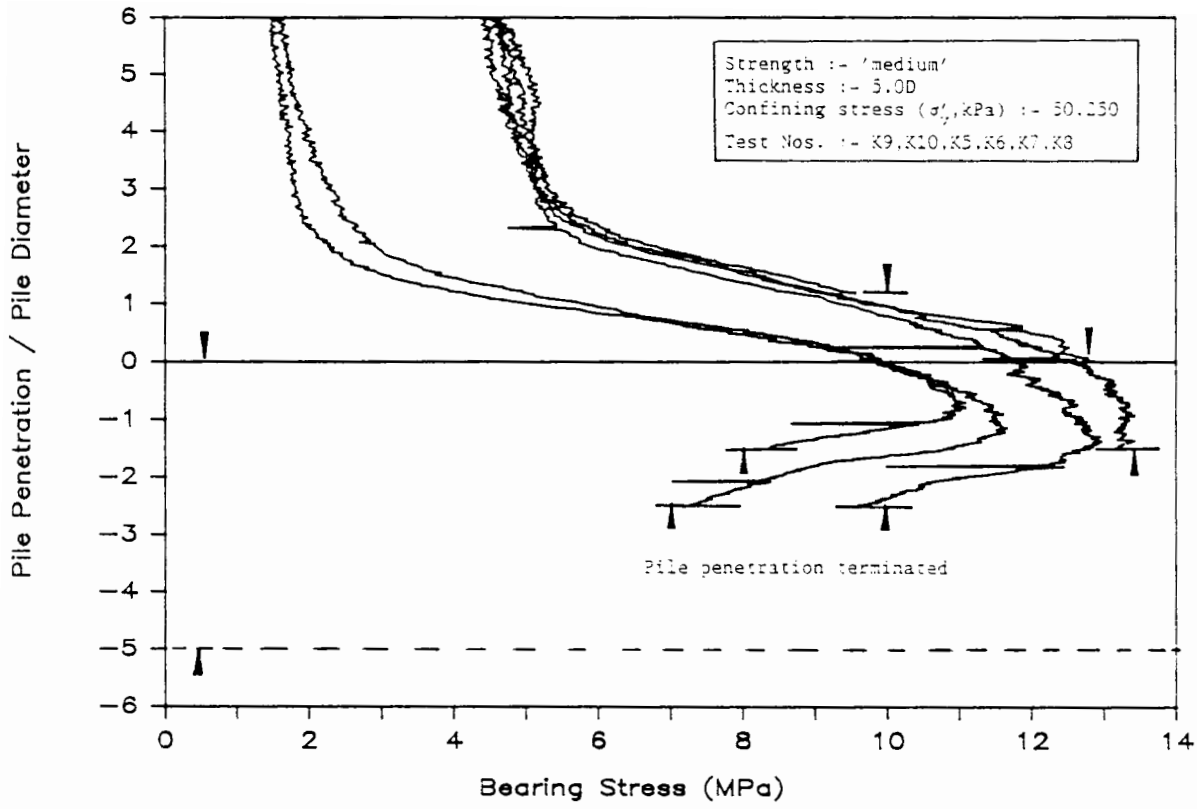

Figure 6.17 - Failure mechanism tests

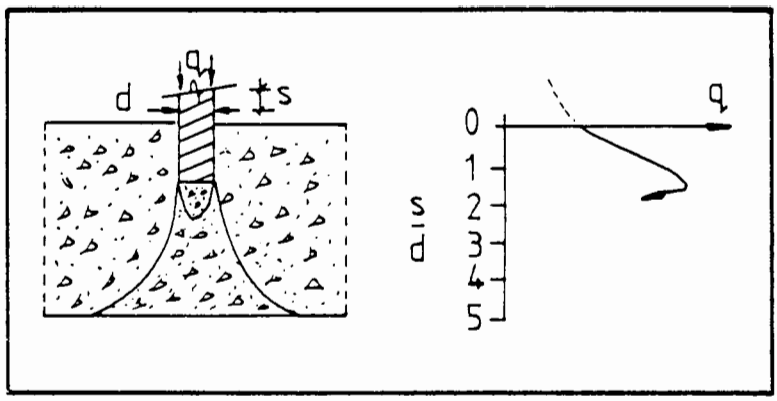

(a)

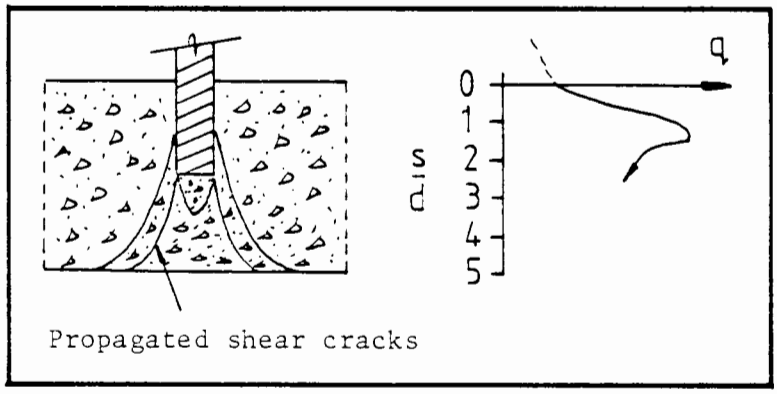

(b)

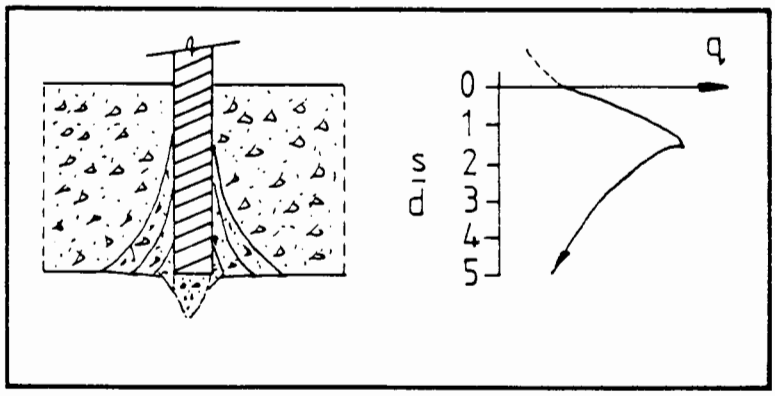

(c)

Figure 6.18 - Development of brittle failure mechanism

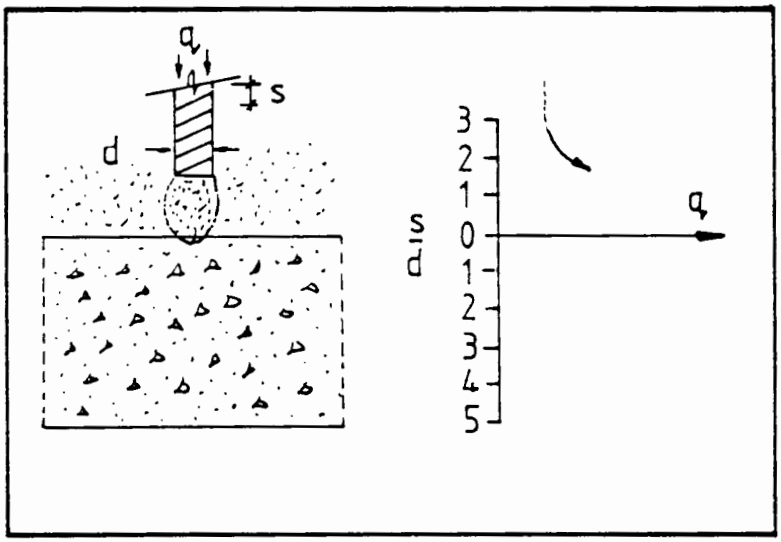

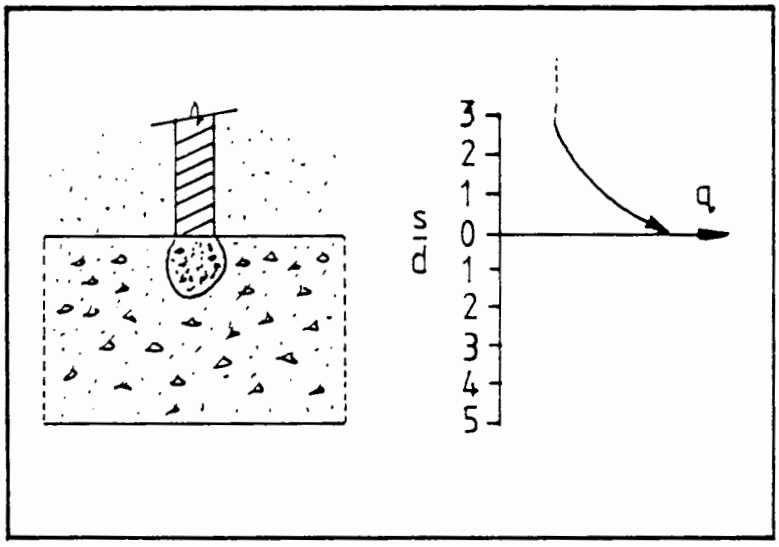

Figure 6.19 - Mechanism development prior to penetration of cemented layer

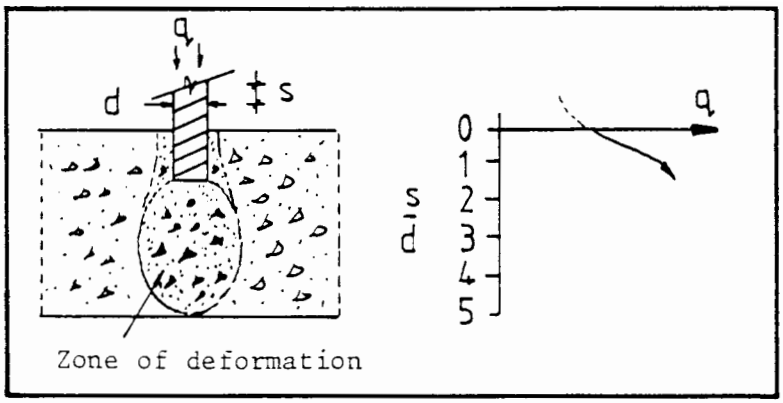

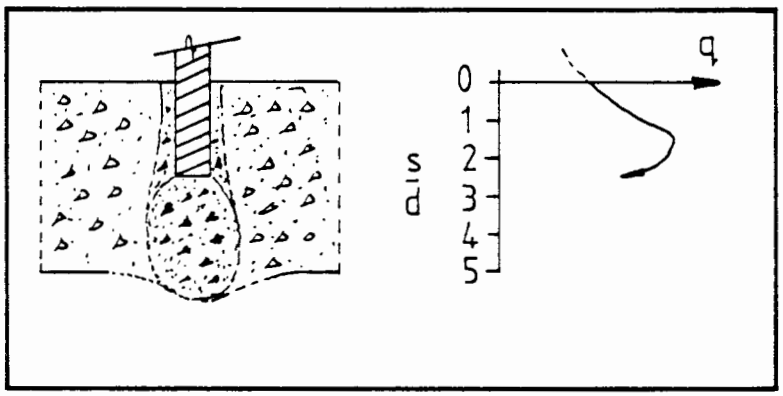

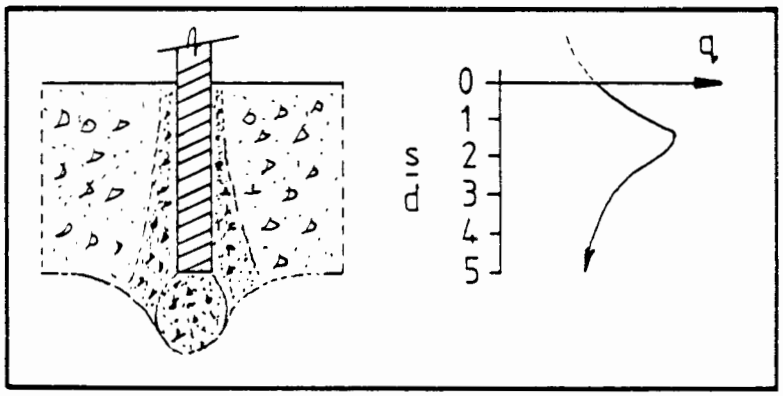

Figure 6.20 - Development of ductile failure mechanism

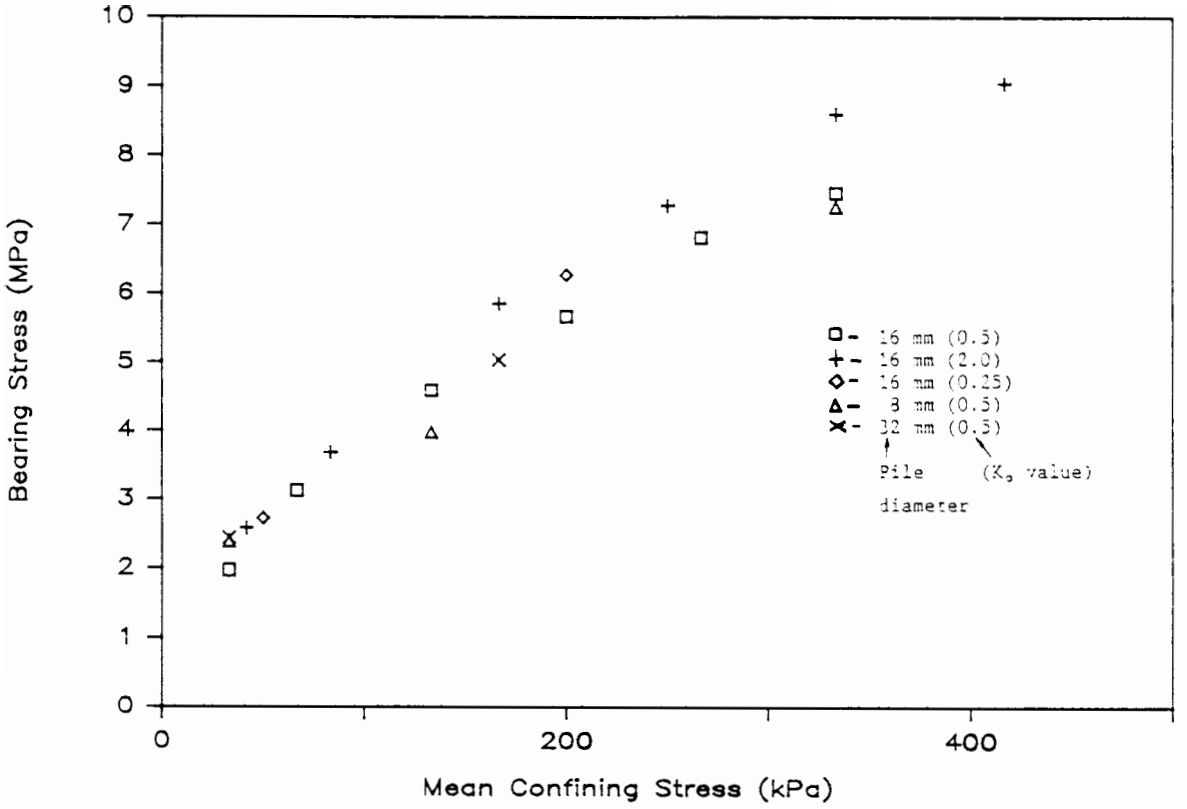

Figure 7.1 - Variation of pile diameter, test results in carbonate sand

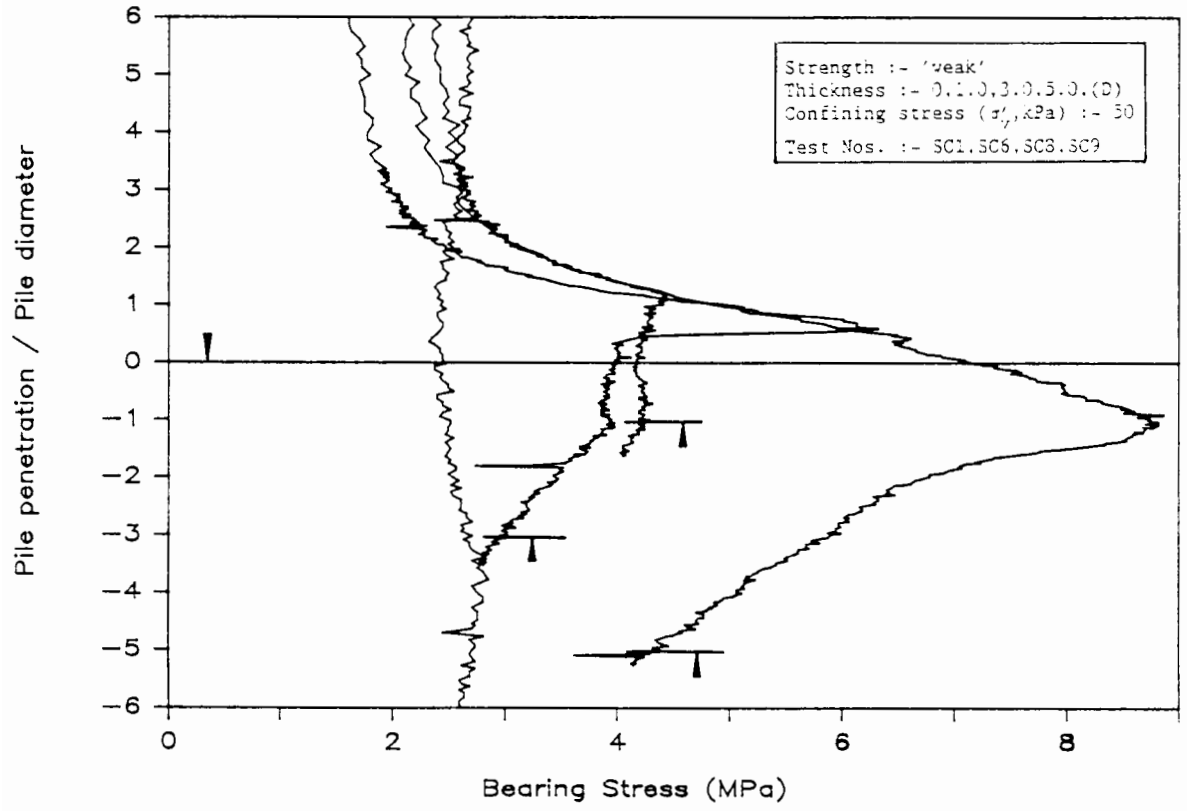

Figure 7.2 - Variation of pile diameter, 8 mm test results (1/2)

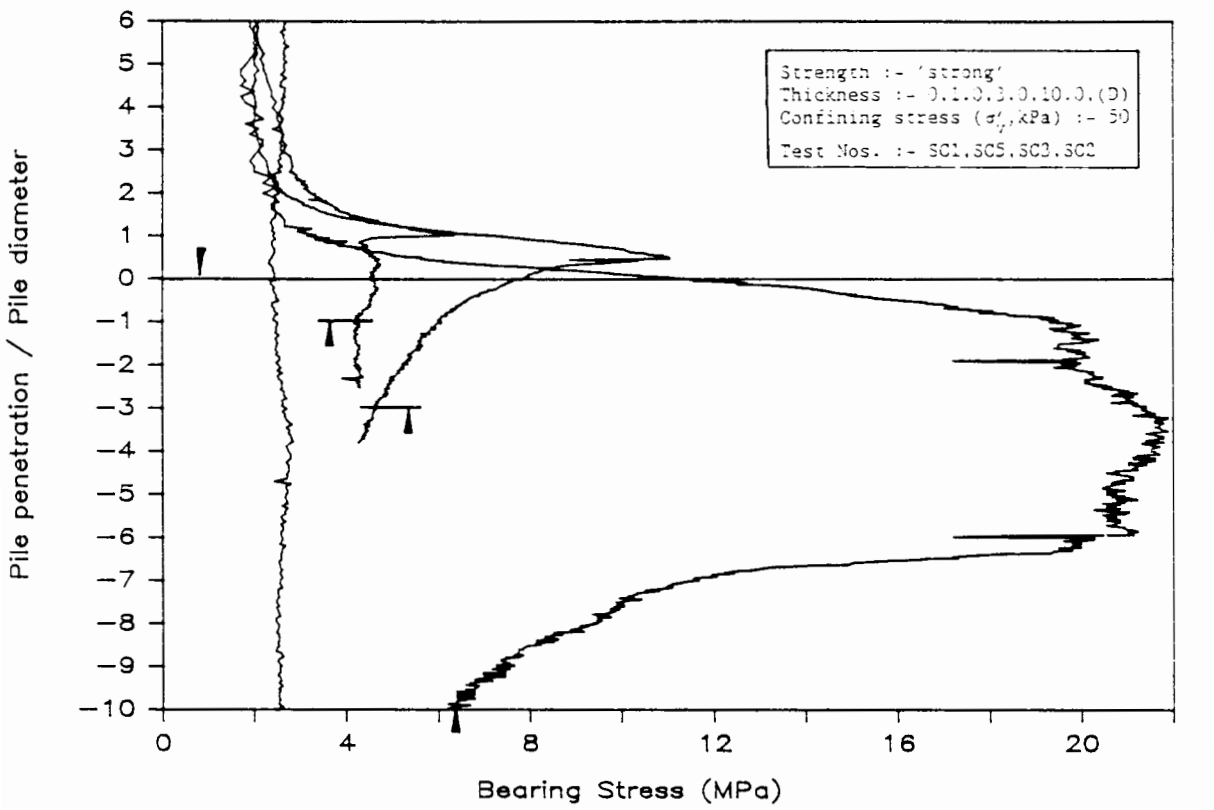

Figure 7.3 - Variation of pile diameter, 8 mm test results (2/2)

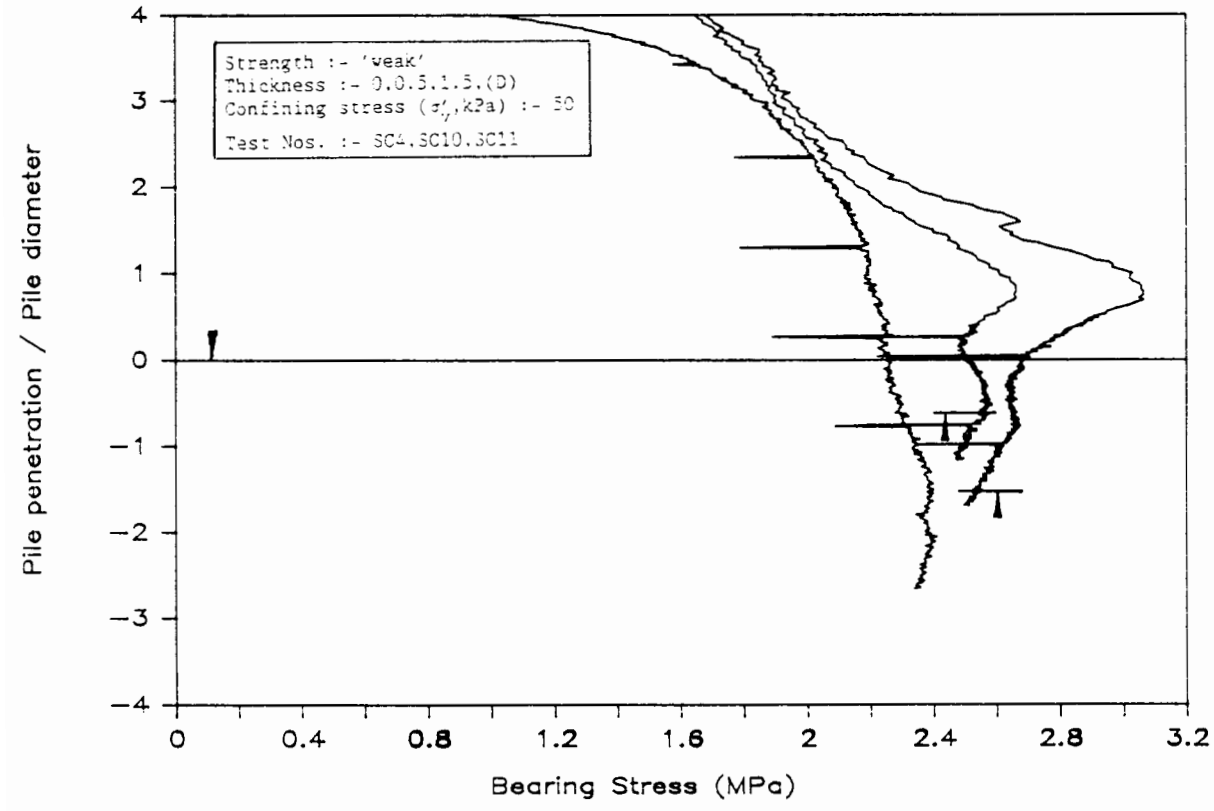

Figure 7.4 - Variation of pile diameter, 32 mm test results (1/2)

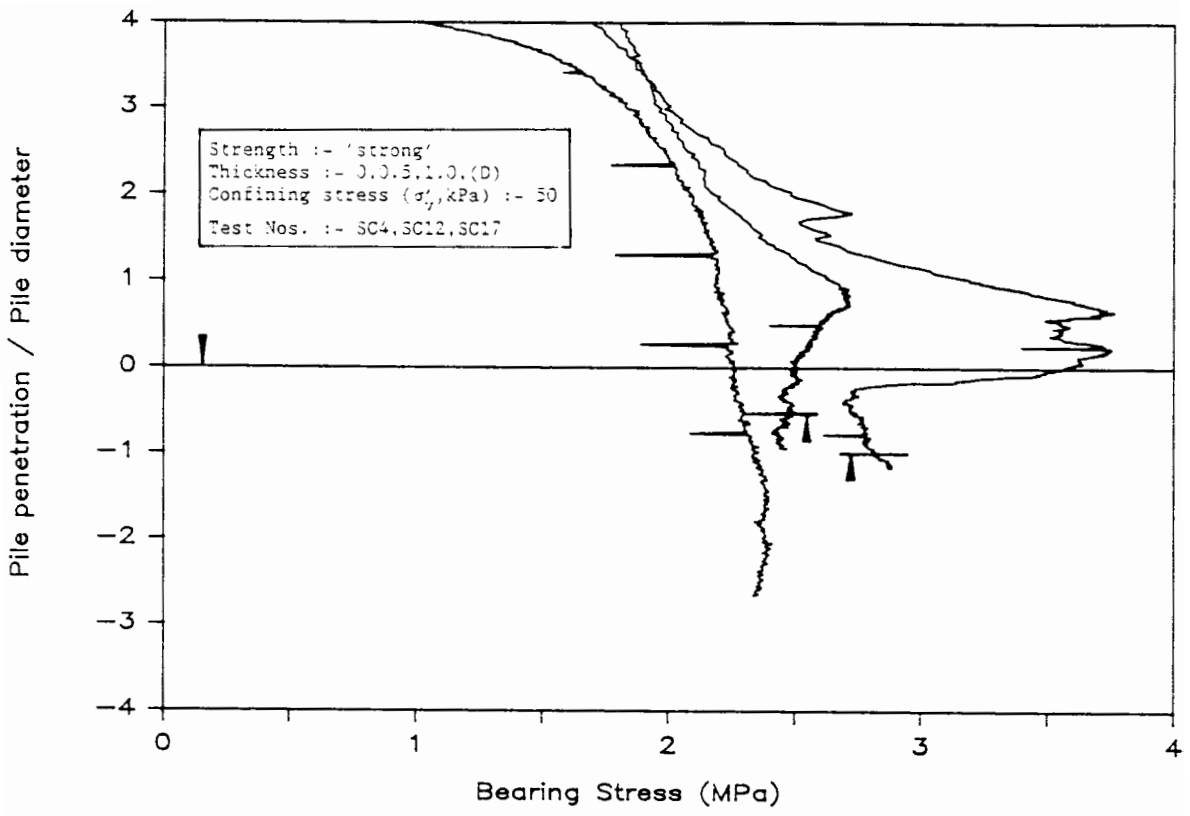

Figure 7.5 - Variation of pile diameter, 32 mm test results (2/2)

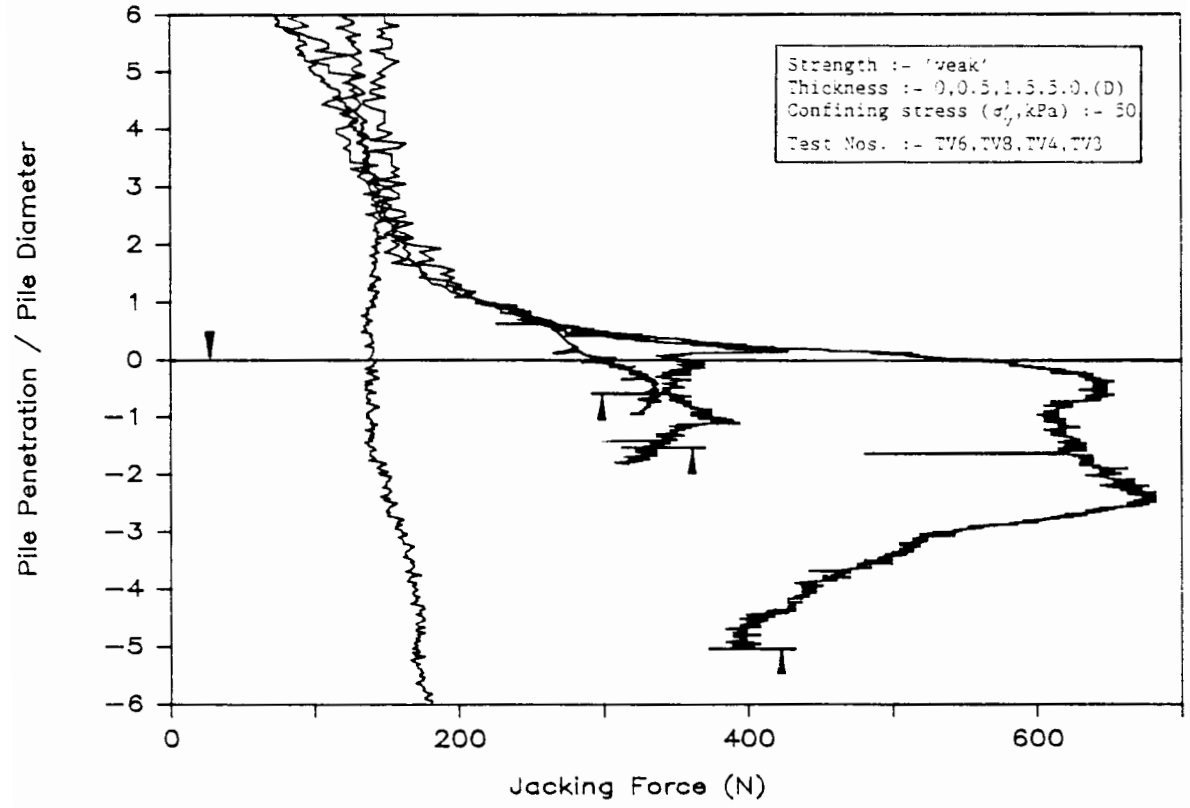

Figure 7.6 - Open end test results (1/2)

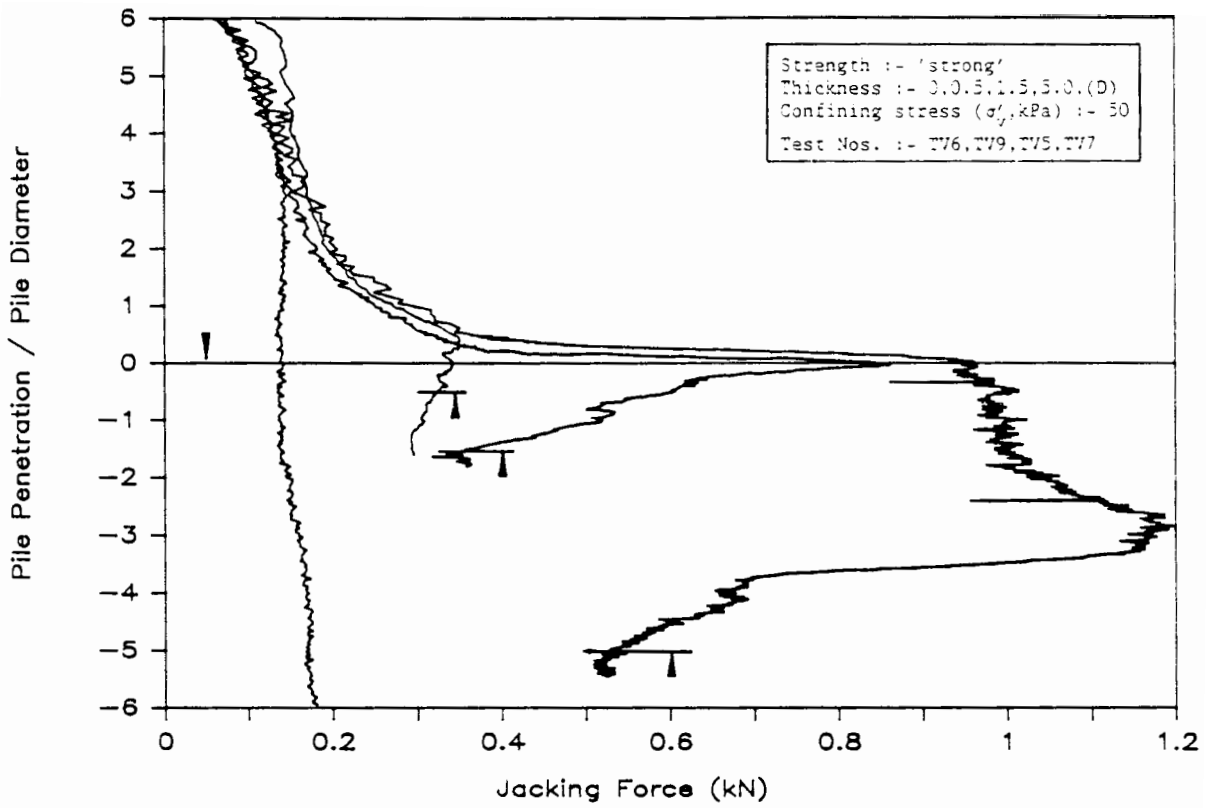

Figure 7.7 - Open end test results (2/2)

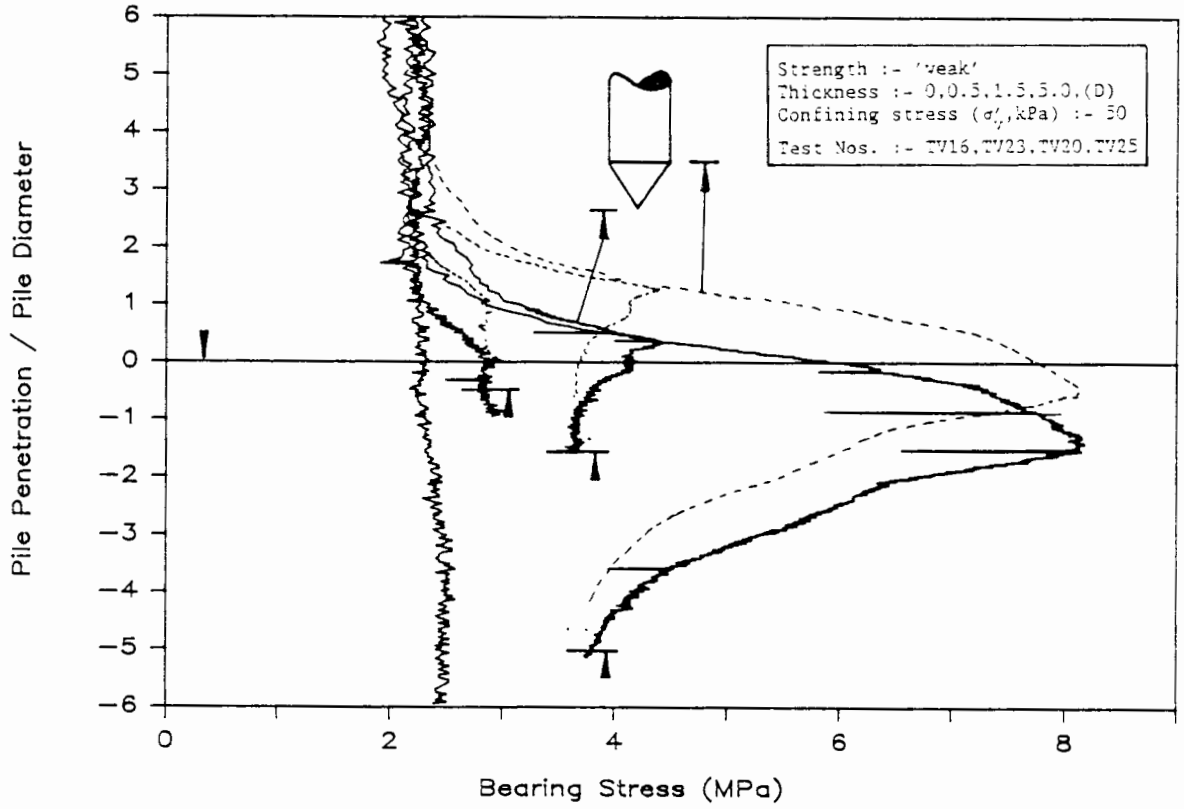

Figure 7.8 - Cone tip test results (1/2)

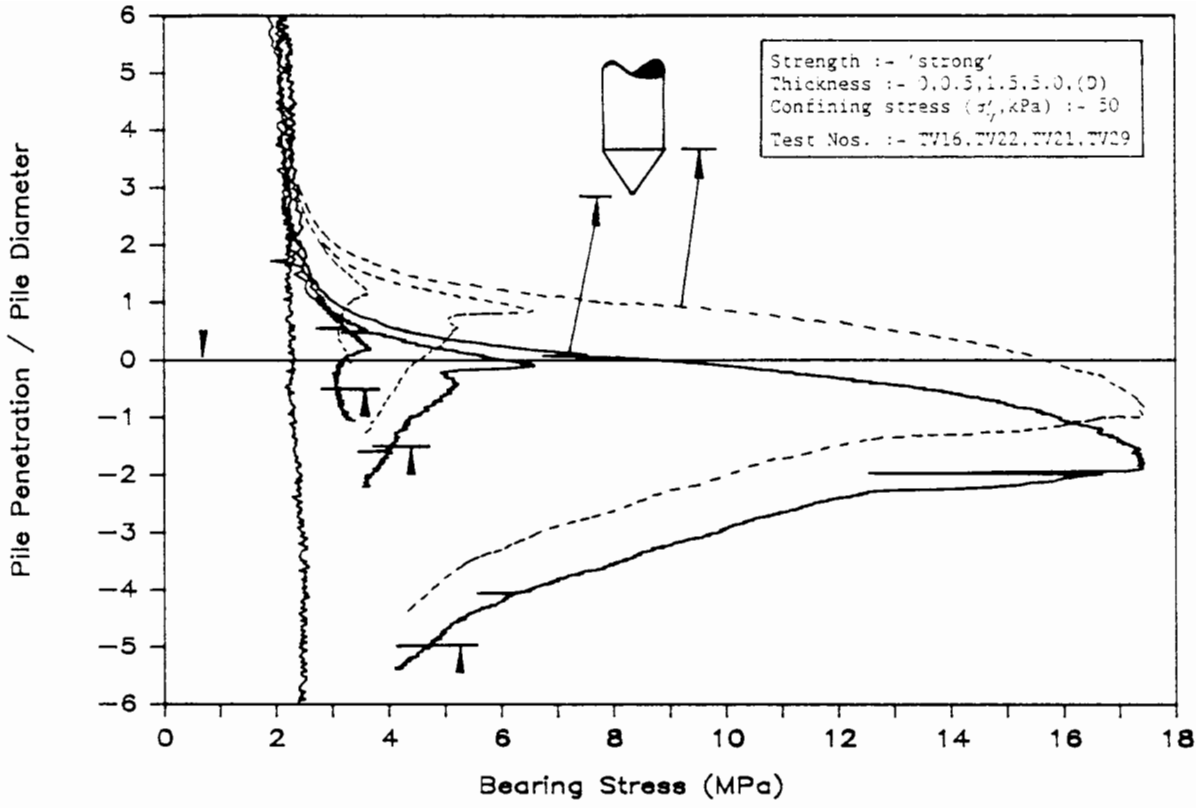

Figure 7.9 - Cone tip test results (2/2)

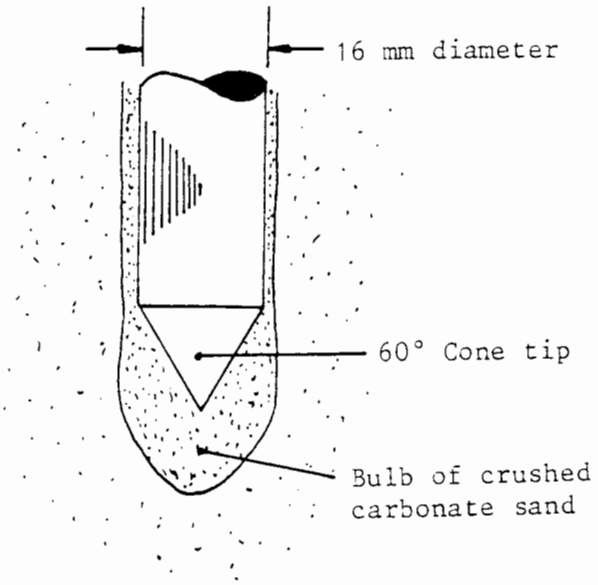

Figure 7.10 - Formation of bulb of crushed sand around cone tip

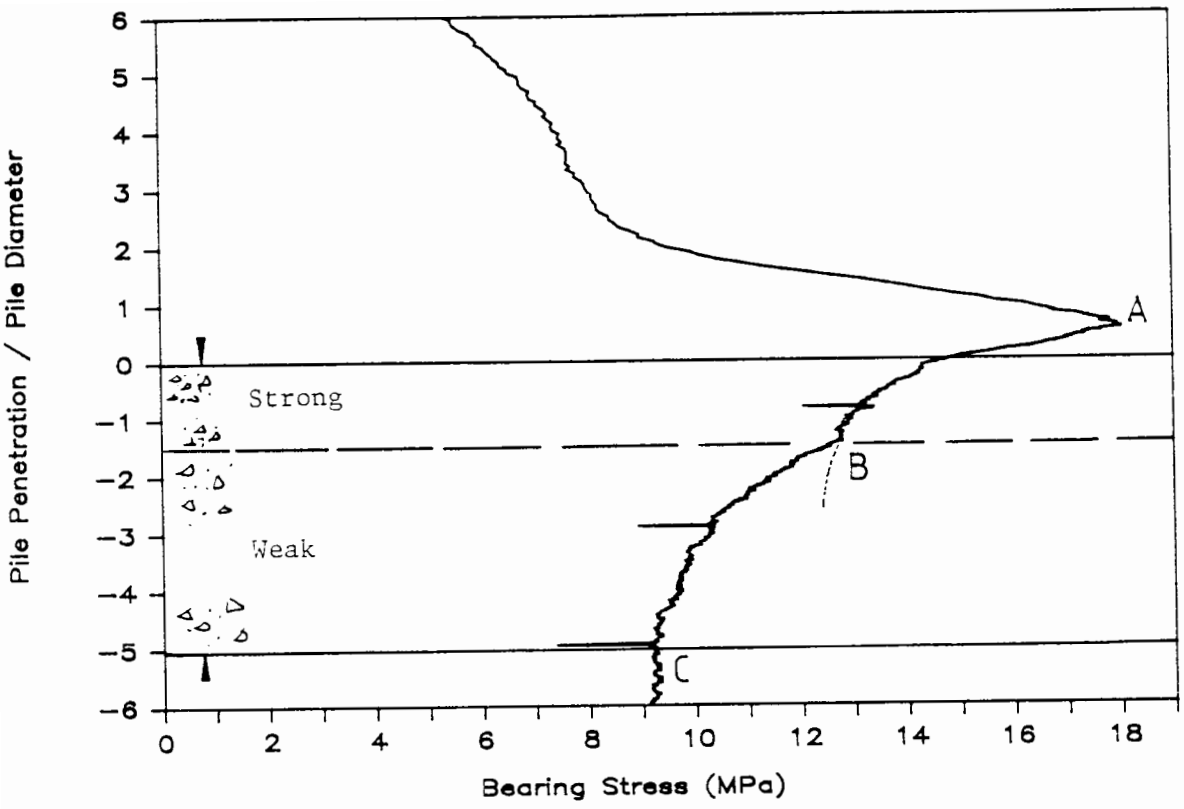

Figure 8.1 - Multi cemented layer system (1/3)

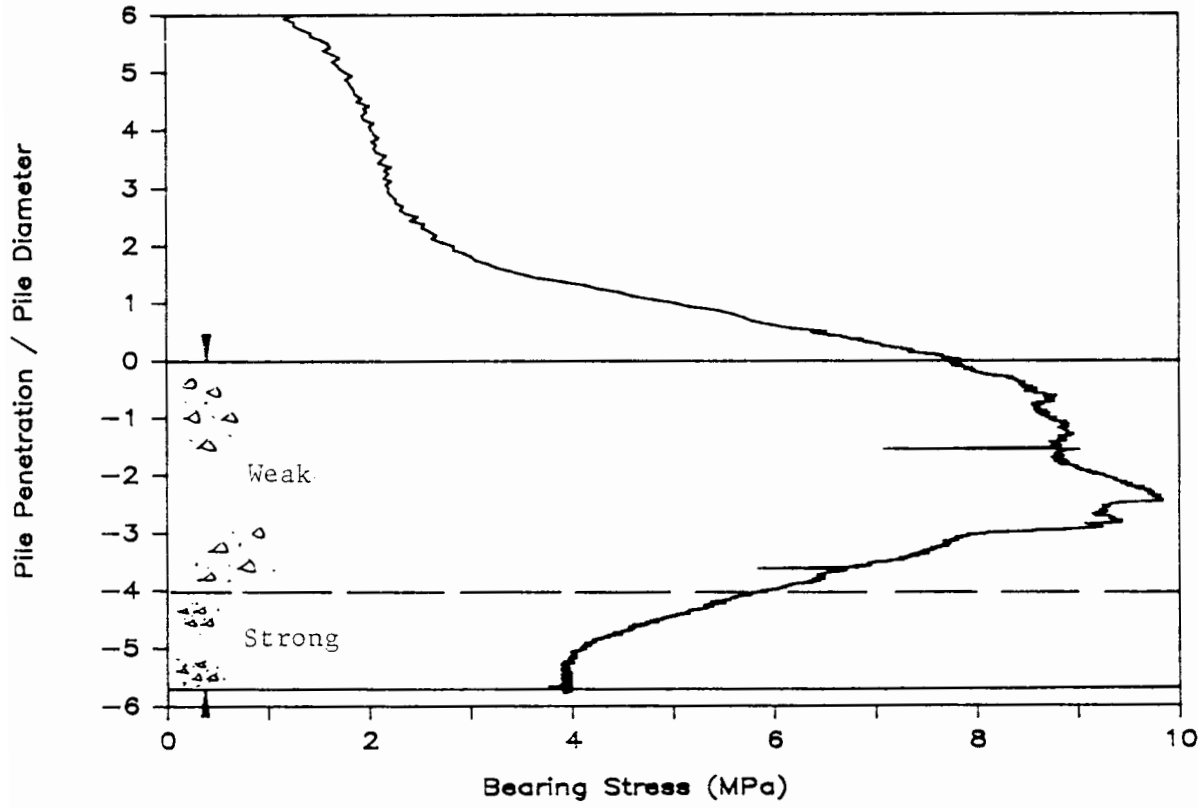

Figure 8.2 - Multi cemented layer system (2/3)

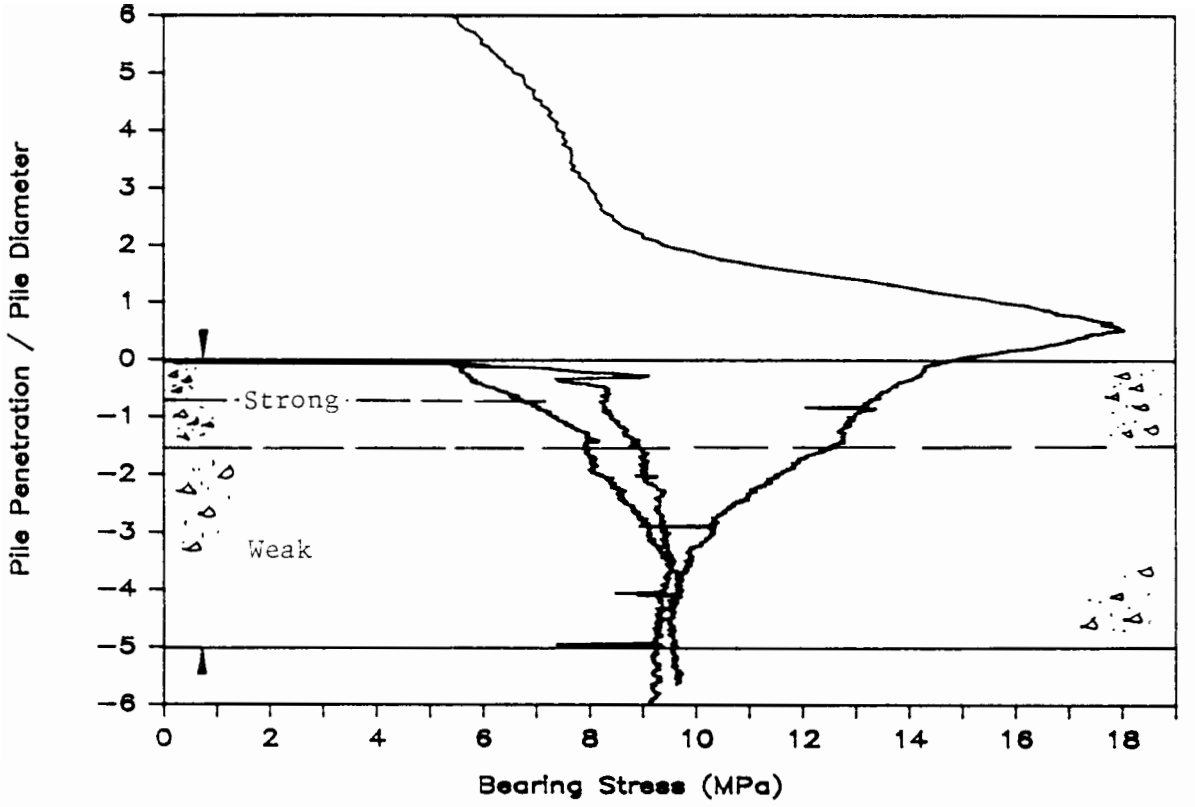

Figure 8.3 - Multi cemented layer system (3/3)

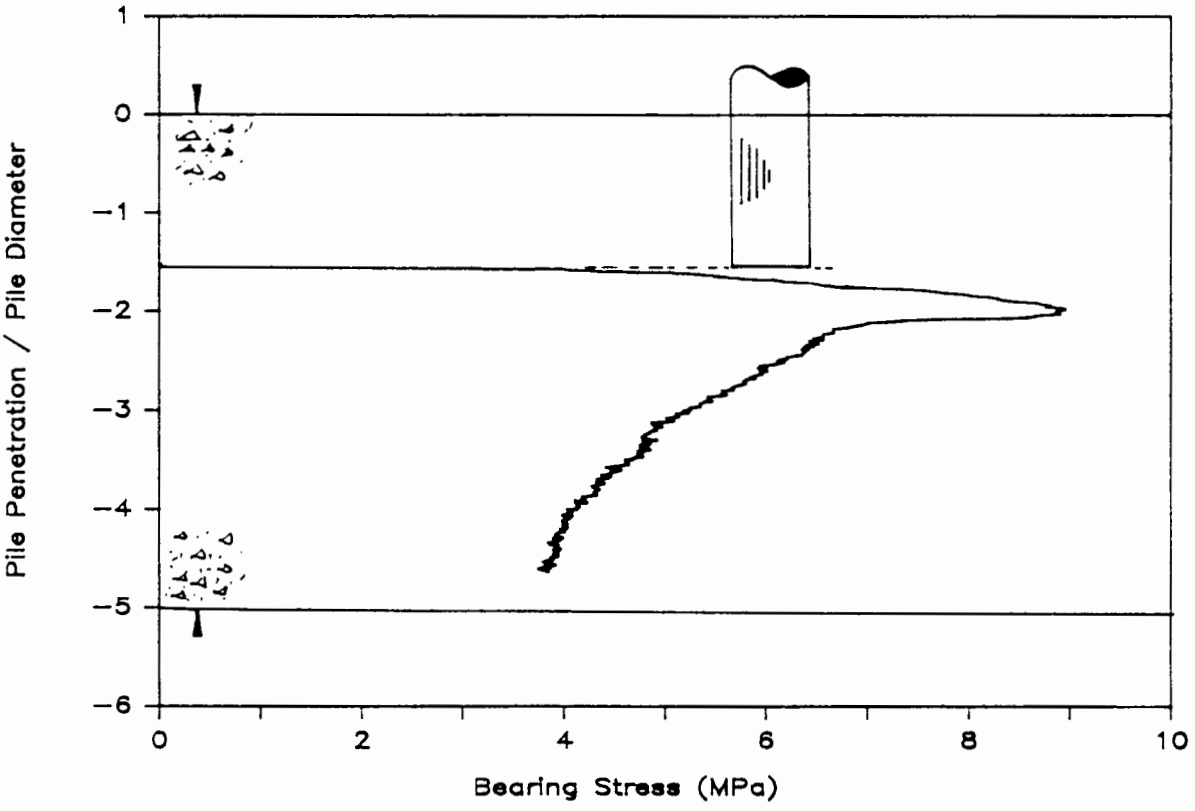

Figure 8.4 - Test result for a pile embedded into a cemented layer

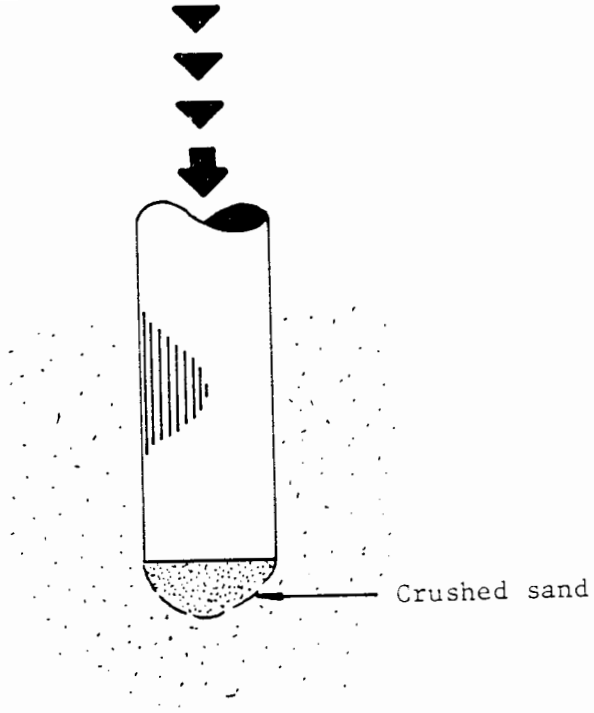

Figure 8.5 - Bulb of crushed material beneath pile tip following dynamic installation

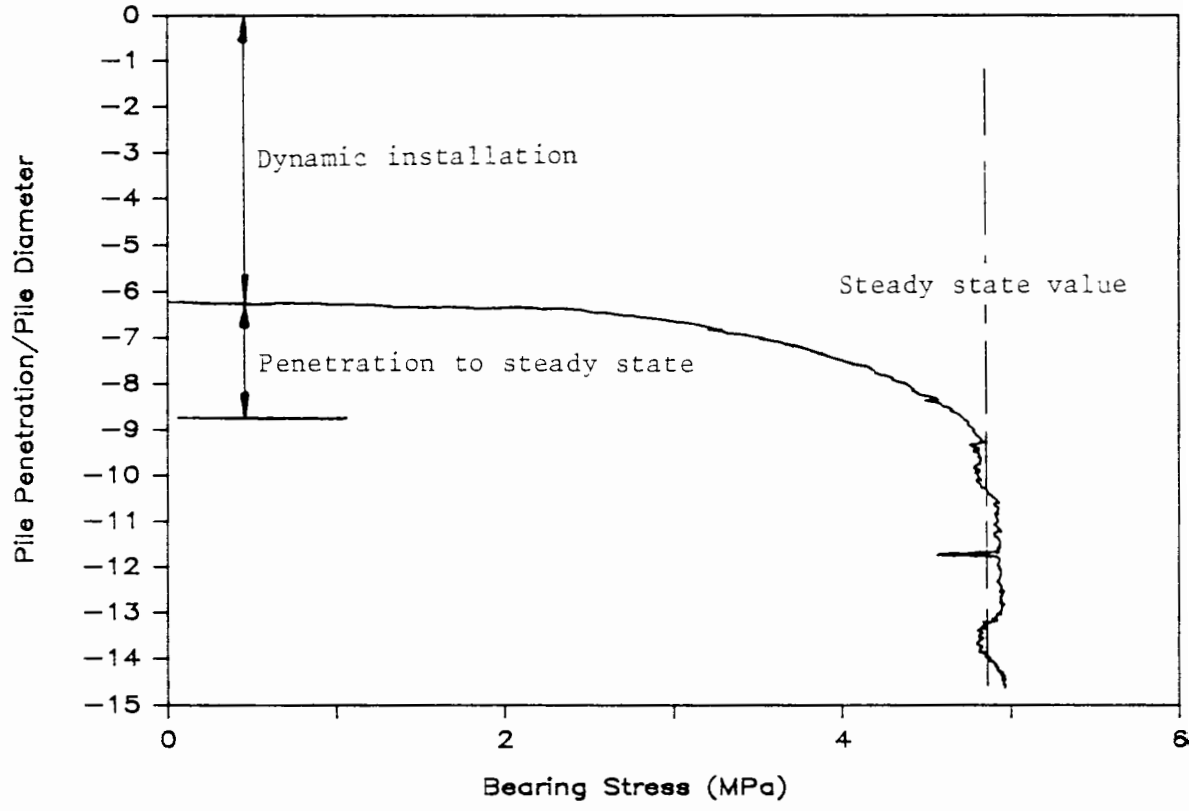

Figure 8.6 - Dynamic installation test (1/2)

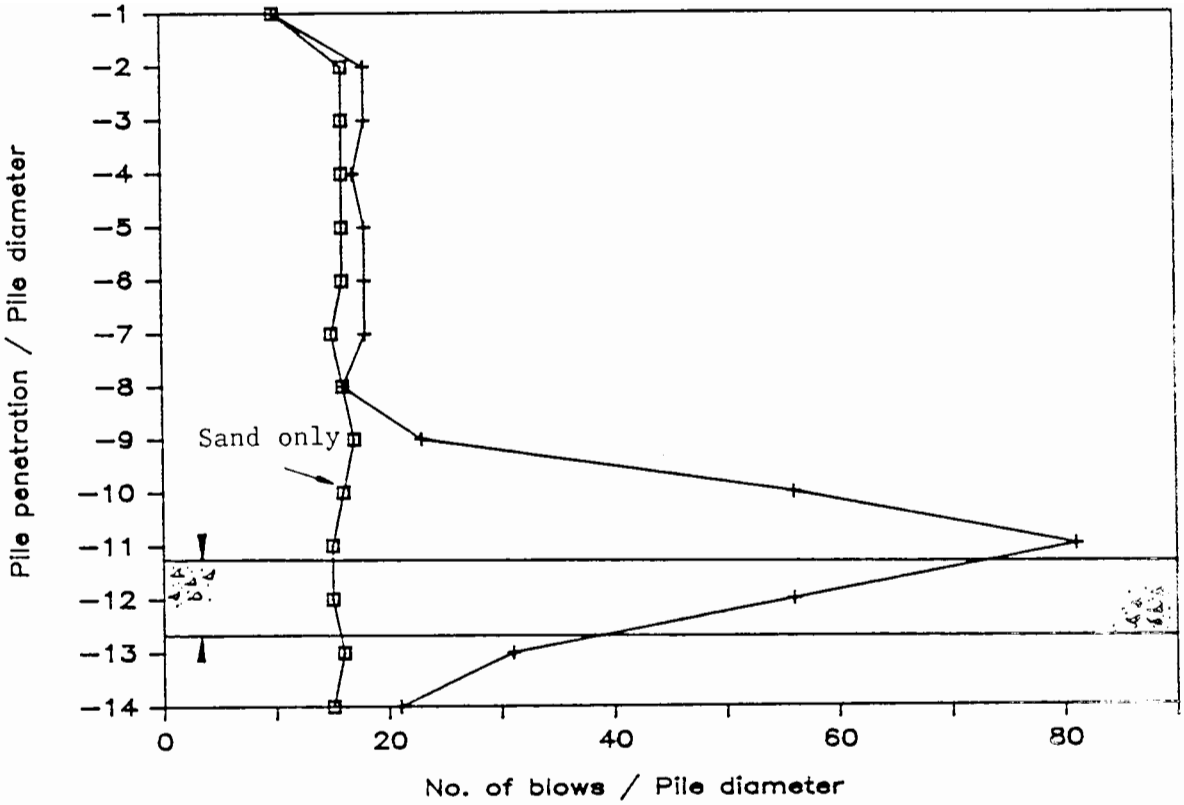

Figure 8.7 - Dynamic installation test (2/2)

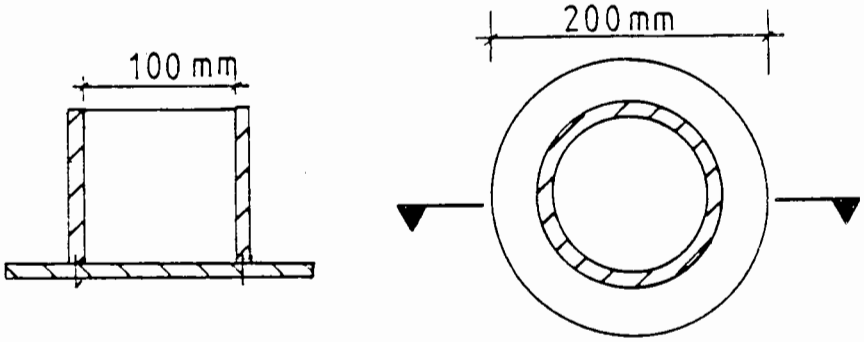

Figure 8.8 - Physical model of numerical analysis constraints

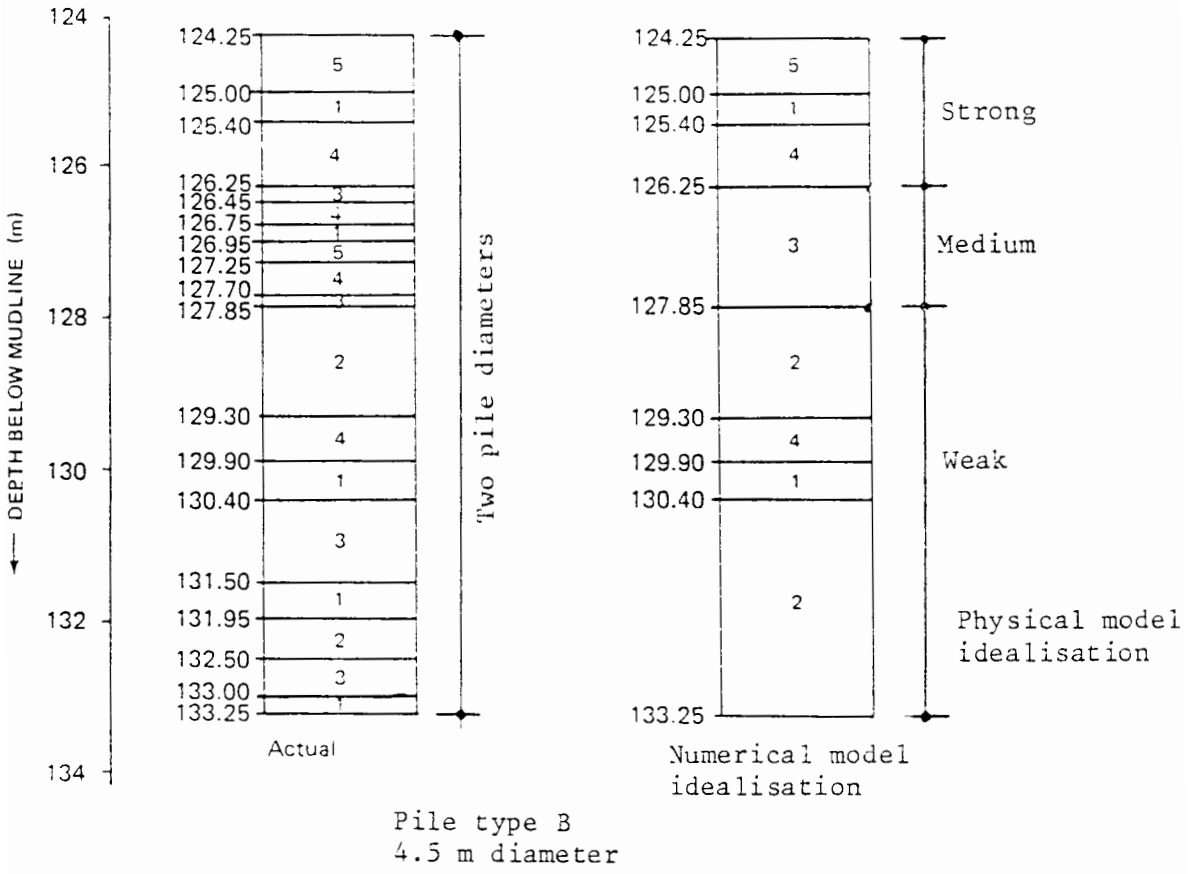

Figure 8.9 - Physical and numerical model idealisations of soil profile

(1/2)

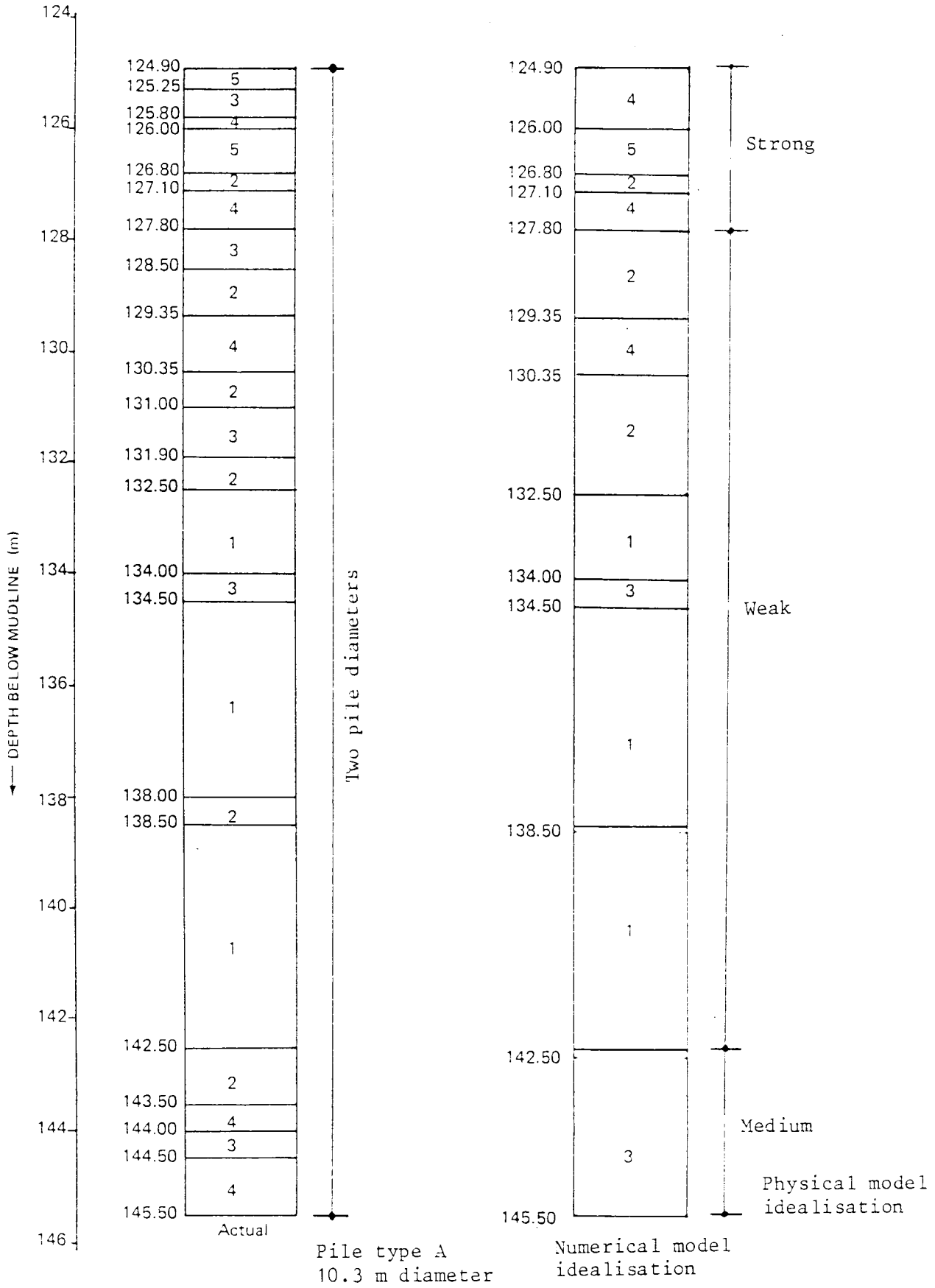

Figure 8.10 - Physical and numerical model idealisations of soil profile

(2/2)

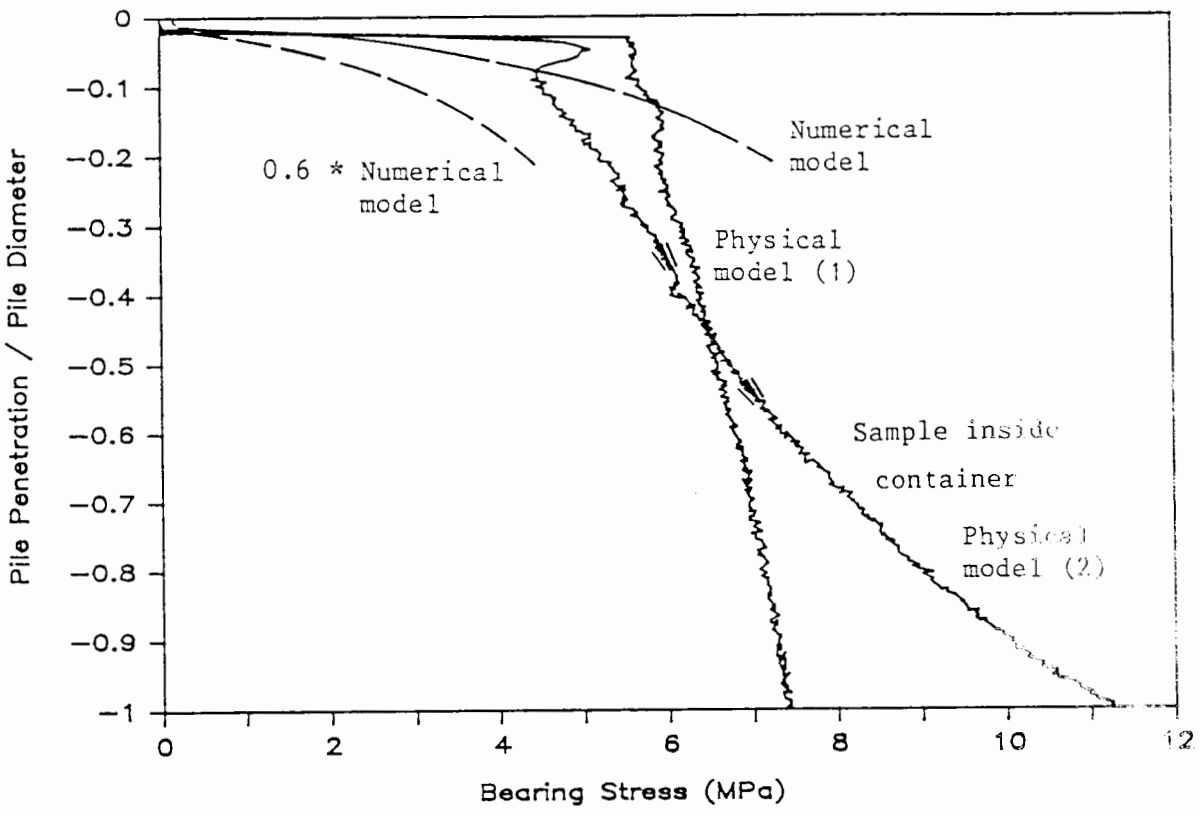

Figure 8.11 - Comparison of numerical analysis and physical test (Type B)

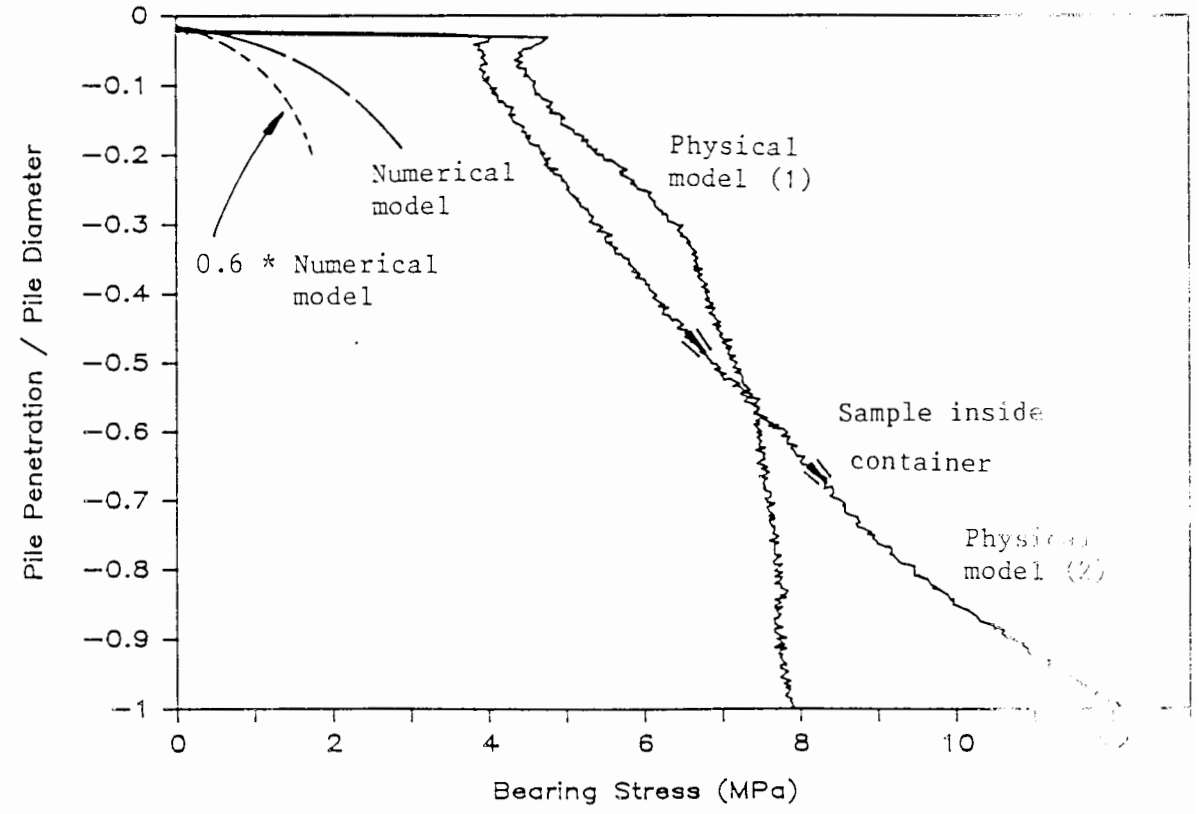

Figure 8.12 - Comparison of numerical analysis and physical test (Type A)

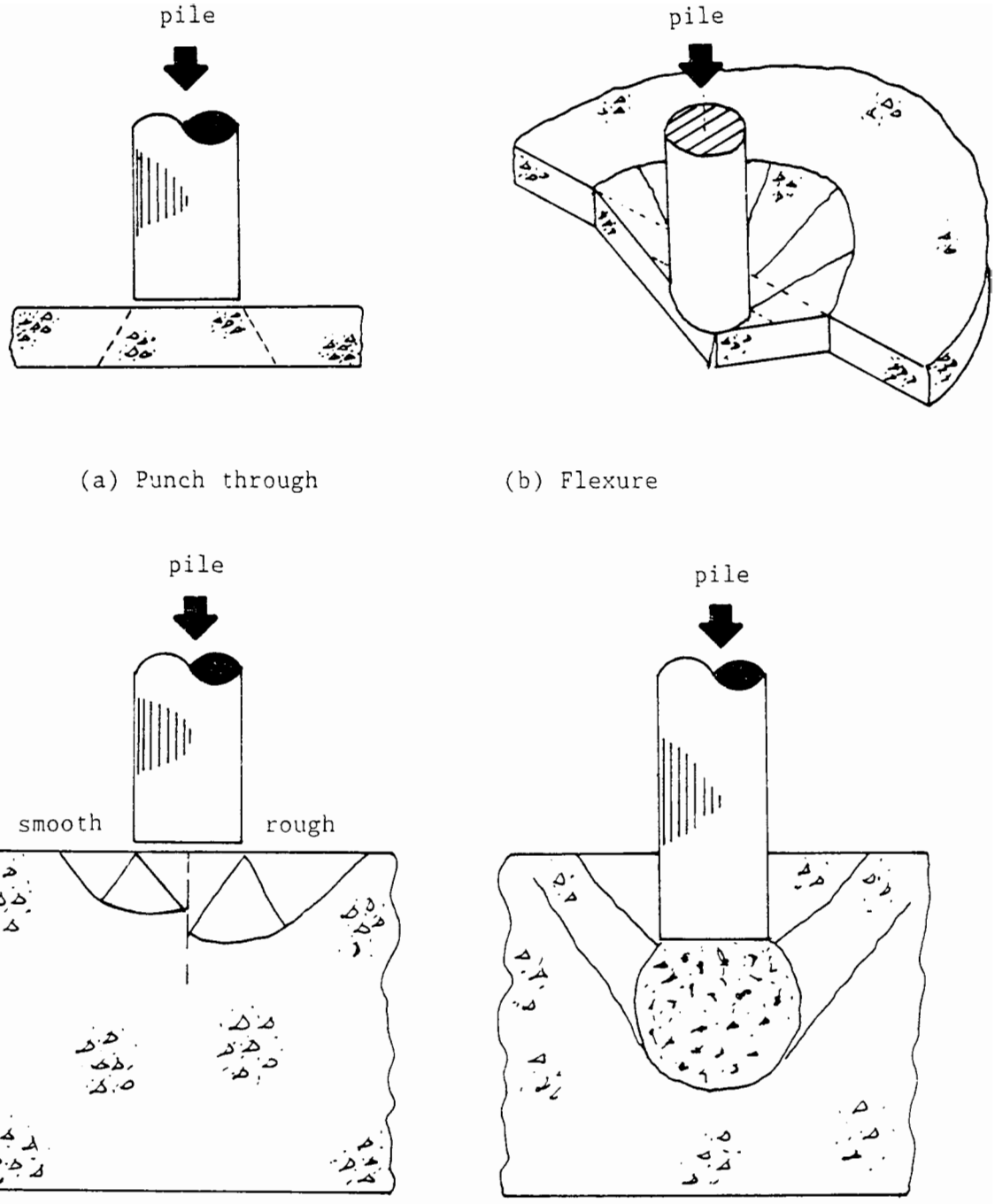

(a) Punch through (b) Flexure

(c) Classical bearing capacity (d) Indentation

Figure 9.1 - Intuitive failure solutions

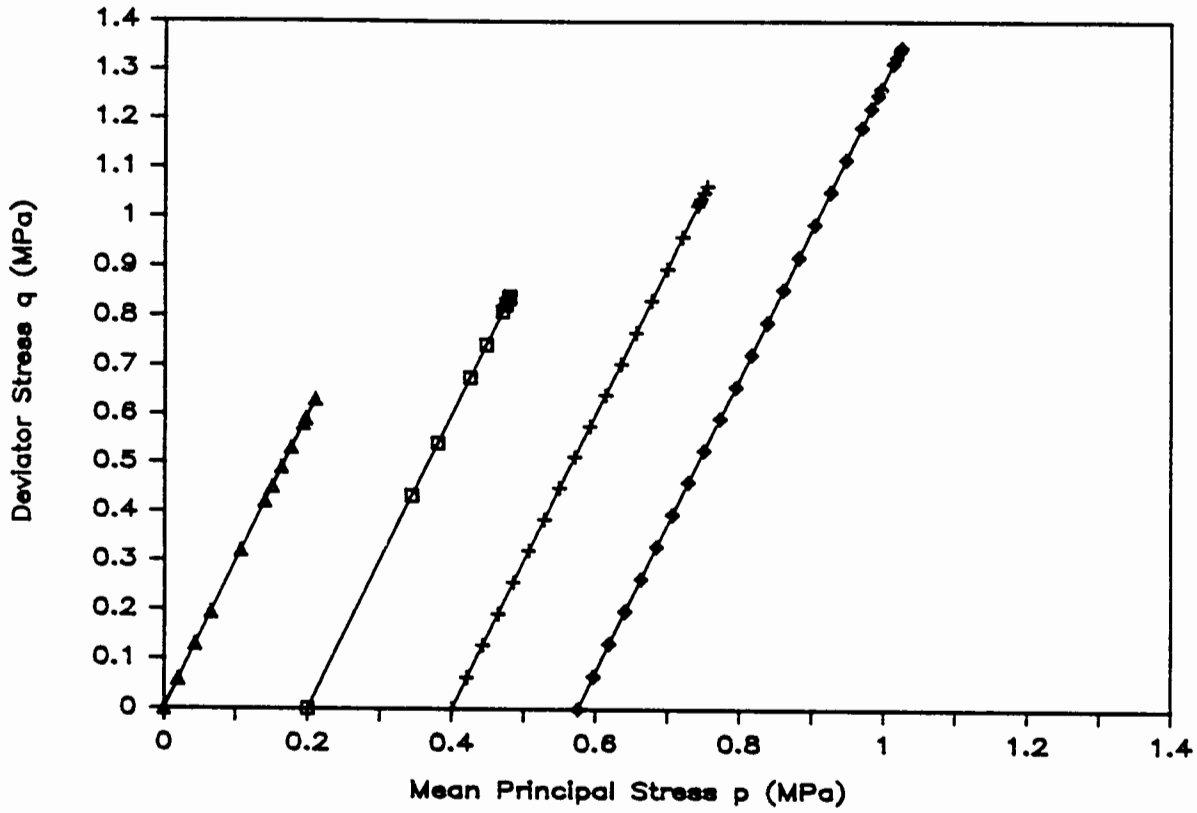

Figure 9.2 - q - p diagram of triaxial test results, 'weak' strength material

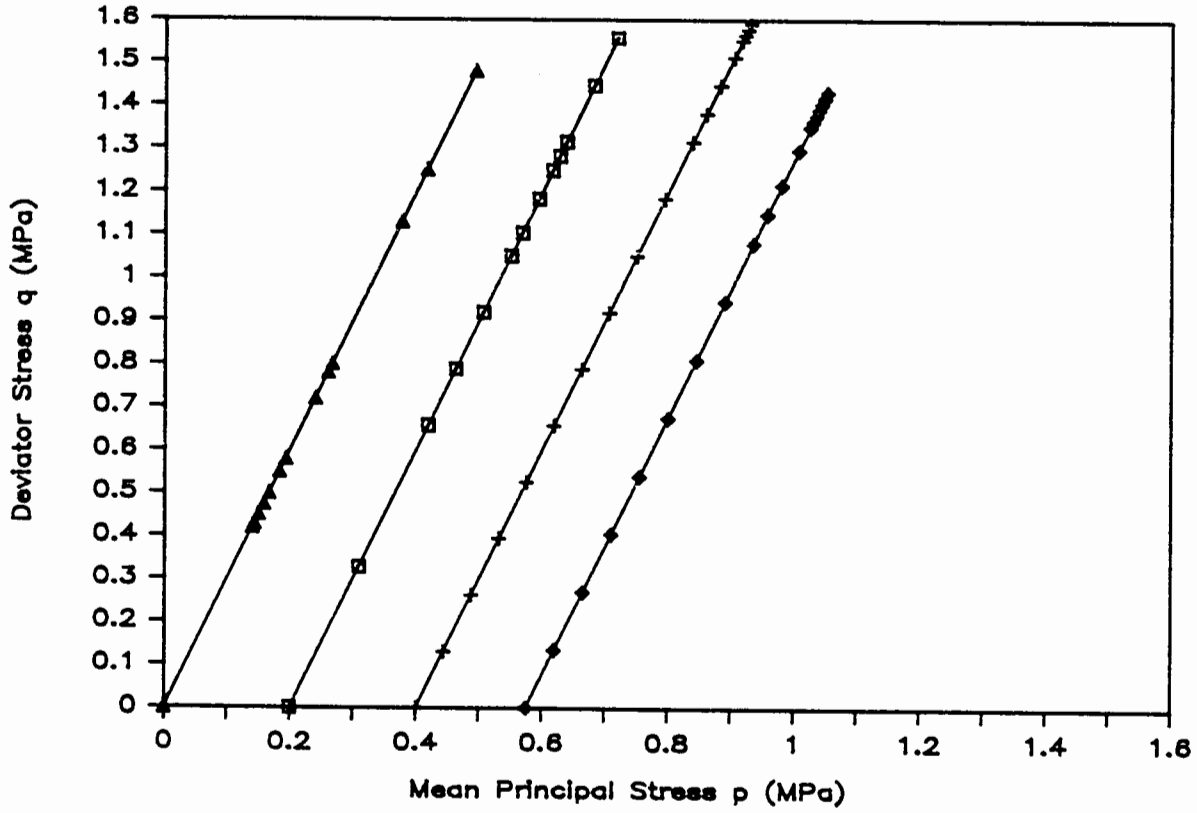

Figure 9.3 - q - p diagram of triaxial test results, 'medium' strength material

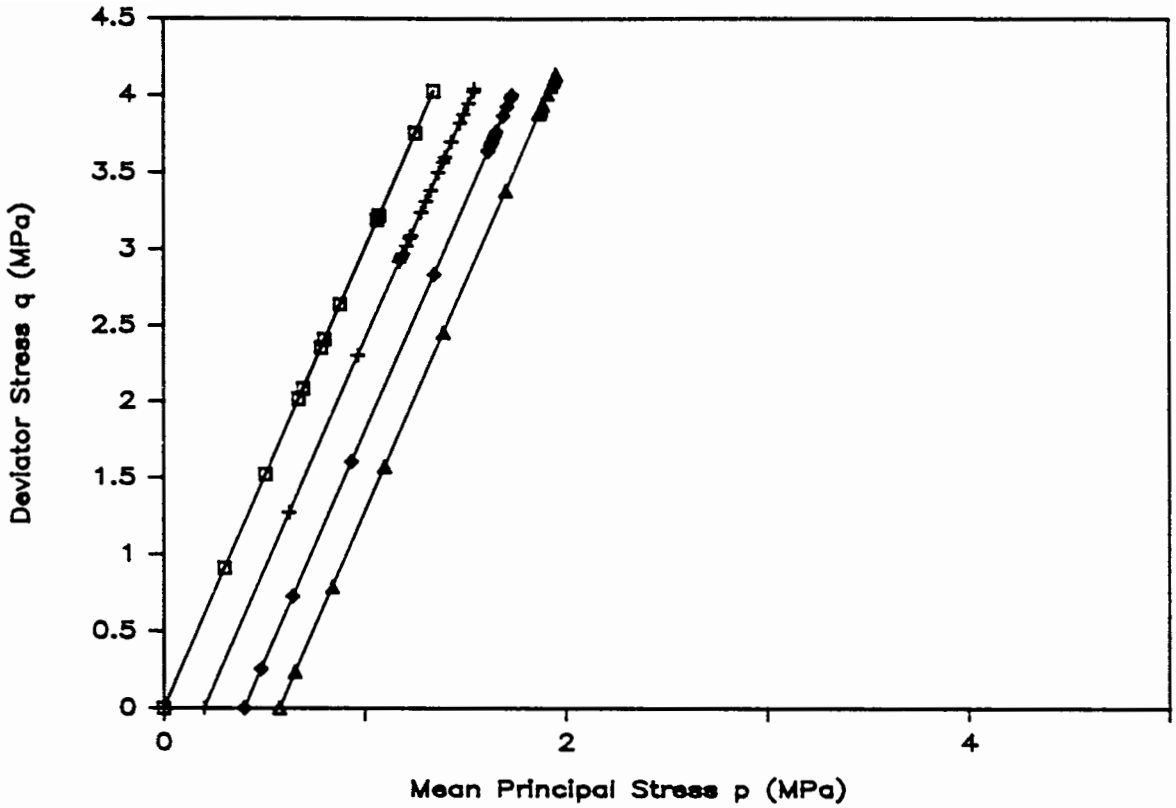

Figure 9.4 - q - p diagram of triaxial test results, 'strong' strength material

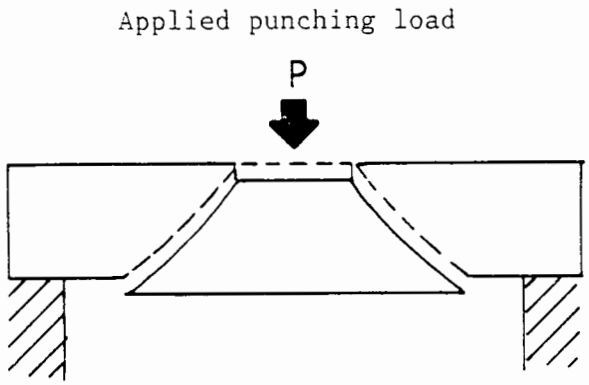

Figure 9.5 - Idealisation of punching shear in concrete slabs

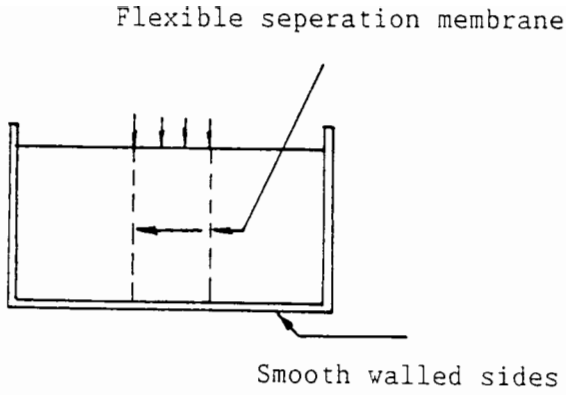

Figure 9.6 - Box model (after Davis, 1980)

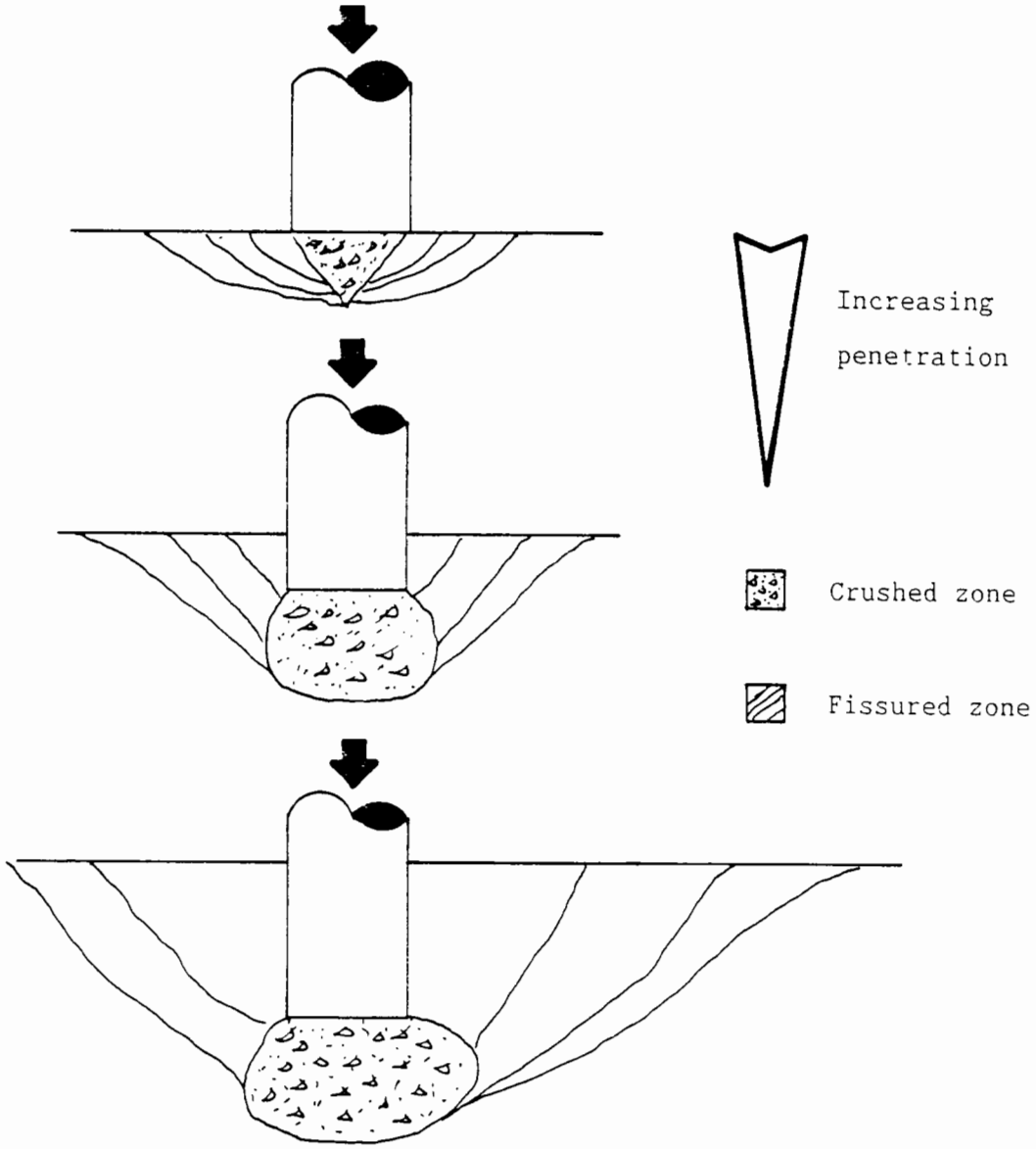

Figure 9.7 - Modes of indentation failure observed in model tests
(after Ladanyi and Roy, 1972)

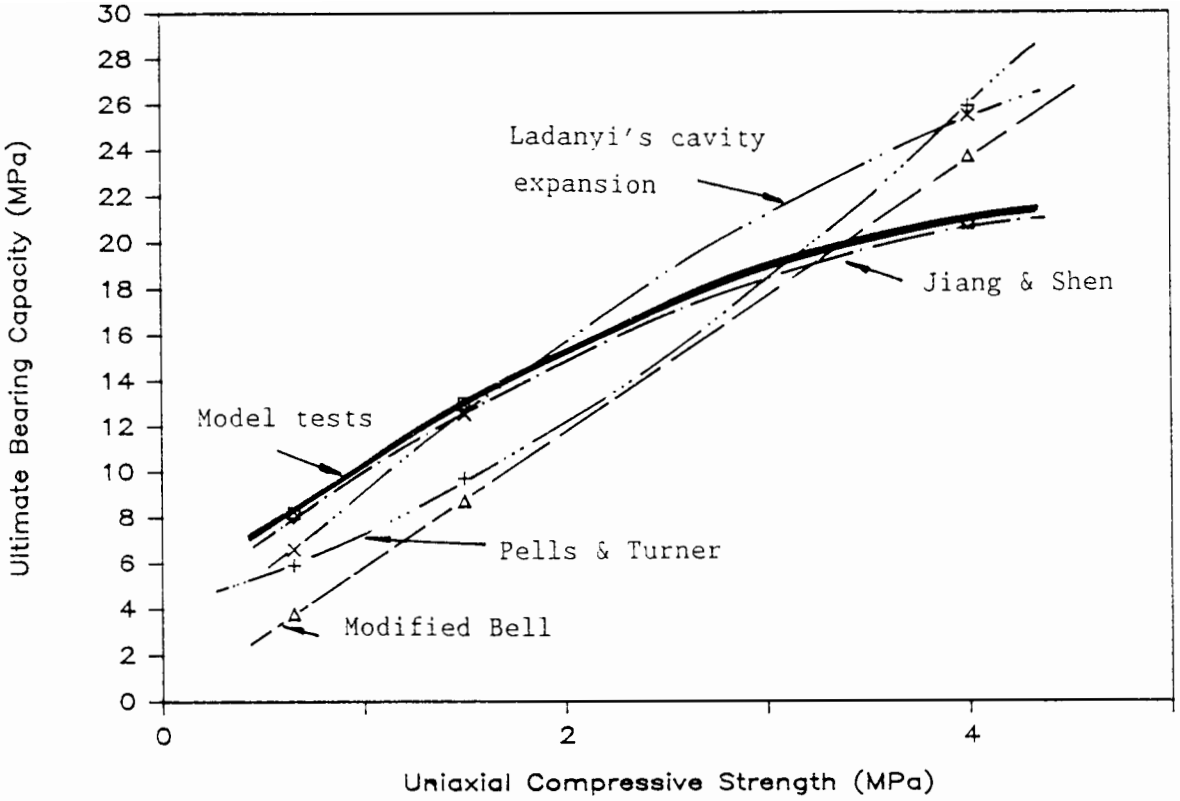

Figure 9.8 - Comparison of calculated ultimate bearing capacities

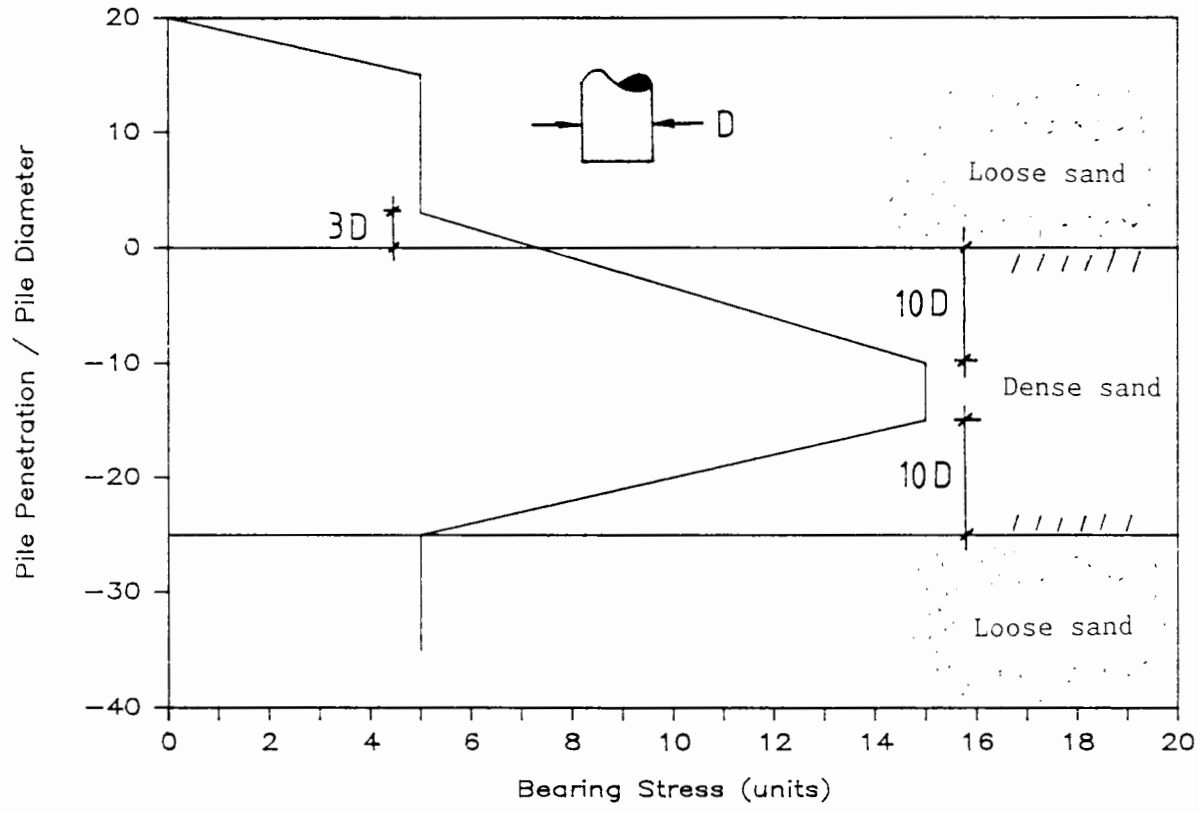

Figure 9.9 - Bearing capacity control envelope (after Meyerhof, 1979)

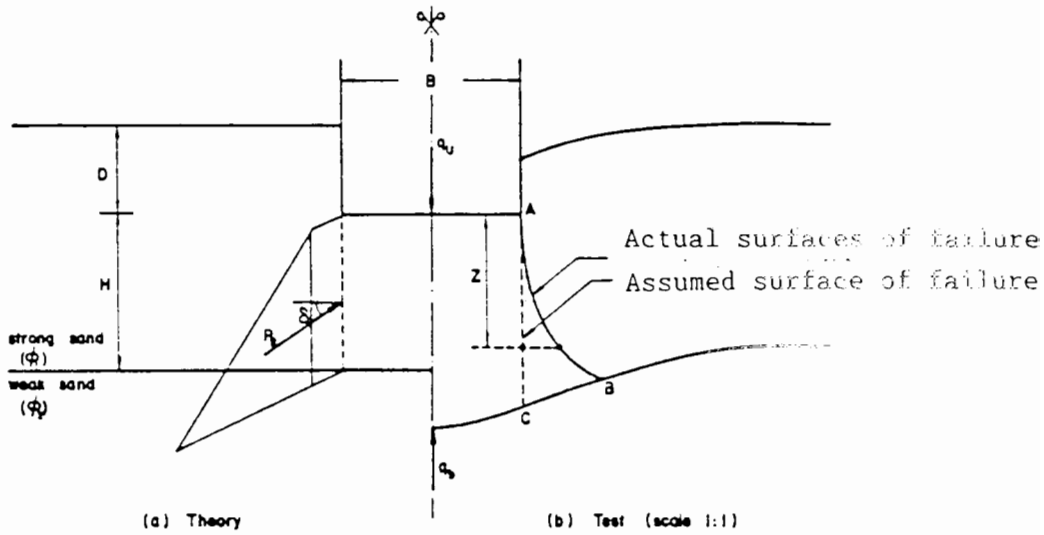

Figure 9.10 - Failure modes of a strip footing on strong sand overlying weak sand (after Hanna, 1981)

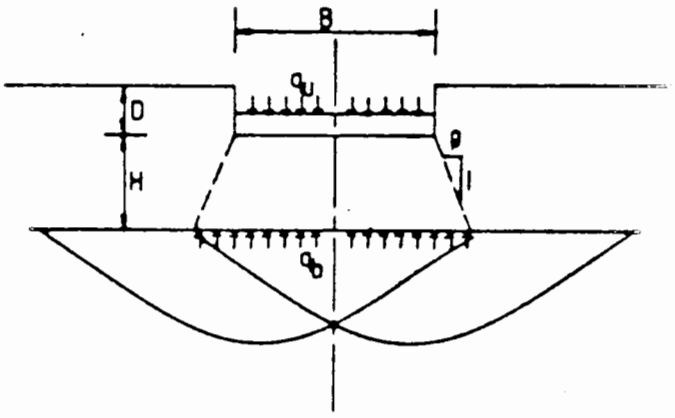

Figure 9.11 - Typical projected area method of analysis

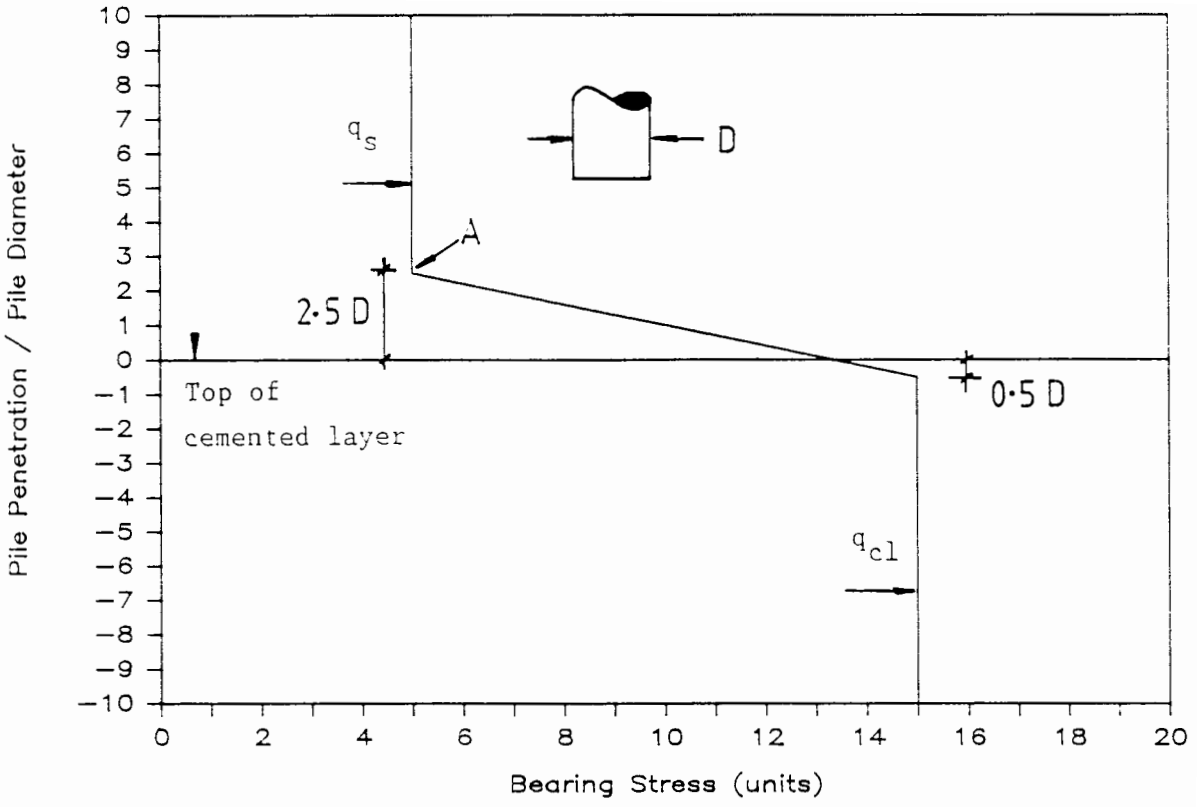

Figure 9.12 - Derived empirical limiting bearing stress response

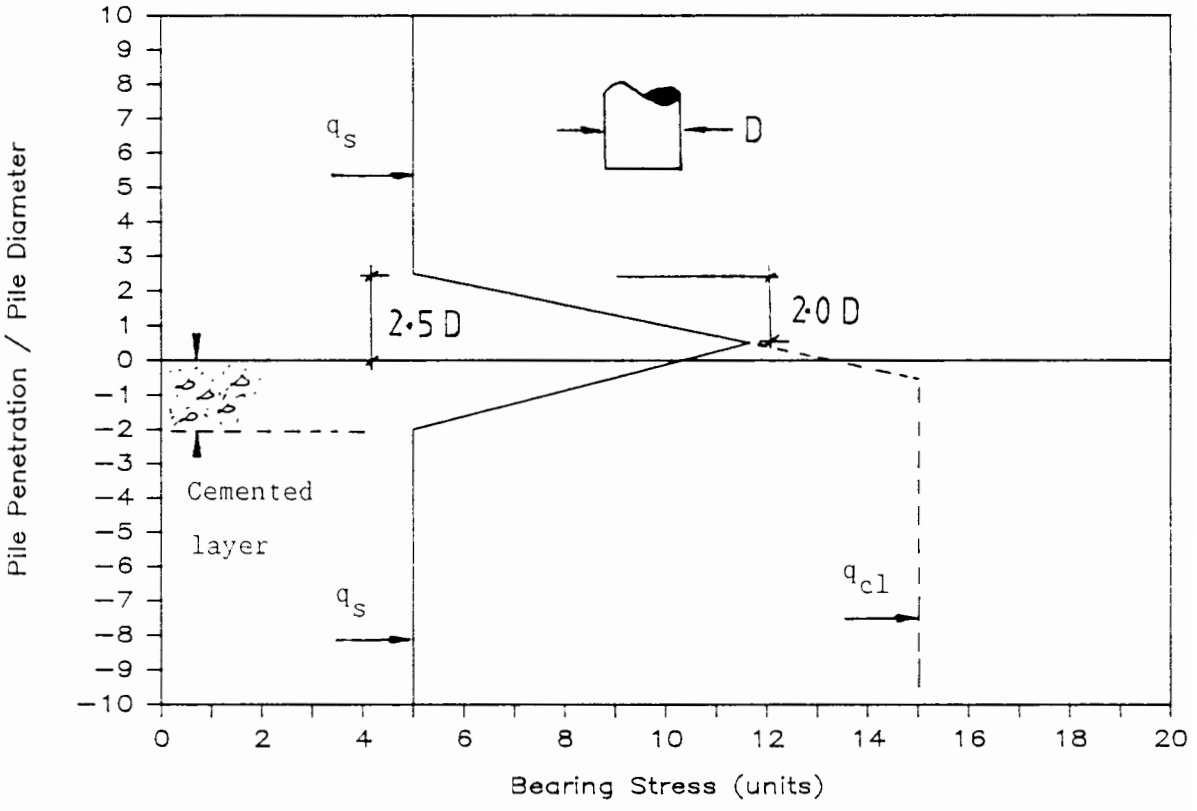

Figure 9.13 - Bearing capacity diagram for cemented layer thickness of two pile diameters

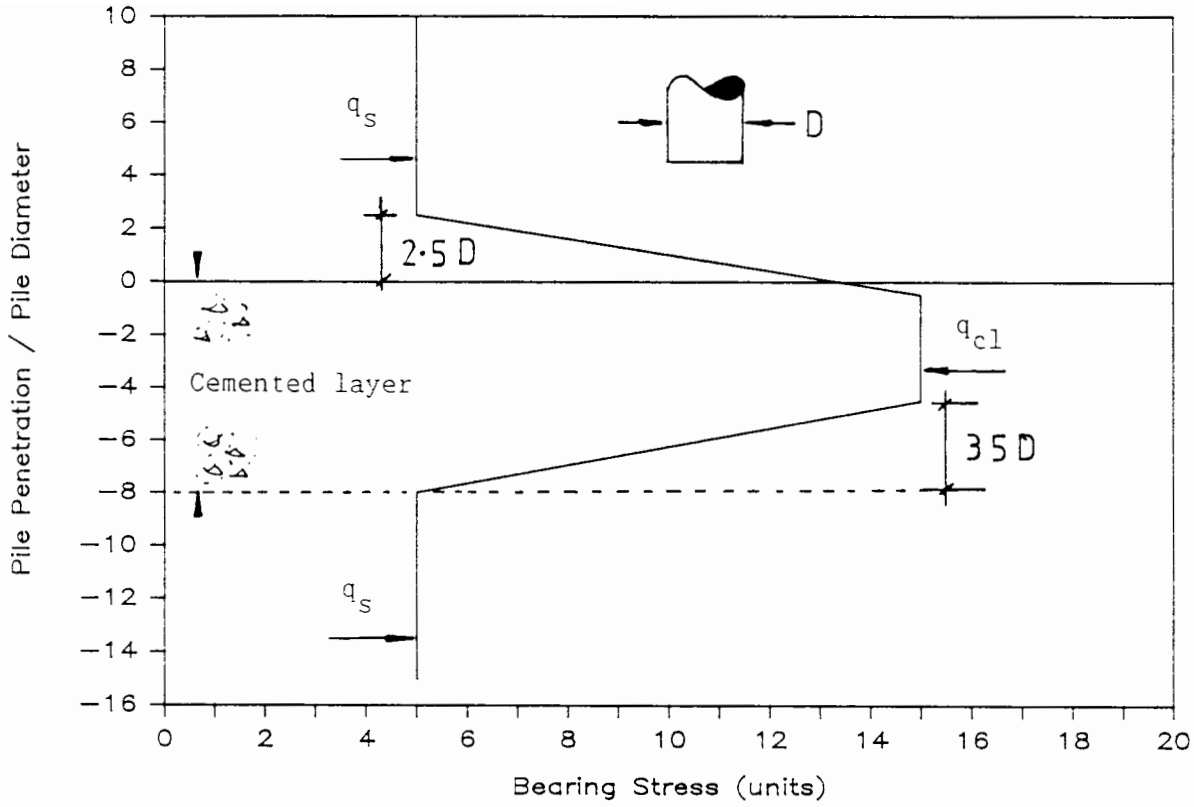

Figure 9.14 - Bearing capacity diagram for cemented layer thickness of eight pile diameters

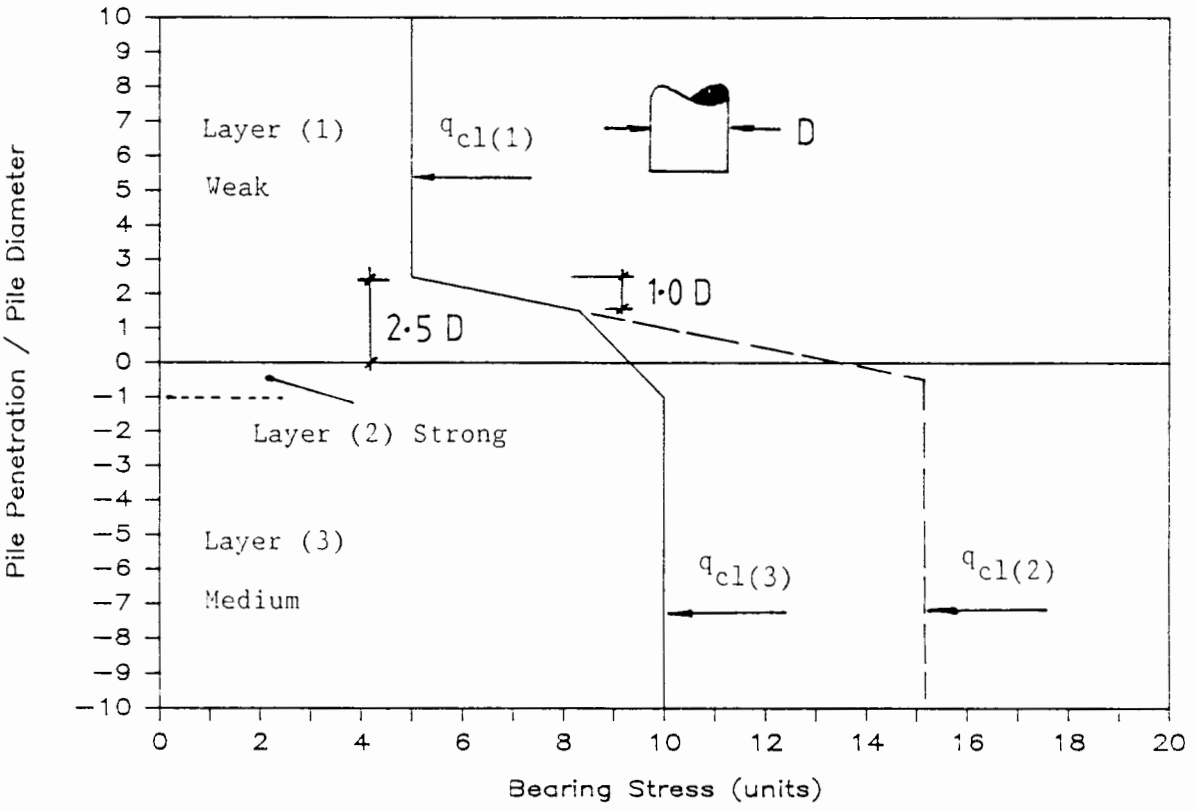

Figure 9.15 - Multi layer system bearing capacity diagram

Plate 2.1

General view (1)

Dogs Bay, Connemara

W. Ireland

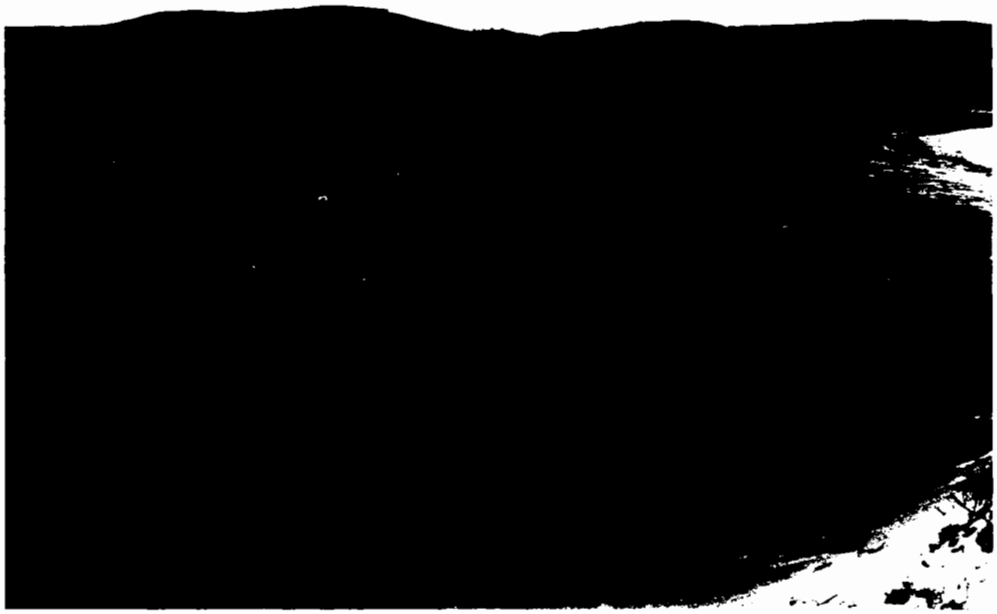

Plate 2.2

Sand extraction area

Dogs Bay, Connemara

W. Ireland

Plate 2.3

General view (2)

Dogs Bay, Connemara

W. Ireland

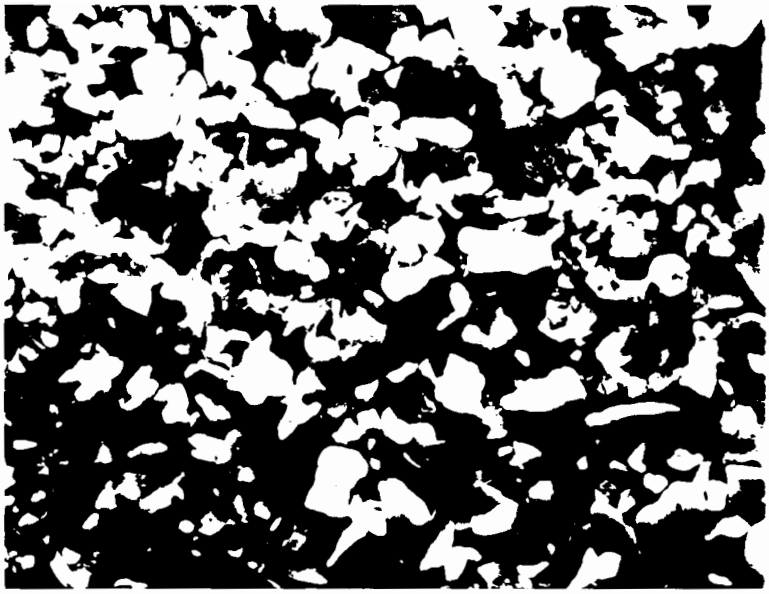

Plate 3.1

Dogs Bay

carbonate sand

1 mm

Plate 3.2

Dogs Bay

carbonate sand

0.1 mm

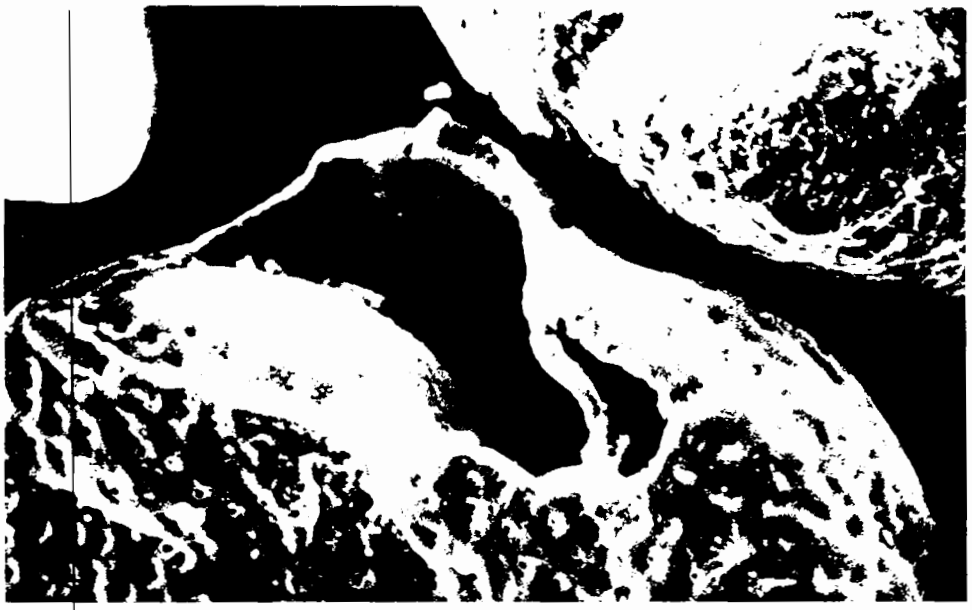

Plate 3.3

Fractured

foraminifera grain

0.01 mm

0.1 mm

Plate 3.4 - Cement coated particle

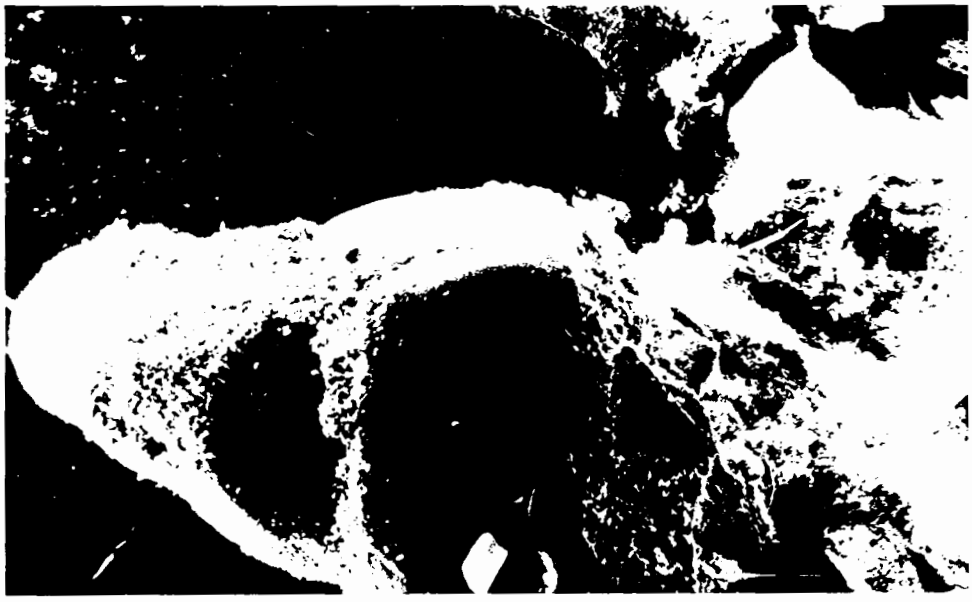

0.1 mm

Plate 3.5 - Cement coated foraminifera grain bonded to other particles

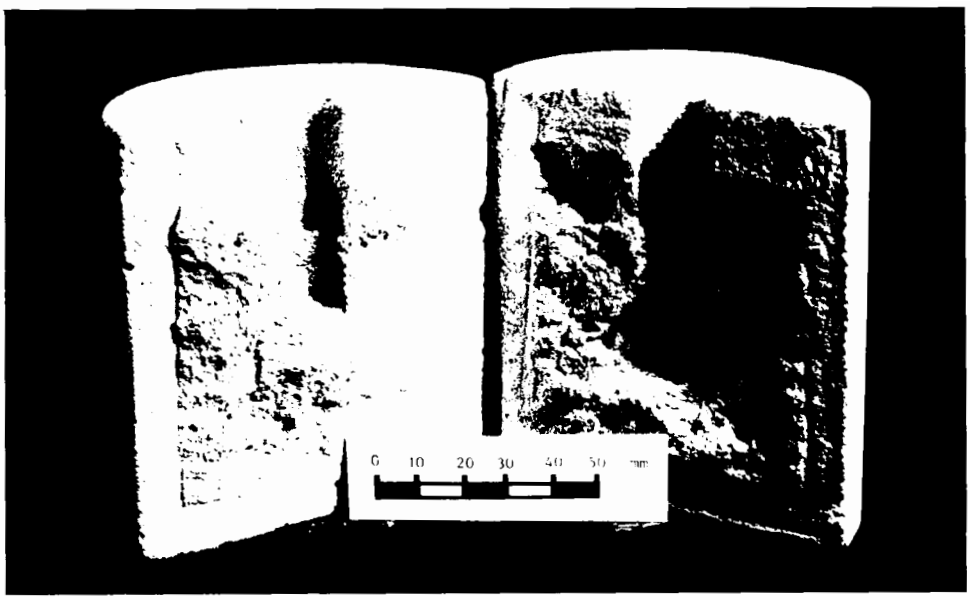

Plate 3.6 - Rod index test, spherical compression zone for 'weak' material

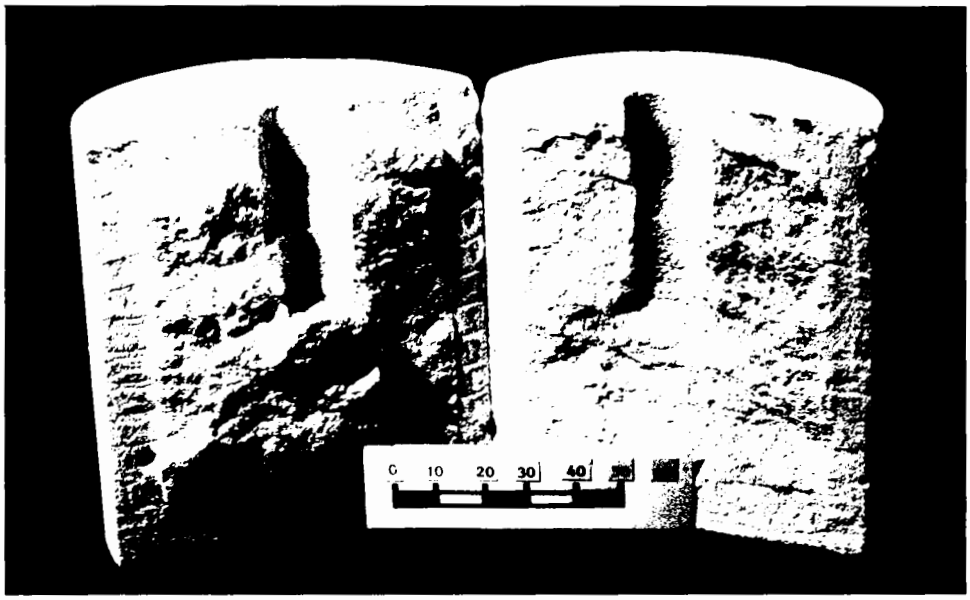

Plate 3.7 - Rod index test, shear cracks for 'strong' material

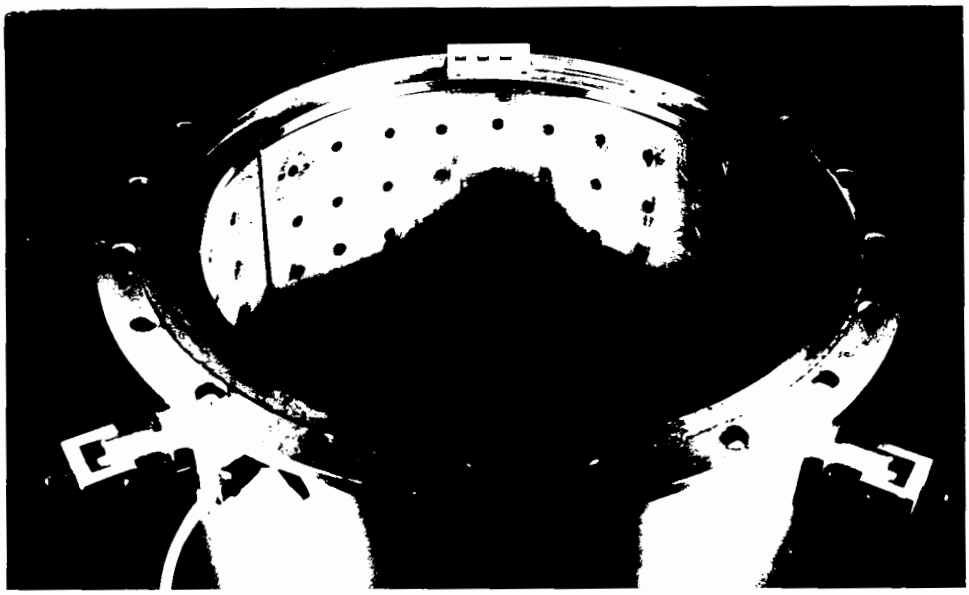

Plate 4.1 - Testing chamber - illustrating sample former

Plate 4.2 - Testing chamber - circumferential membrane fixed in position

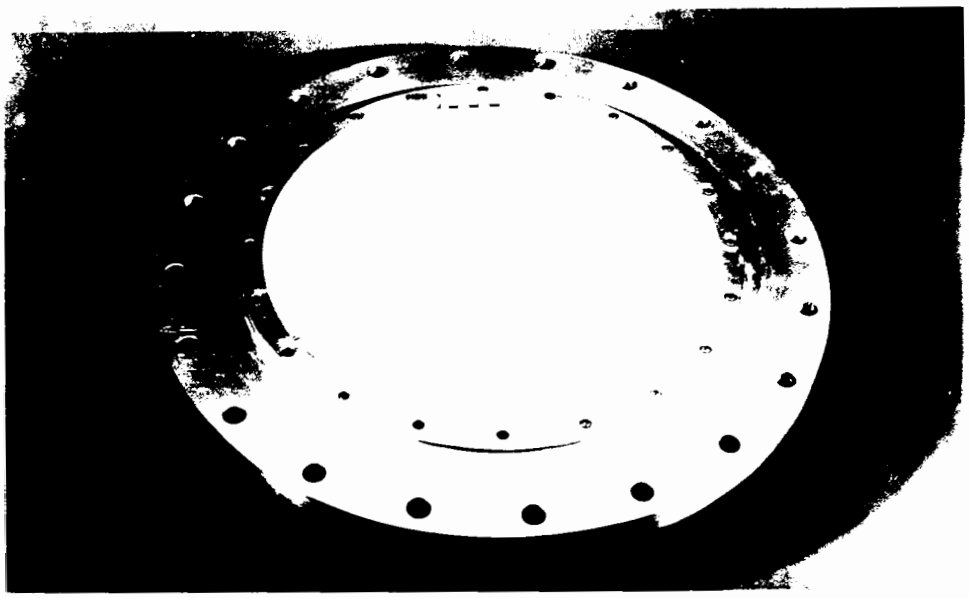

Plate 4.3 - Testing chamber - base membrane fixed in position

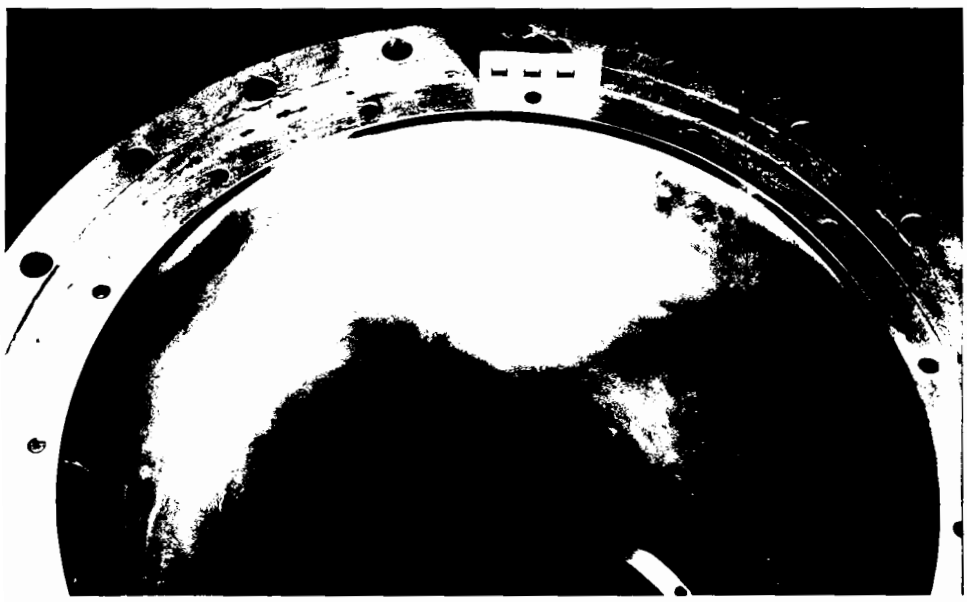

Plate 4.4 - Testing chamber - ready to receive test sample

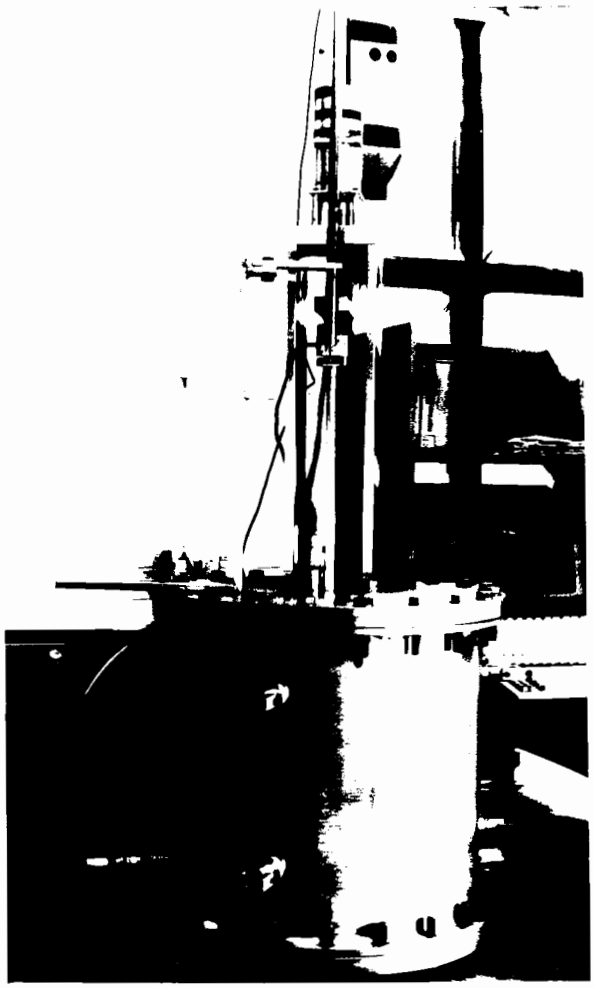

Plate 4.5 - Testing chamber with jacking mechanism attached

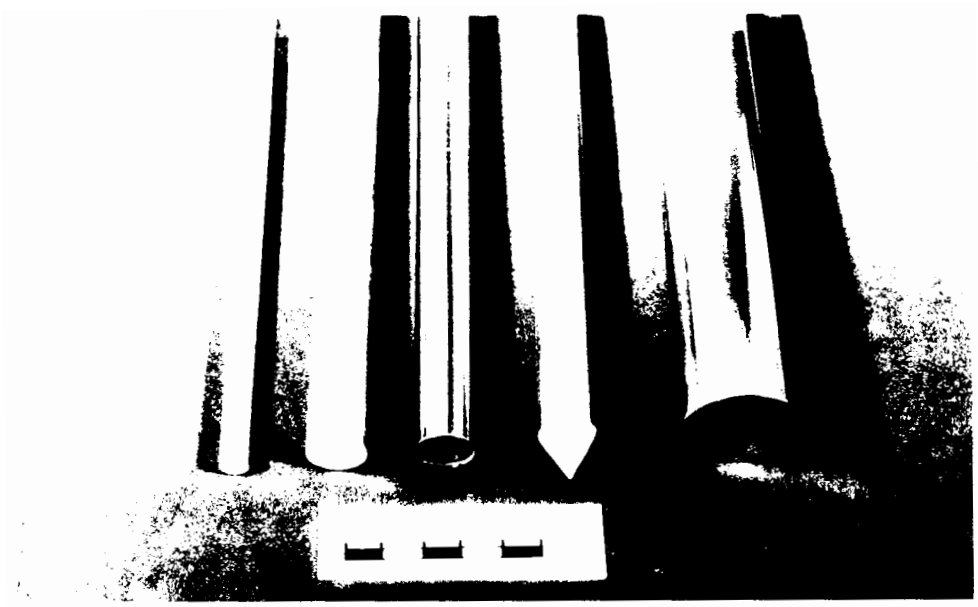

Plate 4.6 - Types of model pile

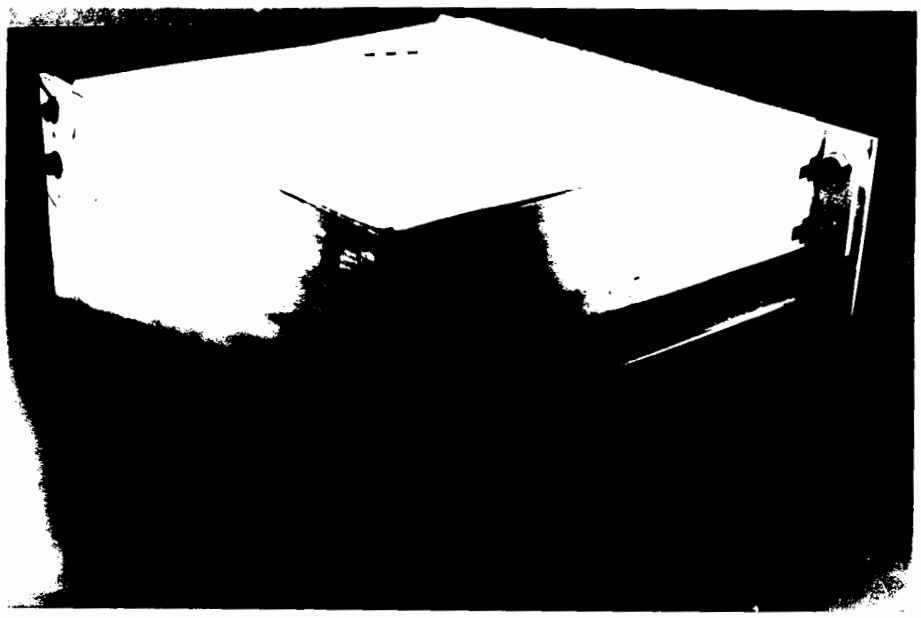

Plate 4.7 - Cemented layer preparation mould

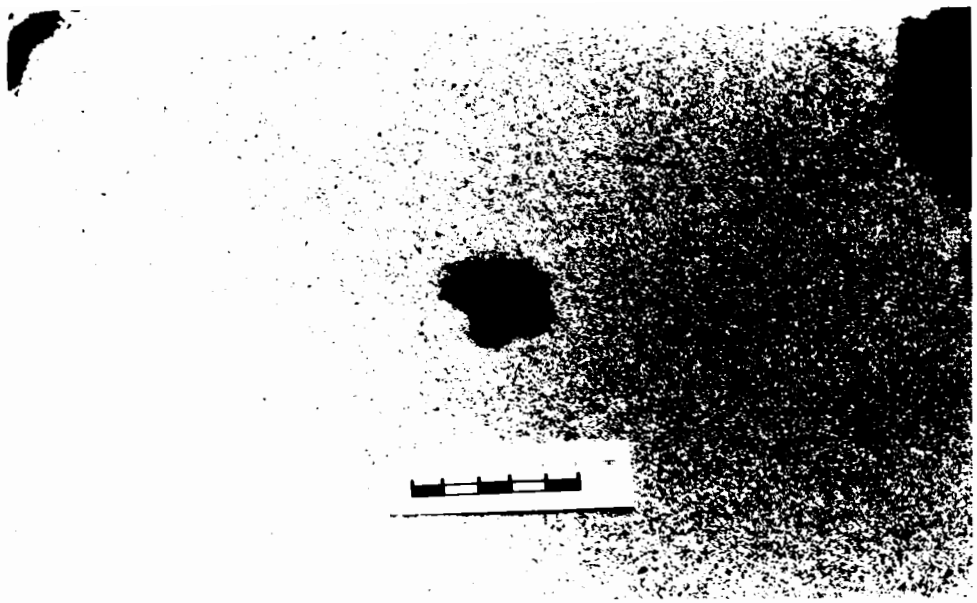

Plate 5.1 - Open hole and annulus of crushed material following push-in and pull-out test

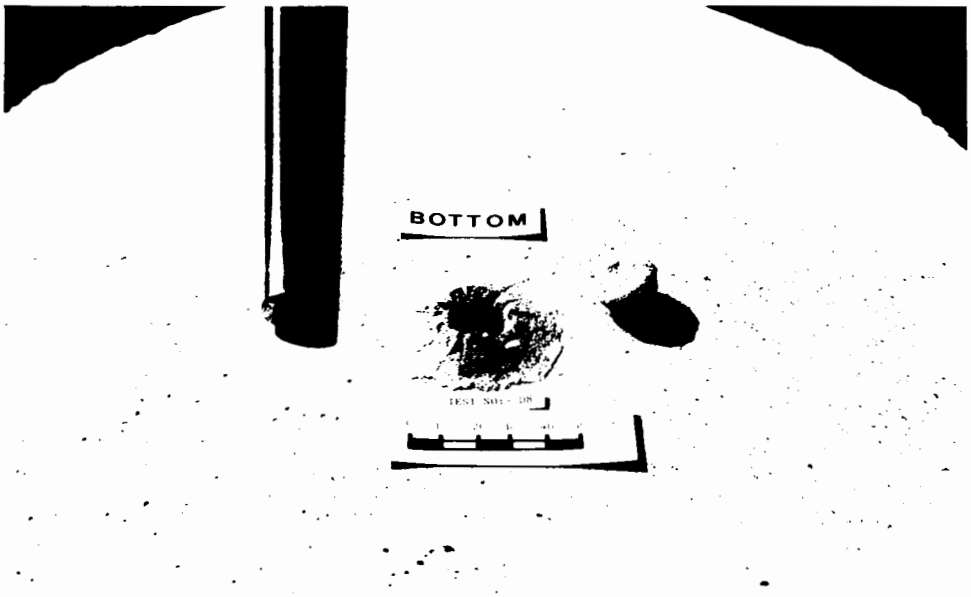

Plate 6.1

0.5 pile diameter

cemented layer

brittle failure

Test No - D8

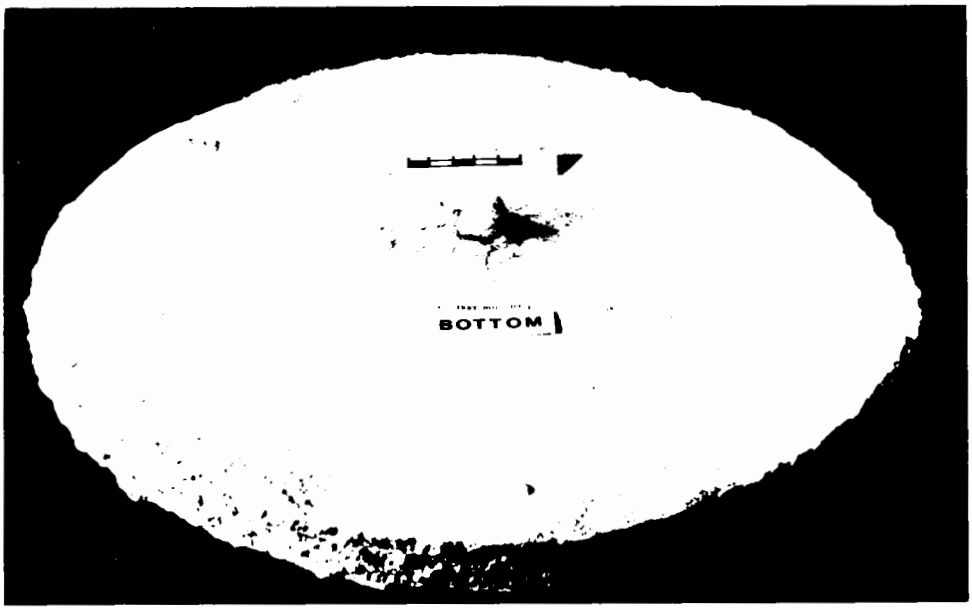

Plate 6.2

1.5 pile diameter

cemented layer

brittle failure

Test No - D9

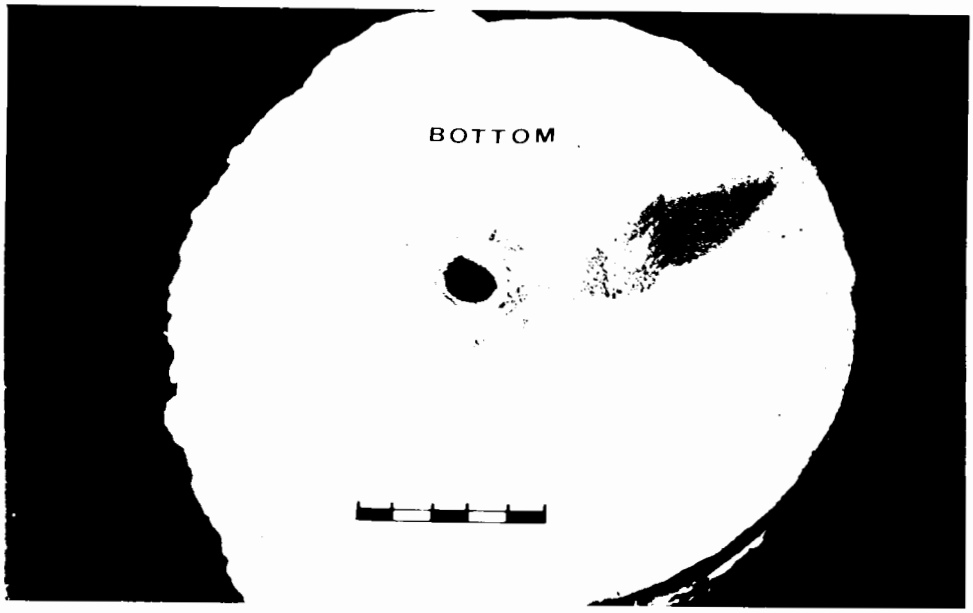

Plate 6.3

5.0 pile diameter

cemented layer

brittle failure

Test No - D21

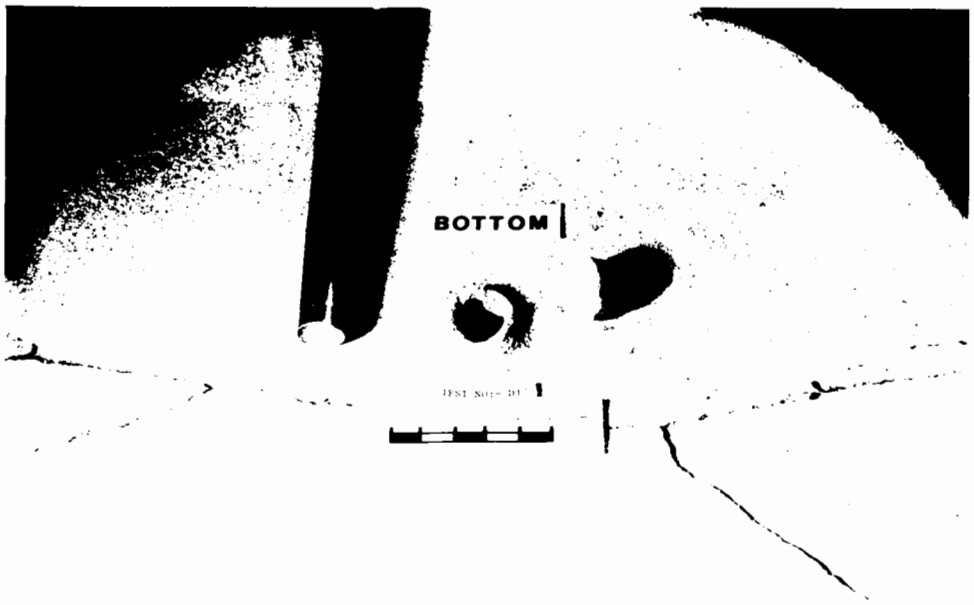

Plate 6.4

0.5 pile diameter cemented layer ductile failure (cracks due to sample extraction)
Test No - D17

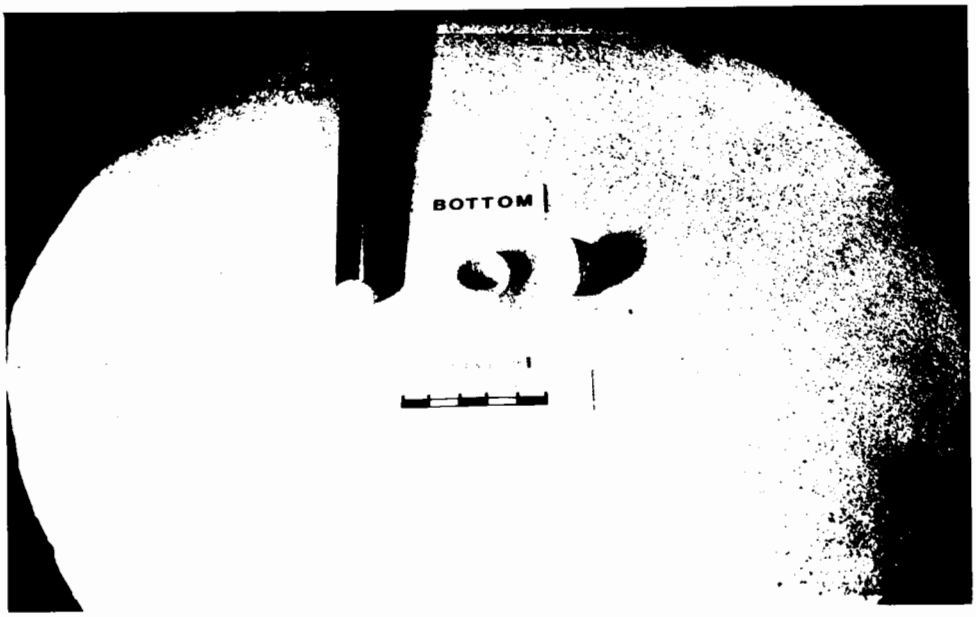

Plate 6.5

1.5 pile diameter cemented layer ductile failure
Test No - D16

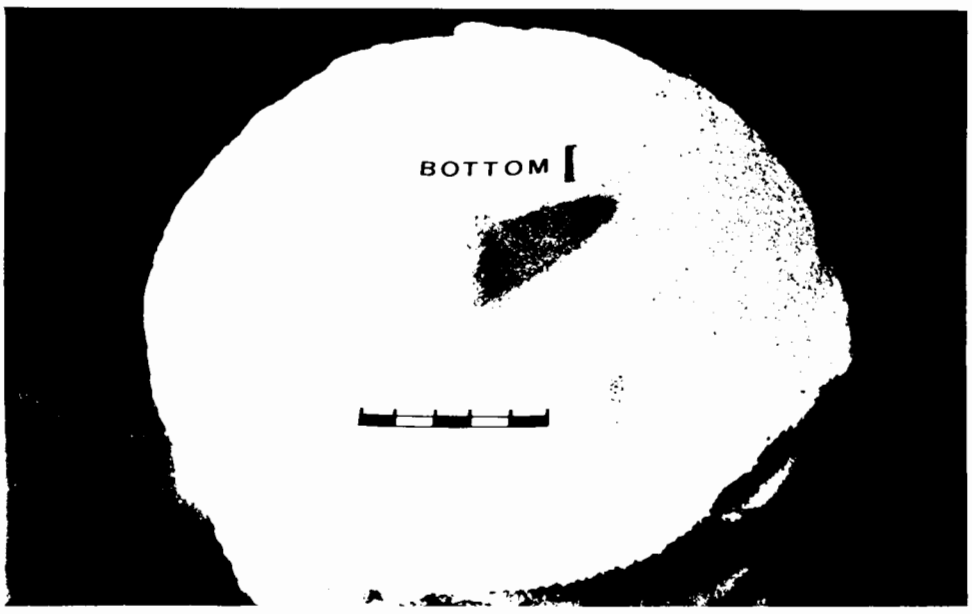

Plate 6.6

5.0 pile diameter cemented layer ductile failure
Test No - D20

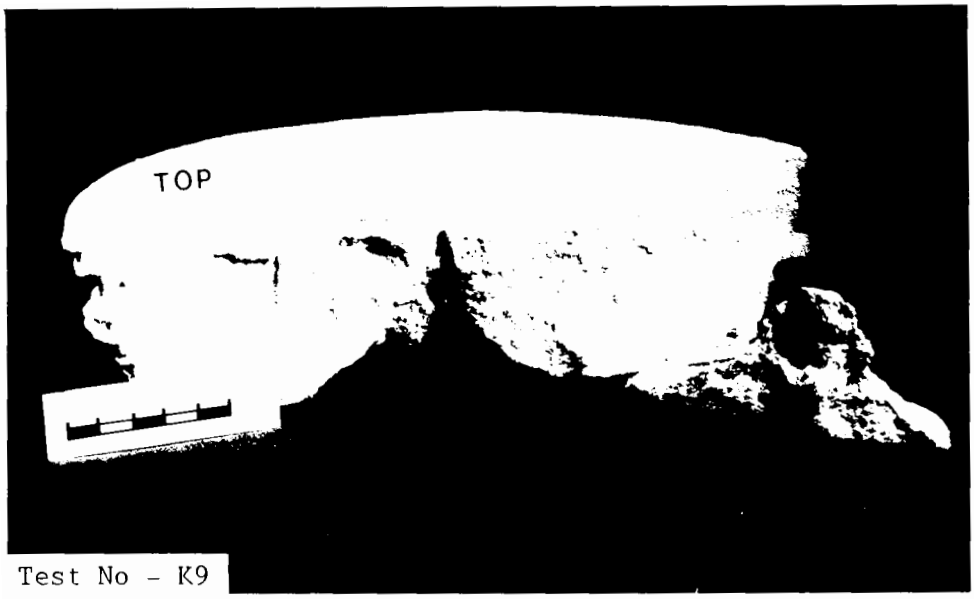

Test No - K9

Plate 6.7 - Punched out section - brittle type failure

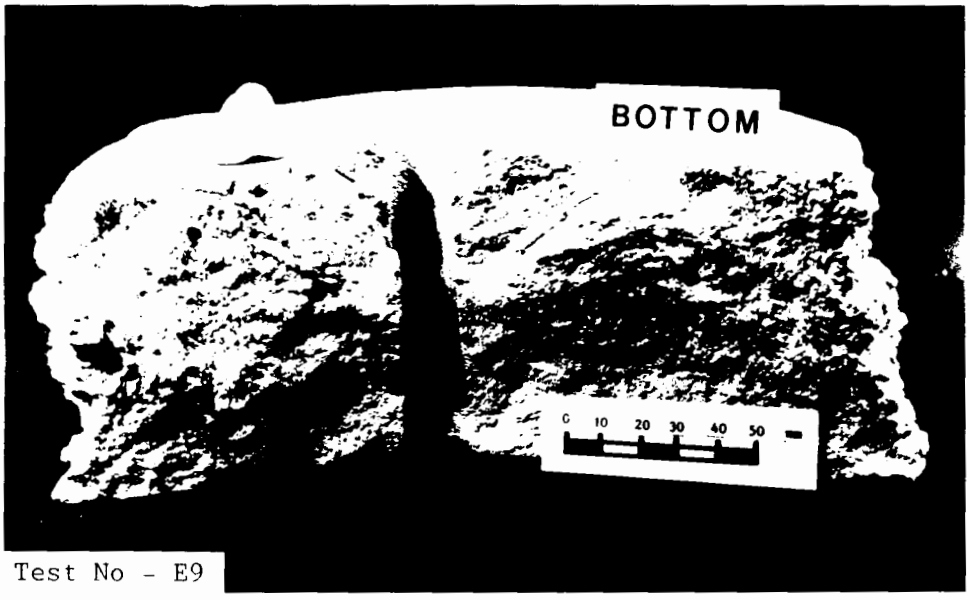

Test No - E9

Plate 6.8 - Continued penetration - brittle type failure

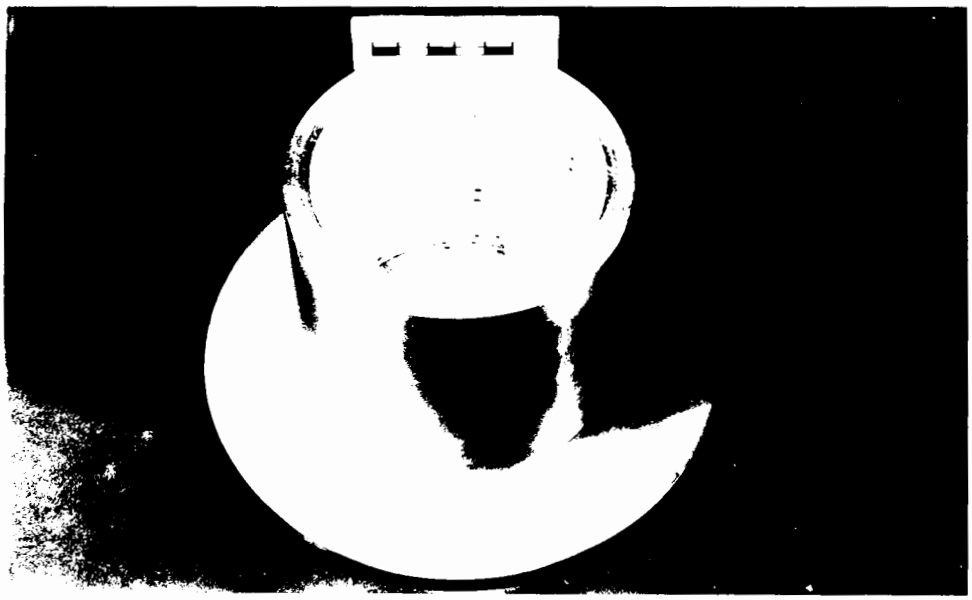

Plate 8.1 - 'Test pot' for physical modelling of numerical analyses boundary conditions

Plate 9.1 - Punching shear failure surface from pull-out test (after Braestrup, 1979)

REFERENCES

REFERENCES

Abbs, A.F. and Needham, A.D. (1985). Grouted piles in weak carbonate rocks. Offshore Technology Conference, Paper No. 4852.

Agarwal, S.L., Malhotra, A.K. and Banerjee, R. (1977). Engineering properties of calcareous soils affecting the design of deep penetration piles for offshore structures. Offshore Technology Conference, Paper No. 2972.

American Petroleum Institute (API) (1984). RP2A: Planning , designing and constructing fixed offshore platforms.

Angemeer, J., Carlson, E. and Klick, J.H. (1973). Techniques and results of offshore pile load testing in calcareous soils. Offshore Technology Conference, Paper No. 1894

Baglioni, V.P., Chow. G.S. and Endley, S.N. (1982). Jack-up rig foundation stability in stratified soil profiles. Offshore Technology Conference, Paper No. 4409.

Baligh, M.M. (1976). Cavity expansion in sands with curved envelopes. Proc. A.S.C.E., Jnl. Geotech. Eng. Div., Vol. 102, No. GT11, pp 1131 - 1146.

Barton, N.R. (1970). A low strength material for simulation of the mechanical properties of intact rock in rock mechanics models. Proc. 2nd Congress, Int. Soc. for Rock Mechanics, Vol. 2, Paper No. 3-15, pp. 99-110.

Barton, N.R. (1976). The shear strength of rock and rock joints. Int. Jnl. Rock Mech. and Min. Sci., 13, pp. 255 - 279.

Bassett, R.H. (1979). Discussion: The use of physical models in design. Proc. 7'th ECSMFE, Brighton, Vol. 5, pp. 253 - 270.

Baumann, R.A. and Weisgerber, F.E. (1983). Yield line analysis of slabs on grade. A.S.C.E., Journal of Structural Engineering, Vol. 109, No. 7, July 1983.

Beake, R.H. and Sutcliffe, G. (1980). Pipe pile driveability in the carbonate rocks of the Southern Arabian Gulf. B.P. personal files.

Bell, A.L. (1915). The lateral pressure and resistance of clay, and the supporting power of clay foundations. Proc. Instn. Civ. Engrs., pp. 233-272.

Beringen, F.L., Kolk, H.J. and Windle, D. (1982). Cone penetration and laboratory testing in marine calcareous sediments. Geotech. Props. Behaviour and Performance of Calcareous Soils, ASTM STP 777. K.R.Demars and R.C.Chaney, Eds., Amer. Soc. for Testing Mtls., 1982, pp. 179-209

Bieniawski, Z.T. (1974). Estimating the strength of rock materials. Jnl. S. Afr. Inst. Civ. Eng.,15, pp. 335 - 344.

Boatman, A.R.C. (1976). The depositional environment of the Red Crag, Ph.D. Thesis, University of London.

Boillot, G., Boysse, P., Lomboy, M. (1971). Morphology, sediments and Quaternary history of the continental shelf between the straits of Dover and Cape Finisterre. The geology of the east atlantic continental margin, 3, Europe. Ed. by F.M. Delany. Report no. 70/15. Inst. Geol. Sci. London, pp. 79 - 90.

Bosence, D.W.J. (1976). Ecological and sedimentological studies of some carbonate sediment producing organisms, Co. Galway, Eire. Ph.D. Thesis, University of Reading.

Braestrup, M.W. (1979). Punching shear in concrete slabs. International association of bridge and structural engineers. Report of the working commission. 1979, Vol. 28, pp. 115-136.

Brinch Hansen, J. (1970). A revised and extended formula for bearing capacity. Bulletin No. 28, Danish Geotechnical Institute, pp. 5 - 11.

Broadhead, A. (1970). A marine foundation problem in the Arabian Gulf. Q. Jnl. Engng. Geol. Vol. 3, pp. 73 - 84.

Brown, E.T. (1984). An assessment of pile end bearing capacity, North Rankin 'A' Platform. Personal report to B.P., February 1984.

Buller, A.T. (1969). Source and distribution of calcareous skeletal components in recent marine carbonate sediments, Mannin and Clifden Bays, Connemara, Ireland. Ph. D. Thesis, University of Reading.

Carter, J.P., Booker, J.R. and Yeung, S.K. (1985). Cavity expansion in cohesive frictional soils. University of Sydney, Research Report No. R507.

Chaney, R.C., Slonim, S.M. and Slonim, S.S. (1982). Determination of calcium carbonate content in soils. Geotech. Props., Behaviour and Performance of Calcareous Soils. ASTM STP 777, K.R.Demars and R.C.Chaney Eds., Amer. Soc. for Testing and Mtls., 1982, pp. 3-15.

Chiu, H.K. and Johnston. I.W. (1984). The application of critical state concepts to melbourne mudstone. Fourth Australia - N.Z. Conf. on Geomechanics, Perth, 1984.

Clark, A.R., and Walker, B.F. (1977). A proposed scheme for the classification and nomenclature for use in the engineering description of Middle Eastern sedimentary rocks. Geotechnique, vol. 27, No. 1, pp. 93-99.

Cole, E.R.L. (1967). The behaviour of soils in the simple shear apparatus. Ph.D. Thesis, Cambridge University.

Dames and Moore (1974,1978). Foundation Investigation Report, North Rankin A location, Northwest Shelf, Australia, B.P. files.

Dames and Moore (1982). Foundation investigation report to B.P. International Ltd., Zakuum and Umm Shaif fields, B.P. files.

Datta, M., Gulhati, S.K. and Rao, G.V. (1979). Crushing of calcareous sands during shear. Offshore Technology Conference, Paper No. 3525.

Datta, M., Gulhati, S.K. and Rao, G.V. (1980). An appraisal of the existing practice of determining the axial load capacity of deep penetration piles in calcareous sands. Offshore Technology Conference, Paper No. 3867.

Datta, M., Gulhati, S.K. and Venkatappa Rao, G. (1979a). Undrained shear behaviour of calcareous sands. Proc. Indian Institute of Engs., Indian Geotechnical Journal, Vol. 9, Part 4, pp. 365-380.

Datta, M., Venkatappa Rao, G. and Gulhati, S.K. (1981). The nature of carbonate material in marine carbonate soils. Proc. 1st Indian Conf.in Ocean Engineering, Indian Institute of Technology, Madras, February, 1981.

Datta, M., Gulhati, S.K. and Rao, G.V. (1982). Engineering behaviour of carbonate soils of India and some observations on classification of such soils. Geotech. Properties, Behaviour and Performance of Calcareous Soils. A.S.T.M. STP 777, K.R.Demars and R.C.Chaney Eds. ASTM 1982, pp. 113-140.

Davis, E.H. (1980). Some plasticity solutions relevant to the bearing capacity of rock and fissured clay. Proc. 3rd Aust.-N.Z. Conf. Geomech.Wellington, Vol. 3, pp.3.27-3.36.

Davis, E.H. and Booker, J.R. (1974). The bearing capacity of strip footings from the standpoint of plasticity theory. Proc. 1'st Aust.- N.Z. Geomechanics Cong., Melbourne, pp. 276 - 282.

Dennis, J. A. N. (1976). Engineering problems associated with ground conditions in the Middle East. Offshore structures. Paper presented at the Engineering Group meeting of the Geological Society, 9th November, 1976.

Dennis, N.D. and Olson, R.E. (1983). Axial capacity of steel pipe piles in sand. Proc. A.S.C.E. Conf. - Geotechnical practice in offshore engineering. Texas, Austin, pp. 389 - 402.

Dunham, G. (1962). Classification of carbonate rocks according to depositional texture. In : Classification of carbonate rocks (ed. W.E. Ham), Mem. Amm. Ass. Petrol. Geol., I, pp. 108 - 121.

Dutt, R.N. and Cheng, A.P. (1984). Frictional response of piles in calcareous deposits. Offshore Technology Conference, paper No. 4838.

Dutt, R.N. and Teferra, W. (1986). CAPWAP analyses increase ability to properly design piles in calcareous sands. Offshore Technology Conference.

Dutt, R.N., Doyle, E.H., Nandal, S. and Ingram, W.B. (1986). Frictional characteristics of calcareous sands from offshore Florida. Offshore Technology Conference. Paper No. 5149.

Elloitt, G.M. (1983). An investigation of a yield criterion for rock. PhD thesis, University of London.

Elliott, G.M. and Brown, E.T. (1985). Yield of a soft, high porosity rock, Geotechnique 35, No. 4, pp. 413 - 423.

Ertec Western Inc. (1983). Investigation of the effects of grain crushing on the engineering analysis of calcareous sediments. AD A126 860. U.S. Govt. Research Contract N62474-82-C-8269.

Evans, K.M. (1985). A model study of the end bearing capacity of piles in layered calcareous soils - The choice of a soil model. Oxford University Engineering Laboratory Report No.OUEL 1576/85. Restricted issue.

Fahey, M. (1980). A study of the pressuremeter test in dense sand. Ph. D. Thesis, University of Cambridge.

Farmer, I. (1983). Engineering Behaviour of Rocks. Second edition, published by Chapman and Hall Ltd., London.

Folk, R.L. (1959). Practical petrographic classification of limestones. Bull. Am. Assoc. Petrol. Geol., 43, pp. 1-38.

Fookes, P.G. and Higginbottom, I.E. (1975). The classification and description of near shore carbonate sediments for engineering purposes. Geotechnique 25, No. 2, pp. 406-411.

Fugro (1978,1981,1986). Soils Reports to Woodside Petroleum, and various other reports, B.P. files.

Fuller, F.M. (1979). Raymond cylinder piles meet the challenge of high load tests. Foundation Facts, Vol. XII, No. 1, 1979. A publication of Raymond International Builders Inc..

Grabau, A.W. (1913). Principles of Stratigraphy, pp. 1185, A.G. Seiler & Co., New York.

Gunatilaka, H.A. (1972). A survey of the geochemistry and diagenesis of recent carbonate sediments from Connemara, W. Eire. Ph.D. Thesis, University of Reading.

Gue, S.S (1984). Investigation of ground heave around driven piles in clay. D.Phil. Thesis, University of Oxford.

Hagenaar, J. (1982). The use and interpretation of SPT results for the determination of axial bearing capacities of piles driven into carbonate soils and coral. Proc. 2nd European Symposium on Penetration Testing, Amsterdam, May 1982, pp. 51-55.

Hagenaar, J. and Vandenberg, J. (1981). Installation of piles for marine structures in the Red Sea. Proc. Xth Int. Conf. S.M.F.E., Stockholm, 1981, pp. 727-730.

Ham, W.E. (1962). Classification of Carbonate Rocks - A Symposium. Mem. Am. Ass. Petrol. Geol., 1, Tulsa.

Hanna, A.M. (1981). Foundations on strong sand overlying weak sand. Proc. A.S.C.E., Jnl. Geotech. Eng. Div., Vol. 107, No. GT7, July 1981 pp. 915-927.

Hoek, E. and Brown, E.T. (1980). Empirical strength criterion for rock masses. Proc. A.S.C.E. Jnl. Geotech. Eng. Div., Vol. 106, pp. 1013 - 1035.

Houlsby, G.T. and Hitchman, R. (1987). Private discussions, Oxford University Soil Mechanics Group.

Houlsby, G.T. and Wroth, C.P. (1983). North Rankin Foundation Studies, Values of shear modulus obtained from pressuremeter tests. Report to Fugro B.V., July 1981, B.P. files.

Jamiolkowski, M. (1986). Presentation to Oxford University Soil Mechanics Group, December 1986.

Jacobsen, M., Christensen, K.V. and Sorensen, C.S. (1977). Gennemlokning of tynde sandlag. Vag-och Vattenbyggaren pp. 23-25, Stockholm, Svenska Vag-och Vattenbyggaren Riksforbund.

Jaeger, J.C. and Cook, N.G.W. (1969). Fundamentals of Rock Mechanics, Chapman and Hall, London.

Jewell, R.J. (1985a). Report on model pile tests performed in cores of calcarenite from the North Rankin 'A' platform. Report No. RJ84016/2 January 1985, B.P. files.

Jewell, R.J. (1985b). Summary report on series I, II, III and IV model pile rod index tests, North Rankin 'A' platform. Report No. RJ85017/5 April 1985, B.P. files.

Jiang, D. and Shen, J. (1986). Strength of concrete slabs in punching shear. Proc. A.S.C.E. Jnl. Struc. Eng., Vol. 112, No. 12, pp. 2578 - 2591.

Johnston, I.W. (1985). Strength of intact geomechanical materials. Proc. A.S.C.E. Jnl. of Geotech. Eng., Vol. 111, No. 6.

Johnston, I.W. and Chiu, H.K. (1984). Strength of weathered mudstone. Proc. A.S.C.E. Jnl. of Geotech. Eng., Vol. 110, No. 7.

Kerisel, J. (1972). La langage des models en mecanique des sols. Proc. 5 th Europ. Conf. Soil. Mech., Madrid, Vol. 2, pp. 9 - 30.

King, R.W., Van Hooydonk, W.R. and Windle, D. (1980). Geomechanical investigations of calcareous soils on the North West Shelf, Australia. Offshore Technology Conference, Paper No. 3772.

Kulhawy, F.H. (1984). Limiting tip and side resistance: Fact or fallacy. Proc. A.S.C.E. National Conv. on Analysis and Design of Pile Foundations, San Francisco, pp. 80 - 98.

Ladanyi, B. (1966). Failure mechanism of rock under a plate load. Proc. 1st. Congress, International Soc. for Rock Mechanics, Lisbon, 1966, pp. 415-420.

Ladanyi, B. (1967). Expansion of cavities in brittle media. Int. Jnl. Rock. Min. Sci., Vol. 4, No. 3, pp. 301-328.

Ladanyi, B. (1972). Rock failure under concentrated loading. Basic and applied rock mechanics, Proc. 10th Symposium Rock Mech., Austin, K.E.Gray (Ed.), A.I.M.E., New York, pp. 363-387.

Ladanyi, B. (1976). Quasi-static expansion of a cylindrical cavity in rock. Proc. 3rd Symposium on Engineering Applications of Solid Mechanics, Univ. of Toronto Press, Vol 2, pp. 219-240.

Ladanyi, B. and Roy, A. (1972). Some aspects of the bearing capacity of rock mass. Proc. 7th Canadian Rock Mech. Symposium, Edmonton, Mines Branch, Dept. of Energy, Mines and Resources, Ottawa, pp. 161-190.

Last, N. (1984). Notes from a seminar held at Southampton University, November 1984 on 'Calibration Chambers'.

Lees, A. (1975). Possible influence of salinity and temperature on modern shelf carbonate sedimentation. Marine Geology, 19, p. 159.

Lees, A., Buller, A.T. (1972). Modern temperate water and warm water shelf carbonate sediments contrasted. Marine Geology, 13, M67.

Lees, A., Buller, A.T. and Scott, J. (1969). Marine carbonate sedimentation processes, Connemara, Ireland. Reading University, Geology Dept., Report No.2.

Lu, B.T.D. (1986). Axial behaviour and capacity of driven piles in calcareous sands. Offshore Technology Conference.

McClelland, B. (1974). Design of deep penetration piles for ocean structures. Proc. A.S.C.E. Journal of Geotechnical Engineering Division, No. GT7, Vol. 100, pp. 709-747

McClelland Ltd. (1985). Report to B.P. Engineering Dept., June 1985, B.P. files.

Meyerhof, G.G. (1960). Bearing capacity of floating ice sheets. Proc A.S.C.E., J.Eng. Mechanics Division, Vol. 86, No. EM5, 1960, pp. 113-145

Meyerhof, G.G. (1962). Load carrying capacity of concrete pavements. Proc. A.S.C.E., J. Soil Mechanics & Founds. Div., Vol. 88, No. SM3, 1962, pp. 89-116.

Meyerhof, G.G. (1974). Ultimate bearing capacity of footings on a sand layer overlying clay. Canadian Geotechnical Jnl., 11, pp. 223-229.

Meyerhof, G.G. (1976). Bearing capacity and settlement of pile foundations. Proc. A.S.C.E., Jnl. Geotech. Engng. Div., Vol 102, No. GT3, pp. 197 - 228.

Miller, D.G. and Richards, A.F. (1969). Consolidation and sedimentation-compression studies of a calcareous core, Exuma Sound, Bahamas. Sedimentology, 1969, pp. 301-316.

Mogi, K. (1966). Pressure dependence of rock strength and transition from brittle to ductile flow. Bull. Earthquake Res. Inst. Tokyo Univ., 44, pp. 215 - 232.

Nauroy, J.F. and Le Tirant, P. (1983). Model tests of piles in calcareous sands. Proc. Conf. on Geotechnical Practice in Offshore Engineering. Austin, Texas, 1983, pp. 356-369.

Nauroy, J.F. and Le Tirant, P. (1985). Driven piles and drilled and grouted piles in calcareous sands. Offshore Technology Conference, Paper No. 4850.

Nielsen, M.P. (1984). Limit Analysis and Concrete Plasticity. Prentice-Hall, Inc., Englewood Cliffs, N.J..

Noorany, I. (1985). Side friction of piles in calcareous sands. Proc. of 11th Int. Conf. on Soil Mech. and Foundation Engineering, San Francisco, Vol. 3, pp. 1611-1614.

Offshore Engineer (1985). Foundation pile problem - the full story, April, p.43.

Ovesen, N.K. (1979). Discussion: The use of physical models in design. Proc. 7'th ECSMFE,, Brighton, Vol. 5, pp. 253 - 270.

Parry, R.G.H. (1978). Estimating foundation settlements in sand from plate bearing tests. Geotechnique, 28, No.1, pp. 107 - 118.

Parry, R.H.G. (1983). Evaluation of North Rankin A Platform Foundations Report to Fugro B.V., March 1983, B.P. files.

Pells, P.J.N. and Turner, R.M. (1980). Endbearing on rock with particular reference to sandstone. Int. Conf. on Structural Foundations on Rock. Sydney, May 1980

Pettijohn, F.J. (1957). Sedimentary Rocks, p. 718, Harper, New York.

Poskitt, T. (1983). Pile driveability analysis - North Rankin A Platform, B.P. files.

Poulos, H.G. (1981). Review of pile acceptance criteria for North Rankin A Platform. Univ. of Sydney Investigation Report No. S322, Nov. 1981

Poulos, H.G. (1982). Review and interpretation of pile driving data from the North Rankin A Platform. Univ. of Sydney Investigstion Report No. S435, December 1982.

Poulos, H.G. (1983). Review of final reports relating to pile installation at the North Rankin A Platform. Univ. of Sydney Investigation Report No. S450, June 1983.

Poulos, H.G. (1984). Cyclic degradation of pile performance in calcareous soils. University of Sydney Research Report No. R477.

Poulos, H.G. (1985). Foundation problems in marine calcareous sands. Ocean space utilisation '85. Proc. International Symposium, Nihon University, Tokyo, Japan, June 1985.

Poulos, H.G. and Chua, E.W. (1985). Bearing capacity of foundations on calcareous sand. Proc. 11'th Conf. on Soil Mech. and Foundation Engng., San Francisco, Vol. 3, pp. 1619 - 1622.

Poulos, H.G., Chua, E.W. and Hull, T.S. (1984). Settlement of model footings on calcareous sand. Geotechnical Engineering, Vol. 15.

Poulos, H.G., Uesugi, M. and Young, G.S. (1982). Strength and deformation properties of Bass Strait carbonate sand. Univ. of Sydney Research Report No. R412, April 1982.

Price, G.P. (1985). Fabric changes and deformation mechanisms in laboratory tested calcarenite, CSIRO Division of Geomechanics, Internal report No. 76, May 1985, B.P. files.

Price, G.P. (1985a). Fabric investigations of model pile tests in calcarenite - Data report No. 3, CSIRO Division of Geomechanics, Internal report No. 74, April 1985, B.P. files.

Price, A.M. and Farmer, I.W. (1981). The Hvorslev surface in rock deformation. Int. Jnl. Rock and Min. Sci., 18, pp. 229 - 234.

Puyuelo, J.G., Sastre, J. and Soriano, A. (1983). Driven piles in a granular calcareous deposit. Proc. Conf. on Geotechnical Practice in Offshore Engineering. Austin, Texas 1983, pp. 440-456.

Randolph, M.F. (1985). Capacity of piles driven into dense sand. Cambridge University Engineering Dept. Report, CUED/D - Soils TR 171.

Reading, H.G. (1978) Sedimentary Environments and Facies. Blackwell Scientific Publications.

Rodgers, J. (1957). The distribution of Marine Carbonate Sediments. Regional aspects of carbonate deposition, Symposium, Soc. Economic Paleontologists and Mineralogists. Special publication No. 5, Am. Assoc. of Petrol. Geol.

Sabins, G.M. and White, R.N. (1967). A gypsum mortar for small scale models. A.C.I. Journal, November 1967.

Scott. J. (1970). The nature and distribution of living and dead foraminifera, Clifden and Mannin bays, Co. Galway, Eire. Ph.D. Thesis, University of Reading.

Settgast, R.H. (1980). Marine pile load testing in carbonate rocks. Offshore Technology Conference, Paper No. 3868.

Shin, E.A. (1969). Submarine lithification of Holocene carbonate sediments in the Persian Gulf. Sedimentology, 12, pp. 109-144.

Stevenson, S.A. and Thomas, C.D. (1978). Driven pile foundations in coral and coral sand formations. Proc. 7th Int. Harbour Congress, Antwerp, May 1978, Vol. 1, pp. 1.05/1-1.05/13.

Stimpson, B. (1970). Modelling materials for engineering rock mechanics. Int. Jnl. Rock Mech. and Min. Sci., (7), 1970, pp. 77-121.

Terzaghi, K. (1943). Theoretical soil mechanics. John Wiley and Sons, Inc., New York.

Vesic, A.S. (1967). A study of bearing capacity of deep foundations , Final report, Project B-189, Georgia Inst. Tech., Atlanta, pp. 231 - 236.

Vesic, A.S. (1972). Expansion of cavities in infinite soil mass. Proc. A.S.C.E. Jnl. soil mech. and foundation eng., Vol. 98, No. SM3, pp. 265 - 290.

Vesic, A.S. (1977). Design of pile foundations. National co-operative highway research program, Synthesis of Highway practice No.42, National Research Council, Washington D.C..

Williams, A.F., Johnston, I.W. and Donald, I.B. (1980). The design of socketed piles in weak rock. Int. Conf. on Structural Foundations on Rock, Sydney, May, 1980.

Wilson, J.B. (1979). Biogenic carbonate sediments on the Scottish Continental Shelf and Rockall Bank. Marine Geology, Vol. 33, M85-93.

Withers, N.J., Kolk, H.T., Lewis, W.M. and Hyden, A.M. (1986). Grouted section tests in calcareous soils. Offshore Technology Conference. Paper No. 5328.

Woodside Petroleum Development Pty. Ltd. (1979). North Rankin Jacket A Foundation Studies - Analysis of sea bottom sediments (2 vols.). B.P. files.

Young, A.G. and Focht, J.P. (1981). Subsurface hazards affect mobile jack-up rig operations. Soundings, McClelland Eng's Inc., Houston

List of Symbols

c	Cohesion
C_c	Compression index
$\overline{C}_c$	Datta's crushing coefficient
d_c	Pile depth factor
d_g	Average grain size
D	Pile diameter
D_{50}	Diameter at which 50% of the soil is finer
e	Void ratio
E	Youngs modulus
E_i	Initial tangent modulus
E_{10}	Secant modulus at 10% axial strain
G	Shear modulus
h	Thickness of cemented layer
I_r	Rigidity index
I_s	Point load index
K	Maximum principal stress ratio
K_0	Effective stress ratio
m	Ratio of compressive to tensile strength
n	Model scaling factor
$N_c N_q N_\phi$	Bearing capacity factors
p	Mean principal stress
p_a	Atmospheric pressure
p_o	Ambient (mean) effective stress
P	Punching load
P_8	Rod Index Test bearing stress at 8 mm penetration
q	End bearing stress
q'	Deviator stress
q_{cl}	Cemented layer limit state bearing stress

q_s	Steady state bearing stress
q_u	Ultimate bearing stress
r	Pile radius
S_c	Pile shape factor
δ	Pile displacement
δ	Soil pile interface angle
ξq_r	Rigidity factor
ν	Poisson's ratio
ν_t	Effectiveness factor
$\sigma_1 \sigma_2 \sigma_3$	Principal stresses
σ_{fc}	Uniaxial unconfined compressive strength
σ_{ft}	Tensile strength
σ_g	Sand grain crushing strength
σ_h	Horizontal confining stress
σ'_H	Effective horizontal stress
σ_v	Vertical confining stress
σ'_V	Effective vertical stress
σ'_m	Effective mean stress
σ'_n	Effective normal stress
τ_s	Unit skin friction
ϕ	Angle of shearing resistance